

Characterization of avian H9N2 and human 2009 pandemic influenza viruses isolated in Singapore

Sutejo, Richard

2011

Sutejo, R. (2011). Characterization of avian H9N2 and human 2009 pandemic influenza viruses isolated in Singapore. Doctoral thesis, Nanyang Technological University, Singapore.

<https://hdl.handle.net/10356/50960>

<https://doi.org/10.32657/10356/50960>

Characterization of avian H9N2 and human 2009 pandemic influenza viruses isolated in Singapore

Richard Sutejo

School of Biological Sciences

A thesis submitted to the Nanyang Technological University
in partial fulfilment of the requirement for the degree of
Doctor of Philosophy (Ph. D)
2011

ACKNOWLEDGMENTS

For the completion of my Ph. D, first and foremost I would like to thank my supervisor A/Prof. Richard J. Sugrue for his valuable input and guidance during my Ph. D period. I would also like to thank you my co-supervisor Dr. Tan Boon Huan, Head of Detection and Diagnostics Laboratories, DMERI@DSO for guiding and assisting me through various experiments required to complete my Ph. D.

I would also like to convey my gratitude to my colleagues as they have offered me great help and assistance in doing various tasks, both in NTU (Dawn, Liat Hui, Patricia, Laxmi, Raihan, Debbie, Anu, Nadine etc) and in DSO (Peijun, Lis, Jasper, Lifang, Kawei, Pusan etc). My greatest gratitude goes especially to Dawn who has been in tremendous colleague in assisting, guiding, and partnering me during the completion of my Ph. D.

Last but not least, I would also like to thank my family and friends, especially my parents who support me from far away to Indonesia, my brother and my sister, and my beautiful partner for standing by my side all the time.

ABBREVIATIONS

aa	amino acid
AIV	Avian Influenza Virus
ATCC	American Type Culture Collection
AVA	Agriculture and Veterinary Association
BSA	Bovine Serum Albumin
cDNA	copy Deoxyribonucleic Acid
CEF	Chick Embryo Fibroblast
CPE	cyto-pathic effect
DMEM	Dulbecco Modified Eagle Medium
dpi	days post infection
EF	Elongation Factor
FBS	Fetal Bovine Serum
FDR	False Discovery Rate
FITC	Fluorescein Isothiocyanate
GCSF	Granulocyte Colony-stimulating Factor
GMCSF	Granulocyte-Macrophage Colony Stimulating Factor
GO	Gene Ontology
HA	Hemagglutinin
HAE	Human Airway Epithelial
HPAI	High Pathogenic Avian Influenza Virus
hpi	hours post infection
IFN	Interferon
IL	Interleukin
KC	Keratinocyte-derived Chemokine
LPAI	Low Pathogenic Avian Influenza Virus
M1	Matrix Protein 1
M2	Matrix Protein 2
MCP	Monocyte Chemotactic Protein
MDCK	Madin Darby Canine Kidney
MIP	Macrophage Inflammatory Protein
moi	multiplicity of infection

mRNA	messenger Ribonucleic Acid
Mx	Myxovirus resistance
NA	Neuraminidase
NPHL	National Public Health Library
NS1	Non Structural Protein 1
NS2	Non Structural Protein 2
nt	nucleotide
OAS	Oligo-Adenylate Synthase
PA	Polymerase Acidic
PAMP	Pathogen Associated Molecular Receptor
PB1	Polymerase Basic 1
PB2	Polymerase Basic 2
PBS	Phosphate Buffered Saline
PCR	Polymerase Chain Reaction
qRT-PCR	quantitative Reverse Transcription – Polymerase Chain Reaction
RANTES	Regulated upon Activation, Normal T-cell Expressed and Secreted
RNP	Ribo Nucleoprotein
RSAD	Radical S-Adenosyl methionine Domain
SA	Sialic Acid
SDS-PAGE	Sodium Dodecyl Sulphate – Poly Acrylamide Gel Electrophoresis
TNF α	Tumour Necrosis Factor α
TPCK	L-(tosylamido-2-phenyl) ethyl chloromethyl ketone
vRNA	viral Ribonucleic Acid

TABLE OF CONTENTS

ACKNOWLEDGMENTS	i
ABBREVIATIONS	ii
TABLE OF CONTENTS	iv
LIST OF TABLES	x
Summary	1
Chapter One: Introduction.....	3
1.1 Virus Classification.....	3
1.2 Morphology and Genome of Influenza Virus	3
1.2.1 Polymerase Proteins	7
1.2.1.1 PA Polymerase	8
1.2.1.2 Polymerase Basic 1 (PB1) and PB1-F2.....	9
1.2.1.3 Polymerase Basic 2 (PB2).....	10
1.2.2 Nucleoprotein (NP)	10
1.2.3 Hemagglutinin.....	12
1.2.4 Neuraminidase (NA)	16
1.2.5 Matrix (M).....	19
1.2.6 Non-structural Protein (NS)	20
1.3 Replication cycle of influenza virus	24
1.3.1 Virus Entry and Uncoating.....	24
1.3.2 Nuclear Import	27
1.3.3 Transcription of Influenza virus mRNA.....	28
1.3.4 Replication of vRNA	30
1.3.5 Nuclear Export of Ribonucleoproteins	31
1.3.6 Extracellular Transport of the Viral Integral Membrane Protein	32
1.3.7 The Viral Assembly.....	33
1.4 Nomenclature of Influenza Virus	34
1.5 Host Specificity and Pathogenicity of Influenza A Virus.....	36
1.5.1 Viral Glycoprotein.....	36
1.5.1.1 Hemagglutinin (HA)	37
1.5.1.2 Neuraminidase (NA)	38
1.5.2 Internal Proteins	39
1.5.3 Polymerase proteins	39
1.5.4 Matrix protein.....	40
1.5.5 Non-structural 1 (NS1) protein.....	41
1.6 Virus-Host Interaction.....	42
1.6.1 Cytokine Response on Influenza Virus Infection	46
1.6.1.1 Myxovirus Resistant (Mx) protein	51
1.6.1.2 2' – 5' Oligoadenylate Synthase (OAS) and RNase L	52
1.6.1.3 Viperin (RSAD2)	53
1.6.2 Cholesterol Metabolism	54
1.7 Influenza Virus in Different Hosts	56
1.7.1 Influenza in Human	56
1.7.1.1 Human Influenza Virus H1N2.....	57
1.7.1.2 Human Influenza H1N1	59
1.7.1.3 Human Influenza H3N2	59
1.7.2 Influenza in Birds	60
1.7.2.1 Avian Influenza Virus Classification	61
1.7.2.2 Outbreaks of High Pathogenic Avian Influenza Virus	62
1.7.2.3 Outbreak of LPAI H9N2 virus	64
1.7.3 Influenza in Swine.....	66
1.7.3.1 Classical Swine H1N1 Viruses.....	67
1.7.3.2 Avianlike H1N1 Viruses	68
1.7.3.3 Humanlike H3N2 Viruses	68
1.7.3.4 Pandemic 2009 H1N1 Swine influenza virus	69
1.8 Research Objective	72
Chapter Two. Materials and Methods.....	75
2.1 General Reagents	75
2.1.1 Cells	75
2.1.2 Virus.....	75
2.1.3 Tissue Culture Reagents.....	76
2.1.4 Antibodies	76

2.1.5	Immunofluorescence and Immunostaining Reagents	77
2.1.6	Commercially available kit.....	77
2.1.7	Cloning Vector and E. coli growth medium	78
2.1.8	Tissue Culture Media and Solution	78
2.1.9	Bacterial Culture Media and Solution	79
2.1.10	DNA Analysis.....	79
2.1.11	Protein Analysis by SDS-PAGE gel	79
2.1.12	Western Blotting.....	80
2.2	Methods	80
2.2.1	General Methods for Biochemistry and Molecular Biology	80
2.2.1.1	RNA extraction	80
2.2.1.2	Reverse Transcription	81
2.2.1.3	Polymerase Chain Reaction (PCR)	81
2.2.1.3	DNA separation by Agarose Gel Electrophoresis	82
2.2.1.4	Gel Extraction	82
2.2.1.5	Ligation.....	82
2.2.1.6	Transformation of Ligation Mix into Competent Cells	83
2.2.1.7	Positive gene insertion by colony screening	83
2.2.1.8	Plasmid Extraction.....	84
2.2.1.9	Sequencing Reaction Preparation.....	84
2.2.1.10	Sequence Alignment and Phylogenetic Tree.....	84
2.2.1.11	Protein Separation by SDS-PAGE	85
2.2.1.12	Western Blotting	85
2.2.2	Tissue Culturing and Infection	86
2.2.2.1	Culture and maintenance of MDCK and A549 cells	86
2.2.2.2	Harvesting and Culture of CEF cells.....	87
2.2.2.3	Mouse Macrophage Harvesting.....	87
2.2.2.4	Virus Propagation.....	88
2.2.2.5	Infection of the cells with virus and the determination of multiplicity of infection used	89
2.2.2.6	Cells harvesting for RNA extraction.....	90
2.2.2.7	Cells harvesting for SDS-PAGE or ³⁵ S-radiolabel imaging	91
2.2.3	Immunofluorescence Assay.....	91
2.2.4	Plaque Assay	92
2.2.4.1	Overlay Assay	92
2.2.4.2	Microplaque Assay.....	93
2.2.4.3	Immunofluorescence Microplaque Assay	93
2.2.4	Growth curve of influenza virus.....	94
2.2.5	[³⁵ S]-Methionine Metabolic Radiolabelling	94
2.2.6	Viral Kinetics	95
2.2.6.1	Cell Infection and Harvesting.....	95
2.2.6.2	Reverse Transcription	95
2.2.6.3	qRT-PCR.....	95
2.2.6.4	Data Analysis	96
2.2.6.4.1	Viral kinetics	96
2.2.7	cDNA Microarray	98
2.2.7.1	Experimental Design and Preparation	98
2.2.7.2	Data Analysis.....	99
2.2.7.3	Confirmatory Experiment.....	100
Chapter Three. Sequence Analysis of H9N2 isolates		102
3.1	Nucleotide and Amino Acid Sequence Similarity Comparison	103
3.2	Phylogenetic and amino acid sequence analysis	106
3.2.1	Non-structural protein (NS).....	106
3.2.2	Matrix Protein (M).....	109
3.2.3	Neuraminidase (NA)	112
3.2.4	Nucleoprotein (NP)	114
3.2.5	Hemagglutinin (HA).....	116
3.2.6	PA polymerase	118
3.2.7	Polymerase protein 1 (PB1).....	121
3.2.8	Polymerase Protein 2 (PB2)	124
3.3	Conclusion	126
Chapter Four. Growth Characteristics of H9N2		128
4.1	Immunofluorescence Assay	130
4.1.1	Madin-Darby Canine Kidney (MDCK).....	130
4.1.2	Chicken Embryo Fibroblast (CEF).....	132
4.1.3	Human Lung Adenocarcinoma cells (A549).....	133
4.2	Growth Curve.....	135

4.2.1	MDCK.....	137
4.2.2	CEF	137
4.2.3	A549.....	139
4.3	Plaque Morphology.....	141
4.4	Viral Genes Expression Profiles in Different Cell Lines.....	143
4.4.1	Replication (vRNA) Profiling in Different Cell Lines.....	144
4.4.2	Transcription (mRNA) Profiling in Different Cell Lines	145
4.4.3	Comparison of Viral Replication and Transcription in Infected Cell Lines	151
4.5	[³⁵ S]-Methionine Metabolic Radioabelling	154
4.6	Conclusion	155
Chapter Five. Analysis on Host Response upon Influenza Virus A Infection		158
5.1	Host Response in MDCK.....	159
5.2	Host Cells Response in CEF	171
5.3	Host Cells Response in A549.....	182
5.4	Validation of cDNA microarray result.....	194
5.4.1	qRT-PCR.....	194
5.4.2	Localization of Mx1 protein by Immunofluorescence Assay	197
5.4.3	Detection of MAP Kinase Related Protein by Western Blotting	199
5.5	Host-virus Interaction in Mouse Lung Macrophage.....	200
5.5.1	Viral kinetics in mouse lung macrophage	201
5.5.2	Measurement of Antiviral Proteins Response in Infected Mouse Lung Macrophage.....	201
5.5.3	Cytokine profiling of mouse lung macrophage	202
5.6	Conclusion	206
Chapter Six. Characterization of 2009 Pandemic Influenza Virus Isolated From Patients in Singapore.....		208
6.1	Genetic Analysis of Strains.....	209
6.2	Growth Characteristics.....	220
6.3	Viral Kinetics in host-cell lines.....	221
6.4	Cell response in host-cell lines.....	224
6.5	Viral kinetics in mouse lung macrophage	230
6.7	Cytokine profiling in mouse lung macrophage	233
6.8	Conclusion	238
Chapter Seven. Conclusion.....		240
Publication List.....		276
Appendix		277
1.	The Primer used for viral kinetics PCR Amplification and Sequencing (Hoffmann <i>et al.</i> , 2001)	277
2.	The Primer used for viral kinetics qRT-PCR Analysis	278
3.	Upregulation of probe sets in MDCK cells at 10 hpi	280
4.	Upregulation of probe sets in CEF cells at 10 hpi	281
5.	Upregulation of probe sets in A549 cells at 10 hpi	283
6.	Cloning Vector for H9N2 gene for sequencing	287
7.	Accession Number List of Influenza Virus Sequence Used in This Experiment.....	288

LIST OF FIGURES

Fig 1.1. Schematic structure of Influenza virion and Viral RNPs.....	5
Fig 1.2. Electron microscope image of negatively stained influenza virus particle.....	5
Fig 1.3. The genome organization of influenza H1N1/PR/8/34, with segment number written on the left	6
Fig. 1.4. X-Ray crystallographic structure of mature HA protein monomer of the 1918 Spanish Flu H1N1 (left). ..	12
Fig. 1.5 Schematic diagram of surface sialic acid receptor recognized by influenza A virus.	14
Fig. 1.6. Epitope mapping of all 16 HA subtypes of influenza A.	15
Fig. 1.7 Schematic Diagram of influenza Neuraminidase (NA) protein.....	16
Fig. 1.8 Epitope binding site in NA protein.....	18
Fig 1.9. Replication cycle of influenza A virus.	23
Fig 1.10. Schematic diagram of the membrane fusion of hemagglutinin (HA) with the endosomal membrane.....	26
Fig 1.11 Schematic diagram of the nuclear import of several influenza virus proteins and RNP.	28
Fig. 1.12 Schematic representation of the viral mRNA transcription.	30
Fig. 1.13 Schematic representation of the nuclear export of influenza protein and RNPs. CRM1 denotes host exportin-1 molecule which facilitates nuclear export with RAN-GTP as a cofactor.	32
Fig 1.14 Schematic diagram of influenza virus budding.	34
Fig. 1.15 Phylogenetic tree of 16 HA (A) and 9 NA (B) subtypes of influenza virus	35
Fig. 1.16 The cleavage site of HA protein.	38
Fig. 1.17 Immunological pathway signalling by Influenza A virus	48
Fig. 1. 18 Schematic representation of influenza A virus inducing MAP kinase pathways.....	50
Fig 1.19 Schematic Diagram of Cholesterol Metabolism.....	55
Fig 1.20 . The origin of 2009 swine influenza virus	71
Fig. 3.1 Phylogenetic tree of non-structural (NS) genes.....	107
Fig. 3.2 Amino acid sequence NS1 from A/Duck/Malaysia/01(H9N2) compared to human derived H9N2 and H5N1 avian influenza virus sequence.....	108
Fig. 3.3. Amino acid sequence NS2 from A/Duck/Malaysia/01 (H9N2) compared to human derived H9N2 and H5N1 avian influenza virus sequence	109
Fig. 3.4. Phylogenetic tree of matrix (M) genes.	110
Fig. 3.5 Amino acid sequence M1 from A/Duck/Malaysia/01(H9N2) compared to human and avian influenza virus sequence.	110
Fig. 3.6. Amino acid sequence M2 from A/Duck/Malaysia/01 (H9N2) compared to human and avian influenza virus sequence.	111
Fig.. 3.7. Phylogenetic tree of neuraminidase (NA) gene.....	113
Fig. 3.8. Amino acid sequence NA from A/Duck/Malaysia/01(H9N2) compared to other avian and human influenza virus sequence.	113
Fig 3.9 Phylogenetic tree of nucleoprotein (NP) genes.	114
Fig.. 3.10 Amino acid sequence NP from A/Duck/Malaysia/01 (H9N2) compared to other avian influenza virus sequence.	115
Fig. 3.11 Phylogenetic tree of hemagglutinin (HA) genes.....	117
Fig. 3.12 Amino acid sequence of HA from A/Duck/Malaysia/01(H9N2) compared to human H9N2.	118
Fig. 3.13 HA Cleavage sites (red arrow) of HA from A/Duck/Malaysia/01 (H9N2) compared to other human and avian influenza virus sequence.....	118
Fig. 3.14 Phylogenetic tree of PA genes.....	119
Fig. 3.15. Amino acid sequence of PA from A/Duck/Malaysia/01(H9N2) compared to other human and avian influenza virus sequence.....	120
Fig. 3.16 Phylogenetic tree of PB1 genes.....	122
Fig. 3.17 Amino acid sequence of PB1 from A/Duck/Malaysia/01(H9N2) compared to other human and avian influenza virus sequence.....	123
Fig. 3.18 Amino acid sequence of PB1-F2 from A/Duck/Malaysia/01(H9N2) compared to other human and avian influenza virus sequence.....	124
Fig. 3.19 Phylogenetic tree of PB2 genes.....	124
Fig. 3.20 Amino acid sequence of PB2 from A/Duck/Malaysia/01(H9N2) compared to other human and avian influenza virus sequence.....	126
Fig 4.1 Immunofluorescence image of Madin Darby Canine Kidney (MDCK)	131

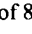
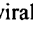
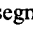
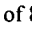
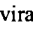
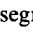
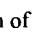
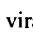
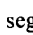
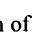
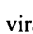
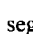

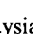
Fig 4.2 Immunofluorescence image of Chick Embryo Fibroblast (CEF)	134
Fig 4.3 Immunofluorescence image of Human Adenocarcinoma lung cells (A549)	136
Fig 4.4 The growth curve profile of MDCK cells infected with A/WSN/33(H1N1) and A/Duck/Malaysia/01(H9N2)	138
Fig 4.5 The growth curve profile of CEF cells infected with A/WSN/33 (H1N1) and A/Duck/Malaysia/01 (H9N2)	139
Fig 4.6 The growth curve profile of A549 infected with A/WSN/33 (H1N1) and A/Duck/Malaysia/01 (H9N2) ...	140
Fig 4.7 The plaque morphology of A/WSN/33 (H1N1) in (A) and (C), A/Duck/Malaysia/01 (H9N2) in (B) and (D)	141
Fig 4.8 The immuno-staining of infected with A/WSN/33 (H1N1) (A), A/Duck/Malaysia/02 (B) for 24 hours. ...	142
Fig 4.9 Relative vRNA expression of 8 viral segments in H1N1 in MDCK (), CEF () and A549 ()	146
Fig 4.10 Relative vRNA expression of 8 viral segments in H9N2 in MDCK (), CEF () and A549 ()	147
Fig 4.11 Relative mRNA expression of 8 viral segments in A/WSN/33 (H1N1) in MDCK (), CEF () and A549 ()	149
Fig 4.12 Relative mRNA expression of 8 viral segments in A/Duck/Malaysia/01 (H9N2) in MDCK (), CEF () and A549 ()	150
Fig 4.13 The absolute quantification of M vRNA and mRNA in MDCK, CEF and A549 infected with A/WSN/33 (H1N1) (), and A/Duck/Malaysia/01 (H9N2) ()	153
Fig 4.14 The [³⁵ S]-methionine metabolic radiolabelling image of MDCK, CEF and A549 infected with A/WSN/33 (H1N1) and A/Duck/Malaysia/01 (H9N2) after 8 hpi in 12% SDS-PAGE gel with 16h exposure time	154
Fig 5.1 The amount of upregulated (A), downregulated (B) and unchanged (C) probe sets in MDCK infected with H1N1 and H9N2 isolate	161
Fig 5.2 The percentage of upregulated gene expression of MDCK cells infected with H1N1 (A) and H9N2 (B) over time	163
Fig 5.3 The downregulated gene expression of MDCK cells infected with H1N1 (A) and H9N2 (B) over time, grouped based on the gene function.	164
Fig 5.4 The unchanged gene expression of MDCK cells infected with H1N1 and H9N2 over time, grouped based on the gene function.	166
Fig 5.5 The Venn Diagram of the amount of upregulated genes in H1N1 and H9N2 infected MDCK cells in cytokine genes (A), antiviral/innate immune related genes (B)	167
Fig 5.6 The heatmap of the host-gene response in H1N1 and H9N2 infected MDCK cells	169
Fig 5.7 Heatmap on Cholesterol Metabolism related genes in H1N1 and H9N2 infected MDCK cells	171
Fig 5.8 The amount of upregulated (A), downregulated (B) and unchanged (C) probe sets in CEF infected with H1N1 and H9N2 isolate.	173
Fig 5.9 The upregulated gene expression of CEF cells infected with H1N1 (A) and H9N2 (B) over time,	174
Fig 5.10 The downregulated gene expression of CEF cells infected with H1N1 (A) and H9N2 (B) over time, grouped based on the gene function.	175
Fig 5.11 The unchanged gene expression of CEF cells infected with H1N1 and H9N2 over time,	176
Fig 5.12 The Venn Diagram of the amount of upregulated genes in H1N1 and H9N2 infected CEF cells in cytokine genes (A), antiviral/innate immune related genes (B) and cell death (C)	177
Fig 5.13 The heatmap of the host-gene response in H1N1 and H9N2 infected CEF cells	180
Fig 5.14 Heatmap on Cholesterol Metabolism related genes in H1N1 and H9N2 infected CEF cells	181
Fig 5.15. The amount of upregulated (A), downregulated (B) and unchanged (C) probe sets in A549 infected with A/Duck/Malaysia/01 (H9N2)	184
Fig 5.16. The upregulated gene expression of A549 cells infected with H1N1(A) and H9N2 (B), grouped based on the gene function.	185
Fig 5.17 The upregulated gene expression of A549 cells infected with H1N1 (A) and H9N2 (B), grouped based on the gene function.	186
Fig 5.18 The unchanged gene expression of A549 cells infected with H1N1 and H9N2 over time	188
Fig 5.19 The Venn Diagram of the amount of upregulated genes in H1N1 and H9N2 infected A549 cells in cytokine genes (A), antiviral/innate immune related genes (B) and cell death	188

Fig. 5.20. The heatmap of the host-gene response in H1N1 and H9N2 infected A549 cells.	191
Fig 5.21 Heatmap on Cholesterol Metabolism related genes in H1N1 and H9N2 infected A549 cells.	193
Fig. 5.22. The qPCR result of various genes in A549 infected with A/WSN/33 (H1N1) and A/Duck/Malaysia/01 (H9N2)	195
Fig. 5.23 The qPCR result of various genes in MDCK infected with A/WSN/33 (H1N1) and A/Duck/Malaysia/01 (H9N2)	196
Fig. 5.24 The qPCR result of various genes in CEF infected with A/WSN/33 (H1N1) and A/Duck/Malaysia/01 (H9N2)	197
Fig 5.25. The staining pattern of Mx1 protein in Mock, H1N1 and H9N2 infected A549 cells at 24 hpi, with enlarged view of the Mx1 staining in inset.....	198
Fig 5.26. The Western Blot result of total JNK, phosphorylated JNK, total p38, phosphorylated 38, total STAT1, phosphorylated STAT1 and β -actin as a control in A/WSN/33 (H1N1) and A/duck/Malaysia/01 (H9N2) infected A549 cells.....	199
Fig 5.27 The immunofluorescence image of mouse lung macrophages infected with A/WSN/33 (H1N1) (left) and A/Duck/Malaysia/01 (H9N2) (right)	200
Fig 5.28 The replication (vRNA) and transcription (mRNA) rate of A/WSN/33(H1N1) and A / Duck / Malaysia /01 (H9N2) infected mouse lung macrophage	201
Fig 5.29 The antiviral host response in A/WSN/33(H1N1) (red bar) and A/Duck/Malaysia/01(H9N2) (green bar) infected mouse lung macrophage	202
Fig 5.30 The cytokine profiling of H1N1 and H9N2 infected mouse lung macrophages. The bar color represents infection time, starting from Non-Infected/Mock (■), 4 hpi (■), 8 hpi () and 20 hpi (■).....	204
Fig. 6.1 The HA gene phylogenetic tree analysis of 2009 Singapore swine influenza virus isolates.	211
Fig. 6.2. The NA gene phylogenetic tree analysis of 2009 Singapore swine influenza virus isolates.	212
Fig. 6.3. The NS gene phylogenetic tree analysis of 2009 Singapore swine influenza virus isolates.	213
Fig. 6.4. The M gene phylogenetic tree analysis of 2009 Singapore swine influenza virus isolates.....	214
Fig. 6.5 The NP gene phylogenetic tree analysis of 2009 Singapore swine influenza virus isolates.	215
Fig. 6.6 The PA gene phylogenetic tree analysis of 2009 Singapore swine influenza virus isolates.	216
Fig. 6.7 The PB1 gene phylogenetic tree analysis of 2009 Singapore swine influenza virus isolates.	217
Fig. 6.8. The PB2 gene phylogenetic tree analysis of 2009 Singapore swine influenza virus isolates.	218
Fig. 6.9 Amino Acid Sequence of M2 in 2009 pandemic strains isolates.....	219
Fig. 6.10 Amino Acid Sequence of NA in 2009 pandemic strains isolates.	219
Fig. 6.11. The growth curve of the 2009 pandemic strains isolates grown in MDCK cells.....	220
Fig 6.12 Replication (vRNA) and Transcription (mRNA) rate of 2009 pandemic strains isolates as compared to A/WSN/33(H1N1) and A/PR/8/34(H1N1) in MDCK, CEF and A549 cells.....	222
Fig 6.13 Relative quantification of mRNA expression of selected genes expressed in virus infected MDCK cells denotes fold change with comparison with mock-infected cells.....	226
Fig 6.14 Relative quantification of mRNA expression of selected genes expressed in virus infected CEF cells	227
Fig 6.15 Relative quantification of mRNA expression of selected genes expressed in virus infected A549 cells....	229
Fig 6.16 Replication (vRNA) and Transcription (mRNA) Rate of 2009 pandemic strains isolates as compared to A/WSN/33(H1N1) and A/PR/8/34(H1N1).....	232
Fig 6.17 Relative quantification of mRNA expression of selected genes expressed in virus infected mouse lung macrophage cells denotes fold change with comparison with non-infected cells, for infection time of 24 hpi (■) and 48 hpi (■).....	233
Fig 6.18 Cytokine profiling of 2009 pandemic strains-infected mouse lung macrophage for infection time of 24 hpi (■) and 48 hpi (■).....	236
Fig 6.18 (Cont.) Cytokine profiling of 2009 pandemic strains-infected mouse lung macrophage for infection time of 24 hpi (■) and 48 hpi (■)	237

LIST OF TABLES

Table 1.1. List of RNA segments of influenza H1N1/PR/8/34 and proteins they encodes (adapted from Lamb and Krug, 2001)	7
Table 1.2. List of important domain in NA protein N1 and N2 subtype.....	18
Table 1.3. List of currently known influenza virus – host interaction	42
Table 1.4 List of cytokines, producing cells, target cells and their function, as summarized by Decker (2006)	47
Table 1.5. Examples of subtypes of Influenza A virus which have infected humans	61
Table 1.6. Clade classification by CDC in 2010.....	63
Table 1.7. The Origin of Swine Influenza Virus Segments	70
Table 3.1 Nucleotide comparison of eight genes of A/Malaysia/01(H9N2) with the three most similar isolates from GenBank.....	105
Table 3.2. Host signature of M protein in influenza A virus	111
Table 3.3 Host signature of NP protein in influenza A virus.....	116
Table 3.4. Host signature of PA protein in influenza A virus.....	121
Table 3.5. Host signature of PB2 protein in influenza A	125
Table 3.6 The summary of the origins of H9N2 isolate.....	127
Table 4.1 Virus Titre at 72 hpi	140
Table 4.2 Tabulated copy number of A/WSN/33 (H1N1) and A/Duck/Malaysia (H9N2) infected MDCK, CEF and A549 cells at 10 hpi, as shown in Fig 4.13. The result shown was based on the copy number of the M segment per 10 ⁴ EF.....	152
Table 5.1 List of upregulated cytokine, antiviral/innate immune related genes in MDCK cells	167
Table 5.2 List of upregulated cytokine, antiviral/innate immune, and cell death related genes in CEF cells.....	178
Table 5.3 List of upregulated cytokine, antiviral/innate immune, and cell death related genes in A549 cells.....	189
Table 5.4 Fold change value of genes on A549, to be compared with qPCR result.	195
Table 5.5 Fold change value of genes on MDCK, to be compared with qPCR result	196
Table 5.6 Fold change value of genes on CEF, to be compared with qPCR result.....	197
Table 6.1 Sequence similarity among 2009 Singapore swine influenza virus isolates, control strains and laboratory strains.. ..	210
Table 6.2 Tabulated copy number of 2009 pandemic strains, WSN and PR8 infected MDCK, CEF and A549 cells at 10 hpi.....	223

Summary

Influenza A virus infection imposes major public health problem. In the past, there were several influenza pandemic outbreaks that killed millions of people. One of the most notable is the 1918 “Spanish Flu”, followed by “Asian Flu” in 1957 and “Hong Kong Flu” in 1968. Since then, highly pathogenic avian influenza virus H5N1 outbreaks have been highlighted for the potential of the pandemic emergence. The emergence of high pathogenic avian influenza (HPAI) strains was resulted from the mutation of low pathogenic avian influenza (LPAI) strains. Similarly, H9N2 influenza viruses also have spread around the world, from wild birds to domestic poultry, especially in Asia. There is a documented evidence of the infection of H9N2 influenza viruses in humans, thus posing them as potential pandemic risks. Recently the 2009 pandemic swine influenza virus also emerged in April 2009, which has reached pandemic level, and co-circulates with seasonal influenza virus.

The efficacy of the influenza virus infection depends on how well the virus interacts with the host cells. The virus should be able to direct the host cell machinery to assist replication and transcription of viral genes, as well as to evade immunological response. Hence, the virus – host interaction is an important aspect towards understanding the nature of the virus, as well as the development of the therapeutic strategy against the influenza virus.

We have isolated a low pathogenic H9N2 influenza virus isolated from ducks as a routine surveillance conducted in Singapore and performed characterization of the virus *in vitro*, which includes sequence analysis, viral growth characteristics and effects on host gene expression using microarrays, using canine, chicken and human cells as host model in tissue culture platform. For the comparison, we also use

A/WSN/33 (H1N1) to determine the efficacy of the viral replication in the tissue culture model, since it is one of the well characterized influenza virus. We found that H9N2 isolate grows poorly in canine and human based cell lines, but able to grow well in chicken based cell lines. This is also supported by the host – interaction analysis, where both canine and human based cell lines exert higher immunological response to fight against the H9N2 infection as compared to H1N1/WSN/33. Further, cytokine profiling shows that the H1N1 infected mouse lung macrophages showed higher expression of IL-1 α , IL-1 β , IL-6, IL-12(p70), IL-13, IL-17, G-SCF, MCP-1, while the H9N2 infected cells showed higher expression of IL-13, MIP-1b and RANTES.

We also conducted similar experiment to 2009 pandemic swine influenza virus. The virus isolates were obtained from patients in Singapore which tested positive for 2009 swine influenza virus. From those, four isolates were chosen and further characterized. The result showed that the isolates were able to grow and replicate in canine, chicken and human based cell lines, although in much lower rate than the laboratory strains. All of the isolates behaved similarly. Furthermore, cytokine profiling in mouse lung macrophages also showed that the isolates induces various cytokine signalling such as IL-1 α , IL-6, IL-9, KC, MIP-1 α , MIP-1 β , MCP-1, TNF- α , and RANTES. The swine influenza virus generally induced higher expression of IL-1 α , TNF- α and RANTES compared to WSN, and generally lower expression of IL-6, KC, MIP-1 α and MIP-1 β .

Chapter One: Introduction

1.1 Virus Classification

Influenza virus belongs to the *Orthomyxoviridae* family. *Orthomyxoviridae* family is a class of virus which possesses a negative sense, single-stranded, and segmented RNA genome. Currently, there are five genera in this family, which are influenza virus A, influenza virus B, influenza virus C, *Thogotovirus* and *Isavirus*. All of the influenza viruses have different characteristics. Influenza A and B virus encode eight segments of RNA and eleven proteins, whereas influenza C only encodes seven segments and nine proteins (Palese, 1980). Influenza A virus can infect a wide range of host, mostly birds and mammals. Influenza B is known to infect humans and occasionally seals (Osterhaus *et al.*, 2000). Influenza C is found in humans and pigs (Guo *et al.*, 1983). Influenza A, B and C are also distinct from each other by the difference in matrix protein structure and antigenicity (Biddison *et al.*, 1977). Furthermore, there are differences in their glycoproteins. Influenza A and B main surface glycoproteins are encoded from two genes, giving rise to hemagglutinin (HA) and neuraminidase (NA). Both HA and NA genes in influenza A virus encode one protein each. Similarly, HA gene in influenza B virus encodes one protein, but the NA gene encodes 2 proteins, NA and NB (Shaw *et al.*, 1983). Influenza C virus main surface glycoprotein is only encoded by Hemagglutinin Esterase Fusion (HEF), which functions as hemagglutinin, receptor destroying and fusion (Herrler *et al.*, 1988).

1.2 Morphology and Genome of Influenza Virus

Influenza A virus is an enveloped virus. The envelope contains lipid membrane originated from the host cell it infects. The envelope consists of two main glycoproteins, hemagglutinin (HA), and neuraminidase (NA). In addition, the M2

protein exists in lower abundance and projects from the surface of the virus. The matrix protein (M1) is located beneath the virus envelope. In the viral core, there are 8 RNA segments, packaged together with the 3 polymerase proteins (PB1, PB2, and PA), and the nucleoprotein (NP) to form ribonucleoprotein complex (Compans *et al.*, 1974). The NEP/NS2 (nuclear export protein/non-structural protein 2) protein is also present in purified viral preparations (Richardson and Akkina, 1991). A schematic representation of influenza A virus is shown in Fig. 1.1.

The morphology of influenza A virus particles is characterized by protruding spikes at the surface. A representative Electron Micrograph image of influenza A virus is shown in Fig. 1.2. These spikes have lengths of approximately 10 to 14 nm, and consists of HA and NA proteins with the ratio of HA and NA is approximately 400-500 HA compared to 100 NA. High quality images of influenza A virus morphology have also been successfully obtained by electron microscopy. For example, Fujiyoshi *et al.* (1994) have managed to visualize the influenza A (virus) by cryo-electron microscopy. The influenza A particles were grouped into the diameter of approximately less than 150 nm spherical particles with well organized interiors, with spikes protruding from the surface. Furthermore, the internal components of the influenza A virus have also been imaged successfully as demonstrated by Murti *et al.* (1992) by immuno-gold labelling/electron microscopy. The Electron Microscopy image of influenza virus A and its internal part components are shown in Fig. 1.2. Noda *et al.*, (2006) also reported spherical morphology of influenza virus in grown eggs. The spherical influenza virus particles have a diameter of approximately 100 nm. In contrast, filamentous influenza virus particles can elongate up to 300 nm in length, which derived from tissue culture cells (Chu *et al.*, 1949).

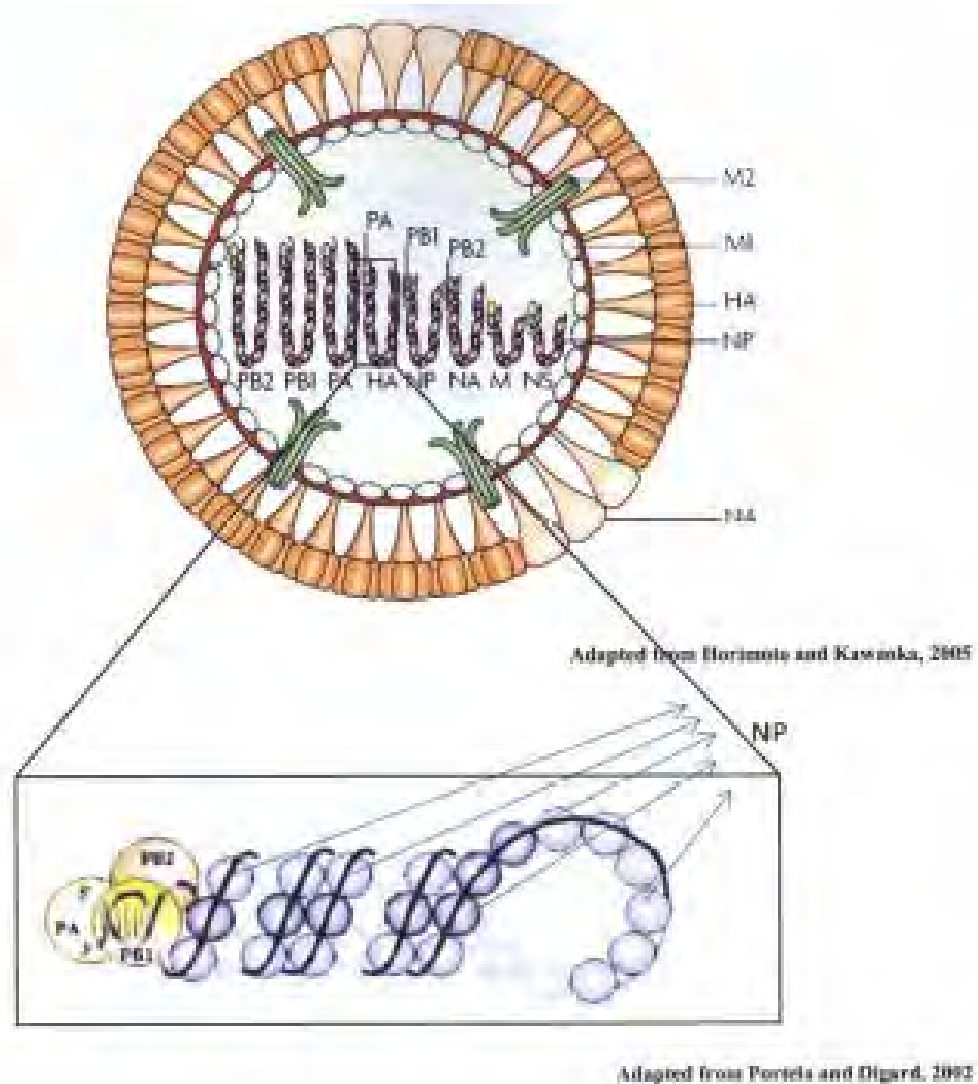
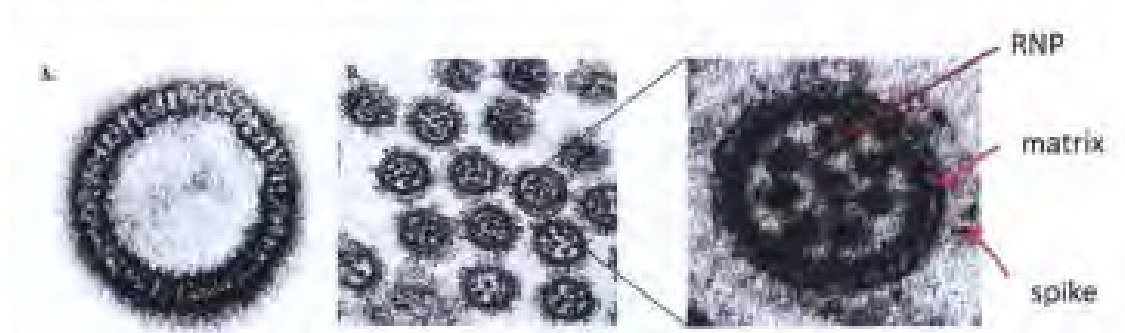


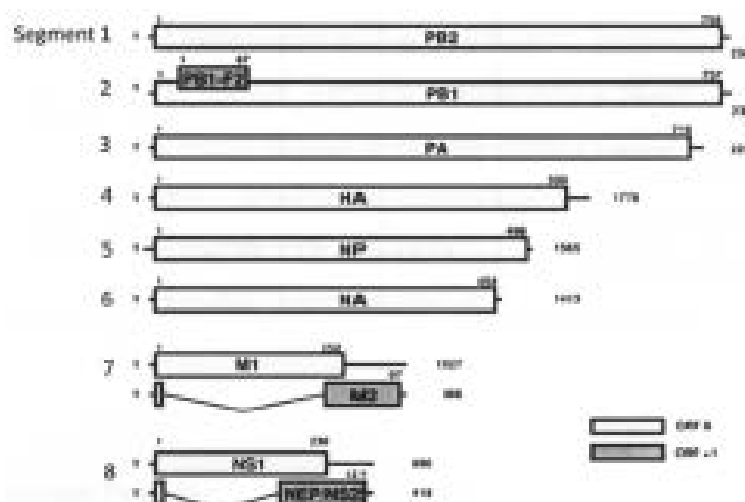
Fig 1.1. Schematic structure of influenza virion and Viral RNPs (inset).



Adapted from Noda *et al.*, 2006

Fig 1.2. Electron microscope image of negatively stained influenza virus particle (A). Electron micrograph of thinned section image of influenza A particles from released cells and its magnification on the inset (B)

The evidence of the segmented nature of influenza A RNA was first shown by using polyacrylamide gel electrophoresis analysis, where 8 bands of RNA were visualized, which later was assigned as segments (Palese and Schulman, 1976). Additionally, each viral segment also contains 5' and 3' non-coding regions. The non-coding regions are conserved among all segments, and this is followed by a segment-specific coding region (Desselberger *et al.*, 1980; Palese *et al.*, 1980). The schematic representation of the genomic organization, the segment numbering referring to the respective gene and protein of influenza A is shown in Fig. 1.3. The segment length, mRNA length, protein size and functions are tabulated in Table 1.1. Most of the segments in the influenza A virus encode one protein, with the exceptions of segment 2, 7 and 8, which encode PB1, M and NS genes, respectively. The segment 2 encodes PB1 protein and the PB1-F2 protein (Mazur *et al.*, 2008, McAuley *et al.*, 2007). The segment 7 encodes M1 and M2 proteins. the NS gene translates to NS1 and NS2 proteins. Both M2 and NS2 proteins are encoded by the splicing mechanism using cellular spliceosome, shown in Fig. 1.3.



Adapted from Lamb and Krug, 2001

Fig 1.3. The genome organization of influenza H1N1/PR/8/34, with segment number written on the left

Table 1.1. List of RNA segments of influenza H1N1/PR/8/34 and proteins they encodes (adapted from Lamb and Krug, 2001)

Segment	Length (nucleotides)	mRNA length (nucleotides)	Encoded poly peptide	Nascent poly peptide length (amino acid)	Molecular weight predicted (kDa)	Approx. Number of copies per virion	Remarks
1	2,341	2,320	PB2	759	85,700	30-60	Host cap recognition of host cell RNA, component of RNA transcriptase complex
2	2,341	2,320	PB1	757	86,500	30-60	Endonuclease activity, catalyzes nucleotide addition, component of RNA transcription and replication complex
		264	PB1-F2	87	10,352	-	Increased pathogenicity, proapoptotic protein, regulates polymerase activity
3	2,233	2,211	PA	716	84,200	30-60	Component of transcription and replication complex, protease activity
4	1,778	1,757	HA	566	61,468	500	Major surface glycoprotein, exist as trimer for sialic acid binding, fusion protein, major antigenic determinant
5	1,565	1,540	NP	498	56,101	1000	Form coiled ribonucleoprotein, involved in nuclear import - export complex, transcription and replication complex
6	1,413	1,392	NA	454	50,087	100	Surface glycoprotein, neuraminidase activity for viral release, antigenic determinant
7	1,027	1,005	M1	252	27,801	3000	Major protein of virion which underlies lipid bilayer, involves in nuclear import - export of cRNA and vRNA
		315	M2	97	11,010	20-60	Integral membrane protein, ion channel activity for virus uncoating
8	890	868	NS1	230	26,815	-	Non structural protein in cytoplasm and nucleus, inhibit cellular pre mRNA 3' end cleavage and polyadenylation, pre-mRNA splicing, sequester dsRNA from PKR kinase to reduce interferon response
		395	NS2/NEP	121	14,216	130-200	Exist in cytoplasm and nucleus, interacts with M1 and involved in nuclear export of RNPs

1.2.1 Polymerase Proteins

Influenza A polymerase proteins are the largest gene segments in the genome with over 2.2 – 2.3 kbps in size. The polymerase complex in influenza A virus consists

of PB1, PB2 and PA proteins. In gene nomenclature, they are encoded as segment 1, 2 and 3 for PB2, PB1 and PA proteins, respectively. PA protein possesses acidic amino acids prevalence while PB1 and PB2 proteins were named for their basic amino acids prevalence. Both PB1 and PB2 segments encode approximately 2,341 nt in length, corresponding to 759 amino acids and 757 amino acids for PB2 and PB1 proteins, respectively. In additions, there is also another open reading frame in PB1 segment which encodes for PB1-F2 protein. The PA segment contains approximately 2,233 nucleotides and 716 amino acids (Horisberger, 1980; Lamb and Choppin, 1976). In SDS-PAGE protein gels, PB1, PB2 and PA have the molecular weight of approximately 96 kDa, 87 kDa and 85 kDa, respectively. The three polymerase proteins, together with viral nucleoprotein (NP), form a complex with the viral RNA, to form the viral ribonucleoprotein (RNP) complex. The expression of the polymerase protein has shown that each of the polymerase proteins has the ability to migrate into the nucleus independently (Akkina *et al.*, 1987, Biswas *et al.*, 1998, Huet *et al.*, 2009, Loucaides *et al.*, 2009), and it was found that PB1 co-migrates with PA in nuclear import (Fodor and Smith, 2004; He *et al.*, 2008). It was reported that the viral polymerase of influenza virus plays a major role in host adaptation and pathogenesis (Gabriel *et al.*, 2005; Gabriel *et al.*, 2007; Gabriel *et al.*, 2008) with nuclear and cytoplasmic host proteins serving as cofactors of the viral polymerase (Deng *et al.*, 2006; Engelhardt *et al.*, 2005).

1.2.1.1 PA Polymerase

Hara *et al.* (2006) suggested that PA is divided into N-terminal domain and C terminal domain, based on the proteolytic cleavage site. The N-terminal domain stretches from 1 to 212 aa, while C – terminal domain lies from 213 to the end.

Furthermore, they also found that many of the critical function of the PA lies in the N-terminal domain which plays critical role in protein stability, endonuclease activity, cap binding, and virion RNA promoter binding. They also observed that mutation K102A caused a general decrease both in transcription and replication in vivo, whereas mutations D108A and K134A selectively inhibited transcription. Both the D108A and K134A mutations completely inhibited endonuclease activity in vitro, explaining their selective defect in transcription. K102A, in contrast, resulted in a significant decrease in both cap binding and viral RNA promoter-binding activity of PB1 protein and consequently inhibited both transcription and replication. (Hara *et al.*, 2004). Recently Yuan *et al.* also discovered endonuclease sites in the PA with the motif similar to endonuclease (P)DX_N(D/E)XK motif at amino acid position 107 (Dias *et al.*, 2009). This also has been confirmed by Yuan *et al.* (2009) in the X-ray crystallography.

1.2.1.2 Polymerase Basic 1 (PB1) and PB1-F2

The PB1 protein plays important role in vRNA binding during transcription (see Section 1.3.3). This activity is due to RNA binding domain of PB1 protein, which located at first 83 amino acids at N-terminal and last 263 amino acids in C terminal. (Gonzales and Ortin, 1999). Poch *et al.* (1989) first identified four motifs in PB1 closely associated with other RNA dependant RNA polymerases. Mutation in these sites will disrupt the transcriptional activity (Biswas and Nayak, 1994). The motifs are named motif I (303-TGDN-306), motif II (398-(D/E)GTASLSPGM-407), motif III (438-WDGLQSSDDFALIVN-452) and motif IV (479-KKKS-482).

The influenza virus PB1-F2 is relatively new protein which is encoded from +1 reading frame of PB1. It has been found to induce apoptosis *in vitro* (Chen *et al.*, 2001) and *in vivo* (Zamarin *et al.*, 2006). The domain critical for the apoptosis function is the mitochondrial targeting sequence located at amino acid position 61 – 74. This domain is shown to interact with ANT3 and VDAC1 to induce apoptosis (Zamarin *et al.*, 2004; Yamada *et al.*, 2004). It is also found that amino acid at the position 66 is critical for increased pathogenicity. It has been found in HPAI H5N1 and “Spanish Flu” pandemic influenza virus contain amino acid S at position 66, while others typically have N (Conenello *et al.*, 2007).

1.2.1.3 Polymerase Basic 2 (PB2)

The role of PB2 protein in influenza A virus is the endonuclease activity, which is very critical during transcription (see Section 1.3.3). The important domain in PB2 includes the bipartite nuclear localization signal (NLS) located at amino acid residue 687–759 (Tarendeau *et al.*, 2007), the cap (7-methyl guanosine triphosphate)-binding domain located at amino acid residue 318–483 (Guilligay *et al.*, 2008). Polymerase basic protein 1 (PB1) can interact with PB2 in the presence or absence of PA protein.

1.2.2 Nucleoprotein (NP)

The nucleoprotein (NP) is the one of the major structural proteins, and is also one of the most abundant virus protein. In addition, NP protein is also one of the critical subunits of the viral ribonucleoprotein (vRNA) binding complex. The NP gene is encoded by RNA segment 5 of the influenza A virus. The NP protein is approximately 1,565 nucleotides corresponding to 498 amino acids with a molecular

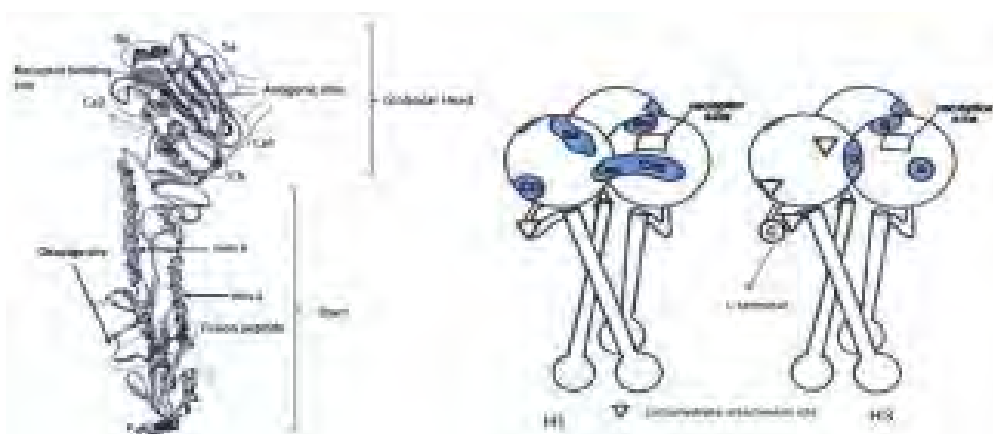
weight of 56.1 kDa. The NP protein has abundant amounts of arginine residues, which are responsible for its strong contribution to RNA bindings (binding) (Winter *et al.*, 1981, Loucaides *et al.*, 2009, Newcomb *et al.*, 2009). Similar to PB2 protein, the NP protein also contains nuclear localization signal (NLS) in its sequence. The NP protein contains an unconventional NLS at amino acid position 4 – 14 , a bipartite NLS at amino acid position 198 – 202, cytoplasmic accumulation signal at amino acid position 337 – 345 and tail loop at amino acid position 402 – 419 (Boulikas, 1997; Neumann *et al.*, 1997; Wang and Krug, 1996; Weber *et al.*, 1998; Melen *et al.*, 2003, Gabriel *et al.*, 2008; Elton *et al.*, 2001; Cros *et al.*, 2005; Wu *et al.*, 2007). This NLS allows the interaction of the NP with several members of the importin family. These interactions allow the RNP complex of the virus to be transported inside the nucleus to initiate the transcription and replication of the influenza virus. The NP protein also has an RNA-binding region at its N terminus at amino acid position 1 – 181, and two NP-NP self-interaction domains, at amino acid residues 189 - 358 and 371 - 465 (Albo *et al.*, 1995; Elton *et al.*, 1999; Kobayashi *et al.*, 1994). NP interacts with PB1 at amino acid position 169 – 358, and PB2 at amino acid position 371 – 465, which is critical for efficient replication and transcription of the virus. (Biswas *et al.*, 1998)

NP protein is most used for detection of viral genomic RNA because of its close association with viral genomic RNA and abundance (Kingsbury *et al.*, 1987, Yamanaka *et al.*, 1990, Baudin *et al.*, 1994). It interacts with virus polymerase unit PB1 and PB2 (Biswas *et al.*, 1998; Medcalf *et al.*, 1999, Poole *et al.*, 2004). It is also a component of nuclear import protein along with three polymerase protein (Mukaigawa and Nayak, 1991; Nieto *et al.*, 1994) and export protein along with M1 protein. (Martin and Helenius, 1991) The amount of NP protein will only start to increase after

it reaches the replication and transcription state, hence it will be a good indicator for viral replication and viral protein expression.

1.2.3 Hemagglutinin

The hemagglutinin (HA) protein is named due to the specific activity of the protein to agglutinate erythrocytes by attaching to specific sialic acid-containing receptors. HA is encoded by RNA segment 4, ranging from 1,742 and 1,778 nucleotides, encoding of 562 to 566 amino acids of polypeptide, dependent on the influenza A strain. The HA is a trimeric rod-shaped glycoprotein of non-covalently linked monomers, with the C-terminal linked to the viral membrane, and the other end projected away from the viral surface (Wiley and Skehel, 1977; Wiley *et al.*, 1977; Skehel *et al.*, 1980; Wilson *et al.*, 1981). The mature structure of HA protein consists of globular head and stem (Fig. 1.4). The receptor binding site and antigenic sites are located in the globular head, whereas the cleavage site and fusion peptide are located in the stem. Another major structure of HA protein is the coiled coil α -helices, which is comprised of two α -helices (Helix A and Helix B) located in the stem area.



Adapted from Stevens *et al.*, 2004

Adapted from Caton *et al.*, 1982

Fig. 1.4. X-Ray crystallographic structure of mature HA protein monomer of the 1918 Spanish Flu H1N1 (left). The HA protein can be divided by 2 domains, globular head and stem. Receptor binding sites and antigenic sites are located on globular head. Fusion peptide and cleavage site are located in the stem region. Schematic representation of different antigenic sites (blue color) between H1 and H3 HA protein (right).

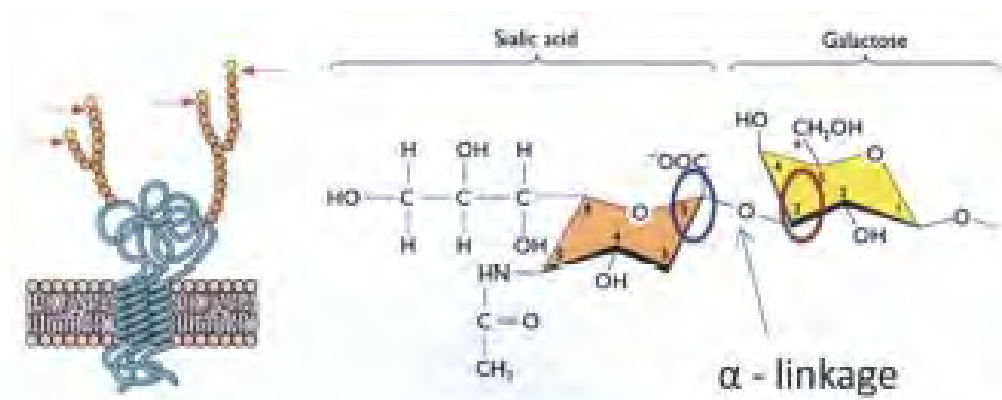
Gerhard *et al.* (1981) first identified the antigenic sites of influenza virus hemagglutinin by generating a panel of hybridoma antibodies targeting HA molecule. Their approach is especially useful to analyze mutations in the HA protein responsible for antigenic drift of the influenza virus. Using the same technique, they successfully mapped 5 antigenic sites of H1 subtype, marked by Ca1, Ca2, Cb, Sa, and Sb (Fig. 1.4 (left)). It should also be noted that the antigenic architecture of the hemagglutinin from different influenza A subtypes varies, as demonstrated by Kaverin *et al.* (2004). They found different antigenic distributions in H3, H5 and H9 subtypes in the globular head of hemagglutinin. For example, the comparison of H1 and H3 HA protein is shown in Figure 1.4 (right).

The HA protein also undergo translational modification. Multiple oligosaccharide chains will be added to the ectodomain of HA in the translation stage. The oligosaccharide chains provide critical functions for evading immunity response as demonstrated by Skehel *et al.* (1984) by comparing the antibody binding level between intact oligosaccharide and the removed oligosaccharide in the HA protein of A/Hong Kong/68 (H3N2). Moreover, three palmitate residues are added to the three C-terminal proximal cysteine residues via a thioether linkage (Schmidt, 1982; Barman *et al.*, 2001; Veit and Schmidt, 2006). The palmitoylation of HA protein has been shown to be critical for influenza virus assembly by increasing HA protein association to lipid raft domain (Chen *et al.*, 2005). The HA segment encode a single polypeptide HA0, which is a precursor form. HA is further cleaved by the host protease to yield HA1 and HA2, which are the prerequisites to the virus' infectivity and pathogenicity. The HA2 sequence is conserved among influenza A strains. and is important for its membrane fusion activity (Skehel and Wiley, 2001). The cleavage site between HA1 and HA2 is also a major determinant for avian influenza virus pathogenicity

(Alexander, 2000). HA is synthesized on the cell membrane-bound ribosomes and translocated into the lumen of the endoplasmic reticulum of the infected cells.

HA has three roles during the influenza virus replication cycle:

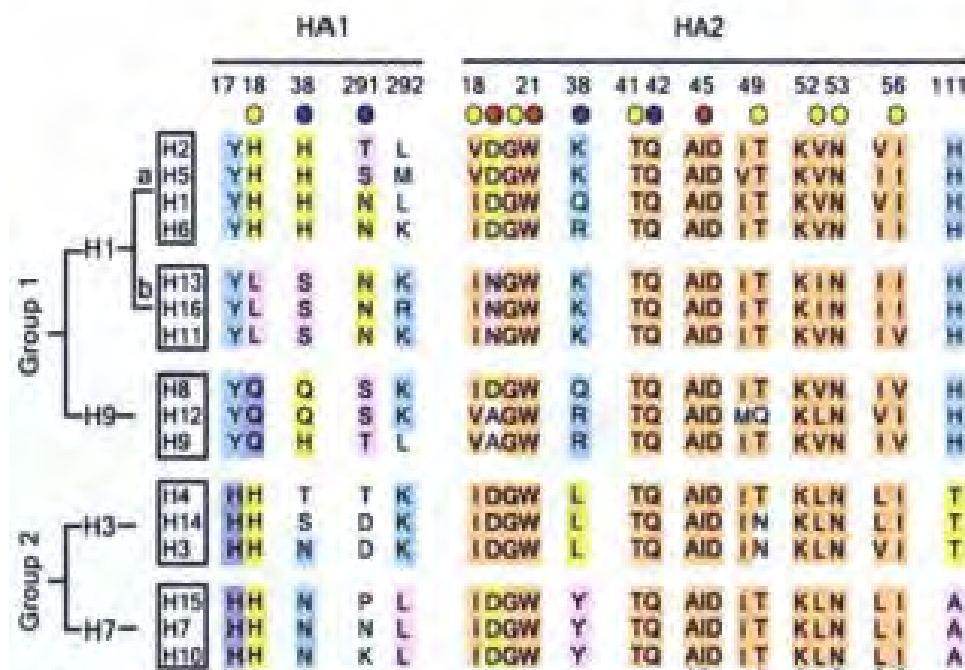
1. HA binds to the receptor containing sialic acid receptors on the cell membrane, which trigger the attachment of the virus. The HA receptor binding site is a grooved pocket located on each unit of HA at the distal end of the molecule. The residues forming the pocket (Tyr-98, Trp-153, His-183, Glu-190, Leu-194) are largely conserved among subtypes (Wilson *et al.*, 1980; Shangguan *et al.*, 1998; Skehel and Wiley, 2000; Glaser *et al.*, 2005). The illustration of the nomenclature of surface sialic acid receptor is shown at Fig. 1.5. The recognition of HA molecules to particular sialic acid receptors expressed by human trachea ($\alpha 2,6$), avian intestine ($\alpha 2,3$) and pig trachea ($\alpha 2,3$ and $\alpha 2,6$) enables the virus to infect the host effectively (Skehel *et al.*, 1980; Vines *et al.*, 1998; Ito *et al.*, 1998; Matrosovich *et al.*, 2000)



Adapted from Racaniello, 2009

Fig. 1.5 Schematic diagram of surface sialic acid receptor recognized by influenza A virus. Note the linkage between sialic acid and galactose. In this diagram, C number 2 in sialic acid carbohydrate (**blue circle**) is linked with C number 3 of the galactose (**red circle**) by an α -linkage (**arrow**), hence the name $\alpha 2,3$ linkage.

2. HA mediates membrane fusion of the endocytosed virus with the host cell membrane to release viral genetic material into the host-cell cytoplasm (Skehel *et al.*, 2000);
3. HA is the major antigen of the virus from which neutralizing antibodies are produced, which together with NA is the major determinant of influenza virus antigenicity (Knossow *et al.*, 2002; Smith *et al.*, 2004). Currently, there are 16 HA subtypes (Fouchier *et al.*, 2006). Sui *et al.* (2009) has performed large scale antibody neutralization to determine epitope location of all subtypes. (Fig. 1.6).



Adapted from Sui *et al.*, 2009

Fig. 1.6. Epitope mapping of all 16 HA subtypes of influenza A. The strength of antibody neutralization is indicated by the colour of the circle below amino acid numbering (Red = strong; Yellow = moderate; Blue = weak). The epitope without the circle has no direct antibody neutralization. The cyan, violet, orange and yellow colours and the amino acid sequence denotes the pattern specific to each subtype.

1.2.4 Neuraminidase (NA)

The neuraminidase (NA) is encoded by segment 6 of the influenza virus. It has 1,413 nucleotides in length encodes a 453-residue polypeptide, which exist as a homotetramer with molecular weight of 220 kDa (Colman, 1984). The NA protein consists of a head domain at C terminal domain that is active enzymatically, and a stalk domain at N terminal domain which is attached to the membrane (Fig. 1.7). The NA polypeptide contains one hydrophobic domain to span the lipid bilayer and N-terminal (Colman *et al.*, 1983). This domain acts as signal domain that targets NA protein to the membrane of the ER and brings about its stable attachment in the membrane (Barman and Nayak, 2000). With regards to the biological activity of the virus, NA protein is responsible for removing the sialic acid from the glycoproteins by catalyzing the cleavage of the α -ketosidic linkage between the sialic acid and an adjacent D-galactose or D-galactosamine (Gottschalk, 1951). This activity allows the viral progeny to be released from the host cell.



Adapted from Varghese *et al.*, 1983

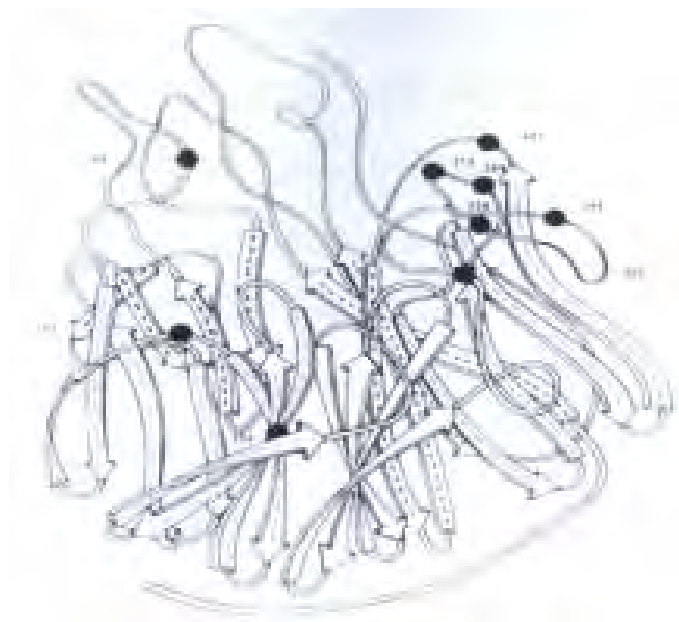
Fig. 1.7 Schematic Diagram of influenza Neuraminidase (NA) protein, which consists of tetramer head and stalk (**right**). The crystal structure of the NA protein tetramer head (**left**). The blue circle in the middle indicates the reactive site

A comparison of NA gene sequences among nine subtypes of influenza A virus reveals that the cytoplasmic tail –MNPNGK- is conserved among influenza A subtypes (Colman *et al.*, 1983). The transmembrane domain of the influenza virus subtypes shares the common property of hydrophobicity, but not the sequence homology. It has been reported that the cytoplasmic tail of NA play an important role in virus packaging (Bilsel *et al.*, 1993), and also affect virion morphology and virulence, but not replication (Mitnaul *et al.*, 1996). Furthermore, both the cytoplasmic tail and transmembrane domain of NA is raft associated (Barman *et al.*, 2004).

The insertion and deletion of stalk region was found in 1982 (Blok and Air, 1982). The length of the stalk in influenza A is typically 62 to 82 residues in most of influenza virus strains, and can be as short as 24 residues, such as in H1N1/WSN/33 (Varghese *et al.*, 1983). Virus with deleted stalk has been found to replicate similarly with parental virus in tissue culture, but better replication in eggs with longer stalk (Castrucci and Kawaoka, 1993). Amino acid cysteine at position 76 was found to be critical in the formation of infectious virus (Luo *et al.*, 1993). Furthermore, any amino acid additions up to 41 amino acids after position 76 do not alter the virus growth (Luo *et al.*, 1993). In H5N1 virus, it has also been confirmed that the stalk length contributes to the pathogenicity to cause systemic infection in avians (Matsuoka *et al.*, 2009; Zhou *et al.*, 2009; Munier *et al.*, 2010). This signifies the importance of the stalk of the NA protein, although it lacks enzymatic sites.

Currently, there are 9 subtypes of NA (Air *et al.*, 1987). An antigenic site analysis done by Colman *et al.* (1984); Air *et al.* (1985, 1989) in N2 subtypes revealed several epitope sites in neuraminidase protein. Later, Webster *et al.* also (1984) first identified important site in N2 which prone to develop escape mutants to reduce antibody binding (Fig. 1.8). Fanning *et al.* (2000) also demonstrate antigenic site in N1

subtype, along with important domain sites by using MacClade phylogenetic amino acid analysis together with already known domain functions (Table 1.2).



Adapted from Webster *et al.*, 1984

Fig. 1.8 Epitope binding site in NA protein (marked in black circle)

Table 1.2. List of important domain in NA protein N1 and N2 subtype (Fanning *et al.*, 2000)

N1 region	N1 amino acids	Properties	N2 regions	N2 amino acids	Properties
A	16-17	Signal-anchor region	A	40-46	
B	41-48	Glycosylation in humans	B	81-82	Stalk
C	67-86	NA stalk, glycosylation/deletions	C	141-149	Glycosylation site
D	188-189		D	197-199	Antigenic site
E	221-222		E	302-308	Antigenic site
F	248-250		F	328-339	Antigenic site
G	263-264		G	344-347	Antigenic site
H	285-289		H	366-368	Antigenic site
I	328-332	Antigenic site	I	368-369	Antigenic site
J	339-344	Antigenic site	J	384-386	
K	351-352		K	400-403	Antigenic site
L	366-369	Antigenic site	L	463-468	
M	385-399	Antigenic site			
N	430-434	Antigenic site			
O	454-455				

1.2.5 Matrix (M)

The matrix (M) segment is 1,027 nucleotides in length and encodes a 51-nucleotide virus specific leader sequence, a 689 nucleotide intron, and a 271-nucleotide body region (Allen *et al.*, 1980; Lamb and Lai, 1982). The M segment encodes 2 proteins, M1 and M2. The M1 protein has 252 amino acid residues, with molecular weight of 27 kDa. The M1 protein lies inside the lipid envelope of the virion and constitutes the most abundant protein in the virion (Schmidt and Lamb, 2005). The M2 protein (M) in influenza A is in segment 7 of the genome. The M2 protein is a minor component of a virion, and possesses ion channel activity (Sugrue *et al.*, 1990). Additionally, a putative alternative splice of mRNA (mRNA₃) has been observed (Lamb and Choppin, 1981). It has a 5' leader sequence of 11 virus-specific nucleotides, and possesses 3' splice site of the M2 mRNA. However, the predicted protein does not exist in the infected cells and virion. (Lamb and Choppin, 1981)

In influenza virus particle, M1 and the viral RNP have close association, which was shown by M1 expression in the purified vRNP protein (Murti *et al.*, 1992). In the virus replication cycle, the dissociation of the M1 protein and vRNP is critical to allow the entry of the RNP into the nucleus, as shown in an experiment using amantadine, an M2 ion protein channel blocker (Hay *et al.*, 1979). The membrane fusion by HA protein occurs undisturbed in endosomes, but the vRNP and M1 protein are not able to dissociate from each other, and transport of vRNP to the nucleus is blocked (Bukrinskaya *et al.*, 1983; Martin and Helenius, 1991). The transport of the M1 protein into the nucleus is also critical to allow the exit of newly assembled RNPs from the nucleus (Martin and Helenius, 1991). M1 consists of 252 amino acids and M2 comprises of 97 amino acids. The M1 protein consists of an N-terminal at amino acid position 1-67, a linker at amino acid position 68-87, a middle region at amino acid

position 88-165 (Sha and Luo, 1997; Arzt *et al.*, 2001) and C-terminal at amino acid position 166-252 to mediate vRNP binding (Baudin *et al.*, 2001). The NLS of M1 protein is located at the amino acid position of 101-106 with the motif of –RKLKR- or –KKLKR- which is critical for interaction with vRNP and NS2/NEP (Noton *et al.*, 2007). There is also an indication of the interaction of the M1 and NS2 proteins in the purified virion (Yasuda *et al.*, 1993).

The M2 protein is abundantly expressed on the plasma membrane of the virus infected cells but only a small amount is incorporated into virions (Lamb *et al.*, 1985; Zebedee *et al.*, 1985). The M2 protein is a disulfide-linked homotetramer with each chain consisting of 97 amino acids with: 24 amino acids in the extracellular; 19 amino acids in the transmembrane domain; and 54 amino acids in the cytoplasmic tail. The M2 protein possesses pH-activated ion channel activity that flows protons, resulting in the uncoating of the influenza virus in the endosomal compartment (Lamb *et al.*, 1985). Another interesting part in M2 protein is the amantadine resistance mutation. The critical points of mutation at amino acids L26, A30 and S31 have been shown to develop amantadine resistance among influenza virus. (Hay *et al.*, 1986; Sugrue and Hay, 1991; Pinto *et al.*, 1992; Suzuki *et al.*, 2003)

1.2.6 Non-structural Protein (NS)

The NS segment is the smallest segment of the influenza A virus genes, which is 890 nucleotides long. It encodes two non-structural proteins (NS), NS1 and NS2/Nuclear Export Protein (NEP), with molecular weights of 26 kDa (202-237 amino acids) and 14 kDa (113 amino acids), respectively (Lamb and Choppin, 1979). The NS1 is encoded by one transcript, whereas the NS2/NEP is encoded by a spliced mRNA with 473 nucleotide intron in between (Inglis *et al.*, 1979; Lamb and Choppin, 1979; Inglis and Almond, 1980). NS1 and NS2 mRNAs share a 56-nucleotide leader

sequence that contains the AUG codon used for the initiation of protein synthesis (Lamb and Choppin, 1979). The NS1 and NS2 proteins also share a sequence of nine N-terminal amino acids before the intron. The translation of the body of the NS2/NEP mRNA is in the +1 ORF position, and overlaps with the NS1 mRNA frame by 70 residues (Lamb and Lai, 1980). The nuclear localization signals of the NS1 is found as two separate signals between residue 34 to 38 and residue 203 to 237 (Greenspan *et al.*, 1988). The NS2 protein also contains nuclear export signal (NES), hence it is named the NS2/NEP. The NES in NS2 protein consists of a short leucine-rich sequence mapped at residues 138 to 147 which mediates the nuclear export of proteins (Gorlic and Mattaj, 1996; 1996; Li *et al.*, 1998). Recently, Robb *et al.* (2009) also proposed the possibility of the role of NS2 in regulating the replication and transcription of the virus.

NS1 protein has been closely associated with virulence (Noah and Krug, 2005), and an antagonist of host cell interferon pathway (Hayman *et al.*, 2007; Hale *et al.*, 2008; Hayman *et al.*, 2009). NS2 serves as a nuclear export protein (Neumann *et al.*, 2000) and packaged in small amount in influenza virus virion (O'Neill *et al.*, 1998). The NS genes are further divided into two groups called alleles A and B. Allele A consists of influenza viruses from human, equine, swine, and avian species, whereas allele B comprises one equine and many avian influenza isolates (Treanor *et al.*, 1989; Ludwig *et al.*, 1991; Guo *et al.*, 1992). The nucleotide sequence similarity within allele A and allele B have been found to be 86.5-99.4% and 89.4-99.6% respectively. The comparison between allele A and allele B is 72.3% (Kawaoka *et al.*, 1998). It has been shown that deleted forms in NS1 protein would still make an infectious particle, but with much lower infectivity and growth (Falcon *et al.*, 2004)

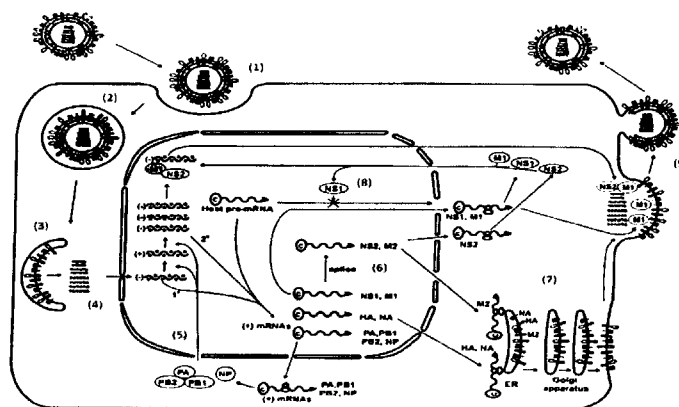
The NS1 protein is expressed in large amounts in influenza virus-infected cells, but is absent in the viral particles, hence the name non-structural (NS) (Lazarowitz *et al.*, 1971; Skehel, 1972). NS1 is found in the nucleus and associated with polysomes (Krug and Etkind, 1976; Krug and Soeiro, 1975).

The NS1 protein plays a major role in the influenza life cycle, which is documented as follows:

1. The binding of the NS1 protein to the Cleavage and Polyadenylation Specificity Factor (CPSF) and Poly(A)-binding protein (PABII) can inhibit the 3' end cleavage and polyadenylation of the cellular pre-mRNAs (Nemeroff *et al.*, 1998). The CPSF binding site is mapped on position 186, and PABII is located on position 223-230. (Nemeroff *et al.*, 1998). In contrast to the cellular pre-mRNAs, the nuclear export of the viral mRNAs is not inhibited by the action of NS1 protein because the poly(A) tails of the viral mRNAs are produced by the viral transcriptase, and not by the cellular 3' end processing machinery (Robertson *et al.*, 1981; Luo *et al.*, 1991; Li and Palese, 1994; Poon *et al.*, 1999)
2. The binding of the NS1 protein can inhibit the host cell pre-mRNA by splicing to a specific stem-bulge in U6 snRNA (Qiu *et al.*, 1995). However, the mechanism of how the NS₁ protein can enhance the virus gene expression, and how the M₁ and NS₁ mRNAs splicing is unaffected needs further investigation.
3. Host cell normally detects the presence of pathogens from the Pathogen Associated Molecular Pattern (PAMP). it was originally thought that influenza virus generates double stranded RNA as PAMP. This activates the Protein Kinase R as one of the important upstream of host-cell immune response. (Hatada and Fukuda, 1992; Hatada *et al.*, 1999; Lu *et al.* 1995). However, an experiment done by Pichlmair *et al.* (2006) showed that influenza A virus does not produce double

stranded RNA as PAMP. Instead, they identified 5'-phosphorylated vRNA in infected cells as PAMP recognized by MDA5 and RIG-I as a critical trigger to the antiviral immunity. Their activities are also blocked by NS1 protein by forming a complex.

The NS2 protein, which originally thought to be a non-structural protein, exists in the virion and forms an association with the M1 protein (Richardson and Akkina, 1991; Yasuda *et al.*, 1993). The NS2 protein is associated with the M1 protein to translocate viral genetic material from the nucleus by its interaction with exportin (O'Neill *et al.*, 1998). The NS2 protein contains one nuclear export signal at the position 12-21 and two C-helical domains at amino acid position 64-81 and 94-116 (Akarsu *et al.*, 2003). The protein mediates RanGTP-dependent binding to crml and the C terminal binds to the M1 protein of the influenza virus to assist in nuclear export of viral RNPs with hydrophobic residue 13L and 21L in NS2 protein (Akarsu *et al.*, 2003; Elton *et al.*, 2001; O'Neill *et al.*, 1998). Further, Akarsu *et al.* (2003) also reported by crystallography analysis that 78W is critical for binding with the M1 and assisting nuclear export.



Adapted from Lamb and Krug, 2001

Fig 1.9. Replication cycle of influenza A virus. The number in parentheses denotes steps of the viral replication : (1) receptor binding; (2) entry; (3) membrane fusion and RNP release; (4) nuclear import of RNP; (5) and (6) replication and transcription of influenza A virus; (7) migration of HA and NA to the cellular membrane; (8) NS1 inhibitory action on host pre-mRNA; (9) viral material packaging and release

1.3 Replication cycle of influenza virus

Briefly the replication cycle step in influenza virus is as follows (Fig. 1.9):

- 1) The virus binds to the host cell sialic acid receptor using HA ;
- 2) The virion enters the cell via endocytosis;
- 3) The low pH of the cytoplasm activates the M2 channel, which allows protons to enter the virion. Viral RNPs and M1 are dissociated, released and imported to the nucleus after the HA protein performs membrane fusion with the host;
- 4) The RNA- dependent RNA polymerase complex, consisting of PA, PB1 and PB2 together with NP begins the replication and transcription of the viral genome;
- 5) The mRNAs are transported from the nucleus for translation, with the copied RNAs (cRNAs) templates for replication;
- 6) Newly synthesized viral envelope proteins HA and NA are transported to the cell surface via the Golgi apparatus, whereas other proteins, including NS1, are transported back into the nucleus for packaging, exporting and optimizing virus replication by inhibiting host defense mechanism (Mahy *et al.*, 1980);
- 7) The packaged RNPs localize and are assembled on the plasma membrane of the host cell (cell) which contains the viral envelope proteins. With the aid of neuraminidase (NA) that cleaves the sialic acid binding with the HA protein, the viral progeny are released.

1.3.1 Virus Entry and Uncoating

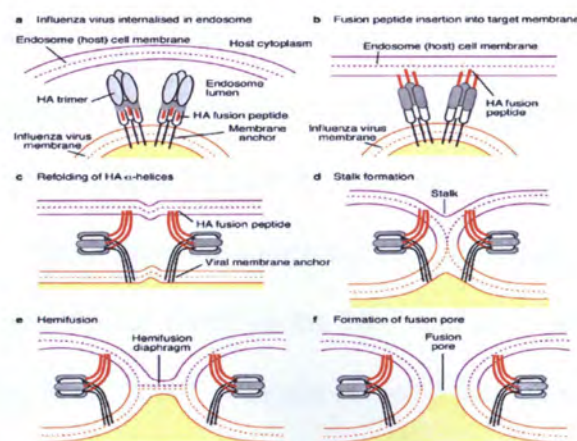
Influenza virus binds to sialic acid receptor which presents in cell surface through HA. Different influenza viruses have different specificities for the sialic acid linked galactose. These specificities are determined by the HA receptor binding pocket (Weis *et al.*, 1988). Ito *et al.* (1998) has shown that different cell lines can contain

different sialic acid linkages. They found that carbohydrate chains of avian intestine predominantly contain $\alpha 2,3$ sialic acid-linked galactose; human trachea carbohydrate chains predominantly contain $\alpha 2,6$ sialic acid-linked galactose, and swine trachea can contain both. This HA specificity is an important determinant in restricting the transmission of the influenza virus in different species. In situations of interspecies transmission to human, Kogure *et al.* (2006) performed lectin affinity assay and found that human trachea lung cells contain both $\alpha 2,6$ in majority and $\alpha 2,3$ in lesser extend. They also found that avian influenza viruses are able to infect human trachea cells with much lower affinity, with multiple low affinity binding events.

The entry of Influenza A viruses into their host cells is mediated by endocytic compartments, which are pH dependent (Conner and Schmidt, 2005). The internalization of influenza virus cells is done by clathrin-coated pits (Matlin *et al.*, 1984). The ability of the influenza virus to enter the cells without clathrin-mediated endocytosis was also observed. This pathway of viral entry requires low pH and that the trafficking of late endosomes requires protein kinase C, Rab5, and Rab7 (Sieczkarski and Whittaker, 2002). Once the virus fully enters the cells, the clathrin coat is removed, and the vesicles fuse with endosomes with a pH-dependent mechanism by the activity of H^+ -ATPase (Stegmann *et al.*, 1987). The usage of acidotropic weak bases and carboxylic ionophores, which raise the pH of the endosomes, can block the uncoating of influenza virus (Matlin *et al.*, 1982).

After the virus has internalized (Fig. 1.10(a)), to release RNPs into the cell cytoplasm, RNPs have to cross both the membrane of the virion as well as the cellular endosomes. The fusion-mediated HA will accomplish this function by fusing the viral membrane with the cellular endosomal membrane (Fig. 1.10(b)) (Martin and Helenius, 1991). The fusion is triggered by the conformation change and cleavage of HA by

cellular proteases (Fig 1.10(c)). The ion channel activity of the M2 protein is also essential to the uncoating process as evidenced from the study using an M2 ion channel inhibitor, amantadine (Bukrinskaya *et al.*, 1982). The uncoating process is started by the forming of membrane-fusion stalk (Fig. 1.10(d)), and thinner structure of fusion diaphragm (Hemifusion diaphragm) (Fig. 1.10(e)) (Cross *et al.*, 2001). Once the particle is endocytosed, the low pH-activated ion channel activity of the M2 protein will let the protons flow from the endosome to the virion. This process will cause the RNPs to dissociate with the M1 protein, which allows the transport of RNPs into the cytoplasm (Fig. 1.10(f)) (Martin and Helenius, 1991). Early crystal structure for pre-fusion confirmation (Fig 1.10(c)) had been resolved as early as 1981 (Wilson *et al.*, 1981). Later, membrane fusion (Fig 1.10(d), Fig 1.10(e)) has also been confirmed with structural study by several groups, for example Bullough *et al.*, 1994, and post-fusion by Carr *et al.*, 1997 and Chen *et al.*, 1999. However, the molecular mechanism for release of the B loop from its metastable state is still unclear (Fig 1.10(b)), although some rearrangement of HA1 is apparently required (Godley *et al.*, 1992; Kemble *et al.*, 1992; Barbey-Martin *et al.*, 2002)



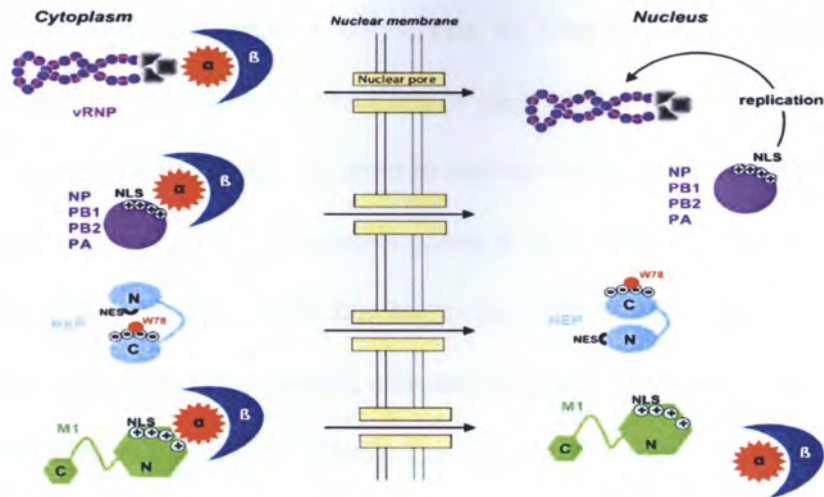
Taken from Cross *et al.*, 2001

Fig 1.10. Schematic diagram of the membrane fusion of hemagglutinin (HA) with the endosomal membrane.

1.3.2 Nuclear Import

The process of RNP transportation is nuclear protein-dependant and is critical for viral replication and transcription. The viral RNAs (vRNAs) are synthesized in the nucleus, and therefore the viral genome trafficking in and out of the nucleus is a critical step in order to achieve good viral replication (Cros and Palese, 2003). The NP protein coats the RNA. The remaining proteins are the three polymerase proteins (PB1, PB2, and PA), which bind to the partially complementary ends of the viral RNA. Polymerase proteins and nucleoprotein create a distinctive panhandle structure together with the viral RNA (Hsu *et al.*, 1987). These RNPs are approximately 10-20 nm wide (Compans *et al.*, 1972; Martin-Benito *et al.*, 2001). The width of RNPs is too large to allow passive diffusion for the entry of the RNPs into the nucleus. Therefore, they must rely on an active nuclear import mechanism, once they are released from the viral particle (Martin-Benito *et al.*, 2001). The polymerase proteins and NP protein possess NLSs, which mediate their interaction with the nuclear import machinery to assist their entry or export from the nucleus (Jones *et al.*, 1986; Wang *et al.*, 1997; Weber *et al.*, 1997; O'Neill *et al.*, 1995; Cros *et al.*, 2005).

After the dissociation with the M1 protein, the RNPs enter the nucleus through the nuclear pore (Fig. 1.11). Importin molecules comprise importin α and Importin β . Importin α proteins recognize the NLS on the cargo proteins (Weis *et al.*, 1995). Once the cargo is bound by importin α , the complex is recognized and bound by importin β that subsequently binds to the fibrils of the NPC and is responsible for the actual translocation (Bayliss *et al.*, 2000). It should be noted that the two viral proteins, the matrix protein (M1) and the nuclear export protein (NS2/NEP) are critical for assisting the nuclear export of RNPs. (Cros and Palese, 2003)



Adapted from Boulon *et al.*, 2007

Fig 1.11 Schematic diagram of the nuclear import of several influenza virus proteins and RNP. Importin α is marked by orange spiky circles, and Importin β is marked by blue crescent shape. Viral RNP protein components (PB2, PB1, PA and NP) are marked by violet circle with (+) symbol representing the NLS amino acids. The NS2/NEP protein is marked by two intertwined elliptical-shaped with N-terminal (N) and C terminal (C) with (-) and W78 together with NES signal. Note the structure before (Cytoplasm) and after (Nucleus) entry. M1 protein is marked with two intertwined elliptical-shaped with N-terminal (N) and C terminal (C) with (+) symbol representing the NLS amino acid.

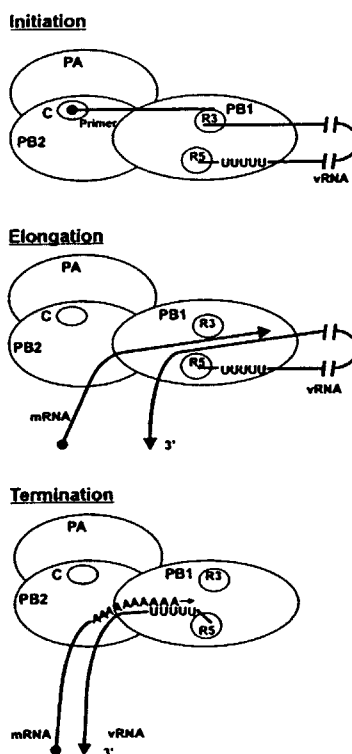
1.3.3 Transcription of Influenza virus mRNA

Influenza virus mRNA synthesis requires the host nuclear function. This can be demonstrated by the addition of α -amanitin, which inhibits the cellular DNA-dependent RNA polymerase II. The inhibition of the polymerase will halt viral mRNA transcription (Lamb and Choppin, 1976; Mahy *et al.*, 1972). The host nuclear protein polymerase will not initiate viral mRNA synthesis until a host-capped primer is supplied and used by the viral mRNA. This capped primer m^7GpppX^m - containing fragments is obtained from the cleavage of host cell RNA polymerase II transcripts. From the ultraviolet light-induced cross-linking studies, it was found that the PB2 protein in this complex recognizes and catalyzes the cap binding of the host capped mRNA (Blaas *et al.*, 1982; Braam *et al.*, 1983), and the PB1 protein initiates the elongation and maturation of the viral mRNA (Blaas *et al.*, 1982; Braam *et al.*, 1983).

Structure study of the influenza A polymerase by Obayashi *et al.* (2008) provides structural basis of the essential interactions of each polymerase protein to carry out their respective functions properly in order to undergo efficient transcription.

The activation of mRNA synthesis occurs in three steps (Fig. 1.12):

1. Initiation : host-capped mRNA binding to the PB2 protein, together with the 5'-vRNA binding to the PB1 protein, activates the binding activity of the PB1 to the 3' - vRNA. (Kawakami *et al.*, 1985). This process will cleave capped RNAs 10 to 13 nucleotides from their 5' ends, preferably at their purine residue (Plotch *et al.*, 1981; Hagen *et al.*, 1994). Nakagawa *et al.* (1996) discovered that PB1 and PA can transcribe mRNA without the presence of PB2. ;
2. Elongation : the availability of the cleaved host-capped mRNA by PB2 (Nakagawa *et al.*, 1995) is used as a primer for the initiation and transcription of the PB1 protein, until the polyadenylation are reached (Beaton and Krug, 1981; Shaw and Lamb, 1984);
3. Termination : since the PB1 protein binds both the 5'- and 3'- ends of the viral mRNA, the polyadenylation and termination of the vRNAs occurs before the 5' end is reached. The polyadenylation is formed due to the steric hindrance of the polymerase itself, resulting the stuttering production of the five to seven uracil residues (Emtage *et al.*, 1979; Robertson *et al.*, 1981; Luo *et al.*, 1991; Li and Palese *et al.*, 1994; Poon *et al.*, 1999; Zheng *et al.*, 1999)



Adapted from Lamb and Krug, 2001

Fig. 1.12 Schematic representation of the viral mRNA transcription. Three polymerase proteins (PA, PB1 and PB2). C in the PB2 denotes cap-snatching sites. R5 and R3 in PB1 denotes vRNA 5' and 3' binding region, respectively. (UUUUU) denotes poly-uracil sites at vRNA for mRNA polyadenylation (AAAAAAAAA) synthesis. The arrow in mRNA denotes direction of the transcription. The arrowhead in vRNA denotes 3' region.

Apart from the full length transcription of mRNA, M and NS segments of influenza A virus also undergo splicing mechanism to produce 2 mRNAs from each gene. M gene produces M1 and M2 mRNAs. NS gene produces NS1 and NS2 mRNAs. These genes have 5'- and 3'- splice sites recognized by cellular splicing machinery (Lamb and Lai, 1982; Lamb and Lai, 1984).

1.3.4 Replication of vRNA

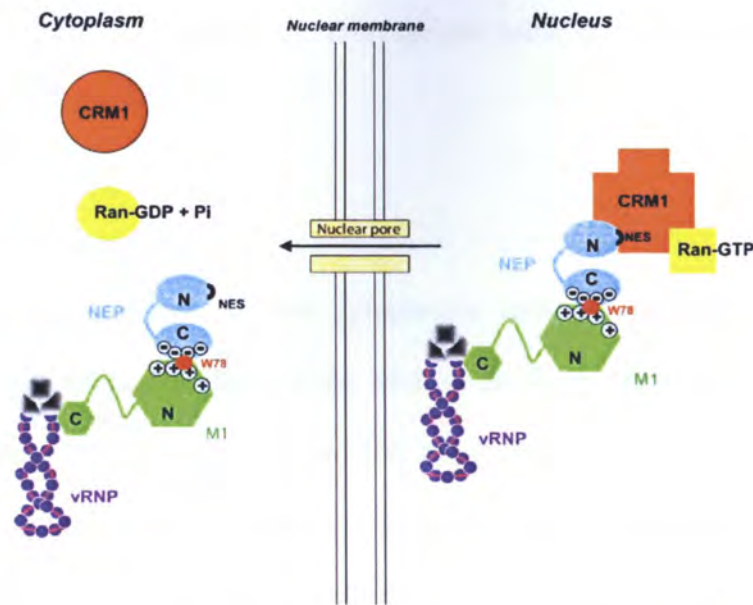
The switch from transcription to the replication of vRNA is currently not well understood. It has been postulated that the availability of free and soluble NP protein controls the switch (Beaton and Krug, 1986). The replication of vRNA occurs in two

steps : (1) the synthesis of template RNAs in full length or anti-genomic, and (2) the copying of the template RNAs into vRNAs. The switch from viral mRNAs to template RNAs requires the change from capped RNA-primed initiation to unprimed initiation. This different initiation strategy will prevent termination and polyadenylation at the poly(A) site, which is used during viral mRNA synthesis (Deng *et al.*, 2006).

The copying of the full-length template RNAs to vRNAs also requires the addition of the NP protein molecules to the elongating RNA molecules (Shapiro and Krug, 1988). No vRNAs are made in the absence of the NP protein, indicating that the elongation of vRNA chains will end as soon as the NP protein is no longer available. The newly synthesized vRNAs in complex with the NP are ready to be exported and packaged into the virus progeny (Shapiro and Krug, 1988).

1.3.5 Nuclear Export of Ribonucleoproteins

The vRNP nuclear export is initiated by forming a vRNP-M1-NS2 complex in the nucleus, with the nuclear export signal provided by NS2/NEP (O'Neill *et al.*, 1998). The nuclear export signal also will overcome the NLS sequence in the NP and polymerase protein (Gorlic and Mattaj, 1996). The NS2/NEP (NS2) interacts with the exportin molecule, a family of cellular proteins which mediate nuclear export of cellular rRNAs and mRNAs (Watanabe *et al.*, 1999). The exportin molecules will associate with RAN-GTP protein to mediate export of the vRNP-M1-NS2 from the nucleus into the cytoplasm (O'Neill *et al.*, 1998) through CRM1 mediated pathway (Elton *et al.*, 2001). The CRM1 – RAN-GTP – NS2/NEP – M1– vRNP protein complex formed from the interaction will allow the nuclear export to occur. After which the complex dissociates, followed by the dephosphorylation of RAN-GTP to RAN-GDP. (Elton *et al.*, 2001) (Fig. 1.13)



Adapted from Sebastien, 2006

Fig. 1.13 Schematic representation of the nuclear export of influenza protein and RNPs. CRM1 denotes host exportin-1 molecule which facilitates nuclear export with RAN-GTP as a cofactor. The conformational change of host factor CRM1 (orange), RAN-GTP \rightarrow GDP + Pi (yellow) mediates nuclear export. Note the binding of the viral NEP (cyan) at C terminal to N terminal of viral M1 protein (green).

1.3.6 Extracellular Transport of the Viral Integral Membrane Protein

The influenza virus HA, NA and M proteins are synthesized on the membrane bound ribosomes and are translocated across the membrane of the Endoplasmic Reticulum (ER) in a signal recognition particle (SRP)-dependent manner (Elder *et al.*, 1979; Hull *et al.*, 1988). there is a step-wise conformational maturation of the HA protein with independent folding of the specific domain in the HA monomer. The monomer will then trimerize and fold according to the neutral form of HA. Once correctly folded and assembled, HA proteins are transported out of the ER to the Golgi apparatus (Fig. 10). The oligosaccharide will be added to the HA during post-translational modification (Doms *et al.*, 1993). Further, three C-terminal proximal cysteine residues of HA and the M2 protein cytoplasmic tail will undergo palmitoylation (Holsinger *et al.*, 1995; Sugrue *et al.*, 1990; Veit *et al.*, 1991). If the

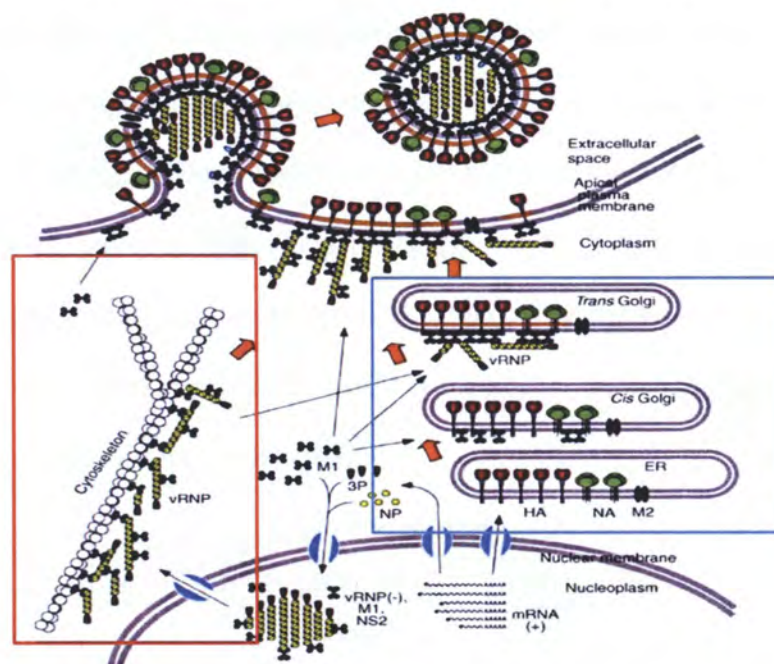
HA contains a furin cleavage site, the cleavage can occur in the Trans Golgi Network (TGN) (Stieneke-Grober *et al.*, 1992).

1.3.7 The Viral Assembly

The interaction between the cytoplasmic tails of the integral membrane proteins and the internal proteins of the virus is necessary for the formation of the budding particle. Eleven residues at the HA cytoplasmic tail and six residues in the NA cytoplasmic tail are highly conserved among HA and NA subtypes (Nobusawa *et al.*, 1991). When both cytoplasmic tails are absent, the virion will possess altered morphology (Jin *et al.*, 1997). The M1 and M2 proteins also assist viral assembly and budding especially in filamentous particle budding (Robert *et al.*, 1998). The amphipathic helix in M2 cytoplasmic tail is shown to be able to bind cellular cholesterol (Rossman *et al.*, 2010). Antibodies targeting the M2 ectodomain reduce the level of cell surface expression of M1 and M2, as well as the level of viral particle formation (Hughey *et al.* 1995). The schematic representation of budding process is shown in Fig. 1.14.

Packaging of an infectious influenza virus particle will require the incorporation of all eight segments of the viral genome. The EM analysis done by Noda *et al.* (2006) demonstrated that most of the influenza virus particles contain 8 gene segments, although it was previously postulated that packaging occurred in random way (Enami *et al.*, 1991). A more advanced EM technique done by two different groups, Harris *et al.* (2006), using cryoelectron tomography and Yamaguchi *et al.* (2008), using Zernike phase-contrast electron microscopy also confirmed the finding of Noda *et al.* (2006). It suggests that an organized packaging method might exist to correctly incorporate eight different segments into the virion, possibly either

by RNA interactions or protein-protein interactions. The glycoprotein HA, NA and M2 translocate into ER through Trans-Golgi networking, and bud through lipid raft microdomain (Takeda *et al.*, 2003 ; Leser and Lamb, 2005). The vRNP will interact with cytoskeleton to assist its movement to the budding virion at the apical plasma membrane. M1 is present under the lipid bilayer and interacts with other viral proteins to cause asymmetry in the lipid bilayer and facilitating membrane bending to initiate budding. (Ye *et al.*, 1999; Baudin *et al.*, 2001; Noton *et al.*, 2007)



Adapted from Nayak *et al.*, 2004

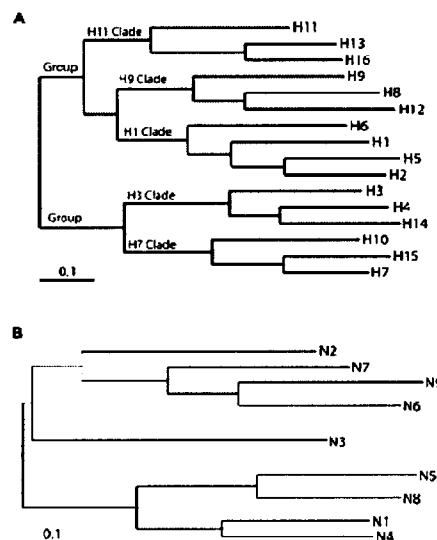
Fig 1.14 Schematic diagram of influenza virus budding. Note the migration of the surface glycoprotein HA and NA, the M2 protein through ER (**blue box**), migration of vRNP through cytoskeleton (**red box**), and M1 complex with all protein and segments before the release of viral progeny.

1.4 Nomenclature of Influenza Virus

The polymerase enzyme of the influenza virus, just as other RNA viruses, lacks the proofreading ability of RNA polymerase to correct mistakes in replication. This causes a high frequency of mutation, the accumulation of which causes a slight shift in the antigenic sites, called antigenic drift (Scholtissek, 1997). In addition, the

segmented nature of influenza virus also allows the reassortment of the gene elements to form new strains if the co-infection among different strains occurs, called antigenic shift (Scholtissek, 1997). Both antigenic drift and antigenic shift may alter the virus characteristics.

To take antigenic drift and antigenic shift into account, along with multiple-species infection capabilities, a standardized nomenclature is used to describe strains of the influenza virus that was developed by World Health Organization. The nomenclature used is based on the hemagglutinin and neuraminidase subtypes, the host origin, geographic origin, strain number and year of isolation (Davenport *et al.*, 1972). For example, A/Duck/Malaysia/62 (H5N2) denotes Influenza Virus with H5 and N2 subtype, collected from ducks in Malaysia in 1962. Currently, there are 16 and 9 NA subtypes identified. (Fouchier *et al.*, 2005). The method of the HA and NA subtype determination approved by WHO is the double immunodiffusion assays with hyperimmune animal sera (WHO, 1972).



Adapted from Fouchier *et al.*, 2001

Fig. 1.15 Phylogenetic tree of 16 HA (A) and 9 NA (B) subtypes of influenza virus (Fouchier *et al.*, 2001). DNA maximum-likelihood trees methods were employed to generate phylogenetic trees. The scale bars represent approximately 10% nucleotide changes between close relatives.

The phylogeny of the hemagglutinin and neuraminidase of influenza virus A has form distinctive clades (Fig. 1.15). The HA subtypes are further grouped into five clades, which are H11, H9, H1, H3 and H7. These clades suggest the origin and diversification of the influenza virus HAs and NAs. The phylogenetic trees also suggest that there are closer relatives among the HA groups compared to NA groups (Fouchier *et al.*, 2001).

1.5 Host Specificity and Pathogenicity of Influenza A Virus

Influenza A viruses infect a wide range of species, ranging from birds, sea mammals, horses, pigs and humans. A phylogenetic analysis done by Gorman *et al.* (1991) suggests that aquatic birds are the natural source (reservoir) of all influenza viruses. These viruses manage to perform interspecies transmission through the frequent mutation nature of the influenza virus (Gorman *et al.*, 1991). The molecular basis for host-range restriction and pathogenicity includes the viral glycoprotein, polymerase proteins, matrix protein and non structural protein, which allows interspecies transmission to other hosts, either through intermediate hosts or direct transmission, like the H5N1 virus case in Asia.

1.5.1 Viral Glycoprotein

Influenza virus glycoprotein consists of the HA protein which mediates binding to its specific host cell cellular receptor sialic acid, and also promotes the membrane fusion to release viral RNP to cytoplasm (Harrison, 2008). The NA protein of the virus removes the sialic acid to release the new progeny virus (Robert and Krug, 2001). The balanced work of both HA and NA protein is substantial for efficient virus-host recognition and release.

1.5.1.1 Hemagglutinin (HA)

The recognition of host cell by the HA protein is influenced by sialic acid moiety, which is N-acetylneuraminic acid (NeuAc) and N-glycolylneuramic (NeuGc) and the galactose linkage. The sialic acid linkage can be either by $\alpha 2,6$ (SA $\alpha 2,6$ Gal) linkage or $\alpha 2,3$ linkage (SA $\alpha 2,3$ Gal) (Rogers and Paulson, 1983). Human influenza viruses preferentially recognize sialyloligosaccharide containing SA $\alpha 2,6$ Gal, which is abundant in human tracheal epithelial cells (Couceiro *et al.*, 1993). Avian influenza viruses preferentially recognize SA $\alpha 2,3$ Gal which primarily exists in epithelial cells of the avian intestine (Rogers and Paulson, 1983). Swine trachea, contains epithelial cells with both SA $\alpha 2,3$ Gal and SA $\alpha 2,6$ Gal linkage, which explains its high susceptibility to both human and avian influenza viruses (Ito *et al.*, 1998). For this reason, it is a very high chance that swines can act as a reassortment vessel between the two viruses which can potentially generate pandemic strains (Kida *et al.*, 1994). Shinya *et al.* (2006) conducted study on the sialic acid population in human airway. They found that SA $\alpha 2,3$ Gal was found predominantly only in particular lung cells in lower respiratory tract, especially on non-ciliated cuboidal bronchiolar cells at the junction between the respiratory bronchiole and alveolus, whereas SA $\alpha 2,6$ Gal was found in upper respiratory tract. This explains the ability of the avian influenza virus to infect humans. The confinement of the avian influenza virus on the lower respiratory tract prevents the direct human to human transmission by coughing and sneezing.

As explained previously, the activity of HA also depends on the availability of the host cell proteases to cleave the precursor protein of HA into two activated subunits : HA1 and HA2 (Fig. 1.16). This cleavage is essential for fusion of the viral and endosomal membranes, and therefore influences viral infectivity (Klenk *et al.*, 1977). Low pathogenic avian influenza viruses possess a single Arginine residue at the

cleavage site, which is recognized by extracellular, trypsin-like proteases, such as plasmin, blood-clotting factor X like protease, clara cells, and miniplasmin (Wood *et al.*, 1993). These proteases are secreted by the respiratory and intestinal tract cells of avian cells, therefore the infection is limited to the tissues and organs (Steinhauer, 1999). Conversely, the highly pathogenic influenza virus strains have multiple basic amino acids at the cleavage site that are recognized by intracellular, subtilisin- and furin-like proteases secreted by most of the host cells, which enable the virus to infect multiple organs, causing systemic infection (Wood *et al.*, 1993). In addition, the presence of a carbohydrate side chain near the cleavage site may interfere with the accessibility of host proteases to the cleavage site (Garten and Klenk, 1999).

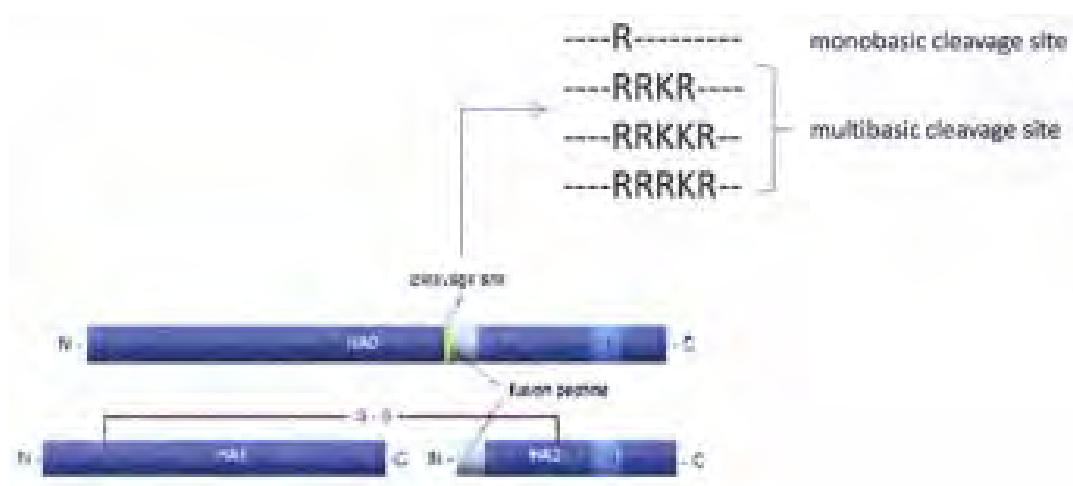


Fig. 1.16 The cleavage site of HA protein. HA0 denotes the HA protein precursor prior to the cleavage. The product is HA1 and HA2 linked by disulfide bonds (S-S). The monobasic and multibasic cleavage site is shown in arrow.

1.5.1.2 Neuraminidase (NA)

The efficient release of the virus progeny requires the removal of the sialic acid by NA (Bilsel *et al.*, 1993). The differences in activity of NA of the avian and human influenza viruses may be attributed to the length and sequence of the NA stalk. A

shorter stalk is less efficient in accessing its substrate (Castrucci and Kawaoka, 1993). However, shortened NA stalks in avian influenza are virulent in poultry including highly pathogenic H5N1, which is characterized by deletion of NA stalks (Zhou *et al.*, 2009). The short NA stalk also allows H5N1 to be able to replicate efficiently in human intestine cells due to its higher pH tolerance (Takahashi *et al.*, 2001). The important feature of the NA protein is also associated with the oseltamivir resistance mutation. The neuraminidase mutations in drug-resistant viruses are attributed to the amino acid residues of E119, R152, H274, and R292 in the N2 strain (Gubareva *et al.*, 2000; Zambon and Hayden, 2001; Kiso *et al.*, 2004).

1.5.2 Internal Proteins

The internal proteins, which include the RNA polymerase complex (PA, PB1 and PB2), nucleoprotein (NP), and matrix protein (M1 and M2) contribute to the host range specificity, such as the efficiency of the nuclear import, viral replication and nuclear export (Gabriel *et al.*, 2005; Gabriel *et al.*, 2007). However, the contribution of the individual proteins may vary based on the polymerase complex compatibility. For example, Gabriel *et al.* (2008) observed that the mutation of D701N in PB2 and N319K in NP caused the H7N7 virus to be efficiently replicated in mammalian cells, but not in avian cells.

1.5.3 Polymerase proteins

PB2 is the most essential polymerase for efficient viral replication, as it mediates the binding of two other polymerases (Obayashi *et al.*, 2008). Reverse genetic studies have shown that K627, which is commonly found in human isolates, determines high pathogenicity (Hatta *et al.*, 2001; Steel *et al.*, 2009; Gao *et al.*, 2009; Jadhao *et al.*, 2009). On the other hand, E627, which is commonly found in avian isolates, determines the low pathogenicity of avian isolates in humans (Hatta *et al.*,

2001). However, several highly pathogenic cases, such as H7N7 isolated from a patient with fatal pneumonia in Netherlands and H5N1 isolated from patients in Vietnam are characterized by 627K in PB2 (Fouchier *et al.*, 2004; Puthavathana *et al.*, 2005). Other experiments using reconstituted human and avian polymerase and NP proteins identified residue 627 of PB2 as the major determinant of replication efficiency in mammalian cells (Naffakh *et al.*, 2000; Labadie *et al.*, 2007).

In addition to PB2, the remaining polymerase proteins, PB1 and PA, and the NP may also contribute to host range restriction. Recently, de Wit *et al.* (2010) identified F666L in PA gene showed indication of increased pathogenicity in human cells as demonstrated by luciferase assay. Kawaoka *et al.* (2009) also found that mutating the PB2(D9N, A199S, R368K, E627K), PA(K142N or K142E, S421I) and NP(V33I, R100V or R100I, L283P, Q357K) of the H5N1 influenza virus caused increased pathogenicity in mice. Although the mechanism is not fully understood, it is hypothesized that the interaction of polymerase proteins and nucleoprotein with host-cell protein contributes to the increased efficiency of replication and pathogenicity.

1.5.4 Matrix protein

M segment encodes the M1 matrix and M2 ion channel proteins. In an experiment, Scholtisek *et al.* (2002) reassorted new viruses by infecting the cells with human influenza virus and avian influenza virus. The result demonstrates that the reassortment of the M gene from early human influenza virus cooperates efficiently with most new avian virus HAs.

Amantadine and rimantadine are drugs that targeted M2 protein (Pearce *et al.*, 1971). Amantadine blocked the M2 protein activity by inhibiting the ion channel activity directly, thereby halting the uncoating and M1-vRNP dissociation (Brown and Redfern, 1976; Skehel *et al.*, 1978). The mechanism of the inhibition is by binding to

the physically to occlude the channel, as demonstrated by NMR (Cady and Hong, 2008; Cady *et al.*, 2010), and X-ray crystallography (Stouffer *et al.*, 2008)

1.5.5 Non-structural 1 (NS1) protein

Non-structural proteins are proteins which do not exist inside the virion, but expressed when the virus replicates with the aim of enhancing infection (Petri *et al.*, 1982). NS1 protein, encoded by segment 8, plays a central role of counteracting the cellular interferon response by:

1. Binding to dsRNA to inhibit the activation of Protein Kinase R (PKR);
2. Preventing activation of transcription factors such as ATF-2/c-Jun, NFkB and IRF-3, IRF-5 and IRF-7 (Kochs *et al.*, 2007).

The highly pathogenic 1918 Spanish Flu NS gene has been shown to block the expression of IFN regulated genes in human cells more efficiently than the NS genes from H1N1/A/PR/8/34 (Geiss *et al.*, 2002). This shows that the more pathogenic strains can exhibit stronger inhibitory actions in counteracting the host immune response. Influenza virus with NS1 from highly pathogenic strain of 1997 H5N1 can also exhibit resistance to IFN and TNF- α , while the growth of the parental strain was blocked by its induction (Seo *et al.*, 2002).

1.6 Virus-Host Interaction

Table 1.3. List of currently known influenza virus – host interaction

Viral protein	Interacting partner	Function	References
HA	Sialic acid on the cell surface	Receptor recognition	Skehel and Wiley, 2000
		Endocytosis initiation and mediation	Matlin <i>et al.</i> , 1981; Patterson <i>et al.</i> , 1979; Sieczkarski and Whittaker, 2002a
		Membrane fusion	Skehel and Wiley, 2000 Cross <i>et al.</i> , 2001
NA	Sialic acid on the cell surface bound on HA of progeny virus	Progeny viral release	Wagner <i>et al.</i> , 2002
PB2	Hsp90	Stimulatory factor for efficient transcription and replication	Momose <i>et al.</i> , 2002;
PA	hCLE	Regulating the replication activity of the polymerase (putative)	Huarte <i>et al.</i> , 2001; Perez-Gonzalez <i>et al.</i> , 2006
	Hypophosphorylated RNA Pol II large subunit	Enhance viral transcription by the degradation of the hypophosphorylated RNA Pol II large subunit	Rodriguez <i>et al.</i> , 2007
	Minichromosome Maintenance (MCM) complex	Stimulating virus genome replication	Kawaguchi <i>et al.</i> , 2007
PB1	Ebp1	Selective inhibitor of viral polymerase	Honda, A. <i>et al.</i> , 2007
Polymerase complex	Hsp90 (with PB1 alone and PB1-PB2)	Assembly and nuclear transport of polymerase subunits	Naito <i>et al.</i> , 2007
	RanBP5 (with PB1 and PB1-PA) (Importin β)	Imports RNA polymerase complex to the nucleus	Deng <i>et al.</i> , 2006
NP	Nucleoprotein Interactor – 1 (NPI-1) and Nucleoprotein Interactor – 3 (NPI-3)	Facilitates the nuclear imports along with viral vRNA	O'Neill <i>et al.</i> , 1995
	RAF-2p48, NPI-5, BAT1, UAP56	Facilitates the formation of NP-RNA complexes	Momose <i>et al.</i> , 2001
	CRM1 (with M1)	Nuclear transport	Elton <i>et al.</i> , 2001
	Nucleosomes (together with vRNP, M1)	Facilitates host pre-mRNAs cap-snatching	Garcia-Robles <i>et al.</i> , 2005)
M1	Cytoskeletal elements	Viral morphogenesis	Avalos <i>et al.</i> , 1997
M2	Caveolin-1	Virus release (via lipid rafts)	Sun <i>et al.</i> , 2010
	Hsp40	Inhibits PKR signalling pathway	Guan <i>et al.</i> , 2010
NS1	CPSF	Inhibits 3' end cleavage and polyadenylation of host pre-mRNA	Nemeroff <i>et al.</i> , 1998
	Poly-A Binding Protein (PABII)	Inhibits polyA tail synthesis	Chen <i>et al.</i> , 1999
	hStaufen	Assists viral mRNA localisation for efficient translation (putative)	Falcon <i>et al.</i> , 1999
	p85 β	Stimulates PI3K signalling	Hale <i>et al.</i> , 2008
	PKR	Blocks PKR - dependent immunity pathway	Li <i>et al.</i> , 2006
NS2	Nucleoporins	Mediates exports of viral RNAs	O'Neill <i>et al.</i> , 1998

When a virus infects a host cell, numerous signalling cascades are initiated as host cell responds to the infection. This response creates interaction among viral and

host proteins, and therefore alters the transcriptional machinery. This change of gene expression can be either in favour of the viral replication as a host defence against viral invasion. To enhance infectivity and replication, viruses have evolved several strategies, such as evasion and inactivation of immunological pathways, and shutdown of host cellular transcription machinery. The difference in interactions among viruses will give more insights on how the virus operates, and from it, novel vaccines and antiviral strategies can be developed. A partial list of the currently known influenza virus protein – host cell protein interacting partners can be seen in Table 1.3.

Studying the interaction between virus and host-cell could pose several challenges. Animal models are generally considered good models for its close resemblance to anatomical and physiological environment, which will be useful to study species adaptation mechanism, and interspecies transmission. However, these models are difficult to control over experimental variables, methods, adaptation and homogeneity. Using tissue culture models to replace animal models will gain advantages for more detailed understandings of the mechanism as compared to the animal models. Besides that, the tissue culture models allow the infection of a variety of cell lines with very high percentage of cells being infected. The high rate of infection will greatly facilitate the ability to measure the changes of gene expression patterns more accurately.

The genome wide analysis technology, such as DNA microarrays is able to analyze the pathogen-host interaction, which allows us to elucidate the global host response by investigating changes of thousand of genes simultaneously. This method is particularly useful for monitoring influenza virus evolved mechanisms of interacting with host-cells, such as evading interferon response, the blocking of mRNA translation. With this technology, it is also interesting to determine viral and cellular

factors responsible for the increased virulence of the HPAI and pandemic strains (Korth *et al.*, 2006).

Among the first use of the technology mentioned above was to monitor gene expression changes HeLa cells infected with influenza virus. The cells were mock infected or infected with either active or heat inactivated human A/WSN/33 (H1N1) influenza virus. The aim of the experiment was to determine distinct subsets of genes whose regulation is replication dependent or independent events during influenza infection, using cDNA microarrays with dual-labelling technique. Further, they found that the replication dependent genes could be classified into five major categories: protein synthesis, cytokine and growth factor signalling, transcription factors and DNA binding proteins, processing and export of mRNA, and the ubiquitin pathway. The replication independent genes were grouped into five categories as well, which are metallothioneins, cell cycle related, transcriptional regulators, ubiquitin pathways and cellular kinases (Geiss *et al.*, 2001).

Further studies using cell culture method using cDNA microarray were aimed to study the NS1 protein, which plays a role in subverting the host response to the virus. In this study, to better understand the effect of NS1 on virus-host interactions, human lung epithelial cell line, A549, was infected with A/PR/8/34 (H1N1), A/PR/8/34 with deleted NS1 and A/PR/8/34 with NS1 contained a deletion in the C-terminus. Numerous genes were preferentially upregulated in response to infection with the mutant viruses compared to parental strain with NS1 present. Many of which were related to the antiviral and interferon responses. This data clearly suggests the role of NS1 of A/PR/8/34 as an antagonist to the interferon response to the virus (Geiss *et al.*, 2002).

This study was also used to examine the role of the specific genes from the pandemic 1918 strain. In this study, A549 cells were infected the viruses from 1918 strain, A/WSN/33 and a recombinant in which the NS1 of A/WSN/33 was replaced with the NS1 of the pandemic 1918 virus. There was greater suppression of interferon stimulated genes in the cells infected with 1918 NS1 recombinant virus than in cells infected with A/WSN/33. This suggests that the NS1 of the 1918 virus is more capable of suppressing interferon responses.

The study of influenza – host interaction using the animal models by means of high throughput genomic technology is also necessary to be used to complement the data from the study using the cell cultured models. This is mainly due to the ability of animal models to correlate genes expression with clinical data, finding key mechanisms in viral clearance, tissue pathology and the response of the infected cells. One of such study was the investigation of the virulence of engineered virus from 1918 strains by using the non-human primate models for their close resemblance and high nucleotide sequence homology with humans. With this advantage, several studies has been done, such as the study of the infection of pigtailed macaques (*Macaca nemestrina*) with A/Texas/36/91 (Baskin *et al.*, 2004), pathogenesis of 1918 virus using cynomolgus macaques (*Macaca fascicularis*), the effect of influenza infection on the early innate immune response in the lung of pigtailed macaques (Kobasa *et al.*, 2007).

Although mice are not a natural host for influenza A virus. But many influenza A strains are adapted to be able to infect mice, and hence can be used as a model host, although some alterations in amino acid sequence occur. There are several studies that indicate HA protein is critical in mouse adaptation, for example N137D and T89A in H1 subtype, and T167L and N246S in H3 subtype (Gitelman *et al.*, 1984; Gitelman *et*

al., 1986; Kaverin *et al.*, 1989; Brown, 1990; Brown and Smeenk, 1994). Kosh *et al.* (2006) utilized mouse as a host model infected with 1918 influenza virus for genomic analysis. They found that mice infected with the reconstructed 1918 influenza virus showed an increased and accelerated activation of host immune response and cell death related genes associated with severe pulmonary pathology.

1.6.1 Cytokine Response on Influenza Virus Infection

Influenza A virus-infected epithelial cells have the ability to respond to the infection by upregulating proinflammatory, chemotactic (chemokines), and other immunoregulatory cytokines. To date, more than 100 proteins of cytokine family are identified (Feldmann, 2008). Representative list of the most common cytokine found in viral infection can be seen in Table 1.4. The chemokines are usually produced constitutively or in response bacterial and/or viral infections. Chemokines attach to the specific cell surface receptors, which lead to a differentiation of immune related cells such as B cells, T cells, NK cells and dendritic cells, and migration to the site of inflammation (Zlotnik and Yoshie, 2000). Influenza A virus-infected macrophages typically secrete numerous cytokines such as RANTES, MCP-1, MCP-3, MIP-1 α , MIP-1 β , MIP-3 α and IP-10, and low amount of IL-8 (Sprenger *et al.*, 1996; Matikainen *et al.*, 2000). Whereas influenza A virus-infected epithelial cells produce RANTES, MCP-1 and IL-8 in response to influenza A virus infection (Matsukura *et al.*, 1996; Adachi *et al.*, 1997). CCL5/RANTES is a chemokine produced upon influenza virus infection, which then recruits leucocytes to the infected sites, and enhance the production of Natural Killer (NK) cells and T cell IFN- γ production and the development of Th1-type immune response (Matsukura *et al.*, 1996; Adachi *et al.*, 1997).

Table 1.4 List of cytokines, producing cells, target cells and their function, as summarized by Decker (2006)

Cytokine	Producing Cell	Target Cell	Function
GM-CSF	Th cells	progenitor cells	growth and differentiation of monocytes and DC
IL-1 α IL-1 β	monocytes macrophages B cells DC	Th cells B cells NK cells various	co-stimulation maturation and proliferation activation inflammation, acute phase response, fever
IL-2	Th1 cells	activated T and B cells, NK cells	growth, proliferation, activation
IL-3	Th cells NK cells	stem cells mast cells	growth and differentiation growth and histamine release
IL-4	Th2 cells	activated B cells macrophages T cells	proliferation and differentiation IgG ₁ and IgE synthesis MHC Class II Proliferation
IL-5	Th2 cells	activated B cells	proliferation and differentiation IgA synthesis
IL-6	monocytes macrophages Th2 cells stromal cells	activated B cells plasma cells stem cells tissue	differentiation into plasma cells antibody secretion Differentiation acute phase response
IL-7	marrow stroma thymus stroma	stem cells	differentiation into progenitor B and T cells
IL-8	macrophages endothelial cells	neutrophils	Chemotaxis
IL-10	Th2 cells	macrophages B cells	inhibit cytokine production Activation
IL-12	macrophages B cells	activated Tc cells NK cells	differentiation into CTL (with IL-2) Activation
IFN- α	leukocytes	tissue	inhibit viral replication MHC I expression
IFN- β	fibroblasts	tissue	inhibit viral replication MHC I expression
IFN- γ	Th1 cells, Tc cells, NK cells	tissue macrophages activated B cells Th2 cells macrophages	inhibit viral replication MHC expression Ig class switch to IgG _{2a} Proliferation pathogen elimination
MIP-1 α	macrophages	monocytes, T cells	Chemotaxis
MIP-1 β	lymphocytes	monocytes, T cells	Chemotaxis
TGF- β	T cells, monocytes	monocytes, macrophages activated macrophages activated B cells tissue	Chemotaxis IL-1 synthesis IgA synthesis inhibit proliferation
TNF α	macrophages, mast cells, NK cells	macrophages tumour cells	CAM and cytokine expression cell death
TNF- β	Th1 and Tc cells	phagocytes tumour cells	phagocytosis, production cell death

Interferon alpha and beta (IFN- α and IFN- β) are the important cytokines produced to fight against influenza A virus infection (Ronni *et al.*, 1997). Epithelial cells and macrophage have different ability to fight against influenza A infection, for example, human lung epithelial cell lines show poor expression of IFN- α/β and

proinflammatory cytokines (IL-1, IL-6, TNF- α) during influenza A virus infection (Ronni *et al.*, 1995). However, influenza A virus-infected monocytes / macrophages efficiently produce large quantities of IFN- α/β , IL-1 β , IL-6 and TNF- α (Ronni *et al.*, 1995; Ronni *et al.*, 1997; Nain *et al.*, 1990 ; Gong *et al.*, 1991; Bender *et al.* 1993, Pirhonen *et al.*, 1999). Influenza virus infection has been found to activate numerous transcription factors involving the expression of cytokine and chemokine gene, for example, Nuclear factor kappa B (NF- κ B), activating protein (AP)-1, interferon regulatory factors (IRFs), signal transducers and activators of transcription (STATs) and nuclear factor-IL-6 (NF-IL-6 or C/EBP β) (Fig. 1.17). These proteins will translocate into the nucleus to initiate transcription of immune response related genes (Matikanen *et al.*, 2000; Ronni *et al.*, 1997; Choi *et al.*, 1996; Hofmann *et al.*, 1995; Pahl *et al.*, 1997; Flory *et al.*, 2000).

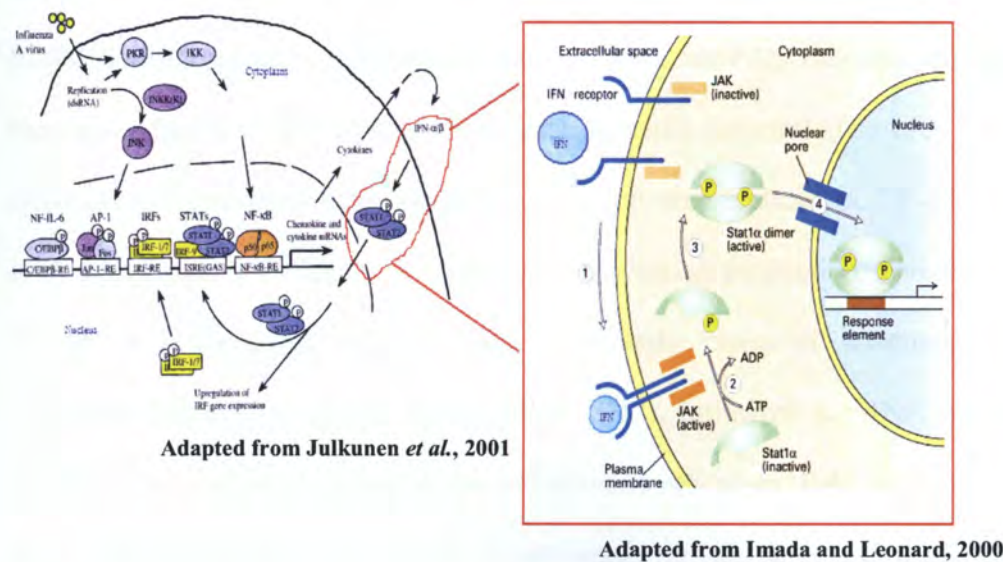


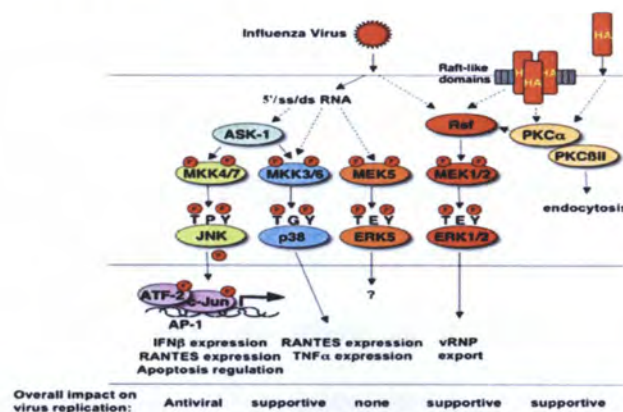
Fig. 1.17 Immunological pathway signalling by Influenza A virus. The viral dsRNA from replication activates several cytokine genes precursor, such as Protein Kinase R (PKR), IKK, and Janus Kinase (JNK). Leading to transcription of chemokine and cytokine genes. This leads to production of IFN- α/β (left). The activation of Jak-STAT pathway is indicated in inset (right). The binding of the IFN to the receptors activates the JAK (1). The JAK phosphorylates the Stat protein to activate it (2). The activated Stats dimerize (3) to be translocated to nucleus to initiate transcription (4).

The Jak-Stat pathway (Fig. 1.17) demonstrates the activation of STATs protein by Jak proteins. Jak proteins are activated by interferons and interleukins. After the binding into the receptors, the Jak proteins phosphorylate the STAT1 proteins (pSTAT1), turning them into activated form. pSTAT1 proteins dimerize and translocate to the nucleus (Imada and Leonard, 2000).

Mitogen-activated protein (MAP) kinases are also critical in regulating cytokines. Influenza A virus infection has been shown to upregulate MAP kinases such as the extracellular signal-regulated kinase (ERK), p38 MAP kinase, and c-Jun-NH₂-terminal kinase (JNK) (Fig. 1.18) (Kujime *et al.*, 2000). During influenza virus infection, p38, JNK and ERK5 MAPK cascades are primarily activated by viral dsRNA. The Raf/MEK/ERK signalling cascade is activated at early and late time of infection. Early activation is initiated by binding of the virus to the cell surface, and late activation is mediated by assembly of the HA to the lipid raft domains. While the Raf/MEK/ERK cascade, the p38 pathway and different PKC isoforms exhibit virus-supportive functions, the JNK pathway acts primarily antiviral. The ERK5 pathway, although activated upon infection has no effect on viral replication. NF- κ B activation is also important in influenza A virus-induced cytokine production. The activation of NF- κ B in Influenza A virus can occur in early phase of infection and viral replication/transcription phase (Ronni *et al.*, 1997). Influenza A vRNA can activate NF- κ B due to a stress response in the endoplasmic reticulum (Pahl *et al.*, 1997; Flory *et al.*, 2000). Protein Kinase R(PKR) is previously thought to be activated by double-stranded RNA of the virus and involved in the activation of IFN- α/β and NF- κ B (Kumar *et al.*, 1994), and PKR/IKK-mediated NF- κ B activation takes place also in influenza A virus infection (Kujime *et al.*, 2000), although influenza A virus infection can activate a cellular inhibitor of PKR, p58IPK, as well (Lee *et al.*, 1994). However,

Pichlmail *et al.* (2006) and Rehwinkel *et al.* (2010) found that IFN- α/β is not induced by PKR binding with dsRNA, but by MDA5/RIG-I binding with 5'-phosphorylated RNA. Similarly, Ludwig *et al.* (2010) suggests that the PKR does not act by inducing IFN- α/β gene transcription, but rather by maintaining the integrity of IFN- α/β mRNA to allow its translation.

In viral infection, IRF-1 was suggested to be an important virus-induced and virus-activated transcription factor that controls the expression of IFN- α/β and IFN-inducible genes (Harada *et al.*, 1989). Presently, the IRF family constitutes nine members, numbered from IRF-1 to IRF-9. From these, IRF-1, IRF-3 and IRF-7 have been shown to be expressed upon IFN- α/β or IFN-related gene expression (Mamane *et al.*, 1999). IRF-3 activation is followed by the translocation to nucleus and the activation of IFN- α/β genes (Yoneyama *et al.*, 1998; Weaver *et al.*, 1998; Schafer *et al.*, 1998). IRF-7, which is under the regulation of IFN- α/β , also regulates the expression of many interferon regulatory genes upon response to infection (Sato *et al.*, 1998; Marie *et al.*, 1998; Wathelet *et al.*, 1998).



Adapted from Ludwig, 2007

Fig. 1. 18 Schematic representation of influenza A virus inducing MAP kinase pathways. Upon the attachment of influenza virus hemagglutinin and/or the detection of viral RNA, several MAP kinase pathways are activated, such as Janus Tyrosine Kinase (JNK), p38, and Extracellular-signal-Regulated Kinases (ERKs). All of the MAP kinases are activated by dual phosphorylation (red P circle) at threonine (T) and tyrosine (Y). The function of each MAP kinases member families is shown by arrow above with the resulting effect of the activation of the MAP kinases.

Besides cytokine and chemokines, the viral infection also induces several antiviral genes closely associated to cytokine and chemokines activation. The most well known antiviral genes associated with influenza virus infection are myxovirus resistance genes (Mx), 2' – 5' oligoadenylate synthase (OAS), RNase L and Viperin (RSAD2). These genes will be discussed in the next section.

1.6.1.1 Myxovirus Resistant (Mx) protein

As discussed previously, the interferon can assist to obstruct the propagation of virus in the potential target cells by enhancing immune responses (Stetson and Madzhitov, 2006). Mx gene is one of antiviral gene induced by the interferons. It has shown antiviral activity against influenza A viruses (Haller *et al.*, 1998). Mx proteins are classified into the dynamin superfamily of large GTPases and are expressed in many species, mainly vertebrates, for examples mouse (Horisberger *et al.*, 1988), chicken (Seyama *et al.*, 2006) and pigs (Palm *et al.*, 2007).

The murine Mx1 protein accumulates in the nucleus and inhibits primary transcription and replication of influenza A virus (Krug *et al.*, 1985; Pavlovic *et al.*, 1992), with the exception of Balb/c mice which contain a deletion in Mx1 gene in the chromosome (Jin *et al.*, 1998). This indicates that the Mx1 targets vRNP. Several studies has shown high inhibitory effect of influenza A virus replication by Mx1 has been observed in tissue cultures (Staeheli *et al.*, 1986) and *in vivo* using mouse model that possess the Mx1 resistance gene (Haller *et al.*, 1987; Salomon *et al.*, 2007; Tumpey *et al.*, 2007). The human MxA protein also exhibits similar effects to murine Mx1 protein (Pavlovic *et al.*, 1992). However, human MxA protein and murine Mx1 protein have different mechanism. Human MxA protein inhibits steps involved in viral replication and transcription, which develop in the later phase of viral replication.

Murine Mx1 inhibits in the early viral transcription steps (Pavlovic *et al.*, 1992). In spite of the difference in mechanism of Mx in different species, it shows that the Mx proteins of the two species act in a comparable way by recognizing the same or similar viral target structures. Dittmann *et al.* (2008) demonstrated that different strains of influenza virus might have different degree of sensitivity against the Mx protein.

1.6.1.2 2' – 5' Oligoadenylate Synthase (OAS) and RNase L

The 2',5'-oligoadenylate synthetase (OAS)/RNase L system is an innate immunity pathway that responds to a pathogen-associated molecular pattern (PAMP). IFN signalling induces transcription of the OAS genes through IFN-stimulated response elements in the promoters (Rutherford *et al.*, 1988). Further, the degradation of viral and cellular RNAs is initiated upon the binding of nuclear factors induced by the interferon (Rutherford *et al.*, 1988). Later, RNase L will recognize this pattern, which results in viral RNA degradation and termination of viral infections (Hovanessian and Justesen, 2007). In humans, OAS family consists of 10 isoforms, but with three genes known to play role in antiviral activity (OAS1 to OAS3) and a single OASL gene encoding a related protein with two C-terminal ubiquitin-like domains that does not synthesize 2'-5' A (Justesen *et al.*, 2000; Mashimo *et al.*, 2003). In mice, there are eight *oas1* genes, in addition to *oas2*, *oas3*, and two *oasl* genes (Kakuta *et al.*, 2004). However, Balb/c mice do not express all of *oas1* gene isoforms (Kakuta *et al.*, 2004). Characteristics wise, all isoforms of OAS exist in different protein conformation and oligomers state. OAS1 isoforms (p40/p46) have one catalytic domain and tetramerize, OAS2 isoforms (p69/p71) have two catalytic domains and form dimers in native state, while OAS3 (p100) has three catalytic domains and is a monomer (Hovnanian *et al.*, 1998; Rebouillat *et al.*, 1999).

Human RNase L is 741 amino acids in length. it possesses nine ankyrin repeats, several protein kinase-like motifs, and the RNase domain. 2' - 5' A binds to ankyrin repeats 2 and 4 (Tanaka *et al.*, 2004) causing catalytically inactive RNase L monomers to form activated dimers with potent RNase activity (Cole *et al.*, 1996; Dong and Silverman, 1995). Specifically, RNase L cleaves within single-stranded regions of RNA, principally on the 3' sides of UpAp and UpUp dinucleotides, leaving 3'-phosphoryl and 5'-hydroxyl groups at the termini of the RNA cleavage products (Wreschner *et al.*, 1981). Therefore, 2' -5' A is an “alarm signal” that signals antiviral innate immunity through RNase L activation.

1.6.1.3 Viperin (RSAD2)

Viperin is a protein inducible by both type I and type II IFNs (Chin and Cresswell, 2001). It has been identified in various organisms, mostly vertebrates, such as fishes (Boudinot *et al.*, 2000; Sun and Nie, 2004), rodents (Grewal *et al.*, 2000), and several primates (Chin and Cresswell, 2001; Zhu *et al.*, 1997). It has also been shown in various studies that virus infections induce viperin expression (Boudinot *et al.*, 2000; Chin and Cresswell, 2001; Helbig *et al.*, 2005; Zhu *et al.*, 1997), suggesting its role in antiviral response.

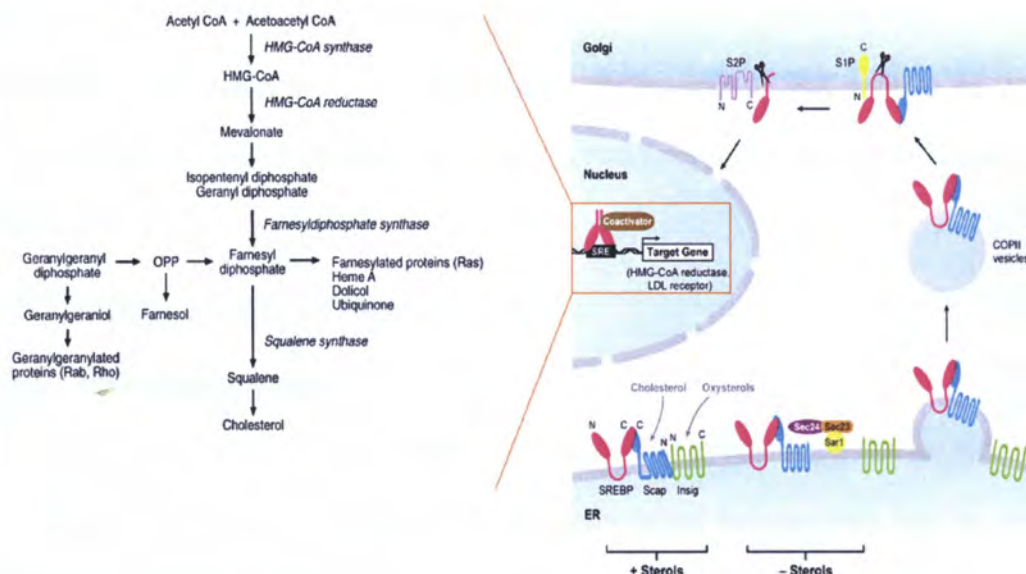
An extensive study done by Wang *et al.* (2007) showed that viperin possesses one of the key role in host defence against influenza virus infection. Viperin inhibits the release of the viral particles from the plasma membrane by disrupting lipid rafts. It has been shown as well that raft microdomain is associated with virus HA (Schmitt and Lamb 2005). Further, Wang *et al.* (2007) also conducted yeast two hybrid screening to determine viperin interacting partner. They found that farnesyl diphosphate synthase, as a viperin-interacting protein, catalyzes formation of farnesyl

diphosphate (FPP). FPP is a precursor of many essential metabolites, such as sterols, dolichols, carotenoids and ubiquinones (Szkopinska and Plochocka, 2005). FPPS is also one of the crucial enzymes involved in cholesterol metabolism pathway (Fig. 1.19). They also found that the viperin interacted in antagonistic way to FPPS, where an overexpression of one causes decrease in the other. It was also shown that the downregulation of FPPS inhibited viral release.

1.6.2 Cholesterol Metabolism

Cholesterol is a sterol compound found in cell membranes of all animals, and blood in mammals. Cholesterol is required for cell membrane integrity (Ikonen, 2008). Cellular membranes in most eukaryotes contain varying amount of cholesterol depending on the cell types, which are controlled by lipid transport in both vesicular and protein-bound pathways (Ikonen, 2008). Schematic representation of cholesterol metabolism pathway is shown in Fig 1.19. Cholesterol synthesis is initiated from acetyl CoA molecule, and processed through multiple form of intermediates. An important enzyme for irreversible cholesterol synthesis is catalyzed by 3-hydroxyl-3-methylglutaryl Co-Enzyme A Reductase (HMGCR), and the transcription of which is regulated by sterol regulatory element binding protein (SREBP) which resides in ER (Brown and Goldstein, 1997). This protein is essential in cellular lipid homeostasis. When cells are low on cholesterol, transcription of genes required for the synthesis and uptake of cholesterol, such as HMG-CoA Reductase and LDL receptor, is upregulated through the action of SREBP. When the cells are abundant on cholesterol, SREBP will be inactivated by the binding of cholesterol to the SREBP-Scap complex, which will halt the transport of SREBP into the nucleus and therefore, the cholesterol synthesis is halted, reducing cholesterol levels to normal (Goldstein *et al.*, 2006). Cellular

cholesterol levels are controlled not only by cholesterol, but also by oxysterols. Oxysterols are intermediates in bile acid synthesis and function in elimination of excess sterol from tissues. Oxysterols are present at low concentrations in cells relative to cholesterol and play an important role in the regulation of systemic cholesterol homeostasis of mammalian cells (Beaven and Tontonoz, 2006). Oxysterols, such as 25-hydroxycholesterol (25-HC), have long been recognized as potent inhibitors of sterol synthesis, which are catalyzed by 25-hydroxycholesterol hydroxylase (Chang and Limanek, 1980).



Adapted from Ikonen *et al.*, 2008

Fig 1.19 Schematic Diagram of Cholesterol Metabolism (left), activated by SREBP-Scap molecule in the low sterol condition (- Sterols) and excess sterol condition (+ Sterols). The SREBP-Scap complex will travel through Golgi in COPII vesicle, which then transported to the nucleus to bind the SRE.

Many of the cellular cholesterol research are done by manipulating cholesterol level. The methods used are the statin drugs, which inhibit the HMGCR, thus blocking the cholesterol synthesis (Frishman and Rapier, 1989; Alberts, 1990), cyclodextrins to remove intracellular cholesterol (Favier *et al.*, 1995; Francis *et al.*, 1999; Shogomori

and Futerman, 2001), cholesterol complexed with cyclodextrin to increase intracellular cholesterol (Tomeczkowski *et al.*, 1993).

Cholesterol have been implicated for its importance in viral infection, for example virus internalization in HIV-1 virus (Liao *et al.*, 2001; Liao *et al.*, 2003), Viral entry in Hepatitis B virus (Kremer *et al.*, 2009), Replication in Dengue virus (Rothwell *et al.*, 2009; Puerta-Guardo *et al.*, 2010), infection and budding of Semliki Forest Virus (Kielian and Helenius, 1984; Chatterjee *et al.*, 2000; Chatterjee *et al.*, 2002), budding in respiratory syncytial virus (Yeo *et al.*, 2009). In Influenza A virus infection, several critical function of cholesterol have been documented, such as to assist entry and fusion (Nussbaum *et al.*, 1992; Keller and Simons, 1998; Sun and Whittaker, 2003; Biswas *et al.*, 2008), and maturation of M2 protein to assist membrane localization (Schroeder *et al.*, 2005) and viral particle release (Barman and Nayak, 2007).

1.7 Influenza Virus in Different Hosts

1.7.1 Influenza in Human

According to Centre for Disease Control (CDC) terminology, human influenza A viruses refer to those subtypes that generally infect humans and can be found widespread throughout the world (CDC, 2007). The most known subtypes of influenza A viruses with common pattern of circulation among humans are H1N1, H3N2 and H1N2, which termed “currently” circulating influenza virus (CDC, 2007). CDC also sets a rule, where any case of human infection with a novel influenza A virus that is different from currently circulating human influenza H1 and H3, such as H5 strain classified as a “recently” circulating virus with the confirmation process from CDC laboratory (CDC, 2010). Due to antigenic drift and antigenic shift, the current circulating human influenza virus will be different antigenically from those circulating

in the past year. This type of influenza is commonly referred as seasonal influenza, or “seasonal flu”, “common flu” or “annual flu” (CDC, 2007). It generally causes annual influenza epidemics that are mostly not lethal to humans except to the elderly (>65 years old) or young (<5 years old) (CDC, 2007). The seasonal influenza is a recurring time period characterized by the prevalence of outbreaks of influenza in a specific region. This occurs during the winter period in both northern and southern hemispheres (CDC, 2007). With genetic analysis, seasonal influenza activity can sometimes be predicted according to geographic regions (NIAID, 2009). The beginning of the seasonal influenza emergence may vary by location. The disease will take approximately 3 weeks to reach the peak, followed by another 3 weeks to diminish (NIAID, 2009).

Currently, there are two HA subtypes (H1 and H3) and two NA subtypes (N1 and N2) that are circulating and transmit efficiently among humans (CDC, 2009). This will increase the possibility for genetic reassortment between the two viruses. The human seasonal influenza prevalence of different subtypes may vary between different seasons. For example, the H3N2 strain has been the predominant influenza A strain worldwide for the last two decades, with the exception of the 1988–1989 and 2000–2001 seasons where H1N1 infections mostly dominated (Lin *et al.*, 2004). A new reassorted human strain from two dominant human influenza virus H1N1 and H3N2 to form H1N2, had emerged in Europe continent and became dominant in the September–November 2001 in the Northern hemisphere (Ellis *et al.*, 2004; Paget *et al.*, 2002).

1.7.1.1 Human Influenza Virus H1N2

The H1N1 influenza virus subtype continued to reoccur and cause disease primarily in children and young adults together with H3N2 subtype (Cox and

Subbarao, 2000). Due to genetic reassorting of influenza virus, these 2 subtypes of human influenza A viruses have a potential to form a new strain of influenza virus. This generally occurs when mixed infection takes place in an individual with both viruses. Initially, the reassortant human influenza A (H1N2) viruses were first documented in 1983 (Nishikawa *et al.*, 1983). These reassortants have been identified in several cases, as demonstrated in research done by Yamane *et al.* (1978), Bean *et al.* (1980), Guo *et al.* (1992) and Xu *et al.* (1993).

More recently, a H1N2 reassortant virus reemerged in North America. It was identified by the WHO and CDC in Atlanta, and named A/Wisconsin/12/2001 (Choi *et al.*, 2001). This virus was detected in December 2001 from a 6-month-old baby with a respiratory illness and fever as the main symptoms (Choi *et al.*, 2001). The study was performed on H1N2 viruses in order to elucidate the origin of the virus and its spread. A total of 51 H1N2 viruses acquired from various regions in the world, including such as Singapore, Malaysia, Canada, India, Egypt, Oman, Romania, the United Kingdom, and the United States, were identified among 890 seasonal influenza viruses screened from 41 countries. The following year, the WHO and the Public Health Laboratory Service reported the emergence of H1N2 viruses from humans in England, Israel, and Egypt (CDC, 2003). During this season, genetic (genetic) analysis of H1N2 showed that the HA of the circulating H1N2 viruses was similar to that of the A/New Caledonia/20/99 (H1N1) vaccine strain antigenically and genetically (Gregory *et al.*, 2002). The H1N2 virus NA was antigenically and genetically related to that of circulating human influenza H3N2 reference viruses such as A/Moscow/10/99 (Gregory *et al.*, 2002). So far, neither fatality cases nor high rate of human to human transmission have been reported (Xu *et al.*, 2004).

1.7.1.2 Human Influenza H1N1

Human Influenza A H1N1 virus is one of the influenza A virus subtypes that is currently endemic in the human population. The typical seasonal influenza virus infects approximately 5% of total population with 100,000 death annually (CDC, 2007). The first H1N1 subtype was first successfully isolated by Wilson and Smith in 1933, which is named A/WS/33 (H1N1) (Wilson and Smith, 1933). There was a major influenza pandemic caused by H1N1 influenza virus strain in 1918, commonly known as “Spanish Flu” (Cox and Subbarao, 2000). After the 1918 “Spanish Flu” pandemic, the H1N1 subtype of virus diminished rapidly for almost 50 years, the pandemic occurred with H2N2 and H3N2 in 1957 and 1968 (Cox and Subbarao, 2000). The first re-emergence of the H1N1 was in 1977 which was called “Russian Flu” (Webster *et al.*, 1992). Since then, both H3N2 and H1N1 recirculate in human population.

Based from the knowledge that waterfowl is the natural reservoir of the influenza virus, the genetics analysis have been carried out on the H1 strain of the influenza circulating in 1930s by Hinshaw *et al.* (1978) in order to determine the origins and relationships of the H1N1 virus with the older H1N1 strain from other species. They found that the H1 variants circulating in humans in the early 1930s were closely related to swine influenza viruses and were later shown to be similar to viruses from wild ducks antigenically.

1.7.1.3 Human Influenza H3N2

H3N2 Influenza A virus is currently the important seasonal human influenza causing higher morbidity and mortality worldwide than H1N1 (CDC, 2007). On average, H3N2 influenza viruses infect 5-15% of the total population, resulting in 500,000 deaths annually (Stohr, 2002). Since 2002, the antigenic evolution of A

(H3N2) viruses has followed from previously dominating the A/Sydney/5/1997-like viruses and A/Fujian/441/2002-like viruses to the A/California/7/2004-like viruses and to the A/Wisconsin/67/2005-like strains in a 5 year span (Russell *et al.*, 2008).

Russell *et al.* (2008) conducted a study on the circulation of the H3N2 influenza virus worldwide by analyzing the genetic and antigenic aspects of the hemagglutinin of 13,000 human derived H3N2 from 2000 – 2007 periods. They found out that there was continuous circulation in east and Southeast Asia via a region-wide network of temporally overlapping H3N2 epidemics, and those epidemics in the temperate regions were seeded from this network each year. This suggests that the new strain of seasonal H3N2 emerging worldwide may have originated from and appeared initially in this area. Additionally, Okada *et al.* (2009) also classified the human H3N2 influenza virus into three distinct groups based on the neutralizing human monoclonal antibody: 1968-1973, 1977-1993 and 1997-2003.

1.7.2 Influenza in Birds

Ducks are believed to be the natural reservoirs of influenza A viruses. The H3 and H6 subtypes of influenza A viruses are found most predominantly in ducks, H7 subtype is found in chickens, H4, H9, H11, and H13 subtypes are observed more frequently in shorebirds and gulls, the H5 subtypes have been found in wide range of both domesticated and wild birds, especially in Southeast Asia region (Webster and Kawaoka, 1988). The N2, N6, and N8 subtypes of the NA gene predominate in ducks, while N6 and N9 are more prevalent in shorebirds and gulls. In the process, Influenza A viruses have also been isolated from domesticated poultry such as turkey, chicken, quail, pheasant, goose, and duck (Webster and Kawaoka, 1988).

In ducks, avian influenza A viruses replicate well in the epithelial cells in the intestines and the respiratory tract (Webster *et al.*, 1977; Webster *et al.*, 1978). The viruses are resistant to the low pH environment in the digestive tract. The infection of ducks with influenza A viruses is asymptomatic (Webster *et al.*, 1978). This suggests that the virus may adapt in ducks without showing symptoms. However, there is a case where the avian H5N1 are lethal to ducks in Hong Kong (Strum-Ramirez *et al.*, 2004). Several avian influenza virus strains have also been shown to infect humans. Some of those even have a very high mortality rate. (Table 1.5)

Table 1.5. Examples of subtypes of Influenza A virus which have infected humans

Subtype and year	Remarks	Selected Reference
H5N1 1998	Originated from avian in Hong Kong, highly pathogenic to avians, human case confirmed, no efficient human to human transmission observed. 216 deaths out of 349 reported case in human (CDC, 2007)	Cox and Subbarao, 2000; Capua and Alexander, 2004
H7N7 2003	Originated from poultry farm in Netherlands, 89 people confirmed for the infection with one death	Fouchier <i>et al.</i> , 2003; Koopmans <i>et al.</i> , 2004; Munster <i>et al.</i> , 2007;
H9N2 1999	Infection confirmed, 2 children infected and recovered	Peiris <i>et al.</i> , 1999; Capua and Alexander, 2004; Butt <i>et al.</i> , 2003;

1.7.2.1 Avian Influenza Virus Classification

The avian influenza A viruses can be grouped based on their pathogenicity. This classification is based on their lethality in chickens. Avian influenza viruses can be classified as high pathogenic avian influenza (HPAI) or low pathogenic avian influenza (LPAI) viruses. LPAI viruses may have been considered of negligible risk, but there is evidence that HPAI might arise from LPAI by mutations (Horimoto and Kawaoka, 1995). An avian influenza virus is classified as HPAI if it exerts following characteristics (Alexander, 2000):

- 1). Avian influenza virus that is lethal for at least 6 out of 8 “8-week-old susceptible chickens” in 10 days following intravenous inoculation with 0.2 ml of a 1/10 dilution of an infective allantoic fluid;
- 2). If the influenza virus kills less than 6 out of 8 chickens, the growth test in cell culture will be done without the addition of trypsin. If there is growth, it will be considered HPAI. This classification is made for avian influenza virus with the exception of the H5 and H7 subtypes of virus;
- 3). For all H5 and H7 viruses, if growth is observed in cell culture without trypsin, the amino acid sequence of the HA must be determined. If the sequence is similar to that observed for other HPAI isolates, it will be classified as HPAI, which can be characterized by the multiple basic cleavage site.

1.7.2.2 Outbreaks of High Pathogenic Avian Influenza Virus

Among the most well known HPAI outbreaks was HPAI H5N1. The first outbreak of H5N1 HPAI was reported in Hong Kong in 1997 in poultry (Shortridge *et al.*, 1998). Later, this virus was classified as HPAI because of its high mortality rate (70%-100%) in chickens (Suarez *et al.*, 1998; Subbarao *et al.*, 1998). It also possess 60% mortality rate in humans (Gambotto *et al.*, 2008). The main characteristic of the HPAI H5N1 viruses is its multibasic sequence at the cleavage site in the HA, which is a characteristic of highly pathogenic viruses (Shortridge *et al.*, 1997). Many of the H5N1 isolates contain a shortened NA stalk. This characteristic of viruses is found in an adapted influenza virus in land-based poultry (Matrosovich *et al.*, 1997). Later, the infection of the HPAI H5N1 to the human population also shows high mortality rate (>60%) (Subbarao *et al.*, 1998).

Table 1.6. Clade classification by CDC in 2010 (CDC, 2010)

Clade	Year	Geographic location	Isolation source	Description and strain name
0	1996–2002	PRC, Hong Kong	Avian/human	Early progenitors of H5N1; HK/PRC 1997 avian influenza outbreak Gs/Guangdong/1/96
3	2000–2001	PRC, Hong Kong, Vietnam	Avian	Ck/Hong Kong/YU562/2001
4	2002/2003	PRC, Hong Kong	Avian	Gs/Guiyang/337/2006
	2005/2006	Guiyang, PRC	Avian	Described as Guiyang 1
5	2000–2009	PRC, Vietnam	Avian	Gs/Guangxi/914/2004
	2004	Guangxi, PRC	Avian	
6	2002/2004	PRC	Avian	Ck/Hunan/01/2004
7	2002/2004	PRC	Avian/human	Human case from Beijing in 2003
	2005/2006	Yunnan, Hubei, and Shanxi, PRC	Avian	Described as Yunnan 2 Ck/Shanxi/2/2006
8	2001–2004	Hong Kong, PRC	Avian	Ck/Hong Kong/YU777/2002
9	2003–2005	PRC	Avian	Dk/Guangxi/2775/2005
1	2002/2003	Hong Kong, PRC	Avian/human	Described as Guangdong
		Vietnam, Cambodia, Thailand, Laos, Malaysia	Avian/human	Spread of H5N1 to southeast Asia; described as Vietnam/Thailand/Malaysia Vietnam/1203/2004
2.1.1	2003–2010	Eastern Indonesia	Avian	Described as Indonesia Ck/Indonesia/BL/2003, Ck/CDC12/BL/2010
2.1.2	2005–2009	Western Indonesia	Avian/human	Primarily avian with human cluster from Medan; described as Indonesia Indonesia/538H/2006, East Java/CDC212/2007.
2.1.3	2004–2009	Eastern and western Indonesia	Avian/human	Described as Indonesia Indonesia/5/2005
2.1.4	2009–2010	Western Indonesia	Avian	Id/CDC202/2010
2.2	2005	Qinghai Lake, Jiangxi, PRC	Avian	Progenitors from Qinghai Lake outbreak; described as Qinghai-like
	2005–2007	Mongolia, Europe, Middle East, Africa	Avian/human	Long-distance spread of H5N1; described as EMA clade BHGs/Qinghai/1A/2005
2.3.1	2003–2005	Hunan and Guangdong, PRC	Avian	Described as Hunan Dk/Hunan/303/2004
2.3.2	2004–2006	Hong Kong, southern PRC	Avian	Described as Mixed/Vietnam
	2005	Vietnam	Avian	Described as Mixed/Vietnam 2 Ck/Guangxi/2461/2004
2.3.3	2004	Hunan, PRC	Avian	Ck/Guiyang/3055/2005
	20	Guiyang, PRC	Avian	Described as Guiyang 2
2.3.4	2005–2006	Hong Kong, PRC, Thailand, Laos, Malaysia	Avian/human	Described as Fujian-like Dk/Fujian/1734/2005
2.3.5	2007–2010	Western PRC	Avian	Dk/Nanjing/34/2010
2.4	2002–2005	PRC (predominantly Yunnan and Guangxi)	Avian	Described as Yunnan Ck/Yunnan/115/2004
2.5	2003/2004	PRC, Korea, Japan	Avian	Spread of H5N1 to east Asian countries
	2006	Shantou, PRC	Avian	Described as Guangdong/2006 Ck/Korea/ES/2003

HPAI H5N1 was classified based on the HA and NA protein characteristics, Z and Z⁺ genotype (Li *et al.*, 2004; Kou *et al.*, 2005). Genotype Z is characterized by a multibasic HA cleavage site, a 20-amino acid deletion in the NA stalk, and a 5-amino acid deletion in NS1. Genotype Z⁺ lacks the NA stalk deletion as compared to Genotype Z (Sims *et al.*, 2005).

Since 2003, HPAI H5N1 viruses have become widespread in Southeast Asia, spanning from Vietnam, Indonesia, Thailand, Cambodia, Laos, South Korea, Japan, China, Malaysia, and Myanmar (CDC, 2009). Further, numerous cases of direct avian-to-human transmission have been reported. Another interesting finding by Chen *et al.* (2004) is that the HPAI H5N1 is widespread among domestic ducks in Southern China. These viruses are not pathogenic in birds. From this finding, they suggest that ducks may play a crucial role as a reservoir of H5N1 viruses by transmitting the viruses to wild birds and mammals (Chen *et al.*, 2004). Until recently, there is no evidence of effective and efficient human to human transmission of HPAI H5N1 virus, unless the virus manages to adapt to the human host (Gambotto *et al.*, 2008). Due to rapid divergence and wide geographical spread, World Health Organization (WHO), the World Organization for Animal Health (OIE), and the Food and Agriculture Organization (FAO) grouped the H5N1 into clades based from genetic relatedness.

1.7.2.3 Outbreak of LPAI H9N2 virus

H9N2 subtype avian influenza viruses (AIV) have been circulating worldwide. The first detection of the H9N2 was from turkeys in Wisconsin in 1966 (Homme and Easterday, 1970). In North America, many of the H9N2 viruses were detected in gulls and wild ducks (Kawaoka *et al.*, 1988; Shaw *et al.*, 2002), but no H9N2 viruses have been reported in chickens (Perez *et al.*, 2003).

Before 1990, H9N2 viruses were isolated from only ducks in Asia (Shortridge, 1992). Since then, infections of H9 subtype have been reported in many Asian countries, especially in chickens (Alexander, 2000, Guo *et al.*, 2000 and Naeem *et al.*, 1999). The H9N2 viruses have also been found in swines (Cong *et al.*, 2007; Peiris *et al.*, 2001; Shi *et al.*, 2008). This may suggest a swine potential as “mixing vessel” method for the generation of potentially pandemic H9N2 influenza viruses.

Later, the H9N2 viruses were also isolated from humans with influenza-like illness in Hong Kong and Mainland China (Guo *et al.*, 1999 and Peiris *et al.*, 1999). Two distinct sublineages have become established in Asia, represented by the parent viruses A/duck/Hong Kong/Y280/97 and A/quail/Hong Kong/G1/97, which were predominantly isolated from chickens or quail, respectively (Guan *et al.*, 2000). LPAI viruses generally cause merely mild to moderate symptoms. But the co-infection with other respiratory pathogens such as *pneumococcus* may cause high morbidity (Brown *et al.*, 2006; Nili and Asasi, 2002). The analysis of H9N2 virus genome isolated from the last 20 years showed that these viruses are evolving rapidly and have reassorted with other avian influenza viruses to produce novel genotypes of virus (Li *et al.*, 2003; Li *et al.*, 2005; Xu *et al.*, 2004; Xu *et al.*, 2007).

Many H9N2 field isolates contain human virus-like receptor specificity, with binding preference to α 2-6 linked sialic acid (SA α 2-6) receptors, in contrast to the classic avian virus-like receptor specificity which preferentially binds α 2-3 linked sialic acid (SA α 2-3) receptors (Matrosovich *et al.*, 2001; Choi *et al.*, 2004; Butt *et al.*, 2005; Wan and Perez, 2006). Only a few of the H9N2 viruses that recognize SA α 2-6 receptors actually have infected humans (Saito *et al.*, 2001; Lin *et al.*, 2000). The symptoms are relatively mild, only causing mild flu-like illness. However, their preferential binding to both human and avian cells may bring a potential to cause

interspecies transmission (Peiris *et al.* 1999; Guo *et al.*, 1999; Lin *et al.*, 2000; Butt *et al.*, 2005). Several species of poultry and mammals have been used to study H9N2 viruses (Saito *et al.*, 2001; Humberd *et al.*, 2006; Nili *et al.*, 2007; Kaverin *et al.*, 2004; Aamir *et al.*, 2007). None of these models demonstrate evidence of the potential transmission of the virus in humans. Recently, Iqbal *et al.* (2009) discovered that the H9N2 viruses in Indian sub-continent have undergone extensive genetic reassortment. This leads to a new genotype of H9N2 virus with NS protein from highly pathogenic H7N3 and H5N1 viruses.

1.7.3 Influenza in Swine

The first swine influenza virus A/swine/Iowa/15/30 (H1N1) was isolated by Shope in 1930 (Shope, 1931). Since then, swine influenza has become one of the most prevalent respiratory illnesses in swines. Swines also have a big role to contribute the emergence of pandemic influenza virus based on several findings (Hinshaw *et al.*, 1978; Kida *et al.*, 1994; Ito *et al.*, 1998):

- 1). Swines can be naturally or experimentally infected with avian viruses;
- 2). Epithelial cells in swine trachea contain both human- and avian-type receptors (α 2,6- and α 2,3-linked sialic acid);
- 3). In nature, replication of an avian virus in pigs continuously can lead to influenza virus variants that preferentially recognize human-type receptors; (Scholtissek *et al.*, 1983)
- 4). Swine viruses and avian-human reassortant viruses can infect humans and potentially cause fatal disease.

Three major types of influenza viruses are circulating in pigs (Brown, 2000): the classical swine H1N1 viruses found in pigs since its isolation in 1930 (Hinshaw *et*

et al., 1978), the human-like H3N2 viruses causing frequent infections to pigs. (Castrucci *et al.*, 1993; Hinshaw *et al.*, 1978), and the avian-like H1N1 viruses which were introduced into European Pigs from birds, detected in 1979 (Scholtissek *et al.*, 1983). A prominent human outbreak of swine influenza in humans was described in 1976 (Sencer *et al.*, 2006). A swine H1N1 influenza virus infected soldiers at Fort Dix, New Jersey, resulting in death of one soldier (Nachamkin *et al.*, 2008). Based on concerns that this might be the indicator of a new pandemic, a vaccine was developed and a country-wide vaccination program was established. After the vaccination was done in more than 40 million people, it became clear that vaccination was associated with Guillain-Barré syndrome in about 1 out of 100,000 vaccines indicating a five to tenfold higher incidence than usually observed (Nachamkin *et al.*, 2008). Since the virus was no longer circulating, the vaccination program was stopped. Antibodies that cross-react against peripheral nerve antigen have been suspected to be responsible for the high rate of Guillain-Barré syndromes (Nachamkin *et al.*, 2008).

1.7.3.1 Classical Swine H1N1 Viruses

The descendents of the H1N1 1918/1919 isolate, now referred to as “classical swine viruses” continue to circulate in most parts of the world (Hinshaw *et al.*, 1983; Gorman *et al.*, 1991; Dunham *et al.*, 2009). In Europe, these viruses disappeared for nearly 20 years but were reintroduced in 1976, probably by imported pigs from the United States, starting in Italy (Nardelli *et al.*, 1978). Since their reintroduction, H1N1 viruses have spread and become endemic in Europe with a seroprevalence of approximately 20 – 25 % (Zhang *et al.*, 1989), reported by several studies, for example in the UK (Roberts *et al.*, 1987), The Netherlands (Masurel *et al.*, 1983) and Sweden (Abusugra *et al.*, 1983). For about 60 years since the pandemic 1918, classical swine

viruses were extremely stable, both antigenically and genetically (Easterday, 1980). The emergence of avian-like H1N1 viruses was introduced to European pig from birds in 1979, replacing the dominance of classical swine H1N1 virus (Pensaert *et al.*, 1983). Apart from Europe, various regions in the world also detected classical swine H1N1 virus in local farms, for example, Canada (Morin *et al.*, 1981), Hong Kong (Yip, 1976), Japan (Yamane *et al.*, 1978), India (Das *et al.*, 1981), China and Taiwan (Shortridge and Webster, 1979).

1.7.3.2 Avianlike H1N1 Viruses

In 1979, an avian H1N1 virus, closely related to a duck virus, was introduced into pigs in Europe (Pensaert *et al.*, 1982). In European pigs, cocirculating avian and human H3N2 viruses reassorted. The resultant virus that possessed humanlike HA and NA genes and avian-like internal genes were transmitted to two children in the Netherlands (Castrucci *et al.*, 1993; Claas *et al.*, 1994). Infections of swine with H3N2 viruses containing humanlike surface glycoproteins, but internal genes derived from H1N1 avian origin, are common in Europe (Castrucci *et al.*, 1993). The recent introduction of an avian-like H1N1 virus into pigs in Southern China has not replaced the classical swine viruses, and both lineages continue to cocirculate (Guan *et al.*, 1996).

1.7.3.3 Humanlike H3N2 Viruses

Humanlike viruses of the H3N2 subtype were first isolated from pigs in Taiwan in 1970 (Kundin, 1970). The prevalence of H3N2 viruses in North American pigs is low (Chambers *et al.*, 1991; Bikhor *et al.*, 1994). Since 1984, a humanlike H3N2 influenza virus has caused disease and replaced the original H3N2 virus in

Europe. This resulted from a reassortment of the virus with the avian-like swine H1N1 virus (Castrucci *et al.*, 1993). In 1998, several outbreaks were observed in the swine in the USA, and two antigenically distinct reassortant viruses (H3N2) were isolated: a double-reassortant virus containing genes similar to those of human and swine viruses and a triple-reassortant virus containing genes similar to those of human, swine, and avian influenza viruses (Webby *et al.*, 2000).

1.7.3.4 Pandemic 2009 H1N1 Swine influenza virus

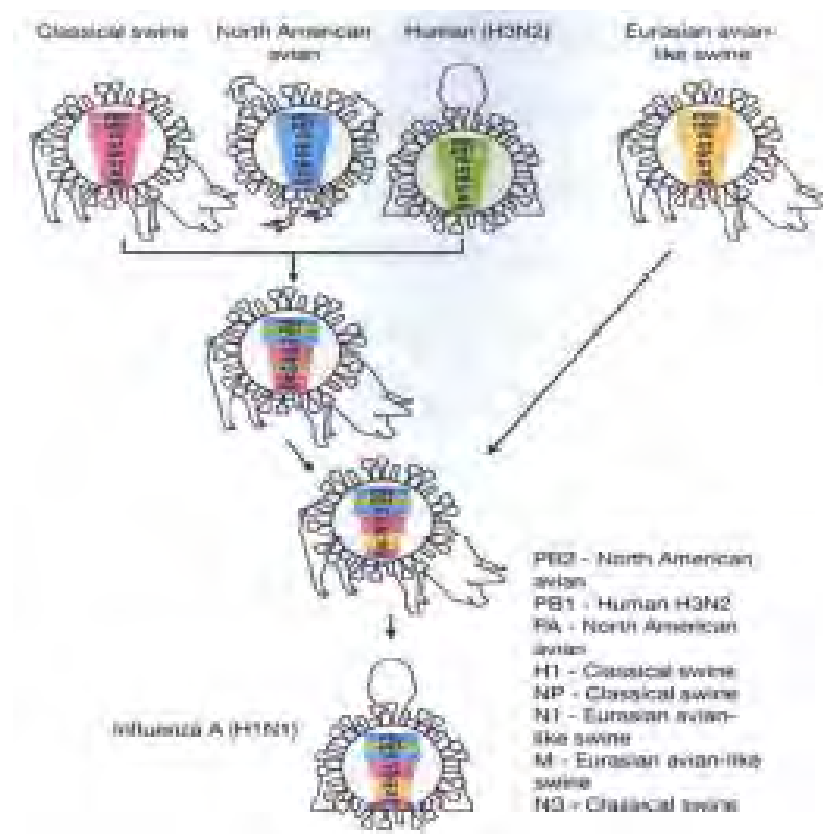
Initially, the 2009 H1N1 swine influenza virus was detected from two specimens in California (Fraser *et al.*, 2009). Retrospectively, the outbreak of pandemic 2009 H1N1 swine influenza virus was reported in the Mexican town of La Gloria, Veracruz, in mid-February of 2009 (Fraser *et al.*, 2009; Kowalczyk and Markowska-Daniel, 2010; Abdel-Haq and Asmar, 2011). Two months later, high numbers of pneumonia/influenza-like illness were observed among the patients. In about the same time, two specimens positive for 2009 swine influenza virus were identified from the outbreak in Southern California in mid-April. Later, the Public Health Agency of Canada also detected 2009 swine influenza virus in specimens received from Mexico. The similarity of all the isolates found in various places in America triggered an alert by the CDC and WHO on 24 April. Not long after that, international spread and clusters of human-to-human transmission prompted the WHO to increase the pandemic alert from phase 3 to phase 5 (human-to-human spread in at least two countries, and signs of an imminent pandemic). Most cases outside Mexico and the United States have been caused by travellers from Mexico. Most infections seem to be mild and do not require hospitalization (Novel Swine-Origin Influenza A (H1N1) Virus Investigation Team). Careful monitoring is critical during the winter

season in order to overcome more virulent variants, as observed with the “Spanish Flu” 1918 pandemic (Fraser *et al.*, 2009).

The pandemic 2009 H1N1 swine influenza virus is a reassortant of triple-reassortant swine influenza A (H1N1) virus that contains classic swine RNA-segments from the North America lineage (HA, NP, non-structural proteins (NS)), avian influenza RNA segments from the North America lineage (polymerase basic protein 2 (PB2), polymerase acidic protein (PA)), and PB1 of human seasonal H3N2 viruses (Neumann *et al.*, 2009) (Table 1.7, Fig. 1.20). Moreover, the NA and M segments, that are of classic North America lineage swine origin in triple-reassortant swine influenza A (H1N1) viruses, were exchanged by NA and M from the Eurasian influenza A (H1N1) swine lineage (Neumann *et al.*, 2009).

Table 1.7. The Origin of Swine Influenza Virus Segments

Segment	Origin
HA	Classical Swine, North American Lineage
NA	Eurasian Swine Lineage
M	Eurasian Swine Lineage
PB2	Avian, North American Lineage
PB1	Human derived H3N2 Swine Lineage
PA	Avian, North American Lineage
NP	Classical Swine, North American Lineage
NS	Classical Swine, North American Lineage



Taken from Neumann *et al.*, 2009

Fig 1.20 . The origin of 2009 swine influenza virus

As of November 2, 2009, the infection of swine influenza virus have been expanded to more than 440,000 cases of pandemic swine H1N1 influenza virus, with more than 5,700 deaths worldwide as documented by WHO (2009). According to Smith *et al.* (2009), the low diversity gives indication that the virus only emerged and infected human in early 2009. The relatively large genetic distance between pandemic swine H1N1 influenza virus and other closely related swine influenza viruses indicates that the gene segments have been circulating around without any detection for more than 10 years, with the estimation of the Times to the Most Recent Common Ancestor (TMRCA) for individual genome segments approximately 9 to 17 years. The attempt of large-scale molecular characterization and the dynamics of the transmission of the virus in human are still at early stage. Nelson *et al.* (2009) found at least 7

phylogenetically distinct clades of swine H1N1 influenza virus have been identified and disseminated globally. The clades are possibly formed because the swine influenza virus co-circulated in with local seasonal strain, hence introducing the genetic materials of the virus. Further, they also analyse the influenza virus outbreak in New York and Wisconsin. They found out that the swine influenza virus derived from those locations was mostly come from two different clades. The clades are both distinct phylogenetically from the viruses first identified in California and Mexico, suggesting an important role for founder effects in determining local viral population structures. Furuse *et al.* (2010) also perform internal genes analysis from 673 strains of influenza A virus derived from human, avian and swine host. Based from their finding, they suggested that the adaptation of 2009 swine influenza virus in human host was due to mutations from continual genetic reassortment.

Many researches have been done to try to elucidate the mechanism of action of the novel 2009 swine influenza virus. This includes growth characteristics in vitro and in vivo (Itoh *et al.*, 2009), transmission study in ferrets and mice (Maines *et al.*, 2009), Cytokine profiling of swine influenza virus (Woo *et al.*, 2009). More recently, Shapira *et al.* (2009) performs yeast-two hybrid combined with genome-wide analysis of the host cells infected with 2009 swine influenza virus in primary lung cells. Their found that, along with antiviral and apoptotic related genes responses, they found some unanticipated host and viral protein interactions, including a network of RNA binding proteins and Wnt signalling.

1.8 Research Objective

It was known that different strains of influenza virus interact with the host in various ways. It is interesting to note that some strains of influenza virus are able to

infect and replicate well in particular host, but not the others. This suggests there are specific interactions between the virus and the host to either assist or inhibit the virus growth. It has been reported that the LPAI viruses have the potential to develop into HPAI. Therefore, the characterization of the host response in the LPAI viruses is as vital as that of HPAI viruses. Most of the host response studies done nowadays focus on HPAI. There are still relatively few studies on LPAI.

The aim of the research is to characterize low pathogenic avian influenza virus H9N2 which has been isolated from ducks imported to Singapore, and current circulating 2009 swine influenza virus currently circulating in Singapore as a routine surveillance conducted by Agri-Food and Veterinary Authority of Singapore (AVA). The characterization is based on the infection profiles in different tissue culture models which represents human, chicken and canine, retaining properties of the species they are derived from. The analysis will be carried out based on:

1. Sequence analysis of the virus for to analyze sequence similarity and clustering pattern of the virus, drug resistance, epitope sites determination, and host signature using phylogenetic tree and sequence comparison,
2. Growth characteristics, assessed by immunofluorescence assay (IFA), Growth Curve, and Plaque Assay to determine virus growth,
3. Host cell response, analyzed by cDNA microarray and cytokine assay to determine global gene response,
4. Viral kinetics for both replication (vRNA) and transcription (mRNA), analyzed by qRT-PCR to determine virus replication efficiency.

The virus growth and replication efficiency relates closely to the virus efficiency to counteract host-cell response and defense mechanism. Therefore, analyzing and comparing the growth characteristics and viral kinetics of different influenza A virus

strains conducted in different cell lines is critical to determine the preference of the influenza virus strains to the particular hosts. Together with the genomic and cytokine analysis, the main keys behind the virus growth preference, virus host-adaptation and interspecies transmission can be revealed.

Chapter Two. Materials and Methods

2.1 General Reagents

All general reagents used in this experiment were of analytical grade obtained from Sigma Adrich Chemical Company Ltd, Becton-Dickenson Ltd, Bio-Rad Ltd., Invitrogen Ltd., USB Corp., unless otherwise stated. For work where sterility is required, all of the reagents are either autoclaved at 121 °C for 20 min or passed through 0.22 µm filter-sterilization (Nalgene).

2.1.1 Cells

MDCK (Madin Darby Canine Kidney)	ATCC
Embryonated Chicken Eggs	Yeo Chew Farm
A549 (Human Adenocarcinomic Lung cells)	ATCC
<i>E. coli</i> One-shot® TOP10	Invitrogen
Lung Macrophage from Balb/c Mice	Laboratory Animals Centre, Singapore

2.1.2 Virus

A/WSN/33 (H1N1)	ATCC
A/Duck/Malaysia/1/01 (H9N2)	AVA
A/Singapore/276/2009 (H1N1)	
A/Singapore/471/2009 (H1N1)	
A/Singapore/478/2009 (H1N1)	DSO
A/Singapore/527/2009 (H1N1)	
A/California/7/2009 (H1N1)	

2.1.3 Tissue Culture Reagents

DMEM+GlutaMAX	Gibco
Foetal Bovine Serum	Gibco
Sterile 1× Phosphate Buffer Saline pH 7.2	Gibco
Penicillin-Streptomycin 100X (10,000 U.I Penicillin and 10,000 µg Streptomycin)	Gibco
Trypsin-EDTA 0.25%	Gibco
Trypsin 2.5%	Gibco
Bovine Serum Albumin (BSA) Fraction V 7.5%	Gibco
Trypsin-TCPK	Worthington
RNAlater	Ambion

2.1.4 Antibodies

Mab 8257 (mouse anti-influenza A nucleoprotein), usage 1:100 (immunofluorescence assay), 1 : 500 (microplaque assay)	Chemicon
AP124F (Goat anti-mouse IgG, FITC conjugated), usage 1:100 (immunofluorescence assay)	Chemicon
Anti-mouse Horseradish Peroxidase , usage 1 : 10,000 (western blotting), 1 : 500 (microplaque assay)	Sigma Aldrich
Monoclonal anti Mx1, usage 1:500 (western blotting)	Gift by Prof Koch, University of Freiburg
Mouse anti-STAT1, usage 1:3,000 (western blotting)	Transduction Laboratory

Mouse anti-phosphorylated STAT1 (pY704), usage 1:3,000	Transduction Laboratory
JNK and phosphorylated JNK	Gift by Dr. Peter Cheung, NTU
p38 and phosphorylated p38	Gift by Dr. Peter Cheung, NTU
β -actin, usage 1:1,000 (western blotting)	Chemicon
ERK1, ERK2 and pERK1/2	Cell Signalling

2.1.5 Immunofluorescence and Immunostaining Reagents

3-amino-9-ethyl carbazole	Sigma Aldrich
Paraformaldehyde	ICN Biochemicals, Inc.
10 \times Phosphate Buffer Saline pH 7.2	1 st Base
Triton X-100	Chemicon
H ₂ O ₂ 3%	Fluka

2.1.6 Commercially available kit

RNAeasy Mini Kit	QIAGEN Ltd.
Gel Extraction Kit	QIAGEN Ltd.
GeneChip [®] One-Cycle Target Labelling and Control Reagents	Affymetrix
Hybridization, Wash and Stain Kit	Affymetrix

QIAprep Spin Miniprep Kit QIAGEN Ltd.

SuperScript™ First Strand Invitrogen

2.1.7 Cloning Vector and E. coli growth medium

pDrive QIAGEN Ltd.

pCR2.1 – TOPO Invitrogen

Difco LB Broth, Miller Becton-Dickinson, Ltd.

Difco LB Agar, Miller Becton-Dickinson, Ltd.

SOC Medium Invitrogen

2.1.8 Tissue Culture Media and Solution

Cell Propagation Medium DMEM+GlutaMAX(Gibco)
supplemented with 10% v/v Fetal Calf
Serum (Gibco) and Penicillin 100 UI/ml
and Streptomycin 100 µg/ml (Gibco)

Cell Infection Medium for single cycle of
infection DMEM+GlutaMAX(Gibco)
supplemented with 10% v/v Fetal Calf
Serum (Gibco) and Penicillin 100 UI/ml
and Streptomycin 100 µg/ml (Gibco)

Cell Infection Medium for multiple cycle
of infection DMEM + GlutaMAX supplemented
with 0.21% BSA (Gibco, USA), 1
µg/ml trypsin-TPCK (Worthington,
USA) and antibiotics (streptomycin 100
mg/ml and penicillin 100 U/ml) (Gibco,
USA)

Fixing Solution 4% Paraformaldehyde (ICN) in PBS

Standard Overlay DMEM (Gibco) and 1% Low
Temperature Agarose (Invitrogen),
0.21% BSA (Gibco) and 1 µg/ml

	trypsin-TPCK (Worthington)
Microplaque Overlay	DMEM (Gibco) with 1.2% Avicel RC-591 (FMC Biopolymer), supplemented with 0.21% BSA (Gibco) and 1 µg/ml trypsin-TPCK (Worthington).

2.1.9 Bacterial Culture Media and Solution

100 mg/ml ampicillin	100 mg/ml in ddH ₂ O, filtered (0.22 µm) and stored at -20 °C
LA broth	LB medium containing 100 µg/ml ampicillin
LA plate	LB agar plate containing 100 µg/ml ampicillin
LA plate for blue/white colony screening	100 µl of 0.1 M IPTG and 250 µl of 40 mg/ml X-Gal in Dimethylformamide were spread on the plate and incubated in 37 °C for 1 h. Plate was prepared fresh

2.1.10 DNA Analysis

1x TBE	100 ml 10x TBE dissolved in 900 ml of ddH ₂ O to make 1 L of 1x TBE stock
0.1% Ethidium Bromide	10 mg of Ethidium Bromide dissolved in 10 ml of ddH ₂ O
Agarose gels	0.5 g of Agarose in 50 ml 1x TBE

2.1.11 Protein Analysis by SDS-PAGE gel

12% Resolving Gel	1.6 ml of 30% Bis-Acrylamide (C : N = 1:29.9) 1.4 ml H ₂ O 1 ml Tris-Cl pH 8.8 60 µl 10% SDS
-------------------	--

	60 µl 10% APS 6 µl TEMED
4% Stacking Gel	266 µl of 30% Bis-Acrylamide (C : N = 1:29.9) 1333 µl H ₂ O 375 µl Tris-Cl pH 6.8 15 µl 10% SDS 15 µl 10% APS 1.5 µl TEMED
Boiling Mix (5x)	31.25 ml 1M Tris-HCl pH 6.8 10 g SDS 25 ml Glycerol 750 µl Bromophenol Blue 2% in ethanol 5 ml 2-mercaptoethanol Add ddH ₂ O to 100 ml
Boiling Mix (1x)	Dissolve Boiling Mix (5x) in ddH ₂ O in 1 :5 ratio.
SDS-PAGE Running Buffer (1x)	57.6 g Glycine 12 g Tris base 4 g SDS Add ddH ₂ O to 4 litres
2.1.12 Western Blotting	
Transfer Buffer	3.03 g Tris base 14.41 g glycine 200 ml methanol water to 1 L
5% Skim Milk Blocking Solution	5 g Skim Milk powder mixed in 100 ml 1x Wash Buffer
WB Wash Buffer	400 ml 10x PBS, add 2 ml of Tween-20, top up with ddH ₂ O to 4 L.

2.2 Methods

2.2.1 General Methods for Biochemistry and Molecular Biology

2.2.1.1 RNA extraction

All starting materials for RNA extraction were 100 µl in liquid form. Pellets or sample lower than 100 µl were added with RNase free water. QIAGEN® RNeasy

Mini Kit was used for this step according to manufacturer's protocol. The final step of elution used in all of the experiment was approximately 40 µl of RNase free water. The RNA samples were kept in -80 °C freezer until ready for use.

2.2.1.2 Reverse Transcription

The starting RNA material was 8 µl. The sample was mixed with 1 µl dNTP 10 mM and 1 µl of primer, and incubated at 65 °C for 15 mins, followed by cooling down on ice for at least 2 mins. RT reaction mix was then added into the sample (one RT reaction contains 2 µl 10x RT buffer, 4 µl MgCl₂ 25 mM, 2 µl DTT 0.1 M, 1 µl RNaseOUT®(Invitrogen)) and incubated for 2 mins at 42 °C. 1 µl RT enzyme SuperScript II (Invitrogen) was added into the sample reaction mix and same incubation condition was continued for 1 hour, followed by RT enzyme inactivation by heating at 70 °C for 15 mins. The sample reaction mix was cooled down on ice for 2 mins. 1 µl of RNase H (Invitrogen) was added to the sample reaction mix and incubated for 20 mins at 37 °C. The sample reaction mix will be in the form of cDNA and ready for next step analysis.

2.2.1.3 Polymerase Chain Reaction (PCR)

The PCR done in this experiment was influenza virus gene segment amplification with the protocol as described in Hoffmann *et al.* (2001). The primers used in this experiment are shown in Appendix 1. 4 µl of cDNA template was used in this experiment. The PCR mix per reaction (50 µl) was: 5 µl 10x HiFi buffer, 5 µl dNTP 2 mM, 2 µl MgSO₄ 50 mM, 2 µl of forward primer 10 µM, 2 µl of reverse primer 10 µM, 0.5 µl of HiFi Platinum Taq (Invitrogen) 100 U/µl, 29.5 µl of nuclease free water. The PCR temperature run setting was set as follows : Initial denaturation at

95 °C for 2 min, followed by 30 cycles of denaturation at 95 °C for 30 sec, annealing at 58 °C for 30 sec, and elongation at 68 °C for 7 mins. The final elongation was set at 68 °C for 10 mins, followed by cooling.

2.2.1.3 DNA separation by Agarose Gel Electrophoresis

The 1% Agarose gel (BioRad) in 1x TBE buffer (1st Base) was used in DNA separation. The sample was prepared in 250 ml Erlenmeyer flask. The agarose was then heated in microwave until completely dissolved and cooled with water until evaporation disappeared. 3 µl of 0.1% ethidium bromide (BioRad) was added into the agarose, and poured into 8 cm gel casting cassette. The appropriate DNA comb was applied and let the agarose sit for 1 hour. The Agarose was loaded into DNA Agarose gel tank PowerPak (BioRad) and was run at 10V/cm for 45 mins. The agarose were then viewed with UV Transilluminator. The DNA band of interest was excised for gel extraction.

2.2.1.4 Gel Extraction

The excised gel was then processed using QIAGEN[®] Gel Extraction Kit, following manufacturer's protocol. The final elution step was 30 – 50 µl in Nuclease Free Water. The sample was then measured with NanoDrop[®] to determine its concentration. The samples were kept in -20 °C freezer until further use.

2.2.1.5 Ligation

The ligation done in this experiment were done using pDrive vector(QIAGEN[®]) and pCR2.1-TOPO vector (Invitrogen[®]). Both vector maps are displayed in Appendix. pDrive vector ligation was done for M, NS, NP, NA, and HA,

and pCR2.1-TOPO was done for PA. Each of the vector system came with its own ligation reaction mix and was done according to the manufacturer's protocol. The ligation reaction mix was stored at -20°C freezer until further use. PB1 and PB2 were unable to be put into both vectors, hence direct PCR product sequencing were utilized.

2.2.1.6 Transformation of Ligation Mix into Competent Cells

4 µl of ligation reaction mix was used for transformation by incubating the mix into TOP10[®] competent cells (Invitrogen) in ice for 30 mins. The cells were then heat shocked at 42 °C for 45 sec, and put on ice for 3 mins. The cells were then topped up with 250 µl SOC Media (Invitrogen) and were incubated in a shaker incubator at 37 °C for 1 hour. Meanwhile, the LB Agar plate was pre-warmed. If pDrive transformant was used, 100 µl 0.1 M IPTG and 250 µl of X-GAL 40 mg/ml in dimethylformamide was added into the plate, spread evenly and let absorbed for 1 hour. 100 µl of the transformant were added into the plate, spread evenly and incubated at 37 °C for 16 hours.

2.2.1.7 Positive gene insertion by colony screening

For pDrive transformant, white colonies were selected and picked for positive gene insertion in the vector, and blue colonies were selected for negative control. For pCR2.1-TOPO transformant, all colonies were selected for colony screening. The colony screening was done using primers used in PCR amplification. The PCR reaction mix in PCR tube was prepared as follows (per reaction(20 µl)) : 2 µl of 10x PCR buffer, 2 µl of dNTP 2 mM, 1 µl of MgCl₂ 50 mM, 0.8 µl of forward primer 10 mM, 0.8 µl of reverse primer 10 mM, 0.5 µl Platinum Taq polymerase (Invitrogen) in 12.9 µl of nuclease free water. The colony was picked with tooth-picks and submerged

evenly into the PCR reaction mix. The tubes were then placed into PCR machine. The PCR incubation settings were set with the same condition mentioned in Section 2.2.1.3. The PCR amplicons were then run into DNA Agarose Gel to check for positive bands. For positive colonies, they were grown in 5 ml LB broth at 37 °C for 16 hours. 1 ml was stored as glycerol stock and the rest would be spun down. Pellet obtained was used for plasmid extraction.

2.2.1.8 Plasmid Extraction

4 ml of the grown *E. coli* culture of positive gene insertion gene were lysed and from this process, purified plasmid was obtained. QIAGEN® MiniPrep was used. The extraction was done according to the manufacturer's protocol. The final elution was 40 µl in Nuclease Free Water.

2.2.1.9 Sequencing Reaction Preparation

200 ng of plasmid, and 30 ng of PCR product (for PB1 and PB2) were used as materials for sequencing. The sequencing reaction mix was prepared as follows : 4 µl BIG-DYE Terminator v3.1® (ABI), 1 µl primer, samples, and later adds nuclease free water at final volume of 10 µl. The reaction mix was loaded into the PCR machine and run with the condition as follows : 95 °C for 5 min, [95 °C for 30 sec, 55 °C for 20 sec, 65 °C for 2 min for 30 cycles], ended with 65 °C for 4 min. The samples were then sent to 1st Base® for sequencing.

2.1.2.10 Sequence Alignment and Phylogenetic Tree

Nucleotide and translated amino acid (aa) sequences for each gene segment were compared between the isolates and other published sequences from GeneBank

(<http://www.ncbi.nlm.nih.gov.ezlibproxy1.ntu.edu.sg/genomes/FLU/FLU.html>) with Megalign (DNASTAR, Lasergene Version 7) using the Clustal X algorithm. Percent (%) sequence homology was calculated for each of the full-length gene. Phylogenetic tree was constructed using the neighbour-joining method at the nt level, with bootstrap analysis performed on 1000 replicates. Phylogenetic trees were viewed with TreeView v1.6.

2.2.1.11 Protein Separation by SDS-PAGE

The gel was cast inside a cassette in advance with appropriate percentage of acrylamide. After the gel were set, loaded into the SDS-PAGE Tank (BioRad) and filled with 1x SDS-PAGE running buffer. Samples in 1x Boiling Mix were then loaded into the wells. The separation was run at 200 V for 50 – 60 mins (until the bromophenol blue migrated to the bottom of the gel close to the edge). The gel was carefully removed from the cassette.

2.2.1.12 Western Blotting

Initially, the PVDF membrane (Poll laboratories) was soaked into methanol for approximately 2 mins. The gel processed by SDS-PAGE was carefully picked up. Transfer unit cassettes were assembled in this order : **Red pole** > clear plate > pad > 3 MM filter paper > PVDF membrane > gel > 3 MM filter paper > pad > black plate > **neg. pole (Black)**. The cassettes were the loaded into the tank together with one block of frozen iced water. 1x Transfer Buffer was laded into the tank until the cassettes were submerged. The run was at 100 V for 60 mins. After that, the PDVF membrane was carefully removed from the cassette and washed with 1x WB Washing Buffer for 2 times. The membrane was blocked with 5% Skim Milk Agar overnight at 4 °C with

slow shaking. The membrane was washed with 1x WB Washing Buffer for 5 mins, 3 times, and incubated with primary antibody for 1 hour at room temperature. The membrane was washed with 1x WB Washing Buffer for 5 mins, 3 times. The membrane was incubated with secondary antibody for 1 hour at room temperature. After the incubation was finished, the membrane was washed with 1x WB Washing Buffer for 5 mins, 3 times. The membranes were then dried and put into Western Blot cassettes. Enhanced Chemiluminescence (Amersham) was applied into the membrane and spread evenly and carefully. The exposure was done with KODAK O-MAT X-ray film in the dark room, and exposed. The films were developed in Kodak Developer Machine. Adjustment of the exposure time was required to make satisfactory result.

2.2.2 Tissue Culturing and Infection

2.2.2.1 Culture and maintenance of MDCK and A549 cells

MDCK and A549 cells were maintained and propagated using Cell Propagation Medium, which contain DMEM+GlutaMAX(Gibco) supplemented with 10% v/v Fetal Calf Serum (Gibco) and Penicillin 100 UI/ml and Streptomycin 100 µg/ml (Gibco). The cells were kept in medium or large flasks (Corning, USA). When the cells reached approximately 90% confluency, the cells were passaged. Briefly, the cells were washed with sterile PBS pH 7.2, incubated in Trypsin-EDTA 0.25% (w/v) until the cells dislodged with tapping the flask. Trypsin was inactivated by adding cell propagation medium, and cells were directly seeded into new flasks or dishes with desired cell density. The cells were then kept in incubator at 37°C, 5% CO₂.

2.2.2.2 Harvesting and Culture of CEF cells

CEF were obtained from embryonated chicken eggs, which were approximately 8-10 days old. Before the harvesting, the eggs were wiped clean using 70% ethanol. The embryos were taken out from the eggs by using forceps. The heads, limbs, internal organs and viscera were removed from the embryos, leaving the intact body part. It was then minced using forceps, washed with PBS and decanted to remove blood and yolk. It was then trypsinized with 0.1% Trypsin in PBS for 20 min until the minced parts became slightly slimy and the solution was turbid. Trypsin was inactivated by addition of DMEM+GlutaMAX(Gibco) supplemented with 10% v/v Fetal Calf Serum (Gibco) and Penicillin 100 UI/ml and Streptomycin 100 µg/ml (Gibco). The trypsinized cells were then passed through a strainer to be separated from larger untrypsinized cell clumps. The cells were then spun down at 400×g for 10 min. The supernatant was removed and the cells were resuspended in fresh cell propagation medium. The cells were seeded into wells and dishes for experiments and kept at incubator at 37°C, 5% CO₂.

2.2.2.3 Mouse Macrophage Harvesting

Balb/c mice aged from six to eight weeks old were purchased from the Laboratory Animals Centre, Singapore and maintained under standard pathogen-free (SPF) conditions. After keeping for one week in the SPF room the mice were sacrificed and the lungs were dissected for cell harvest.

Macrophages from the mouse lungs were harvested using positive selection for CD11b⁺ cells. The lungs were dissected from the mice and digested using collagenase D (Gibco #11088866001, 1mg/mL in application for lung tissues). After meshing

using 100µm strainer, the medium (DMEM + 2% FBS + Pen-Strep) containing cells was collected. The cells were pelleted, and resuspended in FACS buffer(0.5% BSA + 1 x PBS + 2mM EDTA), and filtered through a 30µm filter into single-cell suspension.

The single-cell suspension obtained was incubated with CD11b microbeads (MACS #130049601) and applied to LS positive selection column (MACS #130042401) for magnetic separation according to company specification. Briefly, the cell suspension was incubated together with the CD11b magnetic microbeads. Cells expressing CD11b receptors were attached by the microbeads. The cell suspension was applied into a LS column under a strong magnetic field. The cells labelled by the magnetic microbeads were picked up by the column due to magnetic force, while the non-labelled cells were not picked. The collected macrophages were seeded onto 13mm glass coverslips in 24-well plates at a density of 2×10^5 cells per coverslip and cultured in L929 medium for around 3 to 5 days before infection.

2.2.2.4 Virus Propagation

The H9N2 virus was isolated from duck originated from Malaysia, which imported to Singapore and tested positive by Agri-food and Veterinary Authority of Singapore (AVA) as part of the routine surveillance for Avian Influenza Virus. the H1N1 2009 pandemic strains isolates were obtained from patients in Singapore which had been confirmed positive by qRT – PCR method and Immunofluorescence Assay done by Detection and Diagnostic Laboratory in DSO National Laboratories.

The swine influenza viruses used in this experiment derived from the patients in Singapore tested positive from swine influenza virus. The sample collection was done by nasal swab method stored in viral transport medium. The specimens were then tested by qRT-PCR for the presence of swine influenza virus genes. To confirm the

result further, MDCK cells were infected with the specimens with the shell vial method (Reina *et al.*, 1996). The cells were then incubated for 3 days and stained with anti-NP (Mab 8257) (Chemicon, USA) for the presence of virus antigens. Four strongest signals were selected for further analysis. Four specimens with the strongest signal, labelled as A/Singapore/276/2009 (H1N1), A/Singapore/471/2009 (H1N1), A/Singapore/478/2009 (H1N1) and A/Singapore/527/2009 (H1N1).

The viruses were propagated in 12 day-old embryonated chicken eggs. Before inoculation, all of the eggs used were checked for the viability using candling equipment. The eggs were cleaned with 70% ethanol and then punctured to create small holes just approximately 5 mm above air pocket layer. Virus inoculum of approximately 10^4 pfu or approximately 1 : 10 dilution was injected to the eggs through the holes created previously using syringe. The holes were then sealed with tapes and the eggs were incubated for 2 days in 37 °C incubator. The seal tapes and the egg-shells were carefully removed using scissors and forceps. The allantoic fluid was then carefully harvested without breaking the yolk and veins. The fluid was pooled inside 50 ml Falcon Tubes and spun down at 500 ×g for 15 min to remove debris and blood clots. The clarified fluid containing virus was then aliquoted into cryotubes for future use.

2.2.2.5 Infection of the cells with virus and the determination of multiplicity of infection used

The determination of the moi to infect MDCK, CEF and A549 cells was done to assess the efficacy of each virus strain used in this experiment to infect the majority of the cells (>95%) in the experiment. To fulfill this, the amount of the virus inoculum required to infect the cells was adjusted accordingly, and the percentage of the cell

infected was monitored using the immunofluorescence method. Based from the observation, at moi of 3, all virus strains used in this experiment (A/WSN/33 (H1N1), A/Duck/Malaysia/1/01 (H9N2), A/Singapore/276/2009 (H1N1), A/Singapore/471/2009 (H1N1), A/Singapore/478/2009 (H1N1) and A/Singapore/527/2009 (H1N1)) showed >95% infection at 16 hpi in MDCK, CEF and A549 cells. Based from this, moi of 3 was used as a baseline to achieve all-cell infection.

After the cells reached desired confluency level, the cells were then infected with the virus inoculum. Briefly, the cell propagation medium was removed from the cells, and the virus inoculum was dissolved in PBS, and directly applied to the cells. The cells were then rocked regularly for every 10 mins to evenly distribute the virus inoculum for 1 hour. After the incubation was done, the virus inoculum was then removed and replaced with cell infection medium. For the infection at multiplicity of infection (moi) of 3 or more, the cells are maintained using DMEM + GlutaMAX supplemented with 2% Fetal Calf Serum and antibiotics (streptomycin 100 mg/ml and penicillin 100 U/ml), incubated in 37 °C, 5%CO₂. For infection at moi lower than 1, the cells are maintained using DMEM + GlutaMAX supplemented with 0.21% BSA (Gibco, USA), 1 µg/ml trypsin-TPCK (Worthington, USA) and antibiotics (streptomycin 100 mg/ml and penicillin 100 U/ml) (Gibco, USA) , incubated in 37 °C, 5% CO₂.

2.2.2.6 Cells harvesting for RNA extraction

All medium were removed completely, washed with 1x PBS pH 7.2 for 2 times. RNAlater (Ambion) was applied on the cells sufficient enough to cover the dishes or plates surface. The cells were then scrapped, collected in an eppendorf tube

and spun for 10,000 xg for 15 mins. The supernatant was drained and the pellet obtained was kept in -80 °C freezer until further use.

2.2.2.7 Cells harvesting for SDS-PAGE or ³⁵S-radiolabel imaging

All medium were removed completely, washed with 1x PBS pH 7.2 for 2 times. 1x Boiling Mix was applied on the cells sufficient enough to cover the dishes or plates surface. The cells were then scrapped and collected in an eppendorf tube. The lysates were homogenized using 9.5 mm syringe until water-like viscosity was obtained. The lysate obtained was kept in -20 °C freezer until further use. The samples were then loaded and run in SDS-PAGE setup similar to 2.2.1.10 protocol. The gel was then fixed with 10% acetic acid. The gel were then dried and embedded in a filter paper using a gel drier set at 80 °C for 1 hour. The gel were put into Radiolabelling cassette with KODAK O-MAT X-ray film, and incubated at -80 °C for at least overnight (or until satisfactory result was obtained). The X-ray film was then developed in Kodak developer machine.

2.2.3 Immunofluorescence Assay

Each cell line used was seeded into ±50% confluency at coverslips in 24-well plates, infected with the viruses at moi of 3 at various time points, the cells were incubated at 37 °C, 5% CO₂, fixed with 4% paraformaldehyde (w/v) in PBS, permeabilized with 0.1% Triton X-100 in PBS for 10 minutes, followed by incubation antibody targeted against NP protein (Chemicon, USA) with the dilution of 1:200 in PBS as a primary antibody, which were probed using goat anti-mouse fluorescein isothiocyanate (FITC) (Chemicon, USA) with the dilution of 1:100. The coverslips were washed with PBS pH 7.2 three times for 5 minutes in between the incubation

steps. The cells were mounted using Dakocytomation Fluorescence Mounting Medium (Dako, USA) on glass slide, sealed with nail polish and viewed under Nikon Eclipse 80i Microscope with emission of 532 nm.

2.2.4 Plaque Assay

2.2.4.1 Overlay Assay

The monolayers of MDCK in 6-well plate were infected with the viruses in PBS pH 7.2, incubated for 1 hour with shaking every 10 minutes. The virus inoculum were then removed and the cells were overlayed with DMEM (Gibco) and 1% Low Temperature Agarose (Invitrogen), 0.21% BSA (Gibco) and 1 µg/ml trypsin-TPCK (Worthington). The infected cells were incubated in 37 °C, 5% CO₂ for 3-4 days until plaque was visible. Plaque formation was monitored under phase contrast microscope. The plaque numbers were counted and the titres were determined using the formula specified below :

$$Plaque\ titre\left(pfu/ml\right)=\frac{Plaque\ count}{2}\times\frac{1000}{500}\times\frac{1}{dilution\ factor}$$

After the plaque assay we obtained the titre number of A/WSN/33(H1N1) and A/Duck/Malaysia/01 (H9N2) to be 2.0×10^8 pfu/ml and 1.1×10^7 pfu/ml, respectively. The 2009 pandemic strains isolates failed to form plaque in the assay, therefore, we utilized microplaque immunofluorescence assay to quantify the 2009 swine virus titre. This will be elaborated in Section 2.2.4.3.

2.2.4.2 Microplaque Assay

The monolayers of MDCK in 96-well plate were infected with the viruses in PBS pH 7.2, incubated for 1 hour. after which the virus inoculum were removed, and the cells were overlayed with DMEM (Gibco) and 1.2% Avicel RC-591 (FMC Biopolymer), 0.21% BSA (Gibco) and 1 µg/ml trypsin-TPCK (Worthington), and incubated in 37 °C, 5% CO₂ for 24-48 hours, after which the cells were fixed with 4% paraformaldehyde in PBS at room temperature. All subsequent steps of the staining procedure were performed at room temperature and washed with PBS three times. The cells were permeabilized with 0.5% Triton X-100 and 20 mM glycine in PBS, and incubated with primary antibody targeted against NP (Chemicon, USA), and probed with anti mouse Horseradish Peroxidase (Sigma, USA). The monolayers were later stained with 0.4 mg/ml 3-amino-9-ethyl carbazole (Sigma, USA), 0.09% H₂O₂ in 50 mM Acetate buffer.

2.2.4.3 Immunofluorescence Microplaque Assay

The MDCK cells were seeded into 96-well plates until cell confluency was reached. The cells were then infected with swine influenza virus in a serial dilution manner, incubated for 24 hours without the presence of trypsin in order to restrict the infection into single cycle of infection, when one stained virus equals to 1 pfu. The cells were fixed with 4% paraformaldehyde and permeabilized with 0.1% Triton-X. They were stained with influenza anti-NP (Mab 8257) (Chemicon, USA), continued by anti-mouse FITC. The cells were observed under under Nikon Eclipse 80i Microscope with emission of 532 nm. The cells with obvious pattern of influenza virus infection staining were counted and the titre was determined. For comparison, we used

H1N1/A/California/2009 swine influenza virus strain, along with WSN and PR8

H1N1 virus. Using this method, the plaque titre obtained is as follows:

A/Singapore/276/2009(H1N1)	:	4×10^5 pfu/ml
A/Singapore/471/2009(H1N1)	:	7×10^5 pfu/ml
A/Singapore/478/2009(H1N1)	:	6.4×10^5 pfu/ml
A/Singapore/527/2009(H1N1)	:	3.9×10^6 pfu/ml
A/California/7/2009(H1N1)	:	4×10^5 pfu/ml
A/PR/8/34 (H1N1)	:	1.2×10^8 pfu/ml

2.2.4 Growth curve of influenza virus

The cells was seeded into 35 mm-dishes until confluent and infected with the viruses at moi of 0.1, 0.01, and 0.001. The supernatant was harvested every for 72 hours with 12 hours interval, The supernatant in each well would be replaced with fresh media. The virus harvested from the supernatant will be titered using the microplaque assay described above.

2.2.5 [³⁵S]-Methionine Metabolic Radiolabelling

The cells was seeded into 35 mm-dishes until confluent and infected with the viruses at moi of 3. After 6 hpi, the media then was replaced with methionine and cysteine free DMEM (Sigma Aldrich) and incubated for 1 hour. Radiolabelling with ³⁵S will be done by adding the isotope at the concentration of 10 μ Ci/well and incubated for 1 hour. The radiolabelled media was then removed and replaced with infection media. 150 μ l Boiling Mix (1x) was added after the infection media was removed, followed by scrapping the cells and collecting the cell lysate. The lysate was sonicated until the viscosity was approximately similar to water. The lysate were run on SDS-PAGE, followed by gel drying on a filter paper. The gel were then exposed in an X-ray film for 16 hours and then developed and scanned.

2.2.6 Viral Kinetics

2.2.6.1 Cell Infection and Harvesting

Confluent cells were infected with a multiplicity of Infection (moi) of 3 in 35 mm dishes with either H1N1 (A/WSN/1933), or H9N2. Cells were harvested in one hour interval from 0 to 10 hours post infection (hpi) hourly, plus at 24 hpi. Treatment with RNALater™ (Invitrogen, Carlsbad, CA, USA) in 1x PBS was used to help preserve the harvested RNA. The pelleted cells and viruses as well as the supernatant and 1 ml of the corresponding culture medium have been stored immediately at -80°C. The RNA from the harvested samples was extracted using the RNeasy kit (Qiagen, Valencia, CA, USA) according to the manufactures instruction.

2.2.6.2 Reverse Transcription

The extracted RNA amounts were reverse transcribed using the Superscript II Reverse Transcriptase (Invitrogen) according to the manufacturer's instructions. Reverse transcription was performed either for all mRNAs by the use of Oligo d(T) primer (Invitrogen) or for all Influenza A segments by the use of a modified Uni12 primer ("Chan-Primer" or "Uni12(M)") (Hoffmann *et al.*, 2001). The sequence is 5'-AGRAAAAGCAGG-3'.

2.2.6.3 qRT-PCR

The primer list can be seen in A. Real-time PCR was carried out with the LightCycler ® 2.0 System, software version 5.32 (Roche, Mannheim, Germany) and followed the protocol as described by manufacturer. Amplification and detection of viral genes based on a combination of forward and reverse primers plus an 8-mer of

the Universal Probe Library (UPL) (Roche) located within the expected amplification product, generated with the default settings of the recommended Profinder software (<http://qpcr.profinder.com/organism.jsp>). The threshold cycle (C_T) value was determined by “Fit Points Methods” in the software.

The qPCR assays with the samples were optimized with 5 mM $MgCl_2$ and annealing temperature of 55 °C for all primer sets. The 20 μ l of the sample mixture was prepared using the Taq polymerase (Invitrogen) in microcapillary tube. Each tube contains 4 μ l of samples with reagent mixtures as follows : 6.8 μ l dH_2O , 2 μ l 10x Buffer – $MgCl_2$, 2 μ l dNTP 2 μ M, 1 μ l BSA, 1 μ l $MgCl_2$ 50 mM, 1 μ l of each primer (final concentration 0.5 μ M), 1 μ l UPL and 0.2 μ l Taq polymerase. The thermal cycling protocol was as follows: initial denaturation at 95 °C for 10 min, followed by 50 cycles of 10 s at 95°C, 10 s at 55°C and 10 s at 72 °C. The fluorescent signal was measured at the end of the extension step at 72 °C. After the cycling was completed, the samples were cooled down to 40 °C for 30 s.

2.2.6.4 Data Analysis

2.2.6.4.1 Viral kinetics

Relative quantification method was used to quantify the kinetics of vRNA and mRNA of the virus in the cells using the $2^{-\Delta\Delta C_T}$ method as described by Livak and Schmittgen (2001) with the formula as follows:

$$\text{Relative amount (at x hpi)} = (2)^{-\Delta\Delta C_T}$$

The C_T value denotes the number of cycles needed for the system to detect fluorescence signal of the amplification product with the assumption of 2 fold increase in each cycle. The calculation was done as follows:

1. Determine the ΔC_T value with the formula C_T of the sample - C_T of elongation factor,
2. Determine $\Delta\Delta C_T$ value with the formula ΔC_T of sample from (1) - ΔC_T of sample at 10 hpi

All time points will be measured in relative to 10 hpi time point. The elongation factor of the respective cell lines was used to normalize the relative calculation of each time point.

2.2.6.4.2 Copy number of M genes

The combination of absolute and relative quantification methods were used to calculate the copy number of M gene in each experiment. (Klein, 2002; Livak and Schmittgen, 2001). The method of calculated will be described below.

2.2.6.4.3 Construction of Standard Curve

For the M gene, PCR amplification of M full length is generated as a template for the standard curve. For the Elongation Factor gene, A fragment of elongation factor of each cell line with size approximately 337 bp, 466 bp and 350 bp for canine, chicken and human, respectively, was generated as a template for measurement to construct a standard curve. The fragments were PCR amplified using the HiFi Platinum Taq polymerase (Invitrogen). The fragments were then gel purified and measured in ng. A 10-fold dilution series up to 10^7 times dilution of the fragment was generated to be measured. The amount of the fragment used in ng was converted to copy number using the formula as follows (Whelan *et al.* 2003) :

$$DNA (M \text{ copy}) = \frac{6.02 \times 10^{23} \text{ copy/mol} \times DNA \text{ amount (g)}}{DNA \text{ length (bp)} \times 660 \text{ (g/mol/bp)}}$$

The C_T values in each dilution were measured in duplicate using a real time qPCR to generate the standard curve. The C_T values were plotted against the logarithm of the copy number. Standard curve of M and elongation factor gene were generated by a linear regression of the plotted points. For the slope of each standard curve, the amplification efficiency was performed to ensure that the M and elongation factor is comparable (Rasmussen, 2001). From the standard curve, the conversion from C_T value to copy number was obtained.

2.2.6.4.4 Copy number calculation

The copy number of the M gene from the samples at 10 hpi will be calculated first in relative to 10^4 copy numbers of the corresponding cell lines elongation factor as a basis of normalization. For the rest of the time points, relative quantification methods was used in relative to the 10 hpi samples as base-line calculation. It is also necessary to normalize this result with the 10^4 copy numbers of elongation factor at corresponding time points.

2.2.7 cDNA Microarray

2.2.7.1 Experimental Design and Preparation

Each cell line was seeded into two 100-mm dishes until confluent and infected and incubated with the viruses at the moi of 3 with several time points with 2-hour interval, which will represent the viral entry, nuclear localization and nuclear export of the virus in the cells. The dishes were washed with sterile PBS for two times to remove media and unbound virus particles, 0.5x RNAlater (Ambion) in PBS were applied for the dishes and the cells were scrapped, pooled and aliquoted, which was spun at 10,000 rpm ($9,300 \times g$) for 10 mins in table-top microcentrifuge. The RNAlater

was removed and the aliquots were stored on -80 °C immediately. Each of the experiment was done in triplicates. All harvesting were done in 4 °C.

The cells were later extracted using RNAeasy Mini Kit (Qiagen). Prior to cDNA and cRNA synthesis, the quality of the RNA sample for hybridization was checked with the clear bands of rRNA in agarose gel and the value of $A_{260/280}$ was between 1.9 – 2.2. Three µg of the RNA samples were used to synthesize biotin-labelled cRNA and hybridized into GeneChip® Canine Genome 2.0 Array for MDCK, GeneChip® Chicken Genome Array for CEF and GeneChip® Human Genome U133 for A549 according to the manufacturer protocols (Affymetrix). The samples were washed and stained in GeneChip® Fluidic Station 450 using Hybridization Wash and Stain Kit (Affymetrix) and scanned on GeneChip® Scanner 3000.

2.2.7.2 Data Analysis

GeneChip® Operating Software was used to collect the intensity signal of each gene in the experiments, which were then processed using Genespring 7.3.1. Firstly, the data was normalized using external genes control or spike-in normalization, which includes *dap*, *lys*, *phe* and *thr* for Poly-A controls to normalize cRNA synthesis variability, and *bioB*, *bioC*, *bioD* and *cre* for Hybridization controls to normalize chip hybridization variability. After the signal intensity of each chip was normalized, the data sets were normalized to mock to obtain the fold-change value. The genes from the data set were considered significantly changed if there were more than 2-fold changes in at least two out of three replicate experiments with the False Discovery Rate less than 0.05, using Benjamini-Hochberg False Discovery Rate, and the p-value was less than 0.05. The genes from the data set were considered unchanged across time-points

if there were less than 0.3-fold changes in at least two out of three replicates. The members of genes were grouped based on biological function and cellular component as annotated by Gene Ontology (GO) SLIMS.

2.2.7.3 Confirmatory Experiment

2.2.7.3.1 qRT-PCR

The fold-change of the genes of interest was further measured for verification purpose using qRT-PCR. The RNA samples from the Mock and 10 hpi time point was reverse transcribed as described in the section 2.2.5.1 and qPCR was performed as described in the section 2.2.5.2. Each sample was run in duplicates. The fold change value was obtained using the relative quantification method as described in section 2.2.5.3.1.

2.2.7.3.2 Western Blotting

The cells were seeded until confluency in 35 mm dish, infected with the virus with the moi of 3. The media was removed, and the cells were treated with 1 mM sodium orthovanadate and 50 mM sodium fluoride in PBS for 30 mins. The solution was then removed and 1x Boiling Mix was applied to the cells. The cells were scrapped, collected in the eppendorf tube and sonicated when necessary. The samples were ready to be processed for separation by SDS-PAGE and Western Blotting, with the protocols described previously.

2.2.8 Cytokine Assay

Supernatant from the macrophages during the infection time was collected and stored at -20 °C. Before the cytokine assay, the stored suspension was centrifuged at 1000 rpm for 10 mins after thawing. After that the supernatant was used for cytokine

assay according to the manufacturer's instructions. Cytokines present in the media were analyzed with the Bio-Plex Protein Array System (BioRad) using the Bio-Plex Mouse Cytokine 23-Plex Panel (1 x 96-well, # M60009RDPD, Bio-Rad), including antibodies for interleukin (IL) family members (IL1 α , IL1 β , IL2, IL3, IL4, IL5, IL6, IL9, IL10, IL12 (p40), IL12 (p70), IL13, IL17], Eotaxin (CCL11), granulocyte colony-stimulating factor (GCSF), granulocyte-macrophage colony stimulating factor (GMCSF), interferon γ (IFN γ), keratinocyte-derived chemokine (KC), monocyte chemoattractant protein 1 (MCP1, CCL2), macrophage inflammatory protein 1 α (MIP1 α , CCL3), MIP1 β (CCL4), RANTES (Regulated upon Activation, Normal T-cell Expressed and Secreted; CCL5), and tumour necrosis factor α (TNF α). The levels of these cytokines were measured for infected and mock cells at different time points.

Chapter Three. Sequence Analysis of H9N2 isolates

The outbreak of avian influenza virus in both wild and domesticated birds had been monitored over past decade. The first detection of the H9N2 was from turkeys in Wisconsin in 1966 (Homme and Easterday, 1970). In North America, many of the H9N2 viruses were detected in gulls and wild ducks (Kawaoka *et al.*, 1988; Shaw *et al.*, 2002), but no H9N2 viruses have been reported in chickens in North America (Perez *et al.*, 2003). Mostly, the emphasis has been put on the avian influenza virus strain H5 and H7. It has been shown that both of those subtypes have the ability to adapt and infect non-avian species and to mutate from LPAI to HPAI variant. Although no high pathogenic variant of the H9 strain has been discovered yet. it has shown the ability to infect human, both in China and Hong Kong (Guo *et al.*, 1999; Peiris *et al.*, 1999). The study of the occurrence of H9N2 influenza virus, together with the molecular characterization of the currently circulating H9N2 will be critical to assess their replication, pathogenicity and pandemic potential. H9N2 has been endemic in many Asian countries causing economic loss to poultry industry by egg reduction and approximately 30% of mortality rate in chicken.

In Singapore area, Agri-Food and Veterinary Authority of Singapore (AVA) conducted the routine surveillance and isolation of currently circulating avian influenza virus, including imported poultries, on the annual basis. In this chapter, the characterization of A/Duck/Malaysia/01 (H9N2) was conducted in order to gain more information about the H9 strain of virus, since there is no characterization of the H9 strain done in the region. The characterization and analysis of the A/Duck/Malaysia/01 (H9N2) consists of phylogenetic tree analysis, and protein sequence analysis. From the information given, we will be able to assess the virus origin, species specificity, and

pathogenicity. The molecular characterization was assessed on all eight genes and eleven proteins. These sequences will be further compared with highly pathogenic avian influenza strain, laboratory-adapted strain and human-infected H9N2 strain in order to elaborate further on each gene sequence and its function. It should be noted that different H9N2 subtypes have different combination of internal genes, for example H9N2 with H5N1 internal genes in China (Zhang et al, 2009), H9N2 subtypes with H7N3 and H5N1 internal genes originating from Pakistan (Iqbal *et al.*, 2009).

The aim of the phylogenetic analysis comparison done in this chapter is to determine the origin and lineage of the virus. The origin determination and lineage grouping is important to access reassortment and spreading pattern of the virus. Furthermore, host signature and epitope binding sites are also investigated. This allows the study of amino acid associated with host adaptation in order to determine the probability of antibody escape mutation, host adaptation, and interspecies transmission. More importantly, drug resistance mutation associated amino acids is also accessed to confer the isolate ability to resist currently circulating drugs. Together, this information is critical for assessing the pandemic potential of the H9N2 virus itself.

3.1 Nucleotide and Amino Acid Sequence Similarity Comparison

Each gene of the A/Malaysia/01(H9N2) isolate was sequenced and analyzed for closest similarity with other strains of influenza virus stored in GeneBank using BLAST program by NCBI (<http://www.ncbi.nlm.nih.gov/blast/Blast.cgi>). The three subtypes with highest Max Score are shown in Table 3.1. The sorting of the highest similarity is based on the Max Score, which determined by how many similar

nucleotides in the sequences compared and the length of the gene covered for the comparison. The E-value (or Expect value) is a parameter that calculates the amount of hits one can expect to see just by chance when searching a database of a particular size. It decreases exponentially with the total score that is assigned to a match between two sequences. The high E-value also describes the high random background noise that exists for matches between sequences. In this experiment, low E-value denotes high similarity and low random background noise in the sequence comparison.

Based on the nucleotide sequence similarity analysis presented on Table 3.1, we can observe that all genes of the H9N2 isolate have highest similarity with the avian influenza virus strain in both Hong Kong and China, with the exception of NP and NS which originated from European avian influenza virus strain. All of the internal genes (NS, M, PA, PB1 and PB2) generally have high percentage of identity compared to the other similar isolates. Further, we can also observe that the three highest similarity sequence picked up by BLAST result belongs to avian influenza virus groups.

Based from the finding above, this suggests that the H9N2 isolate most likely reassorted and obtained its gene exclusively from other influenza virus strains. Furthermore, it also shows that based from BLAST search the reassortment most likely occurred in East Asia area and Taiwan. For NP and NS genes, there is a probability that H9N2 isolate obtain during the migration of the waterfowls which occur during seasonal change in the Northern Hemisphere, based from the sequence similarity information.

Table 3.1 Nucleotide comparison of eight genes of A/Malaysia/01(H9N2) with the three most similar isolates from GenBank

NS

Accession	Description	Max score	Total score	Query coverage	E value	Max ident
DQ376771.1	A/duck/Taiwan/WB29/99(H6N1)	1583	1583	100%	0.0	98%
DQ251446.1	A/mallard/Denmark/64650/03(H5N7)	1578	1578	100%	0.0	98%
FJ432766.1	A/duck/Italy/194659/2006(H3N2)	1572	1572	100%	0.0	98%

M

Accession	Description	Max score	Total score	Query coverage	E value	Max ident
EF681873.1	A/chicken/Taiwan/2838N/00(H6N1)	1773	1773	99%	0.0	97%
GU052803.1	A/duck/Singapore/F119/3/1997(H5N3)	1757	1757	94%	0.0	98%
DQ376657.1	A/chicken/Taiwan/0824/97(H6N1))	1753	1753	97%	0.0	97%

NP

Accession	Description	Max score	Total score	Query coverage	E value	Max ident
CY064951.1	A/mallard/Netherlands/5/1999(H2N9)	2562	2562	98%	0.0	96%
CY015118.1	A/chicken/Italy/312/1997(H5N2)	2543	2543	99%	0.0	95%
FJ750568.1	A/chicken/Belgium/150VB/1999(H5N2)	2542	2542	99%	0.0	95%

NA

Accession	Description	Max score	Total score	Query coverage	E value	Max ident
DQ092870.1	A/Pekin duck/Singapore/F59/04/98(H5N2)	2316	2316	96%	0.0	95%
CY005532.1	A/duck/Nanchang/1749/1992(H11N2)	2287	2287	99%	0.0	94%
HM144566.1	A/duck/Shantou/83/2000(H6N2)	2228	2228	95%	0.0	95%

HA

Accession	Description	Max score	Total score	Query coverage	E value	Max ident
CY005632.1	A/duck/HK/784/1979(H9N2)	2287	2287	99%	0.0	90%
AY206673.1	A/duck/Hong Kong/448/78(H9N2)	2239	2239	95%	0.0	90%
CY005639.1	A/duck/HK/147/1977(H9N6)	2178	2178	99%	0.0	89%

PA

Accession	Description	Max score	Total score	Query coverage	E value	Max ident
CY005451.1	A/Chicken/Nanchang/7-010/2000(H3N6)	3808	3808	100%	0.0	97%
CY005458.1	A/Quail/Nanchang/7-026/2000(H3N6)	3797	3797	100%	0.0	97%
EF597428.2	A/migratory duck/Jiang Xi/8624/2004(H6N2)	3757	3757	98%	0.0	97%

PB1

Accession	Description	Max score	Total score	Query coverage	E value	Max ident
CY005477.1	A/duck/Nanchang/1941/1993(H4N4)	3964	3964	99%	0.0	97%
CY005443.1	A/Duck/Nanchang/4-184/2000(H2N9)	3792	3792	99%	0.0	95%
CY005474.1	A/duck/Nanchang/1681/1992(H3N8)	3786	3786	99%	0.0	95%

PB2

Accession	Description	Max score	Total score	Query Coverage	E value	Max ident
DQ376879.1	A/duck/Taiwan/WB29/99(H6N1)	3986	3986	98%	0.0	97%
DQ376878.1	A/chicken/Taiwan/165/99(H6N1)	3975	3975	98%	0.0	97%
CY005453.1	A/Chicken/Nanchang/7-010/2000(H3N6)	3973	3973	98%	0.0	97%

Note :

Max Score, and Total Score denotes level of similarity among the compared sequences,

Query Coverage denotes the percentage of the H9N2 sequence length covered in this comparison

E value denotes the degree of similarity among the compared sequences, low value denotes very similar sequence

Max identity denotes the percentage of similarity among the compared sequences

3.2 Phylogenetic and amino acid sequence analysis

In order to characterize the isolate A/duck/Malaysia/01(H9N2) phylogenetic tree construction was performed. Sequence data of other influenza virus strains representing particular regional groups were also used to determine the clustering of the isolate A/duck/Malaysia/01(H9N2). The grouping pattern on the isolate A/duck/Malaysia/01(H9N2) in the phylogenetic tree will provide clues on the origin of the virus.

The amino acid sequence analysis was performed to access several important aspects of the isolate A/duck/Malaysia/01(H9N2), including host signatures, epitope binding sites and drug resistance mutations. The sequence obtained was compared with A/WSN/33 strains and human derived H9N2, and HPAI H5N1 viruses to assist sequence characterization of the isolate A/duck/Malaysia/01(H9N2).

3.2.1 Non-structural protein (NS)

From the phylogenetic tree (Fig. 3.1), it could be seen that some of the H9N2 strain in China and Hong Kong clustered together with the highly pathogenic H5N1 lineage from the same area. However, the isolate A/duck/Malaysia/01(H9N2) clustered together with European strains of influenza virus. The isolate A/duck/Malaysia/01(H9N2) also clustered separately from A/WSN/33 (H1N1) and “Spanish Flu” strain, and H5N1 high pathogenic strain. Both H9N2 and A/WSN/33 (H1N1) fell into Allele A class of non-structural genes. Allele A and Allele B are main group of NS based on the clustering pattern, which is discussed in Section 1.2.6.

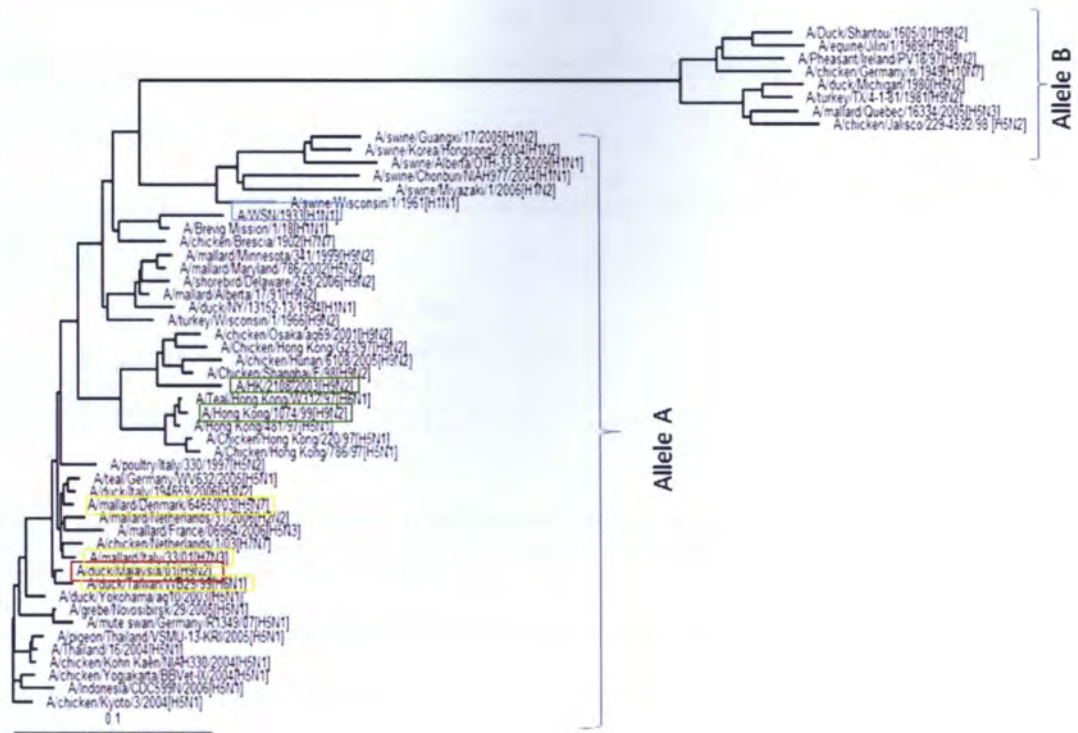


Fig. 3.1 Phylogenetic tree of non-structural (NS) genes. The red box denotes A/Duck/Malaysia/01 (H9N2), green box denotes human H9N2 virus, yellow box denotes the strains from BLAST search, and blue box denotes A/WSN/33(H1N1) indicates the isolate used in the experiment. The 0.1 with a line beneath denotes 10% nucleotide difference per line length.

The comparison of NS1 protein of the isolate A/duck/Malaysia/01(H9N2) with other reference strains is shown below (Fig. 3.2). The nuclear localization signal (NLS) on amino acid position 34-38 of H9N2 isolate has the sequence of –DRLRR–motif, which is typical to the allele A NS1, in which the A/WSN/33(H1N1) also belongs to (Suarez *et al.*, 1998). The isolate A/duck/Malaysia/01(H9N2) also contains R38 and K41, which is critical for dsRNA binding activity and interferon antagonist (Wang *et al.*, 1999; Donelan *et al.*, 2003). All of the The H9N2 isolate has the NLS sequence motif of 216–PKQKRK–221. There are no deletions of the NS1 protein on H9N2 protein, as observed in HPAI A/Ck/Indonesia/PA/2003(H5N1). Deletions on amino acid position 80-84, as reported by Long *et al.* (2008), contributed to the pathogenicity.

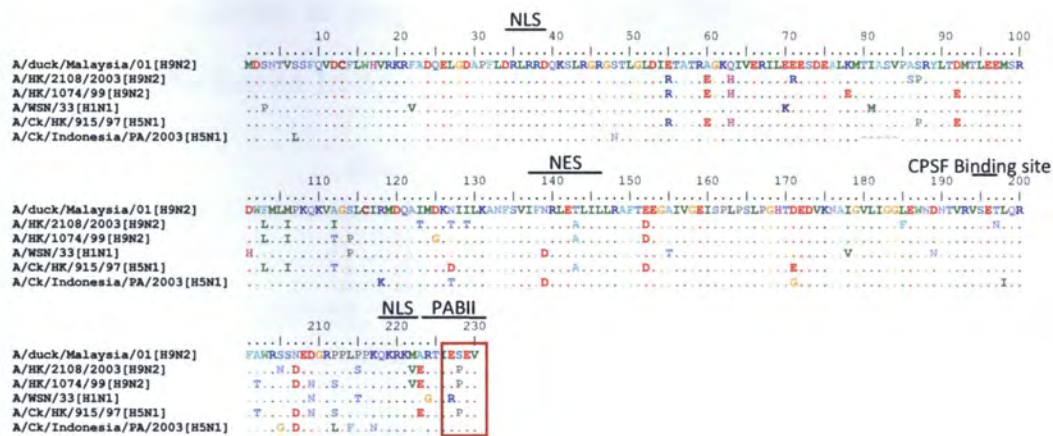


Fig. 3.2 Amino acid sequence NS1 from A/Duck/Malaysia/01(H9N2) compared to human derived H9N2 and H5N1 avian influenza virus sequence. Note the important domains location as marked by an underline on the numbering. Also note the red box which shows PDZ domain.

The isolate A/duck/Malaysia/01(H9N2) possesses 3 hydrophobic residues at 144L, 146L and 147L, which is similar to the nuclear export signal sequences found by Gorlic and Mattaj (1996). The NS1 protein also contains 186E, which is similar to all of the reference strains shown (Fig. 3.2). The isolate A/duck/Malaysia/01(H9N2) contains –ARTIESEV sequence motif at PABII binding domain. The PDZ domain, which lies inside the PABII binding domain at amino acid position 227-230 is attributed to influence various signalling pathways, mostly immunological pathways. The PDZ domain of human influenza viruses has the pattern of either KSEV, RSEV or EPEV (Sheng and Sala, 2001). The H9N2 strains derived from humans, A/HK/2108/2003 (H9N2) and A/Hong Kong/1074/99 (H9N2), as shown above, contain human motif EPEV and A/WSN/33(H1N1) shows RSEV motif.

The comparison of the NS2 protein of the isolate A/duck/Malaysia/01(H9N2) with human derived H9N2, and other reference strain is shown in Fig. 3.3. The isolate A/duck/Malaysia/01(H9N2) and all other isolates contain 78W which is critical for its ability to bind with M1 for the nuclear export. The nuclear export signal of the isolate A/duck/Malaysia/01(H9N2) contains 2 hydrophobic residues at position 13L and 21L

to confirm its ability to undergo nuclear export. This ability has been discussed previously (See Section 1.2.6).

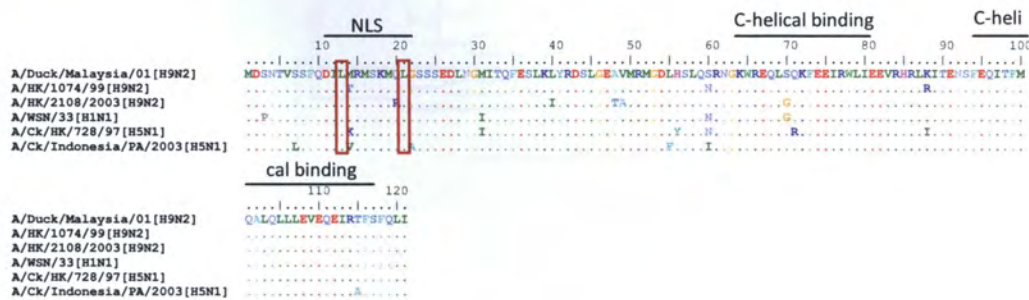


Fig. 3.3. Amino acid sequence NS2 from A/Duck/Malaysia/01 (H9N2) compared to human derived H9N2 and H5N1 avian influenza virus sequence. Note the domains location as marked by an underline on the numbering. Note the red box indicated above with shows important sequence for nuclear export

3.2.2 Matrix Protein (M)

Based from the phylogenetic tree of matrix gene (Fig. 3.4), it can be concluded that the level of conservation of the M gene among influenza A virus is high. The M gene of H9N2 avian influenza virus in Asia, particularly in China and Hong Kong virus, have been grouped into three sub-lineages, based from the region they dominate : Y439 like lineage, G1 like lineage and Y280 like lineage (Guan *et al.*, 1999; Xie *et al.*, 2008). The H9N2 isolate clustered together in the Y439 like sub-lineage. This suggests that M gene of the isolate A/duck/Malaysia/01(H9N2) most likely came from avian influenza virus gene pools in Taiwan, and human derived H9N2 M gene most likely came from Northern China.

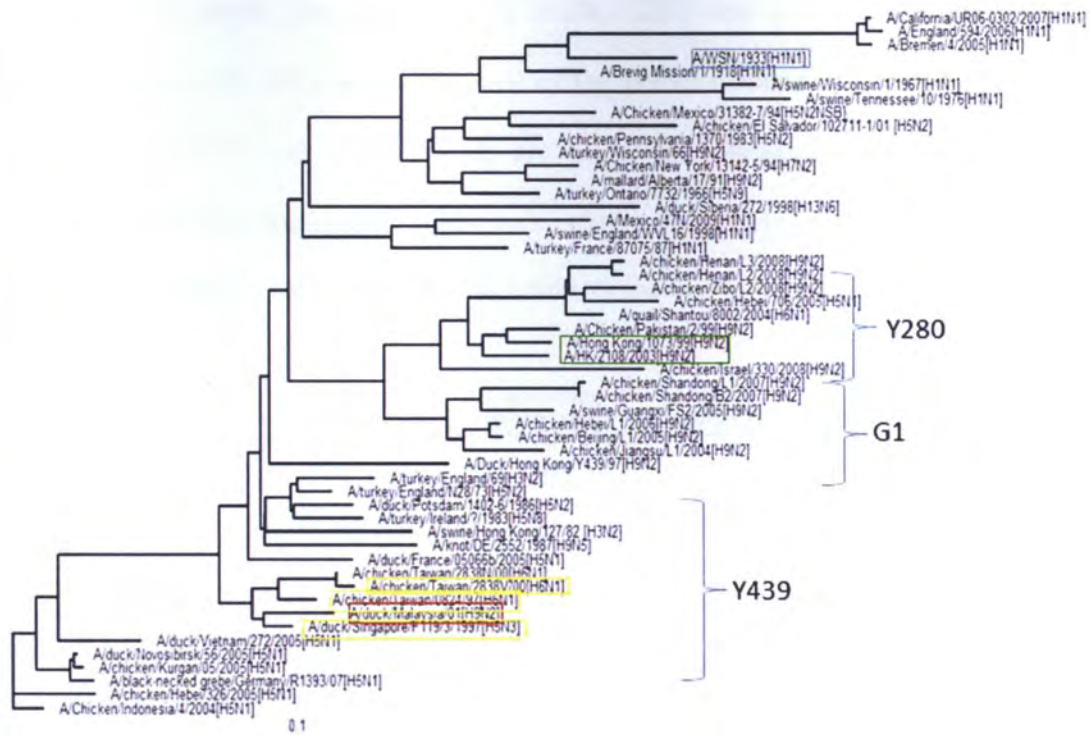


Fig. 3.4. Phylogenetic tree of matrix (M) genes. The red box denotes A/Duck/Malaysia/01 (H9N2), yellow box denotes strains from BLAST search, green box denotes human H9N2 virus and blue box denotes A/WSN/33(H1N1) indicates the isolate used in the experiment. The 0.1 with a line beneath denotes 10% nucleotide difference per line length.

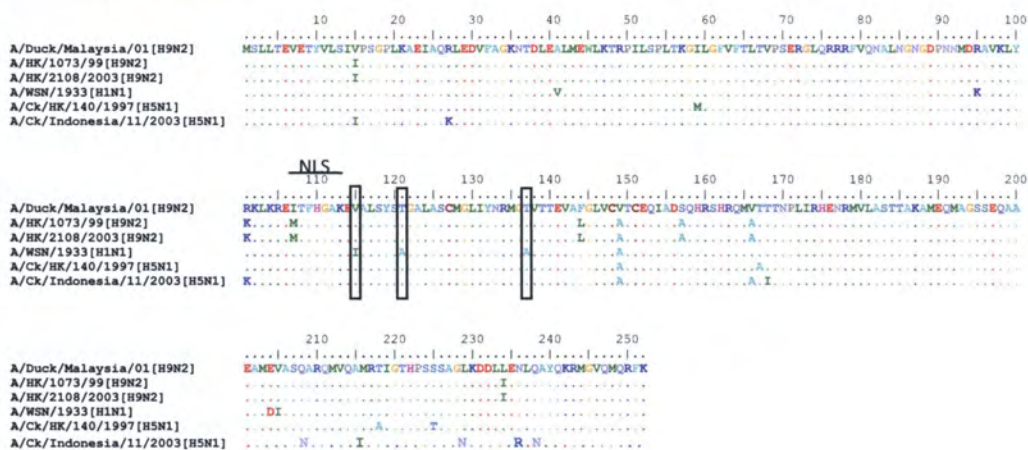


Fig. 3.5 Amino acid sequence M1 from A/Duck/Malaysia/01(H9N2) compared to human and avian influenza virus sequence. Note the domain location as marked by an underline on the numbering.

The amino acid sequence alignment of M1 and M2 proteins are shown in Fig. 3.5 and Fig. 3.6, respectively. According to Shaw *et al.*, (2002) and Chen *et al.*, (2006), host signatures in the M1 protein are located in the amino acid positions 115,

121 and 137. Avian has signatures of 115V, 121T and 137T, while human has signatures of 115I, 121A and 137A. All of the H9N2 isolates compared in Fig. 3.5 have 115V, 121T and 137T, which are all avian signatures. As expected, the A/WSN/33 (H1N1) possesses human-like signature 115I, 121A and 137A.

Table 3.2. Host signature of M protein in influenza A virus (Gorman *et al.*, 1990; Shaw *et al.*, 2002; Chen *et al.*, 2006).

Position	Avian Signature	Human Signature	A/Duck/Malaysia /H9N2(2001)	A/HK/1073/ 1999(H9N2)	A/HK/2108/ 2003(H9N2)	A/WSN/33 (H1N1)
11	T	I	T	T	T	I
16	E	G	E	E	E	G
20	S	N	S	(R)	S	N
55	L	F	L	(F)	(F)	F
57	Y	H	Y	Y	Y	Y
78	Q	K	Q	Q	Q	K
86	V	V	V	V	V	V

Note : Residues in parenthesis denotes human signatures

The host signature of the M2 protein lies in the amino acid position 11, 16, 20, 55, 57, 78, and 86, as shown in Table 3.2. Avian signatures have 11T, 16E, 20S, 55L, 57Y, 78Q, and 86V amino acids in the position mentioned above, respectively. Human signatures have 11I, 16G, 20N, 55F, 57H, 78K, and 86V, respectively. The H9N2 isolate contain all amino acids belonging to the avian signature. A/Hong Kong/1073/99(H9N2) contains two human signatures F55 and R20. A/HK/2108/2003(H9N2) contains one human signature amino acid 55F as well. The laboratory strain A/WSN/33 (H1N1) contains I10, G16, N20, F55, Y57, K78 and V86. All of those amino acid signatures belong to human signatures, with the exception of Y57, which belongs to avian signatures.

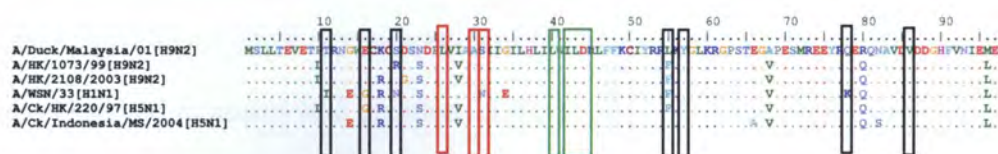


Fig. 3.6. Amino acid sequence M2 from A/Duck/Malaysia/01 (H9N2) compared to human and avian influenza virus sequence. The host signatures are marked by a black box. Amantadine resistance mutation sites are marked by red box. Rimantadine resistance mutation sites are marked by green box.

Another point of interest of doing sequence analysis of the RNA segment 7 is the amantadine drug resistance mutation (see Section 1.2.5 and 1.5.2.2). The M2 protein of all isolates compared in Fig 3.6 possess the L26, A30 and S31 which is the critical amino acid to exhibit amantadine resistance (Hay *et al.*, 1986). In the same time, all isolates showed above also exhibit rimantadine resistance, marked by L40, I42, and L43 (Pielak *et al.*, 2009)

3.2.3 Neuraminidase (NA)

From the phylogenetic tree of the NA gene shown (Fig. 3.7), the isolate A/duck/Malaysia/01(H9N2) clustered together most closely with avian influenza virus of the Eurasian geographical region. Together with the human infected H9N2, this clustering is also similar with that for the M gene.

The amino acid sequence of NA protein sequence comparison is shown below (Fig. 3.8). A close examination of the isolate A/duck/Malaysia/01(H9N2) NA protein reveals that it does not have a stalk deletion, which is observed in highly pathogenic strain A/ck/Pennsyl/1370/1983(H5N2) at the amino acid position of 63 - 82. The stalk deletion of the NA protein is known to be associated with virulence in avian, as they can infect the intestinal area due to the pH resistance (Castruci and Kawaoka, 1993; Zhou *et al.*, 2009). Another important feature of the NA protein is concerning the oseltamivir resistance mutation (see Section 1.5.1.2). The potential oseltamivir resistant sites of the isolate A/duck/Malaysia/01(H9N2) and the other isolates compared do not show any indication of oseltamivir, and peramivir resistant mutation, as observed at amino acid position 119E, 152R, 274H and 293R. These amino acids are located at the the sialic acid binding site in the NA protein (Kobasa *et al.*, 1999; 2001). Also, there is no Q136K mutation observed in all the strains below which confers to zanamivir resistance (Hurt *et al.*, 2009).

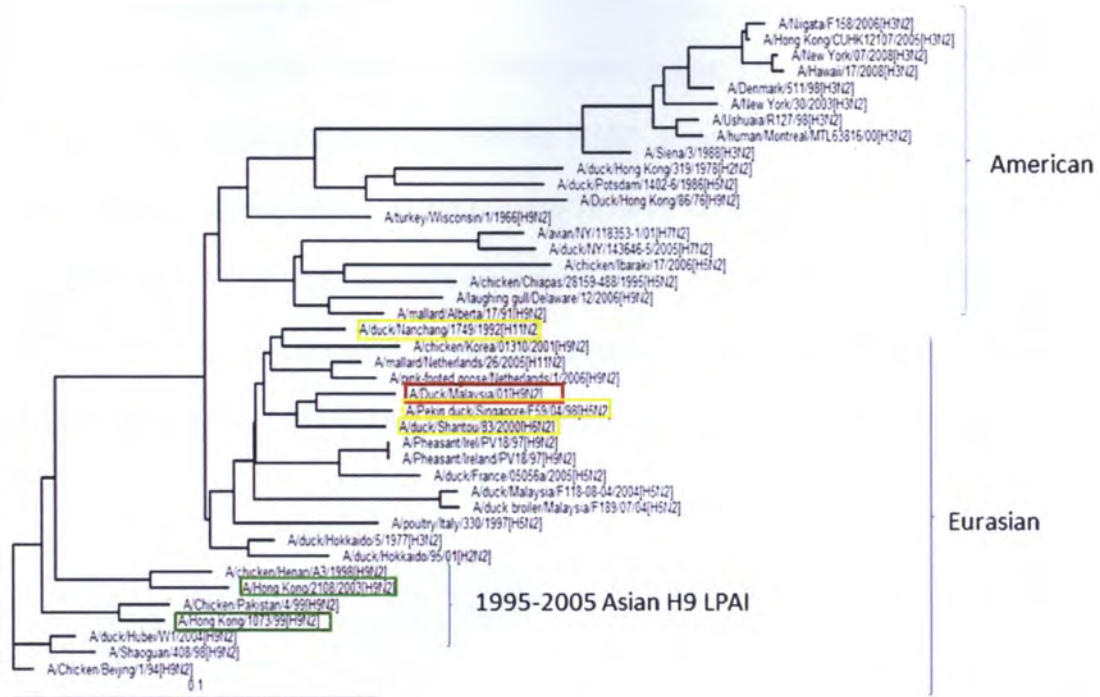


Fig. 3.7. Phylogenetic tree of neuraminidase (NA) gene. The red box denotes A/Duck/Malaysia/01 (H9N2), yellow box denotes strains from BLAST search and green box denotes human H9N2. The 0.1 with a line beneath denotes 10% nucleotide difference per line length.

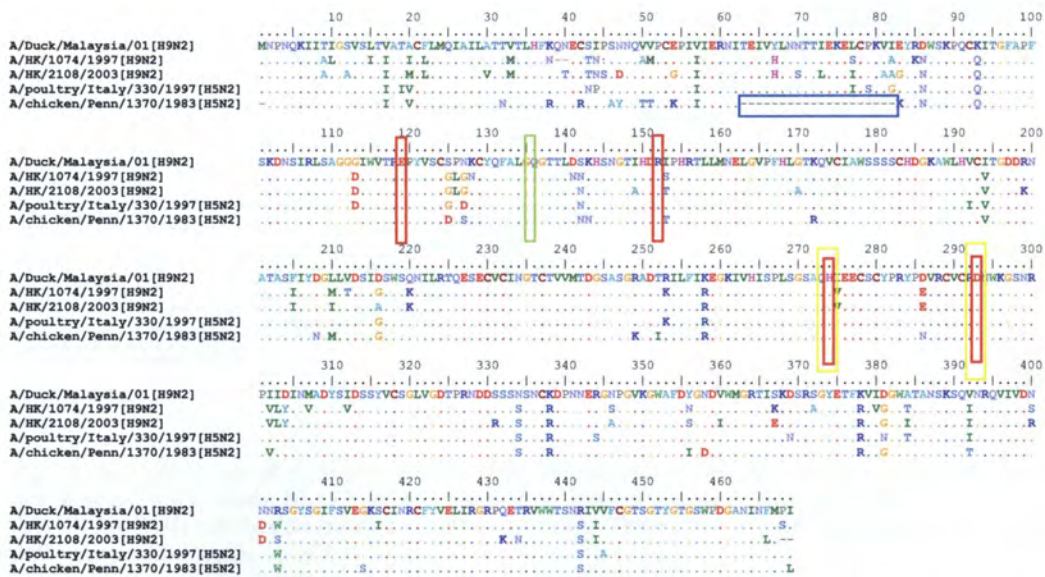


Fig. 3.8. Amino acid sequence NA from A/Duck/Malaysia/01(H9N2) compared to other avian and human influenza virus sequence. Stalk deletion is marked by blue box. Oseltamivir resistance mutation sites are marked by red box. Peramivir mutation sites are marked with yellow box. Zanamivir resistance mutation sites are marked by green box.

3.2.4 Nucleoprotein (NP)

From the phylogenetic tree analysis shown in Fig. 3.9, the A/Duck/Malaysia/01 (H9N2) isolate clustered together with the H5N2 strain of LPAI isolated in Europe area. Human-isolated H9N2 A/Hong Kong/1074/99 (H9N2) clustered together with the HPAI H5N1 1997, and the other human-isolated A/HK/108/2003 (H9N2) did not show any clustering pattern. It can be concluded that the NP gene from the A/Duck/Malaysia/01 (H9N2) most likely derived from the European strain of AIV.

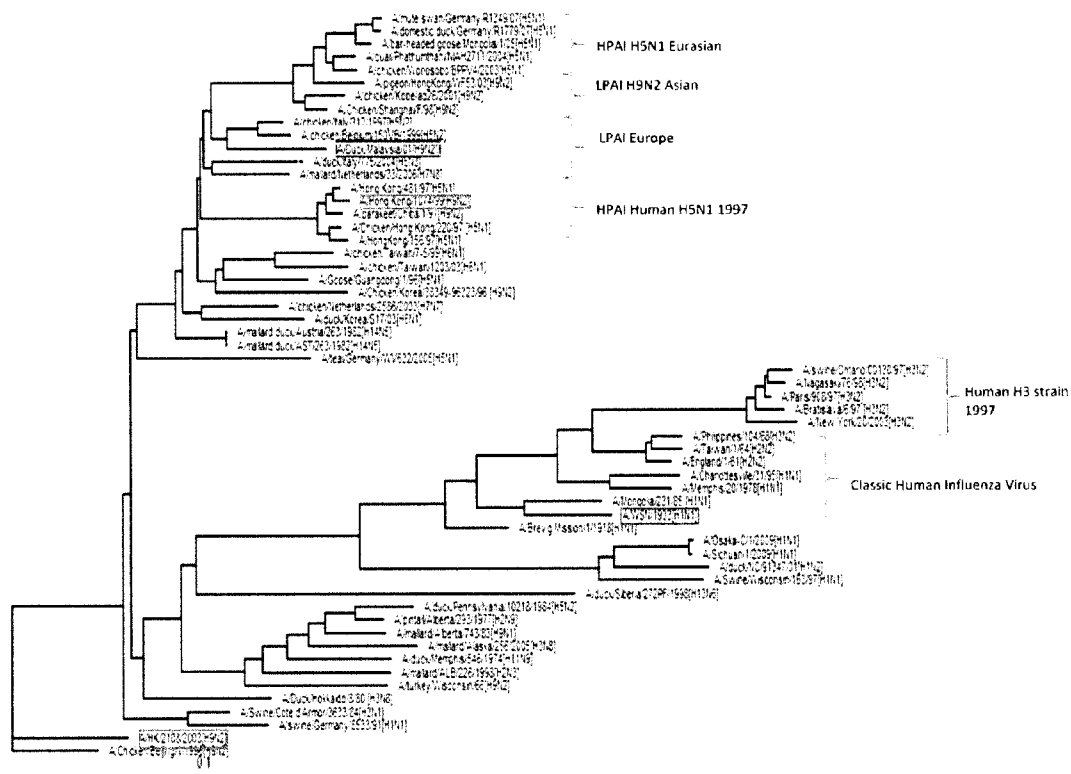


Fig 3.9 Phylogenetic tree of nucleoprotein (NP) genes. The red box denotes A/Duck/Malaysia/01 (H9N2), yellow box denotes strains from BLAST search, green box denotes human H9N2 virus and blue box denotes A/WSN/33(H1N1) indicates the isolate used in the experiment. The 0.1 with a line beneath denotes 10% nucleotide difference per line length.

The amino acid sequence comparison of the isolates is shown in Fig. 3.10. As mentioned earlier, there are 19 positions on NP protein that are associated with host

signatures (Table 3.3). Based on the list below, the entire host signatures of the isolate A/Duck/Malaysia/01(H9N2) belong to avian signatures. This confirms the specificity of the isolate A/Duck/Malaysia/01(H9N2) to avian host. This finding is unlike that for human derived A/HK/1074/1999(H9N2), which contained one human signature at position 136, while the rest belong to avian signatures. The HPAI A/Chicken/HK/220/97(H5N1) also contains similar to the human signature at amino acid position 136. This implication also suggests that both A/HK/1074/1999 (H9N2) and HPAI A/Chicken/HK/220/97 (H5N1) have the potential to be adapted for human transmission.

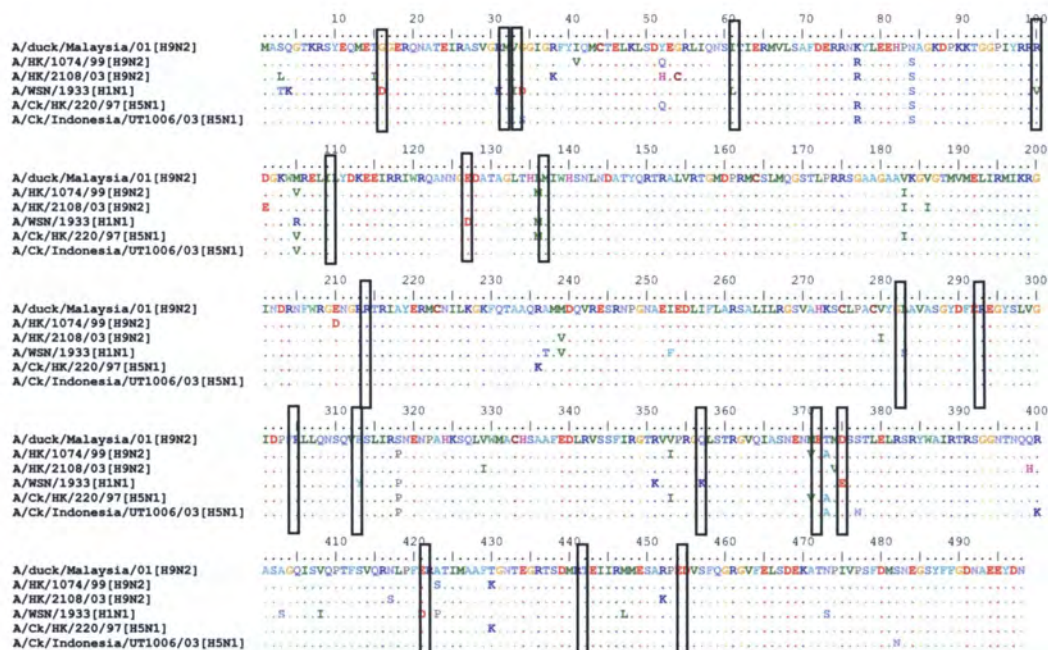


Fig.. 3.10 Amino acid sequence NP from A/Duck/Malaysia/01 (H9N2) compared to other avian influenza virus sequence. Host signature is marked with black box.

Table 3.3 Host signature of NP protein in influenza A virus (Gorman *et al.*, 1990; Shaw *et al.*, 2002; Chen *et al.*, 2006).

Position	Avian Signature	Human Signature	A/Duck/Malaysia /H9N2(2001)	A/HK/1074/ 1999(H9N2)	A/HK/2108/ 2003(H9N2)	A/WSN/33 (H1N1)
16	G	D	G	G	G	(D)
31	R	K	R	R	R	(K)
33	V	I	V	V	V	(I)
61	I	L	I	I	I	(L)
100	R	V	R	R	R	(V)
109	I	V	I	I	I	I
127	E	D	E	E	E	(D)
136	L	M	L	(M)	L	(M)
214	R	K	R	R	R	R
283	L	P	L	L	L	S
293	R	K	R	R	R	R
305	R	K	R	R	R	R
313	F	Y	F	F	F	(Y)
357	Q	K	Q	Q	Q	(K)
372	E	D	E	E	E	E
375	D	G/E	D	D	D	(E)
422	R	K	R	R	R	R
442	T	A	T	T	T	T
455	D	E	D	D	D	D

Note : Residues in parenthesis denotes human signatures

3.2.5 Hemagglutinin (HA)

Guo *et al.*, (1997) classified the H9 HA distributions in Central China region into three sub-lineages, based from the regions of China they dominate: Y280-like strain, G1-like strain and G9-like strain. From the phylogenetic tree analysis (Fig. 3.11), the human-derived H9N2 A/Hong Kong/1073/99 (H9N2) could be grouped into G1-like strain, which clustered together with Western Asia and Middle East H9 strain. A/Duck/Malaysia/01 (H9N2), however, did not cluster together with these sub-lineages. It clustered together with the 1979 Hong Kong strain. This suggests that the HA gene from A/Duck/Malaysia/01 (H9N2) might be derived from classic H9 strain originated in Hong Kong.

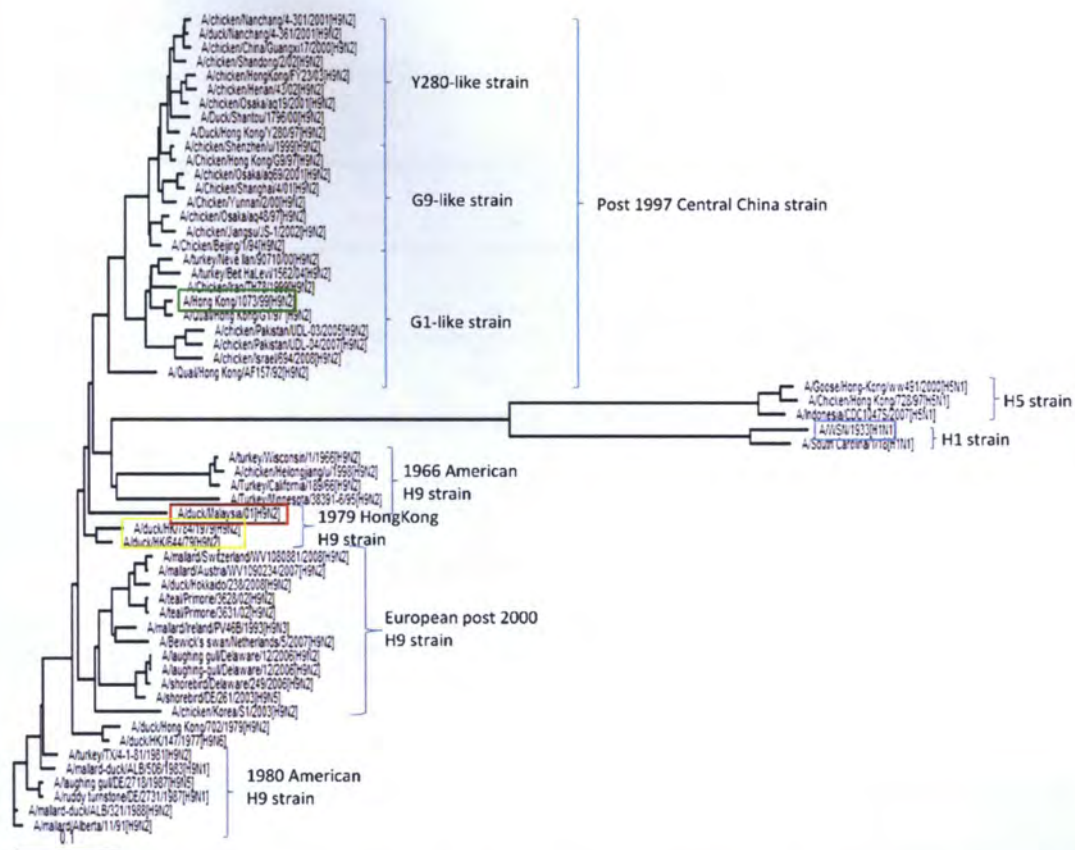


Fig. 3.11 Phylogenetic tree of hemagglutinin (HA) genes. The red box denotes A/Duck/Malaysia/01 (H9N2), yellow box denotes strains from BLAST search and green box denotes human H9N2 virus. The 0.1 with a line beneath denotes 10% nucleotide difference per line length.

The potential N-linked glycosylation sites of influenza viral HA protein is identified by NXS or NXT (X = any amino acids), as shown in Fig. 3.12. The glycosylation serves three biological functions, which include the protein structure stability for virus assembly (Nakamura and Compans, 1978), recognition of antigens (Ertl and Ada, 1981; Thomas *et al.*, 1990) and protection from proteolytic degradation (Reading *et al.*, 2007). The potential N-linked glycosylation sites of A/Duck/Malaysia/01 (H9N2) isolate is identified at 6 positions, which are located at amino acid position 30N, 82N, 141N, 298N, 305N, and 492N. It is also noted that one of the glycosylation site, 298N, is located on one of the neutralizing epitope, which might implicate the reduced sensitivity to antibody in that particular site.

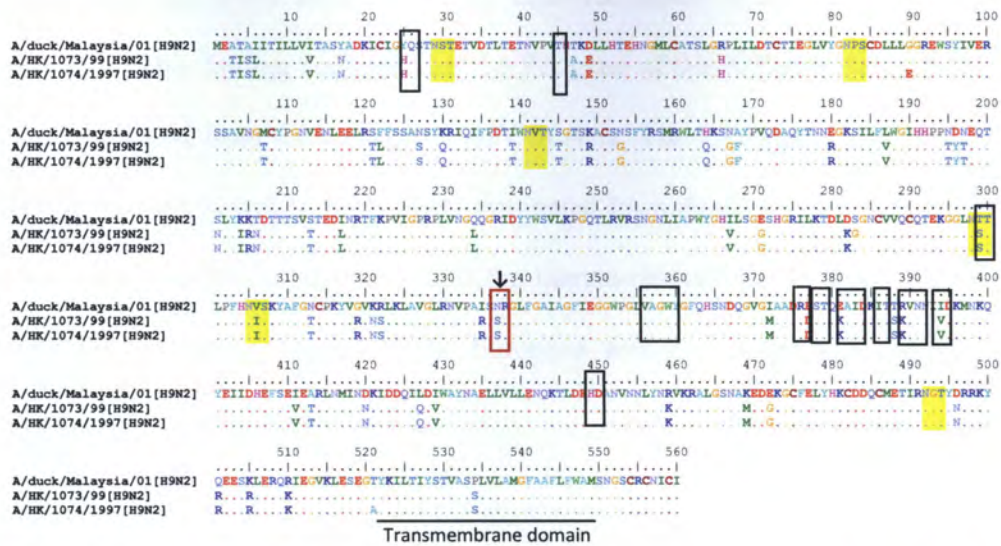


Fig. 3.12 Amino acid sequence of HA from A/Duck/Malaysia/01 (H9N2) compared to human H9N2. The area marked by yellow highlight denotes potential N-linked glycosylation sites. The area in black box denotes epitope sites. Cleavage site is marked by arrow to the red box.

The HA protein cleavage site is shown in Fig 3.13. It is required for membrane fusion and also is a main feature of pathogenicity (Klenk *et al.*, 1977). The cleavage site for the A/Duck/Malaysia/01 (H9N2) isolate and human H9N2 isolate have single amino acid –R cleavage site, hence the isolates are classified as low pathogenic avian influenza virus. A/Indonesia/CDC10478/2007 (H5N1) is classified as high pathogenic avian influenza, since it contains multiple amino acid RRKK cleavage site.

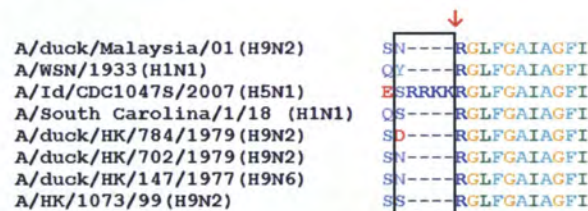


Fig. 3.13 HA Cleavage sites (red arrow) of HA from A/Duck/Malaysia/01 (H9N2) compared to other human and avian influenza virus sequence, boxed area denotes monobasic/polybasic area.

3.2.6 PA polymerase

The phylogenetic tree of PA gene is shown in Fig. 3.14. The clustering of the A/Duck/Malaysia/01 (H9N2) isolate clustered with LPAI Asian strain post 2000. The

human-derived H9N2 strain, however, clustered closer to the LPAI European strain pre 2000. This finding suggests that the PA gene of the A/Duck/Malaysia/01 (H9N2) was originated from the circulating AIV in Asia. The PA gene of the human-derived H9N2 isolates, however, most likely originated from the European strain of AIV. This clustering also rise a possibility that the human-derived H9N2 isolates may reassort with the circulating viruses in the European area to emerge a new H9N2 isolates capable of infecting human.

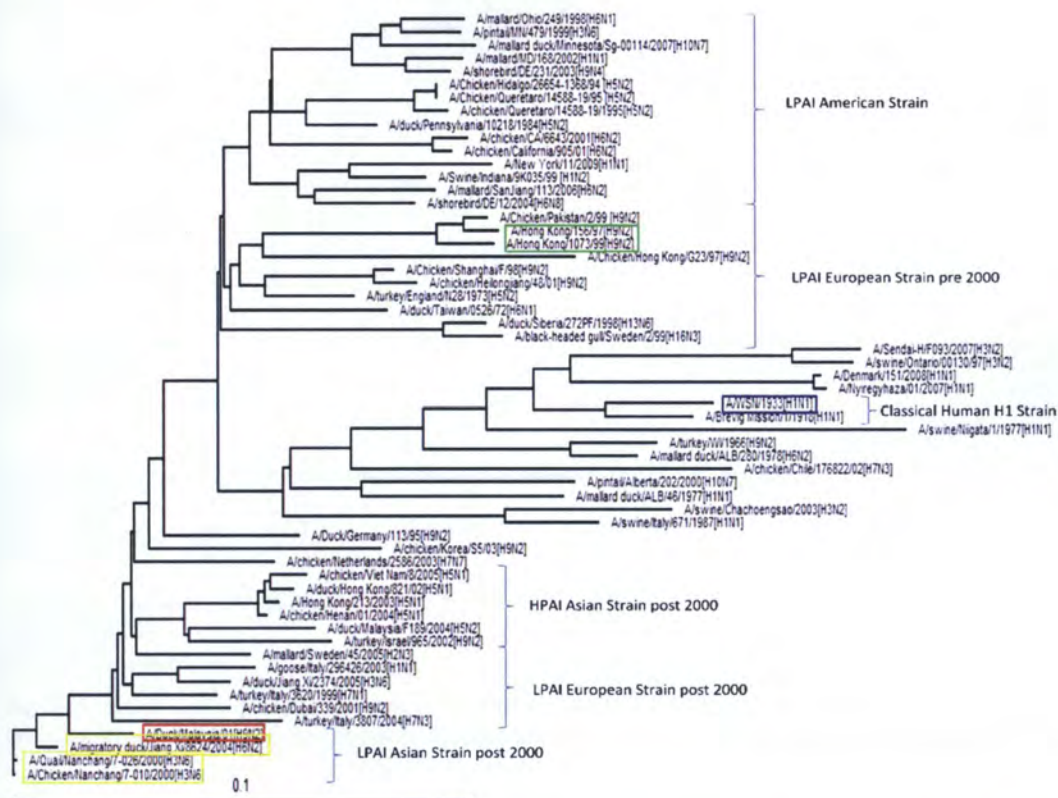


Fig. 3.14 Phylogenetic tree of PA genes. The red box denotes A/Duck/Malaysia/01 (H9N2), yellow box denotes strains from BLAST search, green box denotes human H9N2 virus and blue box denotes A/WSN/33(H1N1) indicates the isolate used in the experiment. The 0.1 with a line beneath denotes 10% nucleotide difference per line length.

The amino acid sequence analysis of the PA protein is shown below (Fig 3.15).

It is important to note that the critical amino acid positions 102K, 108D, and 134K of the isolates are not mutated to ensure PA protein activity to complex with PB1 and PB2 proteins (Hara *et al.*, 2004). All of the isolates have 102K, 108D, and 134K,

which implicate that the PA activity in replication, transcription, cap binding and viral RNA promoter is not impaired due to mutation. (See Section 1.2.1.1)

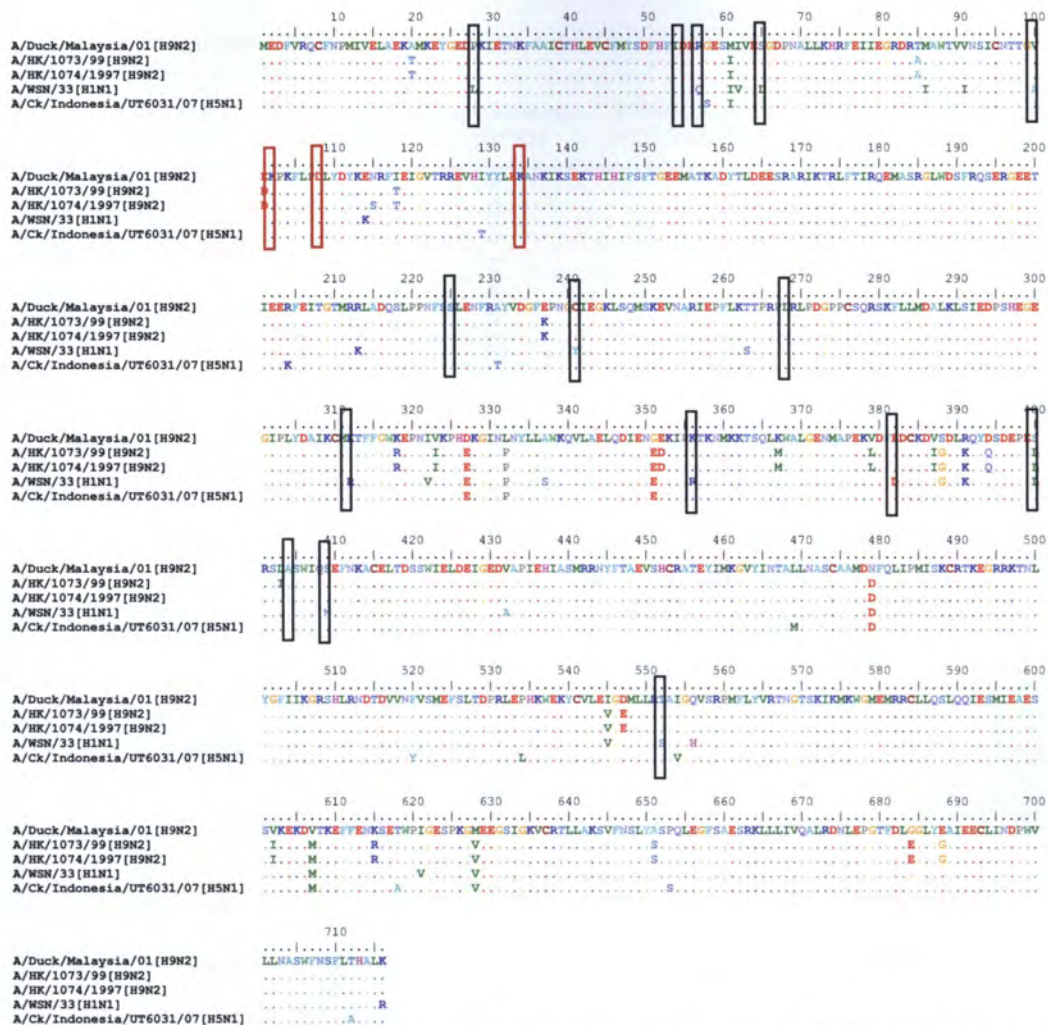


Fig. 3.15. Amino acid sequence of PA from A/Duck/Malaysia/01 (H9N2) compared to other human and avian influenza virus sequence. The host signature is marked by black box. The critical amino acids is marked by red box.

There are 15 host signatures in the PA gene (Okazaki *et al.*, 1989; Shaw *et al.*, 2002; Tautenberger *et al.*, 2005; Chen *et al.*, 2006). The host signature motif of PA protein is shown in Table 3.4. All 15 signatures of the A/Duck/Malaysia (H9N2) isolate were avian signatures. However, the human-derived H9N2 isolates contains human signature 400L. The lab strain A/WSN/33 (H1N1) has mixed host signatures. It

has human signatures on amino acid position 28, 57, 65, 100, 241, 312, 356, 382, 400, 409 and 553, and avian signatures on amino acid position 55, 225, 268 and 404.

Table 3.4. Host signature of PA protein in influenza A virus (Okazaki *et al.*, 1989; Shaw *et al.*, 2002; Tautenberger *et al.*, 2005; Chen *et al.*, 2006)

Position	Avian Signature	Human Signature	A/Duck/Malaysia /01(H9N2)	A/Hong Kong/ 1073/99(H9N2)	A/Hong Kong/ 1074/1997(H9N2)	A/WSN/33 (H1N1)
28	P	L	P	P	P	(L)
55	D	N	D	D	D	D
57	R	Q	R	R	R	(Q)
65	S	L	S	S	S	(L)
100	V	A	V	V	V	(A)
225	S	C	S	S	S	S
241	C	Y	C	C	C	(Y)
268	L	I	L	L	L	L
312	K	R	K	K	K	R
356	K	R	K	K	K	R
382	E	D	E	E	E	(D)
400	Q/T/S	L	S	(L)	(L)	(L)
404	A	S	A	A	A	A
409	S	N	S	S	S	(N)
552	T	S	T	T	T	(S)

Note: Residues in parenthesis denotes human signatures

3.2.7 Polymerase protein 1 (PB1)

The phylogenetic tree analysis of the PB1 gene is shown in Fig 3.16. The A/Duck/Malaysia/01 (H9N2) clustered together with the PB1 gene from Guang Xi and Nanchang area. The human-derived A/Hong Kong/1074/99 (H9N2) strain, as expected, clustered together with the LPAI Asian H9 strain, together with the HPAI A/Chicken/Hong Kong/220/97 (H1N1). This shows that the PB1 gene of the A/Duck/Malaysia/01 (H9N2) might be originated from the central China area.

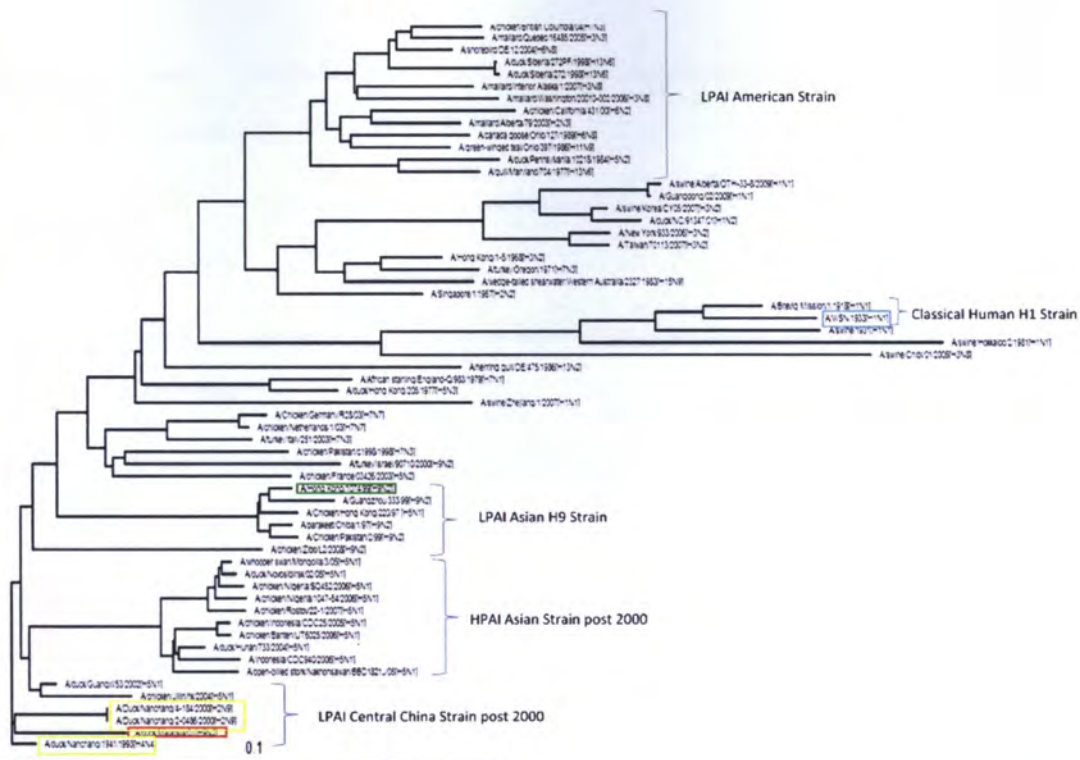


Fig. 3.16 Phylogenetic tree of PB1 genes. The red box denotes A/Duck/Malaysia/01 (H9N2), yellow box denotes strains from BLAST search, green box denotes human H9N2 virus and blue box denotes A/WSN/33(H1N1) indicates the isolate used in the experiment. The 0.1 with a line beneath denotes 10% nucleotide difference per line length.

The amino acid sequence alignment of the PB1 protein is shown below (Fig. 3.17). Firstly, it is important to ensure the motifs I, II, III and IV of the PB1 protein do not contain any mutations which cause the functional impairment. The H9N2 isolates possess motifs I, II, III and IV without any mutations (see Section 1.2.1.2). There are 3 host signatures discovered in PB1 protein. They are located at position 327, 336 and 375. The PB1 protein of avian influenza virus typically contains 327R, 336V and 375(N/S/T), whereas PB1 of human influenza virus contains 327K, 336I and 375S. The isolate A/Duck/Malaysia (H9N2) isolate contains 327R, 336V and 375N. All of the signatures of the isolate A/Duck/Malaysia (H9N2) and human H9N2 isolates belong to the avian signatures.

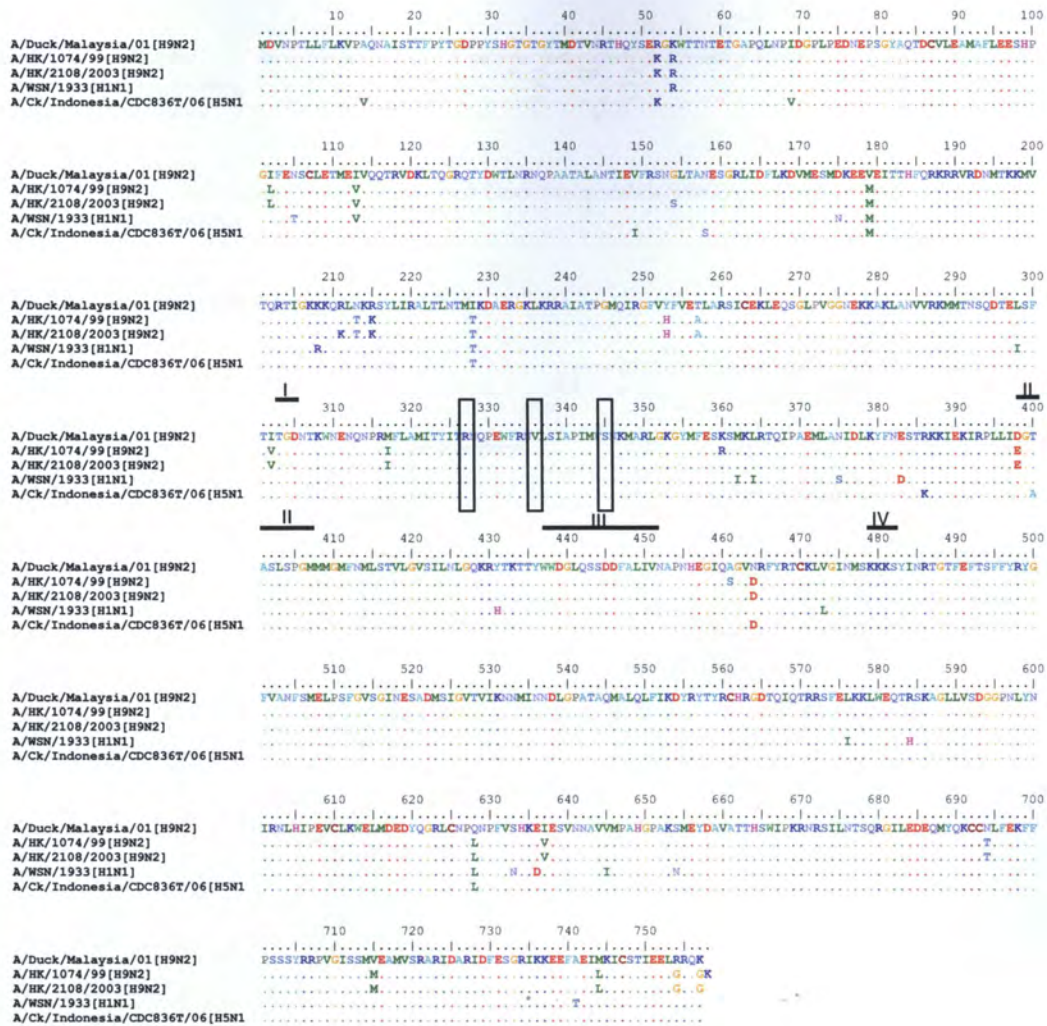


Fig. 3.17 Amino acid sequence of PB1 from A/Duck/Malaysia/01(H9N2) compared to other human and avian influenza virus sequence. Host signatures are marked by black box. The four RNA dependant RNA polymerase conserved motifs have been marked with an underline above the sequence.

The PB1-F2 protein is associated with apoptosis, and the apoptosis inducing sites are located in amino acid position 61-74 (see Section 1.2.1.2). The amino acid sequence of the selected isolates is shown in Fig. 3.18. The H9N2 isolate has amino acid residue 66N, which confers to the low pathogenic variant of PB1-F2. (see Section 1.2.1.2)

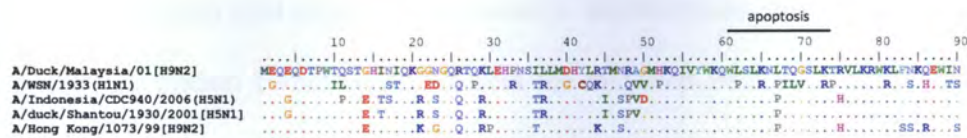


Fig. 3.18 Amino acid sequence of PB1-F2 from A/Duck/Malaysia/01(H9N2) compared to other human and avian influenza virus sequence

3.2.8 Polymerase Protein 2 (PB2)

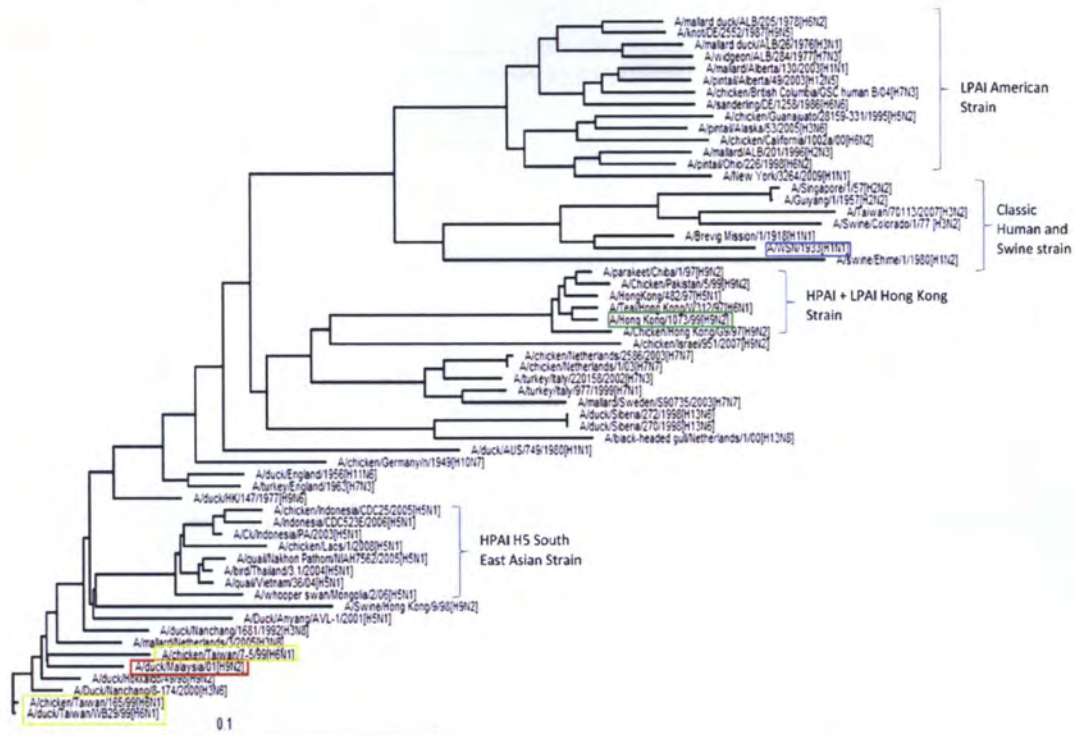


Fig. 3.19 Phylogenetic tree of PB2 genes. The red box denotes A/Duck/Malaysia/01 (H9N2), yellow box denotes the strains from BLAST search, green box denotes human H9N2 virus and blue box denotes A/WSN/33(H1N1) indicates the isolate used in the experiment. The 0.1 with a line beneath denotes 10% nucleotide difference per line length.

The phylogenetic tree of the PB2 gene is shown above (Fig. 3.19). The PB2 gene of A/Duck/Malaysia/01 (H9N2) clustered closely to various LPAI East Asia strains which circulated in 1990 – 2000. The PB2 gene of human-derived H9N2 strain clustered together with the AIVs circulating in Hong Kong area for both LPAI and HPAI.

The amino acid sequence alignment is shown below (Fig. 3.20). Neither H9N2 isolate nor human H9N2 isolate possess the mutation E627K, which confers to high pathogenicity in human (See Section 1.5.3). This mutation has also been found in H5N1 strain infecting human (Hatta *et al.*, 2001; Steel *et al.*, 2009; Gao *et al.*, 2009) and H7N7 strain in Netherlands (Fouchier *et al.*, 2004).

Table 3.5. Host signature of PB2 protein in influenza A virus (Shaw *et al.*, 2002; Tautenberger *et al.*, 2005; Chen *et al.*, 2006). The non-avian signature in the isolate is marked by parenthesis.

Position	Avian Signature	Human Signature	A/Duck/Malaysia/01(H9N2)	A/Hong Kong/1074/1997 (H9N2)	A/Hong Kong/1073/99 (H9N2)	A/WSN/33 (H1N1)
44	A	S	A	A	A	A
81	T	M	T	T	T	(M)
199	A	S	A	A	A	(S)
271	T	A	T	T	T	T
475	L	M	L	L	L	(M)
567	D	N	D	E	E	(N)
588	A	I	A	A	A	V*
613	V	T	V	V	V	A*
627	E	K	E	E	E	(K)
661	A	T	A	(T)	(T)	(T)
674	A	T	A	A	A	P*
702	K	R	K	K	K	(R)

Note: Residues in parenthesis denotes human signature; asterisk (*) denotes neither human nor avian signatures

The list of the host signature of PB2 protein is shown at Table 3.5. The A/Duck/Malaysia/01 (H9N2) isolate has all of the avian signature in PB2, including the position 627, which confers to low virulence and pathogenicity. The human-derived H9N2 isolates, however, possess one novel signature at E567 and human signature at T661. The laboratory strain A/WSN/33 (H1N1) contains mixed signatures. It has human signature at amino acid position 81, 199, 475, 567, 588, 627 661 and 702, and avian signature at amino acid positions 44 and 271.

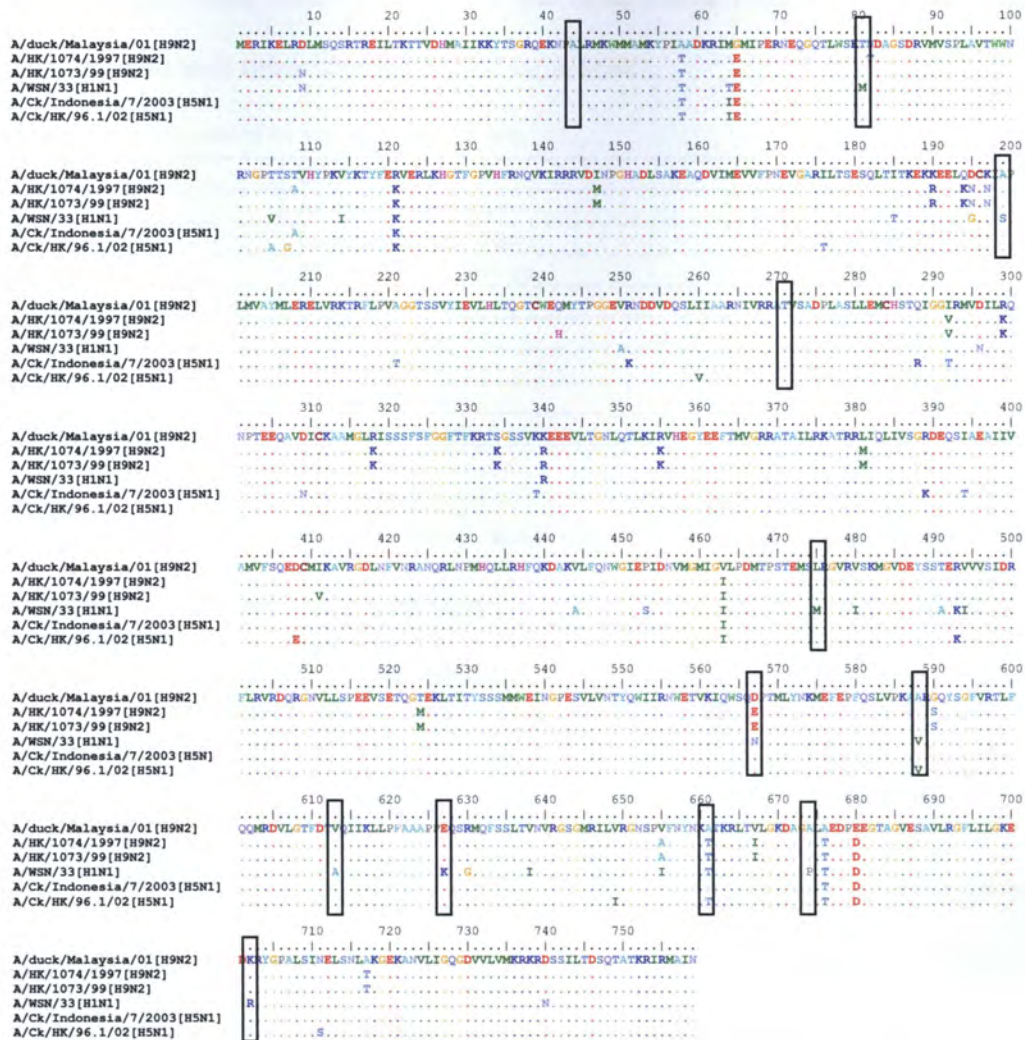


Fig. 3.20 Amino acid sequence of PB2 from A/Duck/Malaysia/01 (H9N2) compared to other human and avian influenza virus sequence. Host signatures are marked by black box.

3.3 Conclusion

Based on the sequence similarity search of the isolate A/Duck/Malaysia (H9N2) isolate, all of the genes are highly similar with the isolates from the Asian origin, with the exception of NP and NS gene, which are most similar with European origin (Table 3.6). The clustering pattern of isolate A/Duck/Malaysia (H9N2) isolate shows that all of the genes mostly grouped together with Asian lineage of the avian influenza virus. This suggests that the H9N2 isolate found in Malaysia was already

circulating in Asian area, mostly China and Hong Kong. Further, the strain underwent reassortment with other subtypes in the same area.

Table 3.6 The summary of the origins of H9N2 isolate.

Segment	Origin
HA	Asian G1-like Lineage
NA	Eurasian Swine Lineage
M	East Asian Y439 Lineage
PB2	East Asian Lineage
PB1	Asian Lineage
PA	Asian Lineage
NP	European Lineage
NS	European Lineage

Based from drug resistance analysis, the isolate A/Duck/Malaysia (H9N2) contains amantadine resistance signature in the M2 protein which shows that the isolate is an amantadine and rimantadine resistance strain. However, there is no indication of oseltamivir, zanamivir and peramivir resistance signature on the isolate A/Duck/Malaysia (H9N2).

The host signature of the isolate A/Duck/Malaysia (H9N2) analysis shows that all of the host signatures in all proteins belong to the avian signatures. However, the human derived H9N2 strains possess several human signatures in M2, NP, PA, and PB2 proteins, which explains the host adaptation capability of the human derived H9N2 strains. In the HA protein, the potential N-linked glycosylation at amino acid position 298 overlaps with the neutralizing epitope binding site. These findings might suggest that the isolate A/Duck/Malaysia/01 (H9N2) is speculated to develop antibody escape mutations important for vaccination by altering the potential N-linked glycosylation site. Similar N-linked glycosylation site were also observed in both human derived A/HK/1073/99 (H9N2) and A/HK/1074/1997 (H9N2). To confirm this, it is necessary to establish HA antibody binding test to address this matter more accurately.

Chapter Four. Growth Characteristics of H9N2

Virus replication efficiency can be assessed in different ways to gain insight into the virus growth characteristics in different cell lines. In this chapter, the growth characteristics of H9N2 avian influenza virus (AIV) was monitored by using several techniques, such as the immunofluorescence assay (IFA), growth curve, plaque morphology and kinetics of both replication and transcription of the virus in both single cycle and multiple cycles manner. Single cycle is the period where a virus particle from inoculum infects a cell, replicates and buds out as a new progeny, whereas the multiple cycle is the period where a virus particle originated from single cycle of infection infects the surrounding cells. Furthermore, single cycle of infection is also done in high multiplicity of infection (moi) where at least more than one virus particle will infect one cell, which means the cell population will be entirely infected with the virus. The statistical prediction of the rate of infection using Poisson distribution to infect all cells is critical to determine the minimum amount of cells infected. Theoretically, by using moi of 3, the proper amount of infected cells is 95% (McDonalds *et al.*, 1977). In our experiment, we demonstrated that > 95% were infected which fulfill Poisson distribution minimum requirement, as described in Section 2.2.2.5 (Fig. 4.1; Fig 4.2; Fig 4.3). Therefore we used moi of 3 as a basis to infect all host cells for subsequent studies. In contrast, multiple cycle of infection is carried out with low moi (i.e less than 1). This means that not the entire cell population will be infected with the virus at the same time. Laboratory human influenza virus strain A/WSN/33 (H1N1) will be used as a comparison of the growth characteristics of the H9N2 AIV, as the A/WSN/33 (H1N1) is among the best characterized influenza A virus.

The immunofluorescence assay can assess the infection cycle of a virus in an infected cell, using antibodies specific to NP protein. This assay is used to investigate viral replication rate in one cycle of infection, which means the observation period was terminated after strong nuclear export signal are observed, which denotes the virus is ready to be released, marking the completion of one cycle of infection. The efficiency of the replication inside the nucleus and the nuclear export can also be assessed in this assay by the examination of intensity and location of the fluorescence signal, which denotes the end point of the single cycle infection.

While the infectivity of the virus during one cycle of infection can be observed with immunofluorescence assay, the growth curve is useful to assess the virus release through multiple cycles of infection. The growth curve experiment has the advantage to assess multiple cycles of virus infection by titering infectious viral particles using plaque assay. Two patterns could be observed in this experiment, which were log or exponential growth and stationary phase. The exponential growth observed in the early time point shows that the virus is capable of replicating in the cells, and able to infect surrounding cells. Similar to the growth curve assay, plaque morphology is also employed to investigate the rate of the viral replication, which can be observed either by an area of dead cells, cells with cytopathic morphology of cells, or immuno-stained infected cells. In this chapter, virus quantification by plaque assay was carried out using standard method and immuno-stained method.

To access the replication kinetics in more details, the quantification of vRNA and mRNA over period of time was carried using quantitative PCR (qPCR). In this experiment, the replication or the synthesis of both vRNA and mRNA replication for all segments were investigated and quantified over a period of time. This finding can be used to elucidate the rate of viral replication and transcription rate in different cells.

This method is especially useful to assess replication efficiency where the released virus may not be infectious, hence can not be detected in the plaque assay method.

4.1 Immunofluorescence Assay

4.1.1 Madin-Darby Canine Kidney (MDCK)

The immunofluorescence image of MDCK infected cells with moi of 3 is shown below (Fig. 4.1). Here, the replication kinetics of A/Duck/Malaysia/01 (H9N2) in MDCK cell lines was monitored by IFA, using anti NP to observe the rate of replication, as compared to A/WSN/33 (H1N1). MDCK is a canine based kidney cell line, which possesses both the NeuAc2,6Ga and NeuAc2,3Ga sialic acid receptors at cell surface, and therefore can be infected by both human influenza virus and avian influenza virus (Hatakeyama *et al.*, 2005). This allows both human and avian influenza virus to grow well in MDCK cells. For this reason, MDCK cells are widely used for influenza virus isolation and growth. From this experiment, it was observed that A/WSN/33 (H1N1) had faster entry and replication kinetic, which could be seen by earlier nuclear localization at 4 hpi. It was then developed into extensive nuclear export from 6 hpi onwards. In A/Duck/Malaysia/01 (H9N2), there was no signal detected up to 4 hpi, which shows that there was little expression of the NP protein until 4 hpi.

Only by 6 hpi, there was weak nuclear localization in approximately 10% of the cell population. Subsequently, more cells had nuclear localization detected with minimal export at 8 hpi. The nuclear export intensified by 10 hpi, although not as strong as in A/WSN/33 (H1N1) infected cells. Based from the observation above, it is clear that A/WSN/33 (H1N1) infected cells showed faster progression of infection than A/Duck/Malaysia/01 (H9N2). This demonstrates that A/WSN/33 (H1N1) has bet-

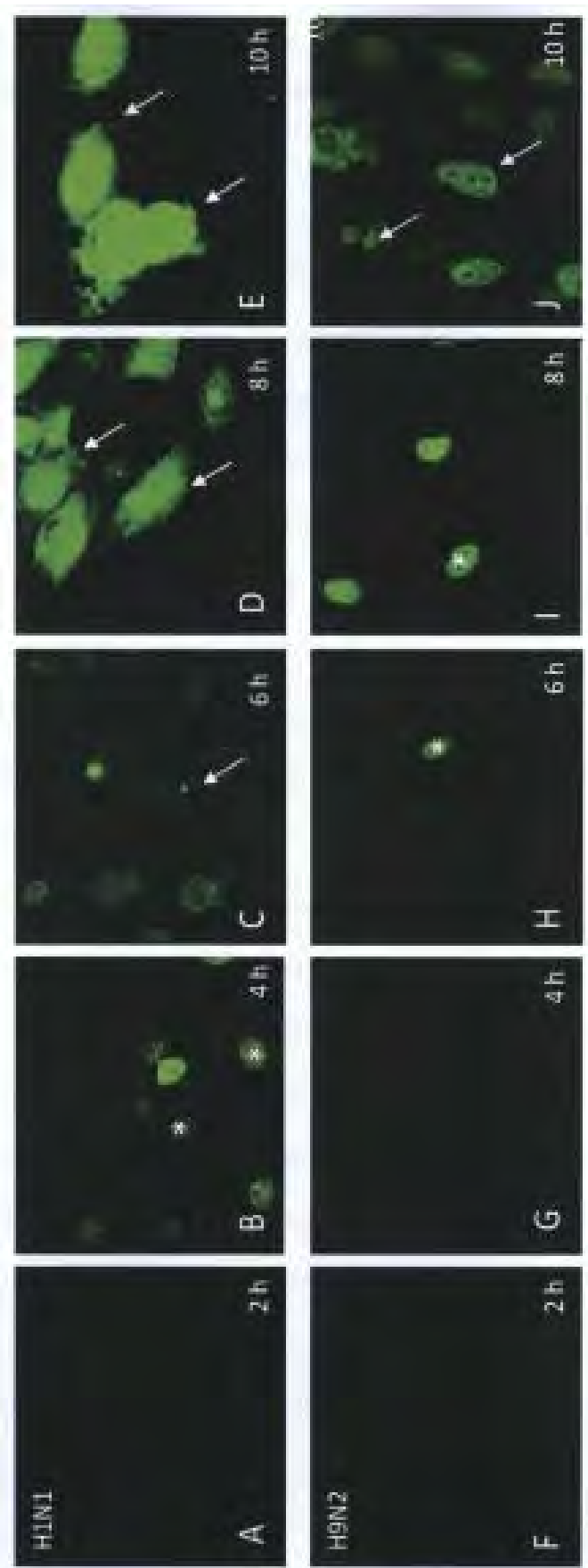


Fig 4.1 Immunofluorescence image of Madin Darby Canine Kidney (MDCK) infected with H1N1/WSN/33 (A to E) for 2 hours (A), 4 hours (B), 6 hours (C), 8 hours (D), and 10 hours (E), and with H9N2/Duck/Malaysia/01 (F to J) for 2 hours (F), 4 hours (G), 6 hours (H), 8 hours (I) and 10 hours (J). Nuclear localization signal is shown with (*) and nuclear export signal is shown with (→).

ter capability to infect and replicate in MDCK cells than A/Duck/Malaysia/01 (H9N2).

4.1.2 Chicken Embryo Fibroblast (CEF)

Chicken Embryo Fibroblast (CEF) is a primary avian fibroblast cells, and possesses mainly of α -2,3 linked glycan which is recognized by avian influenza virus (Gambaryan *et al.*, 2002; Matrosovich *et al.*, 1997, 2000). The immunofluorescence image of CEF infected cells with moi of 3 is shown below (Fig. 4.2). It can be seen that A/WSN/33 (H1N1) could bind to the cell and replicate although the nuclear localization was a bit slower than that for A/Duck/Malaysia/01 (H9N2) infected cells. For the nuclear export, both A/WSN/33 (H1N1) and A/Duck/Malaysia/01 (H9N2) infected cells showed strong signal at around 8 hpi with almost the same intensity, although A/Duck/Malaysia/01 (H9N2) showed earlier nuclear localization and nuclear export. The nuclear emptying was only observed in A/WSN/33 (H1N1), which suggests that the protein expression was lowered significantly towards the late time point of infection.

These results show that human influenza virus A/WSN/33 (H1N1) is able to infect CEF, although A/WSN/33 (H1N1) required more time from the entry until the initiation of replication and transcription as compared to A/Duck/Malaysia/01 (H9N2). Gambaryan *et al.* (1999) reported that the human influenza viruses grown in embryonated chicken eggs can eventually adapt and grow through the chicken embryo chorio-allantoic membrane, resulting from the selection of variants with amino acid substitution around the receptor binding site of the hemagglutinin. The similar rate of nuclear export signal development, which peaked at 8 hpi, as shown in Fig. 4.2, suggests that the rate of viral nuclear export protein complexes of both human and avian influenza virus are approximately similar.

Based from sequence study in Chapter 3, it is shown that all of the H9N2 signatures belong to the avian, while A/WSN/33 (H1N1) only possesses some avian signature. This explains the more rapid signal development in H9N2 isolate than A/WSN/33 (H1N1), and at the same time, the ability of A/WSN/33 (H1N1) to infect chicken based cells. Guan *et al.*, 1999 and Shaw *et al.*, 2002 showed that even incorporation of an amino acid belonging to human signatures in the internal gene of the human-derived H9N2 strain from HPAI H5N1 circulated in China did not impair the replication efficiency. To correlate with our experiment, it is possible that WSN isolate can undergo host signature sequence alteration without changing the efficiency of the initial host, showed by its ability to develop infection in CEF cells.

4.1.3 Human Lung Adenocarcinoma cells (A549)

A549 is a human adenocarcinomic lung cells that possesses predominantly the $\alpha 2,6$ sialic acid receptor, which is ideal for human influenza virus recognition by hemagglutinin. Shinya *et al.*, (2006) reported that majority of the human respiratory tract contain $\alpha 2,6$ sialic acid receptor with the exception of non-ciliated cuboidal bronchiolar cells at the junction between the respiratory bronchiole and alveolus located at lowermost of human respiratory tract. The immunofluorescence image of A549 infected cells with moi of 3 is shown in Fig. 4.3. The A/WSN/33 (H1N1) infected cells showed nuclear localization signal as early as 4 hpi. In A/Duck/Malaysia/01 (H9N2) infected cells, A549 was much slower in showing nuclear colocalization signal, which only appeared at 8 hpi with approximately 20% of the cells showed the signal. The nuclear export signal of both A/WSN/33 (H1N1) infected cells could be detected at 6 hpi. In A/Duck/Malaysia/01 (H9N2) infected

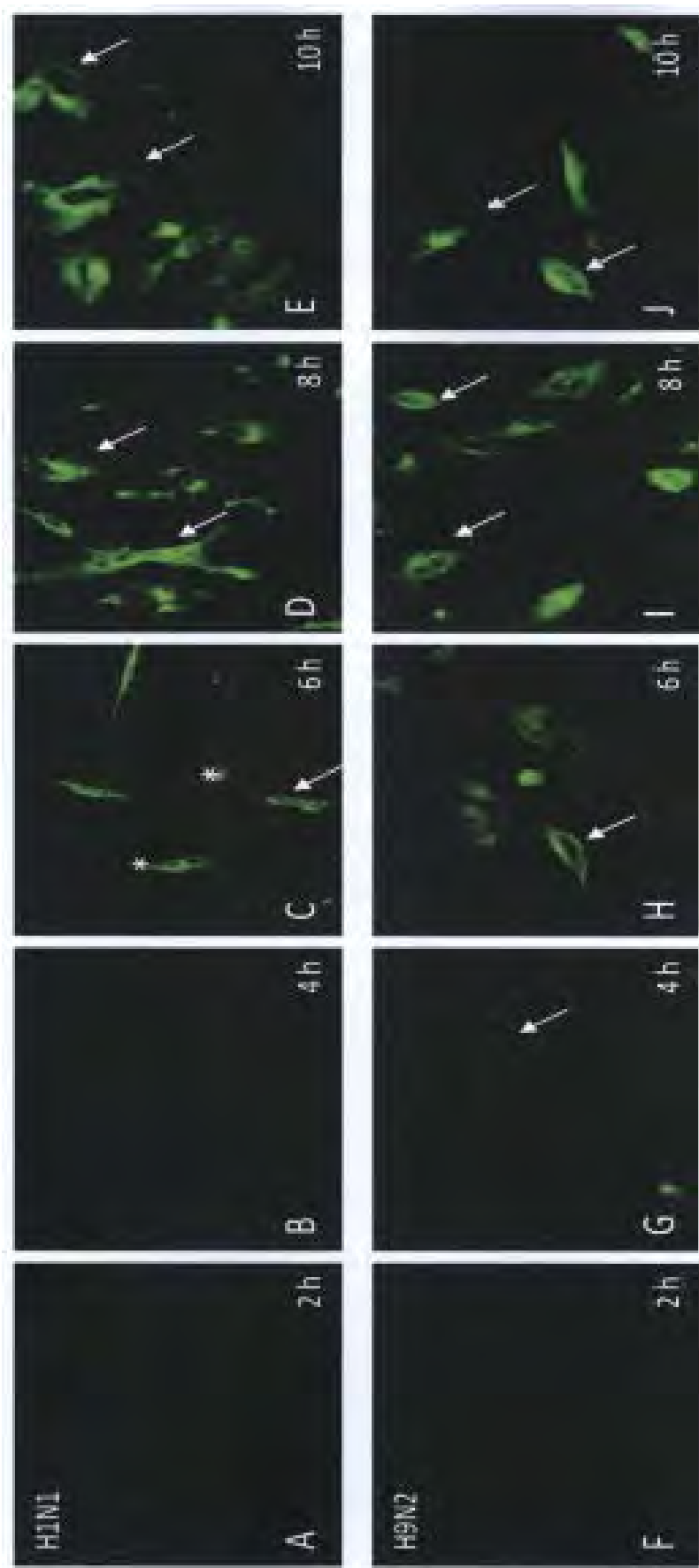


Fig 4.2 Immunofluorescence image of Chick Embryo Fibroblast (CEF) infected with H1N1/WSN/33 (A to E) for 2 hours (A), 4 hours (B), 6 hours (C), and 8 hours (D), and with H9N2/Duck/Malaysia/01 (F to J) for 2 hours (F), 4 hours (G), 6 hours (H) and 8 hours (I). Nuclear localization signal is shown with (*) and nuclear export signal is shown with (→).

cells, the rate of nuclear export was much slower, which could be observed from the weak cytoplasmic staining around the nucleus in approximately 20% of the cells, starting at 10 hpi, which shows as the cells were not entirely infected. Only by 16 hpi we could observe nuclear export signal in approximately 90% of the cells.

The slow signal development of the H9N2 isolate, if to be correlated with the sequence information elaborated in Chapter 3, can be explained by the absence of the human signature in all gene segments in H9N2. However, there is an evidence that a single mutation in the internal genes host signature site, PB1, PB2 and NP from human derived H5N1, is sufficient for the H9N2 strain to be able to infect human (Lin *et al.*, 2000; Butt *et al.*, 2005). A single mutation on G226Q in H9N2 HA protein also confers to its ability for infecting human (Wan *et al.*, 2007). Lee *et al.*, 2010 assessed this finding by infecting the cells with H9N2 strain mentioned above in A549 cells. They found that the small change of the mutation indeed improved the replication efficiency quite significantly by rapid signal development in immunofluorescence assay. This shows the potential ability of the H9N2 isolate to undergo mutation to improve the replication rate.

4.2 Growth Curve

The growth curve experiment aims to observe the rate of viral replication inside the cells within multiple cycles of infection time frame. Hence trypsin was added into the medium. This experiment measures the amount of the infectious viral particles released within a period of time in different cell lines. For titration, Immunostaining method with AEC (See Section 2.2.4.2) was used to calculate the virus titre harvested from the supernatant.

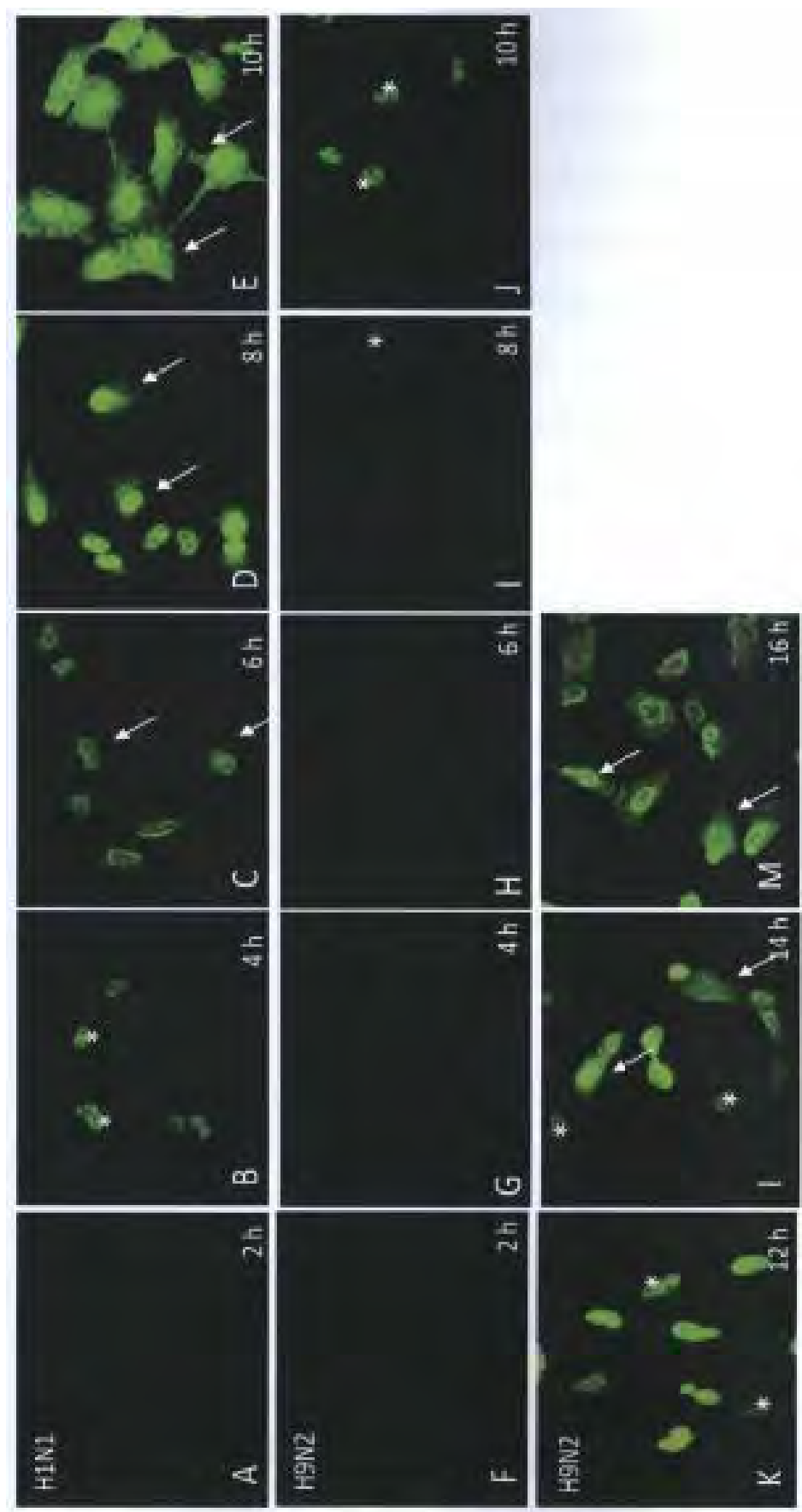


Fig 4.3 Immunofluorescence image of Human Adenocarcinoma lung cells (A549) infected with H1N1/WSN/33 (A to E) for 2 hours (A), 4 hours (B), 6 hours (C), 8 hours (D), and 10 hours (E), with H9N2/Duck/Malaysia/01 (F to M) for 2 hours (F), 4 hours (G), 6 hours (H), 8 hours (I), 10 hours (J), 12 hours (K), 14 hours (L) and 16 hours (M) with moi of 3. Nuclear localization signal is shown with (*) and nuclear export signal is shown with (→).

4.2.1 MDCK

The growth curve on both A/WSN/33 (H1N1) and A/Duck/Malaysia/01 (H9N2) infected MDCK with moi of 0.1, .01, and 0.001 is shown below (Fig. 4.4). The titres of A/WSN/33 (H1N1) reached the peak after 1 day, reaching 10^8 pfu/ml at 30 hpi. In A/Duck/Malaysia/01 (H9N2), the replication endpoint was reached after 1 day with maximum titre of 10^6 pfu/ml. This slower rate concorded with the data in immunofluorescence assay (Section 4.1.1). Although the replication of A/Duck/Malaysia/01 (H9N2) was slower by 2 log (100-fold), both viruses reached the replication endpoint in approximately the same infection time. Most of the cells died after 3 days showing that the virus had reached its maximum growth and no more viral particles were made. The higher titre in A/WSN/33 (H1N1) in this experiment demonstrates the higher rate of the growth of the virus in MDCK cells compared to A/Duck/Malaysia/01 (H9N2). In MDCK cells, H1N1 showed >50% CPE as early as ~24 hpi, and H9N2 showed >50% CPE at ~36 hpi.

The ability of both A/WSN/33 (H1N1) and H9N2 strain in MDCK cells is due to the receptor of the MDCK cells which recognizes both human and avian sialic acid (Gambaryan *et al.*, 2003; Matrosovich *et al.*, 2004). It is also shown that both avian and human influenza virus can replicate more efficiently in MDCK cells than BHK and Vero cells, although the both BHK and Vero cells possess both sialic acid receptors (van Wielink *et al.*, 2011).

4.2.2 CEF

The growth curve of A/WSN/33 (H1N1) and A/Duck/Malaysia/01 (H9N2) in CEF is shown below (Fig. 4.5). H1N1 reached the replication endpoint in 36 hpi with the maximum titre of 10^5 pfu/ml. On the other hand, A/Duck/Malaysia/01 (H9N2) had

significantly higher titre of approximately two to three log higher compared to A/WSN/33 (H1N1). In CEF cells, H1N1 showed >50% CPE at ~36 hpi, and H9N2 showed >50% CPE at ~24 hpi. Consistent with the result obtained in the immunofluorescence assay (Section 4.1.2), the AIV A/Duck/Malaysia/01 (H9N2) had better growth in CEF compared to human influenza virus A/WSN/33 (H1N1).

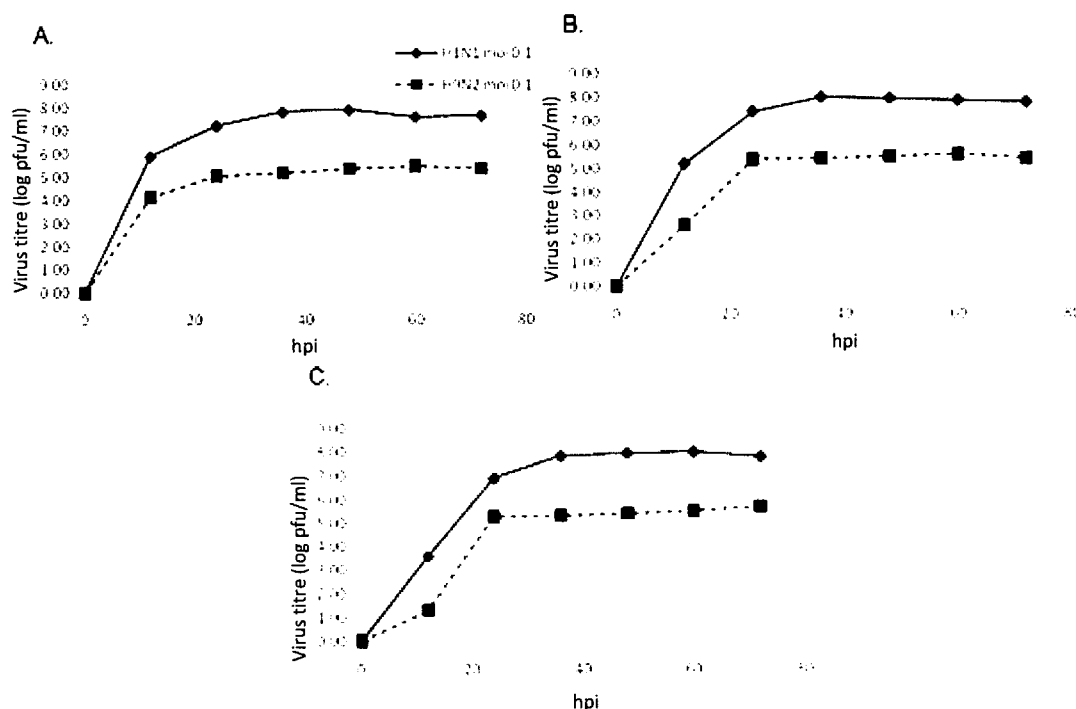


Fig 4.4 The growth curve profile of MDCK cells infected with A/WSN/33(H1N1) and A/Duck/Malaysia/01(H9N2) with moi of (A) 0.1, (B) 0.01, and (C) 0.001

The high growth of the H9N2 isolate was highly attributed to the possession of the avian signatures. To assess cell to cell replication and transmissibility, Shi *et al.*, 2010 evaluated the transmission route and replication efficiency of the H9N2 influenza virus in chicken, they found that the compatibility of the HA and NA genes is critical for generating efficient multiple cycle of infection, even among avian H9N2 strains. In this context, it suggests that the H9N2 used in this study possesses HA and NA protein sufficient for efficient replication in chicken. Lee *et al.*, 2010 also demonstrated that H9N2/G1 strain, which obtained its internal gene from human H5N1 were able to

replicate in human cell lines efficiently while still retained its growth in chicken. This raises the issue of reassortment with human-derived strains to create H9N2 strain capable of infecting human.

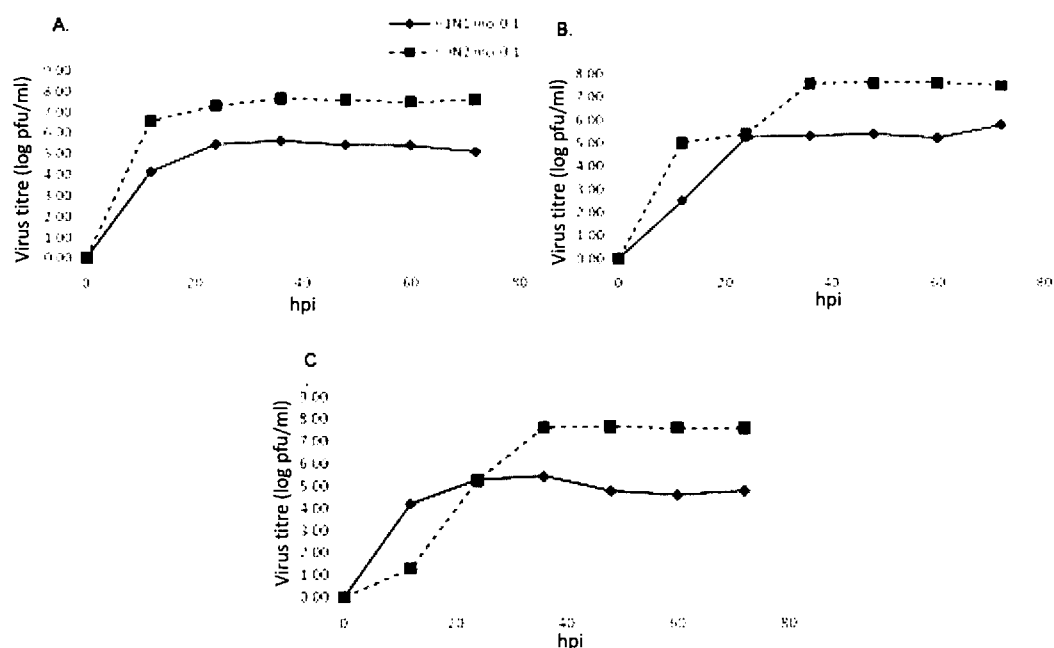


Fig 4.5 The growth curve profile of CEF cells infected with A/WSN/33 (H1N1) and A/Duck/Malaysia/01 (H9N2) with moi of (A) 0.1, (B) 0.01, and (C) 0.001

4.2.3 A549

The growth curve of A/WSN/33 (H1N1) and A/Duck/Malaysia/01 (H9N2) in A549 is shown below (Fig. 4.6). Unlike the other two cell lines, only A549 infected with A/WSN/33 (H1N1) moi 0.1 had detectable infectious viral particle, whereas as A/Duck/Malaysia/01 (H9N2) and A/WSN/33 (H1N1) with moi 0.01 had no infectious viral particle detected. A549 cells showed distinctive cytopathic effect (CPE) at 3 days post infection, which indicate that the cells had been infected. It was previously thought that the cell death was due to the trypsin, but the mock-infected A549 cells did not show any indication of CPE. These observations suggest that the virus is unable to

undergo efficient budding from the host cells, possibly due to host factor inhibiting the efficient budding. Regardless of the budding condition, the higher titre of H1N1 in this experiment shows that the A/WSN/33 (H1N1) have better growth which may strongly correlate to the human signatures possessed by the strain, as explained in Chapter 3. The H9N2 strain, however, do not possess any human signatures to confer good yield in A549 cells, similar with exclusively avian signature strains tested by Lee *et al.*, 2010. There were no marked change in H1N1 WSN and H9N2 even after 72 hpi, which suggested higher infectious dose of the viruses in this cell line.

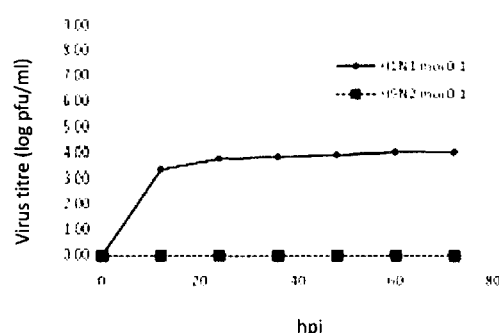


Fig 4.6 The growth curve profile of A549 infected with A/WSN/33 (H1N1) and A/Duck/Malaysia/01 (H9N2) with moi of 0.1

Table 4.1 Virus Titre at 72 hpi

Virus	MDCK			CEF			A549		
	moi 0.1	moi 0.01	moi 0.001	moi 0.1	moi 0.01	moi 0.001	moi 0.1	moi 0.01	moi 0.001
H1N1	1.7×10^7	2.2×10^7	8.8×10^7	2.2×10^5	2.8×10^5	3.1×10^5	2.1×10^3	ND	ND
H9N2	8.5×10^4	5.7×10^4	6.2×10^4	8.5×10^7	1.1×10^8	9.1×10^7	ND	ND	ND

Note :

ND (Non Detected) denotes no virus detected in the supernatant with plaque assay method

The summary of the growth curve experiment is shown in Table 4.1. Based on the virus titre measured at 72 hpi, the A/WSN/33 (H1N1) has higher titre in MDCK cells. A/Duck/Malaysia/01 (H9N2) shows higher titre in CEF cells. This data suggests that A/WSN/33 (H1N1) is more capable of releasing infectious virus particle in MDCK cells. A/Duck/Malaysia/01 (H9N2) shows more release in CEF cells.

4.3 Plaque Morphology

In this experiment, only MDCK cells were used for infection because of its ability to form distinctive CPE and uniform plaque morphology when infected with all subtypes of influenza viruses. Hence, MDCK is used as the standard cell line for plaque assay. A549 and CEF cells were also attempted in this experiment. The extensive cell death was observed in high concentration of virus ($10^5 - 10^7$ pfu/well). The intensity is less with lower concentration without any indication of plaque formation, and no cell death was observed at non-infected cells.

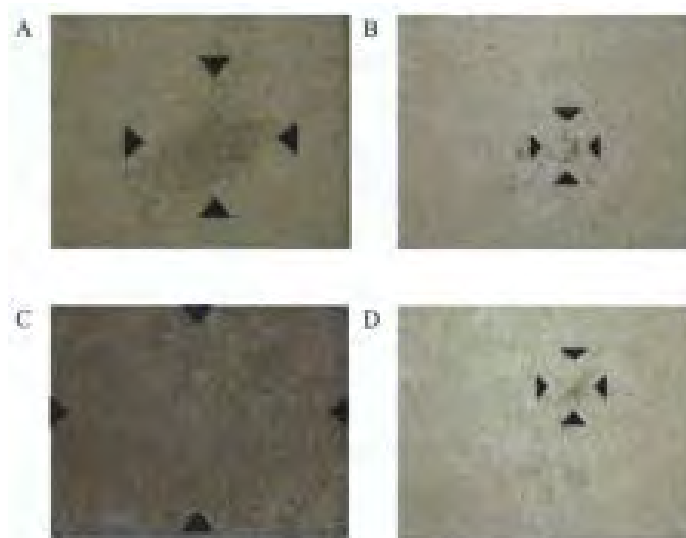


Fig 4.7 The plaque morphology of A/WSN/33 (H1N1) in (A) and (C), A/Duck/Malaysia/01 (H9N2) in (B) and (D) developed in 48 hours (A and B) and 72 hours (C and D) using agarose overlay. Note the accumulated blackened dots which mark the area of dead cells, as indicated by arrows.

The plaque morphology of the MDCK cells infected with A/WSN/33 (H1N1) and A/Duck/Malaysia/01 (H9N2), using agarose overlay as medium is shown below (Fig. 4.7). The plaque morphology observation using agarose overlay is based on a collection of clearing zones consisting of dead cells in 6-well plate format. The A/WSN/33 (H1N1) plaque was visible to the eye after approximately 48 hpi.

However, the A/Duck/Malaysia/01 (H9N2) plaque only showed microscopic size at 4 dpi. The A/WSN/33 (H1N1) plaque continued to enlarge rapidly in size, and at 72 hpi, there was a noticeable increase. The A/Duck/Malaysia/01 (H9N2) had no significant growth in plaque size at 72 hpi. From this experiment, it can be concluded that in MDCK cells, A/WSN/33 (H1N1) undergoes more rapid replication with multiple cycle of infection than H9N2.

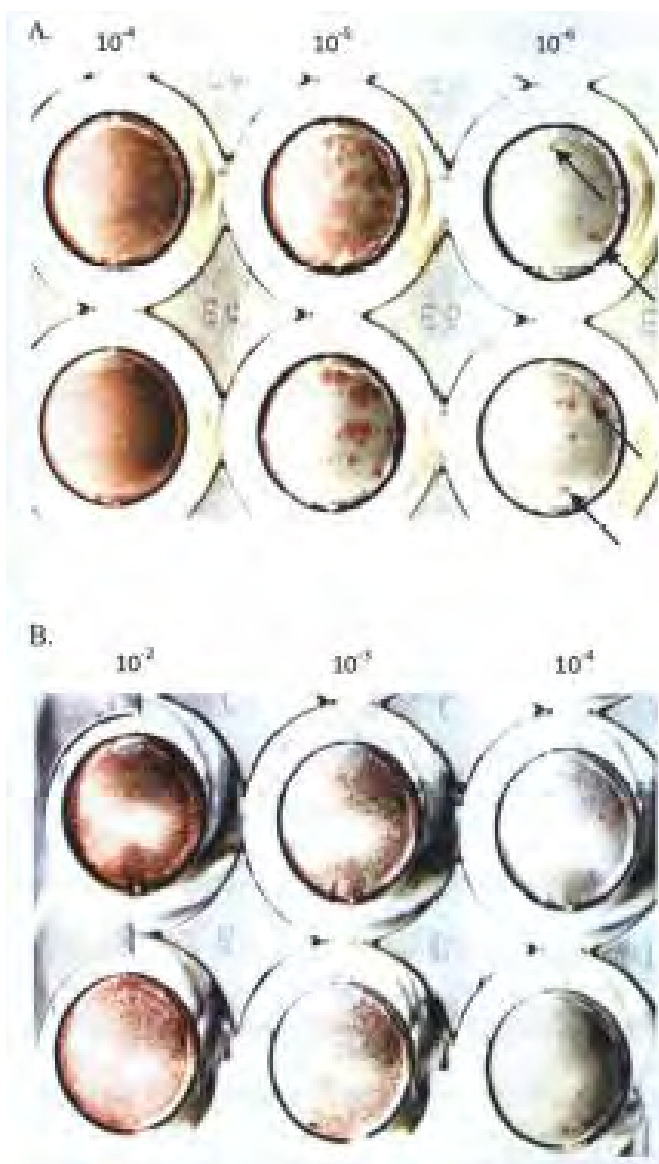


Fig 4.8 The immuno-staining of infected with A/WSN/33 (H1N1) (A), A/Duck/Malaysia/02 (B) for 24 hours. The number above the picture denotes the virus dilution used. Note the visible **red stained punctates** at the two rightmost of each figure, pointed by the arrows, except for H9N2, which is **not clearly visible** for their small size.

The plaque morphology of MDCK infected cells, visualized by immunostaining is shown in Fig. 4.8. This method of plaque formation shows different plaque morphology observation with agarose overlay. In this experiment semi-solid micro crystalline cellulose Avicel® RC-591 was used as an overlay in 96 well-plate formats as demonstrated by Matrosovich *et al.* (2006). The plaque was visualized after the overlay was removed, followed by cell fixation and immunostaining using anti-NP antibody to detect virus NP protein and AEC to stain detected virus NP protein. The plaque was visible as red punctate staining inside the well plate. In this experiment, the A/WSN/33 (H1N1) plaque staining was noticeable after 24 hpi, even with naked eyes. The A/Duck/Malaysia/01 (H9N2) plaque yielded much smaller size. Hence, although with different plaque morphology visualization method, it can be seen that A/WSN/33 (H1N1) is capable of producing plaques more rapidly than A/Duck/Malaysia/01 (H9N2) in MDCK cells. This result concorded with the standard plaque assay method.

4.4 Viral Genes Expression Profiles in Different Cell Lines

In this experiment, we measured the rate of vRNA and mRNA synthesis for both viruses within up to 10 hpi. This method is different from the virus release measured in 4.3, where only vRNA and mRNA produced within a cell is measured. All of the vRNA and mRNA measurement in qPCR method was carried out in two different sets, measured in triplicates independently (n=6). To produce cDNA specific from either vRNA or mRNA, strand-specific primer in the reverse transcription step was used, for example: conserved Uni12 site for vRNA, and poly-A for mRNA. RNase-H was also used after RT to remove any contaminating RNA template to ensure there is no cross-contamination between vRNA and mRNA that

would interfere with qRT-PCR. The result shown below is the representative of one experiment.

4.4.1 Replication (vRNA) Profiling in Different Cell Lines

The relative expression profile of A/WSN/33 (H1N1) is represented in Fig. 4.9, and H9N2 in Fig. 4.10. The overall vRNA expression of A/WSN/33 (H1N1) in all three cell lines generally showed a rapid increase starting from 5 hpi, except for PB1 vRNA which rose from 6 hpi onwards in MDCK and CEF cells, while PB2 gene in A549 and MDCK peaked later at approximately 7 hpi and 8 hpi, respectively. NS started to show an increase as early as 3 hpi in CEF cells. Compared to MDCK and CEF, A549 had the slowest increase of the vRNA expression. The expression of vRNA is closely associated with the replication of the viral genomic material before packaging with the new virion. The slower increase of the vRNA expression profile in A549 cells infected with A/WSN/33 (H1N1) resulted in low viral titres in the growth curve experiment (Section 4.2.3). This result concorded with that from other groups where the vRNA synthesis rate of A/WSN/33 (H1N1) in all viral segments generally peaked at approximately 5 hpi (Smith *et al.*, 1982), and also demonstrated in H7N1/FPV strain (Berrett *et al.*, 1971; Hay *et al.*, 1977)

The vRNA expression of A/Duck/Malaysia (H9N2) differed among the cell lines, irregular increase was observed as early as 1 hpi in MDCK and A549 cells. In CEF, a steady increase was observed starting from 5 hpi in PB2 vRNA and NP vRNA, 6 hpi in HA vRNA and NA vRNA, and 4 hpi in M vRNA and NS vRNA. Based on the IFA and growth curve data, it was observed that A/Duck/Malaysia (H9N2) had better growth kinetics in CEF cells than in MDCK and A549 cells. The rise and drop pattern of A/Duck/Malaysia (H9N2) was not observed in CEF, and this suggests that the

A/Duck/Malaysia (H9N2) virus may be able to counteract the antiviral pathway to prevent the degradation of the viral RNA in CEF cells, of which it is likely that NS1 plays a major factor (de la Luna *et al.*, 1995).

The fluctuation found in generally all gene segments in H9N2 infected MDCK and A549 cells, was highly attributed to stagnancy of the poor and stagnant replication rate. Although the difference is only +1.4 fold-change at 2 hpi and -0.5 fold-change at 7 hpi, since linear unit was used as opposed to log unit in absolute measurement (Fig 4.13), the difference was exaggerated and therefore created an artifact as if the measurement was unusual or inconsistent.

It has been reported that partial changes from avian to human signatures in H9N2 strain confers its ability to infect human cells (Lee *et al.*, 2010), but not otherwise. The same group also observed that the H9N2 strains which did not reassort with human-derived strains A/Duck/Hong Kong/Y280/97 (H9N2/Y280) and A/Chicken/Hong Kong/G9/97 (H9N2/G9) showed poor replication. Further, the H9N2 isolate used in this study did not possess V226Q mutation in the HA protein to support H9N2 replication in human, as described by Wan *et al.*, 2007.

4.4.2 Transcription (mRNA) Profiling in Different Cell Lines

The relative mRNA expression profiling of A/WSN/33 (H1N1) is shown in Fig. 4.11 and H9N2 in Fig. 4.12. Based on findings by Mikulasova *et al.* (2000), the mRNA transcription and protein expression will occur in influenza virus infection first, which then followed by vRNA synthesis.

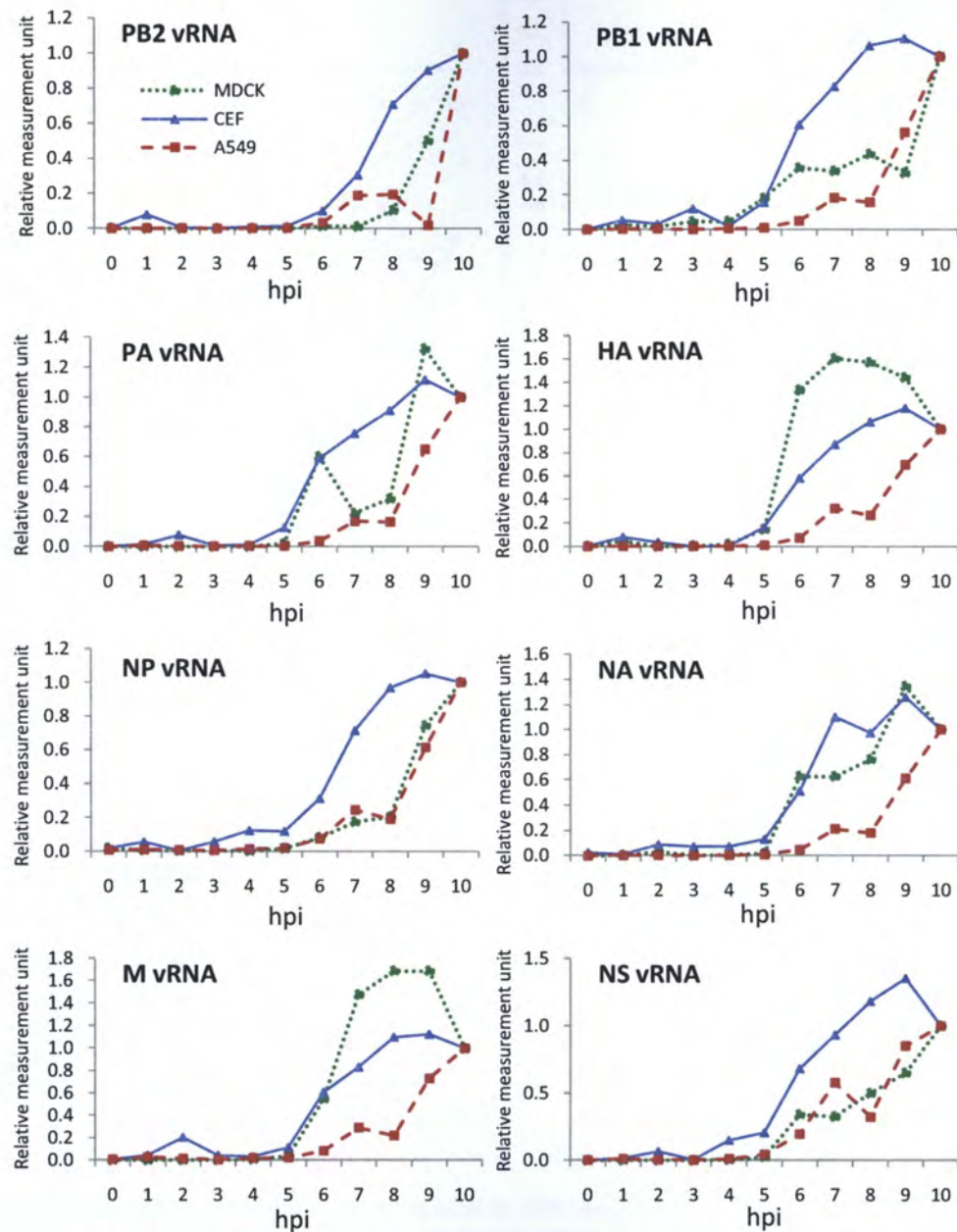


Fig 4.9 Relative vRNA expression of 8 viral segments in H1N1 (moi =3) in MDCK (.....), CEF (———) and A549 (———). All measurement is normalized at 10 hpi as 1.0 relative measurement unit for each cell lines. The experiment was carried out in two sets of experiments, measured in triplicates. Here, the representative of one experiment is shown (n=3).

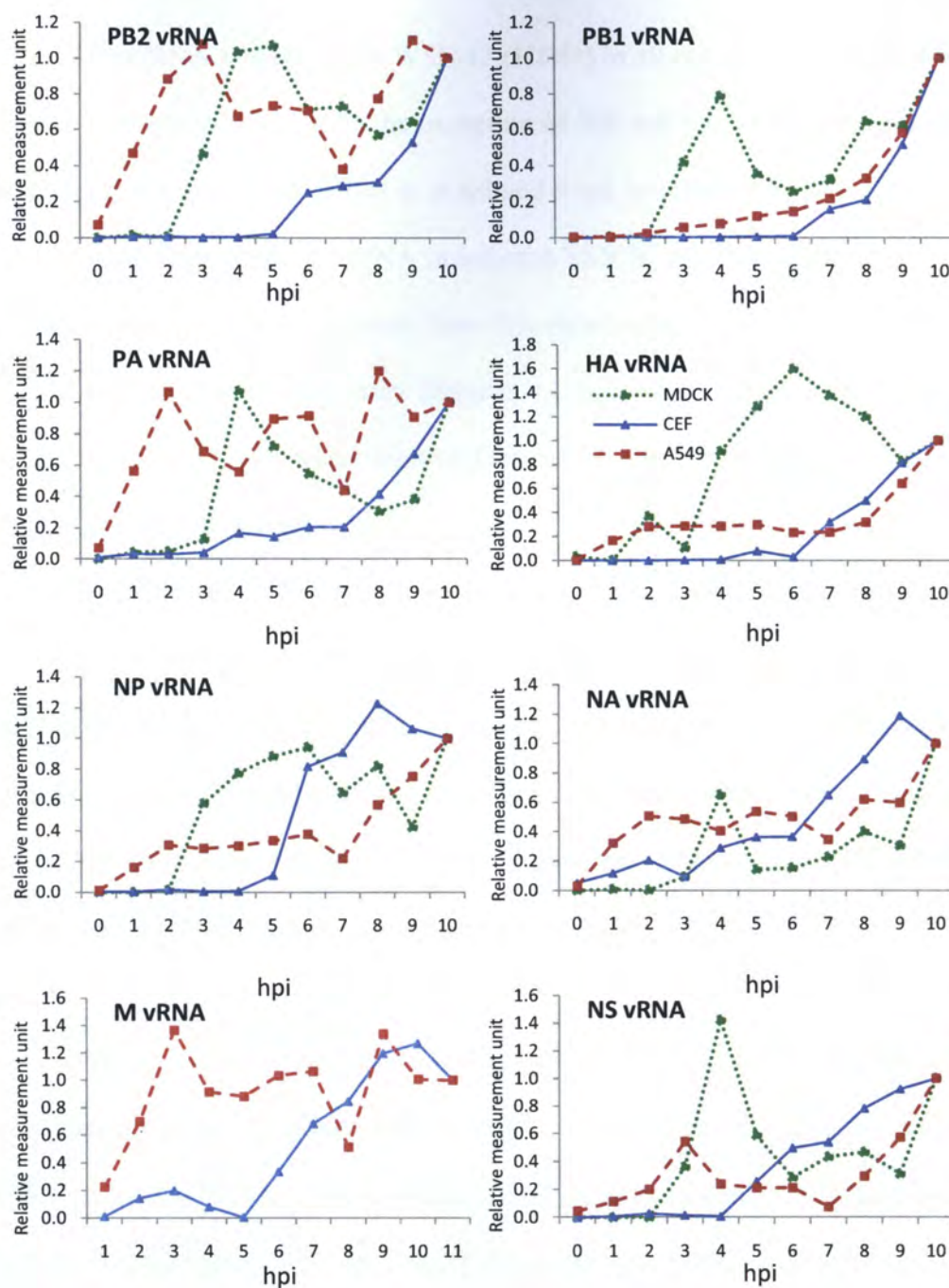


Fig 4.10 Relative vRNA expression of 8 viral segments in H9N2 in MDCK (.....), CEF (—) and A549 (---) (moi =3). All measurement is normalized at 10 hpi as 1.0 relative measurement unit for each cell lines. The experiment was carried out in two sets of experiments, measured in triplicates Here, the representative of one experiment is shown (n=3).

The mRNA profiling of A/WSN/33 (H1N1) in all cell lines generally show an increase at 4 hpi to 5 hpi, with the exception of HA mRNA where the rapid rise in infected MDCK were seen as late as 9 hpi and 6 hpi in infected A549 cells. The late rise was also observed at M mRNA in infected MDCK, which is approximately at 8 hpi. In general, the results obtained from this experiment were consistent the results from in immunofluorescence assay (Section 4.1.1, 4.1.2 and 4.1.3 for MDCK, CEF and A549, respectively), where nuclear localization signal were detected in the cell lines at approximately 4 hpi.

Similar to the vRNA expression profile in A/Duck/Malaysia/01 (H9N2), there was a rise of most of the gene mRNA expression in MDCK cells, which rose at approximately 2 to 3 hpi, dropped subsequently, and rose again starting from 8 hpi. In CEF and A549 cells, no such fluctuation was observed. Instead, most of the genes started to show a rapid rise at 4 to 5 hpi, with the exception of PB1 mRNA and HA mRNA which rose at 6 hpi in CEF cells, while most genes in A549 cells rose only at 8 hpi.

The possession of exclusively avian host signatures in all of the H9N2 strain segments may affect the slower transcription rate of the H9N2 strain, compared to the A/WSN/33 (H1N1). The studies conducted on human-derived H9N2 strain showed that the internal genes NP, PB1 and PB2 is the key factors to confer the H9N2 transmissibility of the strain in human (Lin *et al.*, 2000; Butt *et al.*, 2005). It is shown in this experiment that the mRNA of NP, PB1, and PB2 in H9N2 strain peaked at 7-8 hpi, much later than those of A/WSN/33 (H1N1), which peaked as early as 5 hpi. This also shows the lower compatibility of H9N2 isolate compared to the human strain.

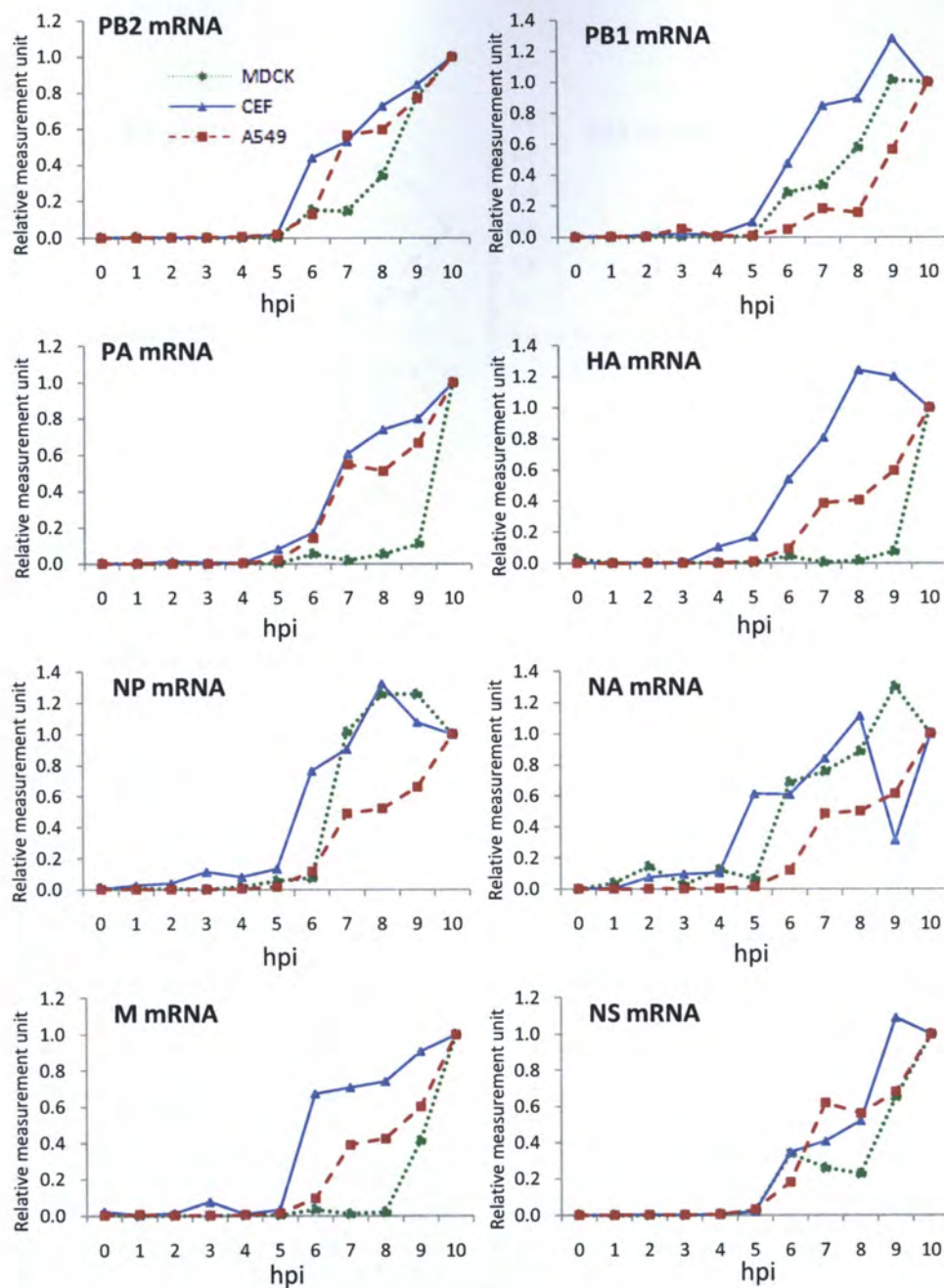


Fig 4.11 Relative mRNA expression of 8 viral segments in A/WSN/33 (H1N1) in MDCK (.....), CEF (—) and A549 (---)(moi =3). All measurement is normalized at 10 hpi as 1.0 relative measurement unit for each cell lines. The experiment was carried out in two sets of experiments, measured in triplicates. Here, the representative of one experiment is shown (n=3).

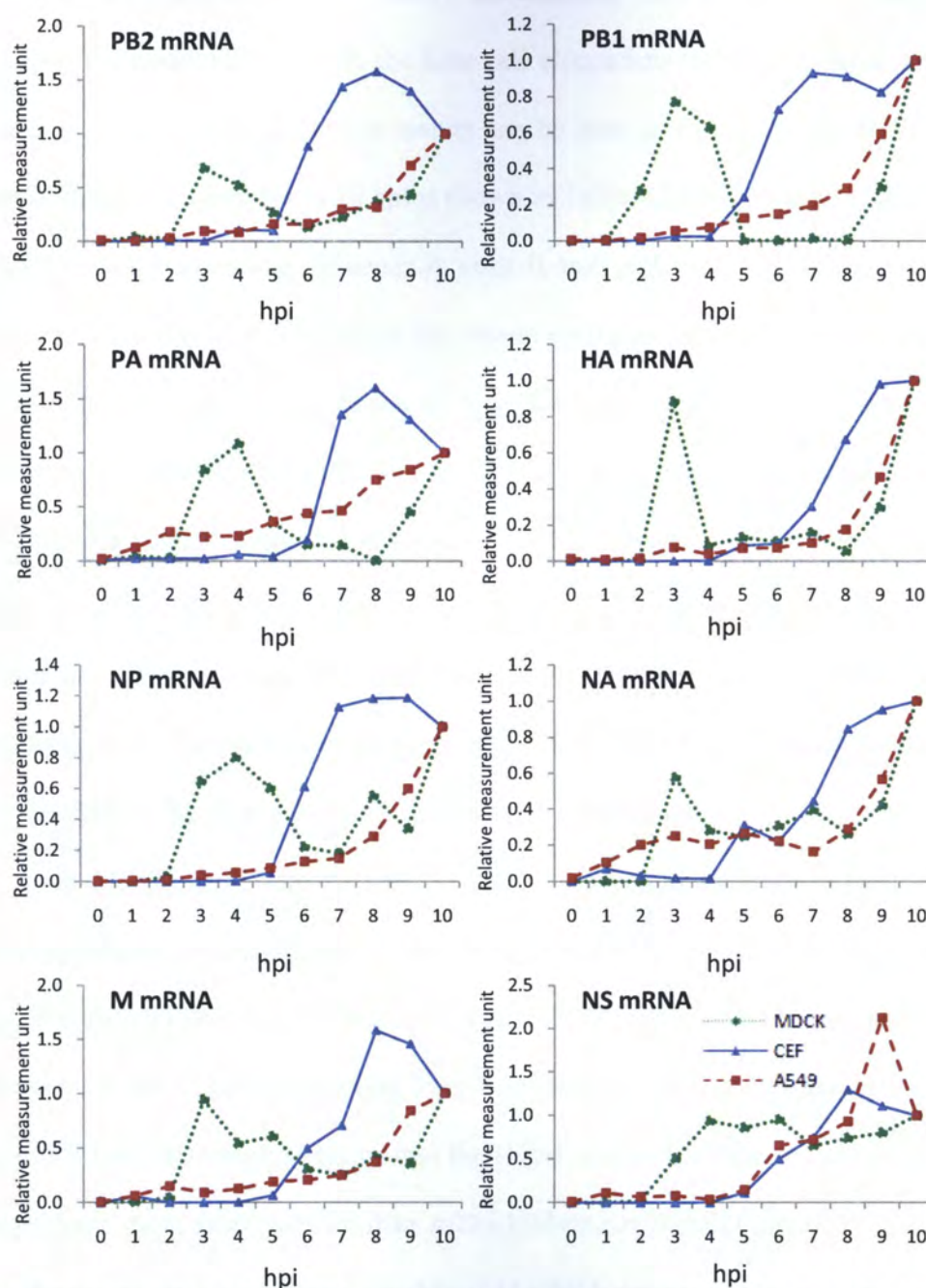


Fig 4.12 Relative mRNA expression of 8 viral segments in A/Duck/Malaysia/01 (H9N2) in MDCK (•••••), CEF (—▲—) and A549 (- -■ - -)(moi =3). All measurement is normalized at 10 hpi as 1.0 relative measurement unit for each cell lines. The experiment was carried out in two sets of experiments, measured in triplicates. Here, the representative of one experiment is shown (n=3).

4.4.3 Comparison of Viral Replication and Transcription in Infected Cell Lines

In this experiment, we quantify the absolute amount of vRNA and mRNA based on the normalization with the host cell elongation factor, and focus on the M gene copies as the parameter. The results can be seen in Fig. 4.13, and the tabulated form of the M copy number at 10 hpi is shown in Table 4.2. The M gene in influenza A is highly conserved among influenza A virus (Lamb and Lai., 1981). The PCR target for quantitative RT-PCR is based on the conserved region of the M gene, and was used for both the absolute quantification of the vRNA and mRNA expression profiling. However, this absolute quantification can only be normalized with the same host cell elongation factor to be compared within the same cell lines. The 0 hpi refers to the non-infected controls (mock) used in the experiment, hence, no virus was introduced to it, and no addition steps were taken to remove the inocula. No subtraction was introduced in the formula since no virus was added in the 0 hpi. This formula has also been applied on the other RNA segments described previously.

In MDCK cells, the A/WSN/33 (H1N1) infection showed an earlier rise in vRNA compared to mRNA, and in term of copies number, the vRNA level is greater as well. The A/Duck/Malaysia (H9N2) infected MDCK cells showed approximately 2 log less copy numbers of vRNA starting from 4 hpi and a log less copies number of mRNA towards 9 hpi. This result suggests that the H1N1 infected MDCK cells could produce and package more viral particles than A/Duck/Malaysia (H9N2) infected MDCK cells, with the assumption of one copy number of M vRNA represents one virion.

In CEF cells, the A/Duck/Malaysia (H9N2) produce approximately a log more for both vRNA and mRNA than to A/WSN/33 (H1N1) infected cells. From these results, it is shown that the H9N2 strain have better replication and transcription in CEF cells. Nevertheless, both A/WSN/33 (H1N1) and H9N2 isolate showed relatively

high copy number at 10 hpi ($>10^6$ M copy number/ 10^4 EF). This is likely due to the possession of avian signatures in all gene segments of H9N2 strain, and partially avian signatures in some gene segments of A/WSN/33 (H1N1) strain. This also may explain the reason of the small difference in both mRNA and vRNA copy number in A/WSN/33 (H1N1) and H9N2 strain.

In A549 cell lines, there were 3 log less copy number of H9N2 strain vRNA compared to A/WSN/33 (H1N1) vRNA, and 2 log less copy number of A/Duck/Malaysia (H9N2) mRNA compared to A/WSN/33 (H1N1) vRNA. Compared to all other cell lines, the A549 cell lines M vRNA and mRNA copy number showed the biggest difference between A/WSN/33 (H1N1) and A/Duck/Malaysia/01 (H9N2) infected A549 cells, which shows that A/Duck/Malaysia/01 (H9N2) can replicate in A549 cells, but with rather low replication rate. This result is expected, because based from the sequence analysis, no human signatures found in gene segments of H9N2 strain. Further, there is no indication of reassortment of human-derived HPAI H5N1 internal genes as demonstrated by Lin *et al.*, 2000 and Butt *et al.*, 2005, and V226Q in the HA protein to allow efficient human infection. Similar study had also been conducted by Lee *et al.*, 2010 to show that original H9N2 strains were not capable to infect human cells efficiently.

Table 4.2 Tabulated copy number of A/WSN/33 (H1N1) and A/Duck/Malaysia (H9N2) infected MDCK, CEF and A549 cells at 10 hpi, as shown in Fig 4.13. The result shown was based on the copy number of the M segment per 10^4 EF.

	MDCK		CEF		A549	
	vRNA	mRNA	vRNA	mRNA	vRNA	mRNA
H1N1	4.29×10^5	3.95×10^4	2.27×10^6	9.50×10^6	8.38×10^4	1.44×10^5
H9N2	3.86×10^3	2.26×10^3	1.84×10^7	1.58×10^7	1.15×10^1	4.26×10^2

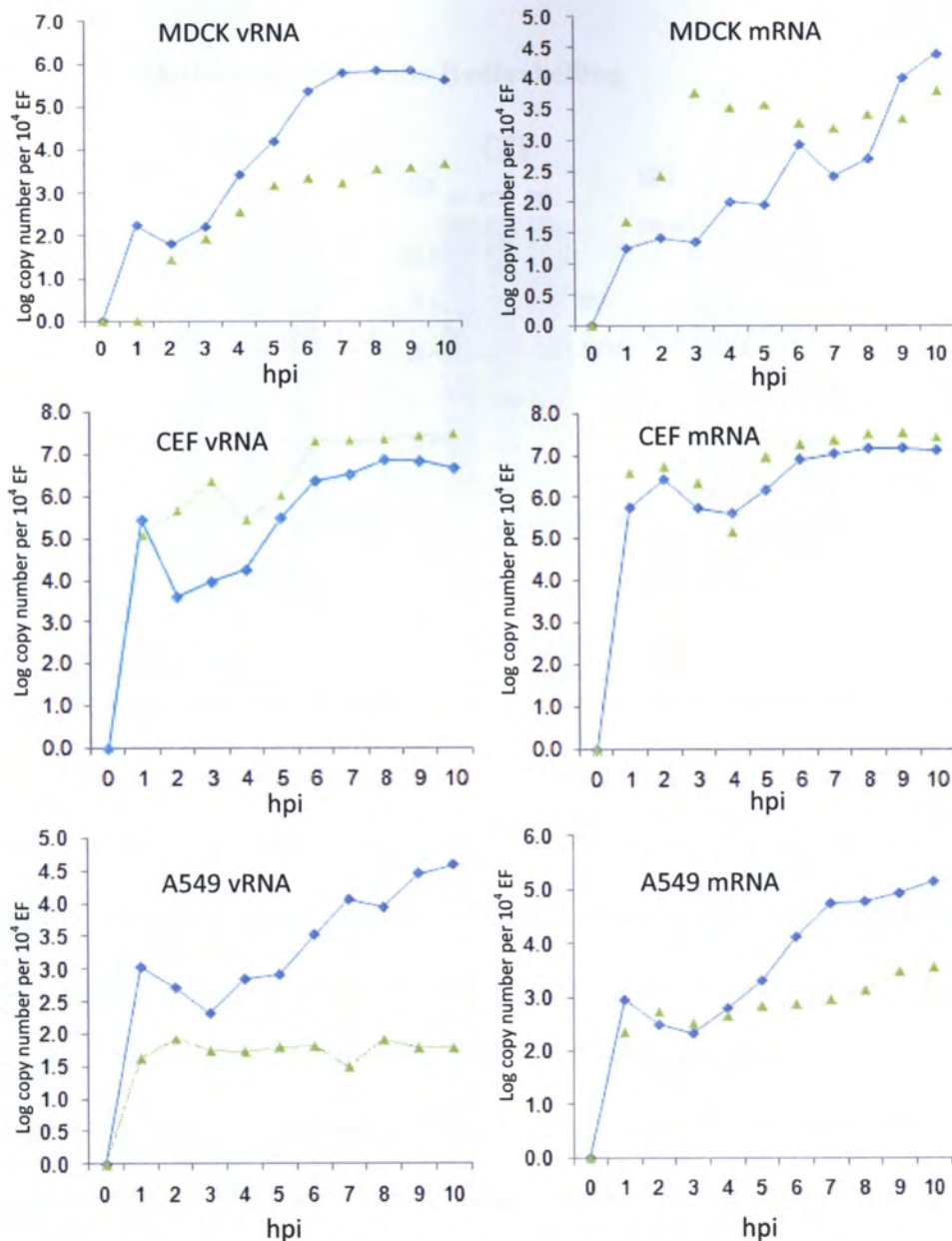


Fig 4.13 The absolute quantification of M vRNA and mRNA in MDCK, CEF and A549 infected with A/WSN/33 (H1N1) (—◆—), and A/Duck/Malaysia/01 (H9N2) (—▲—) (moi =3). All of the graphs shown are normalized to 10⁴ EF copy number. The experiment was carried out in two sets of experiments, measured in triplicates (n=6). Here, the representative of one experiment is shown (n=3).

4.5 [^{35}S]-Methionine Metabolic Radioabelling

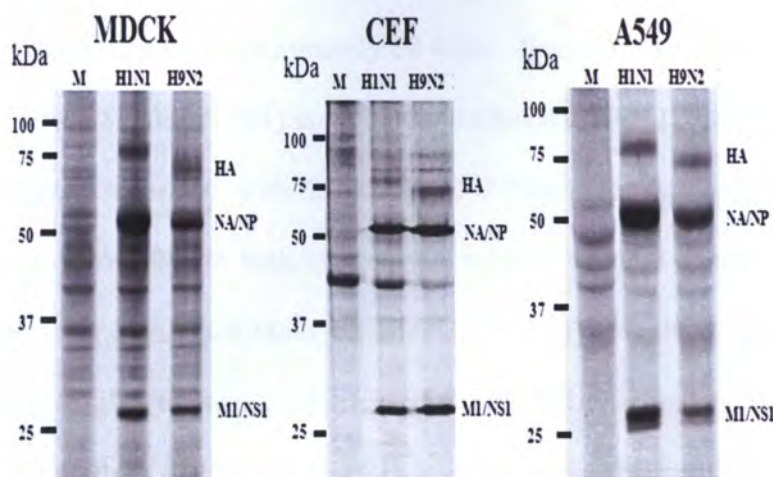


Fig 4.14 The [^{35}S]-methionine metabolic radiolabelling image of MDCK, CEF and A549 infected with A/WSN/33 (H1N1) and A/Duck/Malaysia/01 (H9N2) (moi =3), after 8 hpi, with radiolabelling time conducted at 6 to 7 hpi. The samples were run on 12% SDS-PAGE gel and visualized with 16h exposure time.

The [^{35}S]-methionine metabolic radiolabelling is a method to label virus infected cells, where total viral and host protein expressions can be observed. This labelling can detect protein expression by the incorporation of radiolabelled ^{35}S at approximately 6 hpi for one hour until cell harvesting at approximately 8 hpi. The radiolabelling image is shown in Fig. 4.14. In all cell lines, generally 5 proteins could be observed. Three polymerase proteins, PA, PB1 and PB2 proteins, with the size of approximately 85 kDa, were not detected by this method notably due to the low abundance of the proteins as compared to the other viral and host proteins. A higher exposure time might be required in order to visualize these polymerase proteins, but the host proteins might mask the appearance of these polymerase proteins due to their lower abundance. The protein bands representing NS2 and M2 proteins were not be observed, as they are 14 kDa and 11 kDa, respectively. Therefore it is possible that the proteins have run towards the buffer front on the gel. The HA0 protein was present at

approximately 80 kDa in A/WSN/33 (H1N1) and 72 kDa in A/Duck/Malaysia (H9N2). No HA1 and HA2 proteins were observed since no trypsin was used in this experiment. Both NA and NP protein bands overlapped in A/WSN/33 (H1N1) and H9N2 with similar size at approximately 58 kDa. Both M1 and NS1 protein bands overlapped in A/WSN/33 (H1N1) and A/Duck/Malaysia (H9N2) at approximately 28 kDa, and slightly separated with 28 kDa and 27 kDa for M1 and NS1 proteins respectively in A549 cells. In both MDCK and A549 cells, all 5 bands were at higher intensity than those of A/Duck/Malaysia (H9N2). In CEF cells, NA/NP bands showed approximately similar intensity, whereas HA and M1/NS1 bands showed higher intensity in H9N2 than A/WSN/33 (H1N1) infected cells. This result is similar to the observation in viral kinetics study, where A/WSN/33 (H1N1) replicates better in MDCK and A549 cells, and A/Duck/Malaysia (H9N2) replicates better in CEF cells. In other experiment done by Geiss *et al.* (2001) observed overall decrease in host cellular protein expressions in their [³⁵S]- methionine metabolic radiolabelling image in HeLa infected with A/WSN/33 (H1N1) cells with moi of 50, marked by lighter background. In our experiment, both MDCK and CEF did not exert any obvious decrease in host cellular expression. In A549 cells however, we observed a slight decrease of host cellular expression in A/WSN/33 (H1N1) infected cells. This suggests that the A/WSN/33 (H1N1) is more active in “cap-snatching” in human cell lines than the rest. There is no evidence of decrease in host cellular expression in A/Duck/Malaysia (H9N2) infected cells.

4.6 Conclusion

The growth characteristics of A/WSN/33 (H1N1) and A/Duck/Malaysia/01 (H9N2) were accessed in various methods in three different cell lines, which are

MDCK, CEF and A549 representing canine, chicken and human based cell lines, respectively. The experiments done in this chapter aimed to investigate the virus ability to replicate in different host cells. From the result obtained, the species specificity of the viruses can be further determined.

In immunofluorescence assay, the A/WSN/33 (H1N1) virus showed better replication in MDCK and A549 cell lines. However, A/Duck/Malaysia/01 (H9N2) showed better replication in CEF cell lines. The growth curve experiment also shows similar result, where A/WSN/33 (H1N1) shows higher virus release in MDCK than A/Duck/Malaysia (H9N2). On the contrary, in CEF, A/Duck/Malaysia/01 (H9N2) shows higher virus release than A/WSN/33 (H1N1). Consistent with growth curve experiment, in plaque morphology assay, it could be observed that the plaque formation of A/WSN/33 (H1N1) was much faster than A/Duck/Malaysia/01 (H9N2) in MDCK cell lines.

The vRNA and mRNA quantification of each gene segment in A/WSN/33 (H1N1) and A/Duck/Malaysia/01 (H9N2) also generally concurs with the result obtained from the immunofluorescence assay and growth curve assays. The vRNA and mRNA synthesis of A/WSN/33 (H1N1) could be detected at earlier time point in MDCK and A549 cells than that of A/Duck/Malaysia/01 (H9N2). On the contrary, the A/WSN/33 (H1N1) virus could only be detected at late time point of infection in CEF cells compared to A/Duck/Malaysia/01 (H9N2). Similarly, the M vRNA and mRNA copy number quantification also showed that A/WSN/33 (H1N1) had higher copy number in MDCK and A549, and A/Duck/Malaysia/01 (H9N2) had higher copy number in CEF.

In the [^{35}S]-methionine metabolic radiolabelling, the A/WSN/33 (H1N1) viral bands were generally more intense than those of A/Duck/Malaysia/01 (H9N2) in MDCK and A549 cell lines, which shows that A/WSN/33 (H1N1) has more efficient translation of virus mRNA in those cells. However in CEF, A/Duck/Malaysia/01 (H9N2) showed more intense viral bands than A/WSN/33 (H1N1). Various experiments done in this chapter has shown consistent results to determine the species specificity of A/WSN/33 (H1N1) and A/Duck/Malaysia/01 (H9N2). It can be concluded that A/WSN/33 (H1N1) has better replication rate in A549 and MDCK cells, which suggests that the virus grows better in canine and human cells. However, A/Duck/Malaysia/01 (H9N2) possesses better replication rate in CEF, which shows that the virus grows better in chicken.

Chapter Five. Analysis on Host Response upon Influenza Virus A Infection

The interaction of virus and host upon infection is an important aspect to study mainly with a focus on the host defence mechanism and how the virus can manipulate the host cell to allow efficient replication. In this chapter, we used cDNA microarrays to monitor the progression of the host gene expression over a period of time. The factors that we would aim to examine in this experiment are the upregulated or downregulated population of genes, and their progression toward time.

The Affymetrix[®] cDNA microarrays were employed to monitor the global host gene response of different cell lines infected by the H9N2 isolate. As a comparison, we also used the H1N1/WSN/33 infected cell lines, both with the moi of 3 based on Section 2.2.2.5 validation. The gene expression would then compared to the expression of the mock-infected cells, which was the uninfected allantoic fluid. To ensure the efficient infectivity, immunofluorescence assay was also carried prior to the analysis, as demonstrated in Fig 4.1, 4.2 and 4.3. The parameter observed in this study help us to determine the virus replication ability, the difference of the host defence mechanism and the ability of the virus to counteract it. This strategy also measures the signal intensity in probe sets, which is approximately equivalent to the upregulated or downregulated genes. Probe set is a collection of probes attached in Affymetrix system designed to interrogate a given sequence in an mRNA. One mRNA may be represented by several probe sets depending on the length in order to ascertain the expression intensity. The usage of probe sets for the measurement is useful to identify and include unknown and non-annotated genes as well, and for confirmatory purpose by qRT-PCR and Western Blotting to confirm the biological activity.

To analyze cytokine response, mouse lung macrophages were used as a model cell line. The cells were infected with the viruses, the supernatant harvested, and further analyzed to determine the level of each cytokine. The difference level of cytokine is critical to assess the host immunological response to the virus infection.

5.1 Host Response in MDCK

In this gene expression study, all cells in all time points were infected at moi of 3, where similar number of cells were infected by each virus to enable timepoint by timepoint comparison. The number of the upregulated, downregulated and unchanged probe sets in infected MDCK cells are shown in Fig 5.1. Overall, the amount of downregulated probe sets was much higher in both H1N1 and H9N2 infected cells, which is shown by different scales of the probe sets in the Y-axis. The number of probe sets in the Y-axis refers to the number of differentially expressed mRNAs in the system. This pattern confirms the influenza virus infection characteristics to degrade the host-cell mRNA. This pattern was also found in CEF and A549 cells, as well.

In the upregulated genes, generally there was a steady increase of the number of probe sets in both of the viruses starting from as early as 2 hpi. At 2 hpi, the amount of upregulated probe sets in both H1N1 and H9N2 infected MDCK cells were similar. From 4hpi to 6 hpi, the numbers of upregulated probe sets in the H9N2 isolate were fewer than H1N1, where a significant increase of approximately 50 probe sets from 8 hpi to 10 hpi. The increase in probe sets in H1N1 was observed starting from 6 hpi. At 10 hpi, more than 100 probe sets were upregulated in H9N2, whereas only about 80 probe sets were upregulated in H1N1. This shows that the H9N2 infected cells induces more response than H1N1 infected cells at 10 hpi.

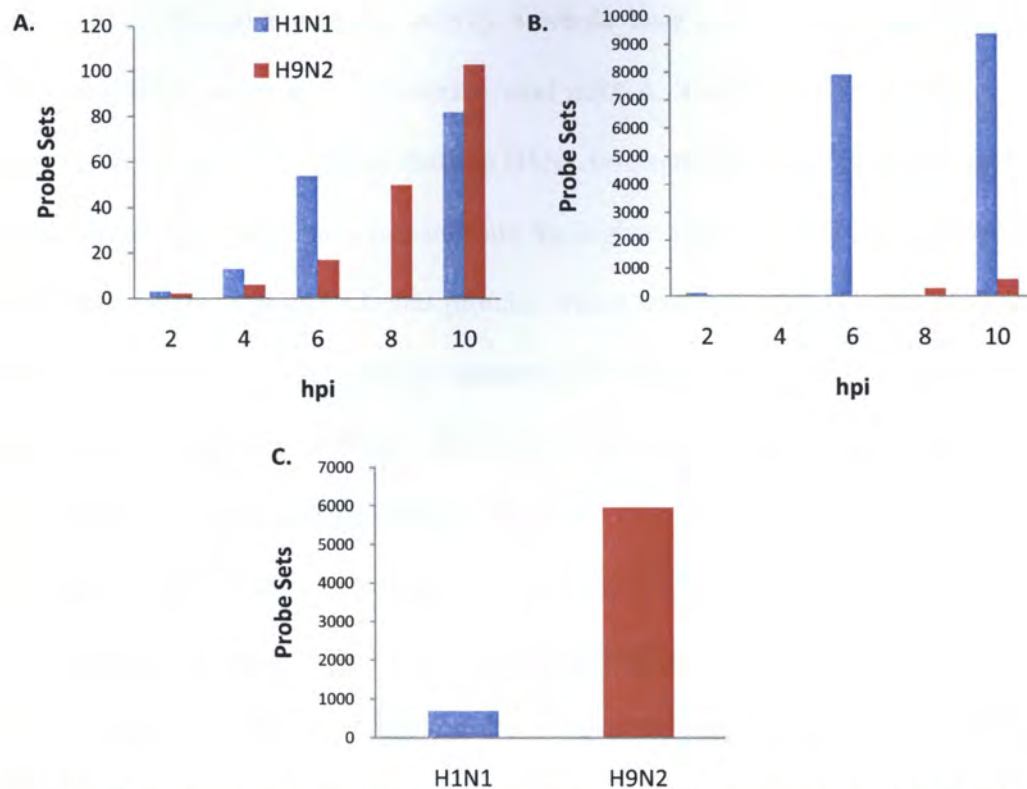


Fig 5.1 The number of upregulated (A), downregulated (B) and unchanged (C) probe sets in MDCK infected with H1N1 and H9N2 isolate. (Note that there is no 8 hpi for for H1N1) (p-value < 0.05, FDR < 0.05, n=3)

From the amount of downregulated probe sets, initially, there were small number of downregulated genes observed in H1N1 infected cells at 2 hpi, and there were insignificant number of downregulated genes observed in H9N2 infected cells. However, starting from 6 hpi, the number of downregulated genes in H1N1 infected cells rose significantly until up to approximately 8,000 probe sets. This increase of downregulated genes in H1N1 infected cells continued until close to 10,000 probe sets at 10 hpi. The H9N2-infected cells did not show any significant increase of downregulated genes until 8 hpi, which also showed slow increase at 10 hpi at approximately 1,000 probe sets. This suggests that the virus is capable of degrading the cellular mRNA in a higher rate in H1N1-infected cells than in H9N2-infected cells. As described in Section 1.3.3, the degradation of the cellular mRNA is due to the

activity of the influenza polymerase complex activity. The polymerase activity is critical to exhibit endonuclease activity towards host cell mRNAs and using the degraded mRNA as primer to transcribe viral mRNA. To relate with the observation found in Section 4.1.1, it is clear that the H1N1 infected MDCK cells started to show nuclear export at 6 hpi, which also indicate the higher activity of the viral polymerase to synthesize new viral mRNA and protein, which suggests high activity of cellular mRNA cap snatching, while H9N2 infected cells only showed steady development only starting from 6 hpi onwards. The more cellular mRNAs are taken over by the virus, the less cellular mRNAs will be detected. This finding is consistent with the observation of the massive decrease of downregulated genes in H1N1-infected MDCK cells, and the slow rise of downregulated genes in H9N2-infected MDCK cells.

It is also interesting to examine the number of unchanged genes in influenza virus infected cells, since the effect of the activity of the viral polymerase protein to cap-snatch the cellular mRNAs is non-specific (Hagen *et al.*, 1994). The definition of unchanged probe sets is that the change in expression does not exceed 1.3 fold change found in all three replicates. The number of unchanged probe sets shown in Fig. 5.2 may indicate the rate of cap snatching activity of the virus. It is noted that the number of unchanged genes in H9N2-infected cells is much more than H1N1-infected cells by approximately 5,000 probe sets in 10 hpi. This finding is also similar to the finding of the number of downregulated genes observed in both H1N1 and H9N2 infected MDCK cells.

The comparison of the upregulated gene grouping in percentage is shown in Fig. 5.2. In both viruses at all time points, the upregulation of each group of genes did not exceed 1% of the total number of probe sets. This is due to the low number of probe sets being upregulated as compared to the total population, for example : total number

of upregulated probe sets in host-pathogen interaction was 15 out of 3310 total probe sets detecting host-pathogen interaction related genes. Similarly, the total number of upregulated probe sets globally was only ~100 out of 22,000 expressed probe sets, which comprised of ~0.45% of the total probe sets. However, the amount of downregulated probe sets showed otherwise where the downregulation could reach up to ~40% of the total probe sets globally in H1N1 infected MDCK cells. The variability and reproducibility of the trends in the graphs below has also been confirmed by statistical significance of $p\text{-value} < 0.05$, $FDR < 0.05$ in three replicates.

There were no upregulated lipid metabolism, and cell death group of genes observed in both H1N1 and H9N2-infected MDCK cells, while there is no upregulated protein metabolism observed in H9N2. This may suggest to the viral activity to halt the progression of apoptosis induction in MDCK cells to optimize the rate of replication. The steady rising number of upregulated genes were clearly observed in H9N2-infected MDCK cells on all groups. However, the H1N1 gene groups showed a slight decrease in the amount of upregulated transcription factors, signal transduction and host-pathogen interactions gene groups from 6 hpi to 10 hpi, and only energy pathways group of genes was detectable at 2 hpi. At 10 hpi, the signal transduction, RNA binding and transcription factor groups of genes also showed more increase in H9N2-infected MDCK cells than H1N1 infected MDCK cells. This activity suggests that the MDCK cells responds and activates more pathways to counteract H9N2 infection than H1N1, which also shows higher cellular activity to counteract viral infection, as shown in higher host-pathogen interaction. In host-pathogen interaction group of genes, the H9N2-infected MDCK cells could be observed as early as 2 hpi, and rose steadily until 10 hpi. At 10 hpi, the percentage of the host-pathogen interaction gene groups in H9N2-infected MDCK cells was also higher than H1N1

infected MDCK cells. This finding suggests that the MDCK cell exhibit higher defense mechanism against H9N2 than H1N1.

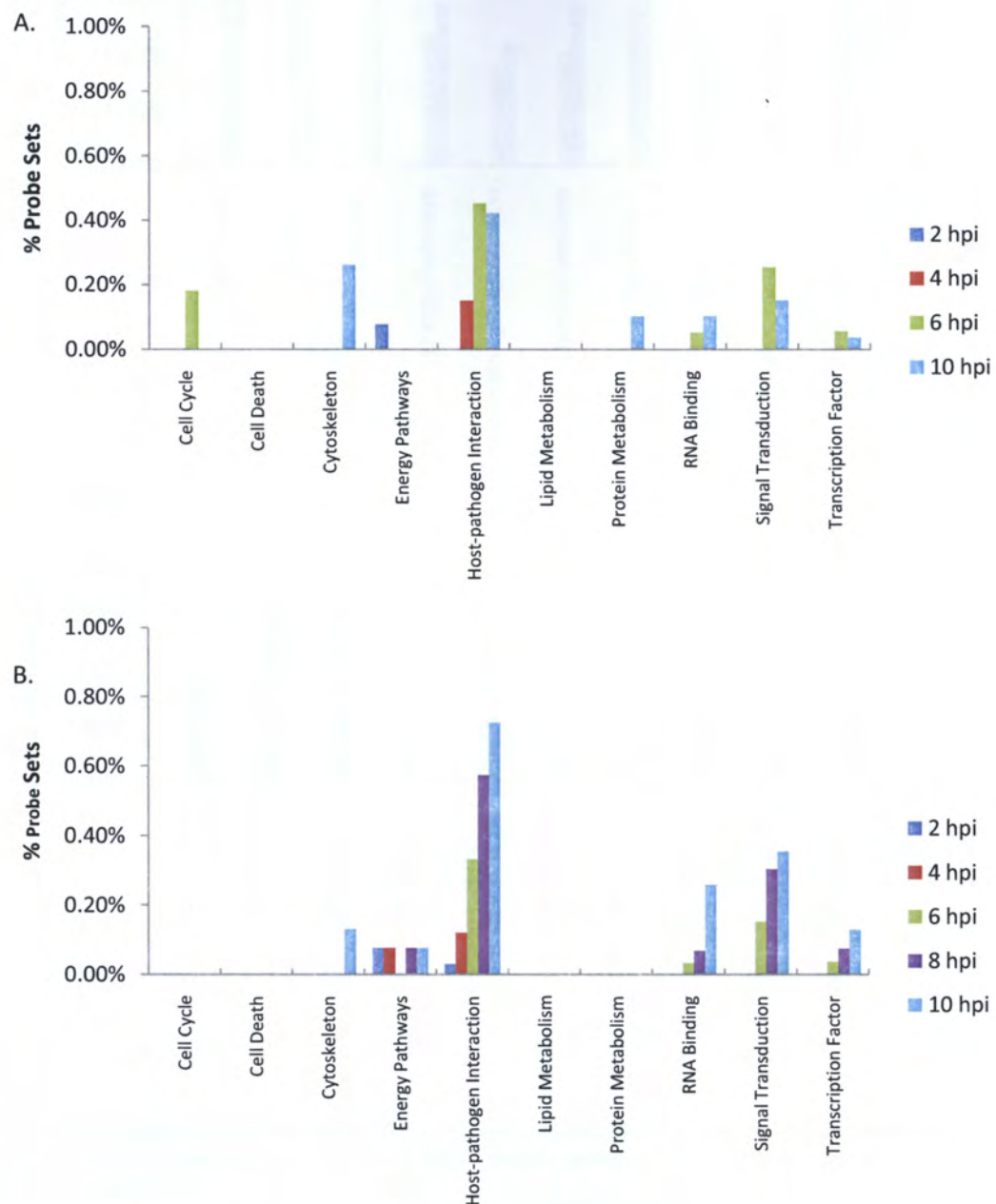


Fig 5.2 The percentage of upregulated gene expression of MDCK cells infected with H1N1 (A) and H9N2 (B) over time, grouped based on the gene function. (p-value < 0.05, FDR < 0.05, n=3)

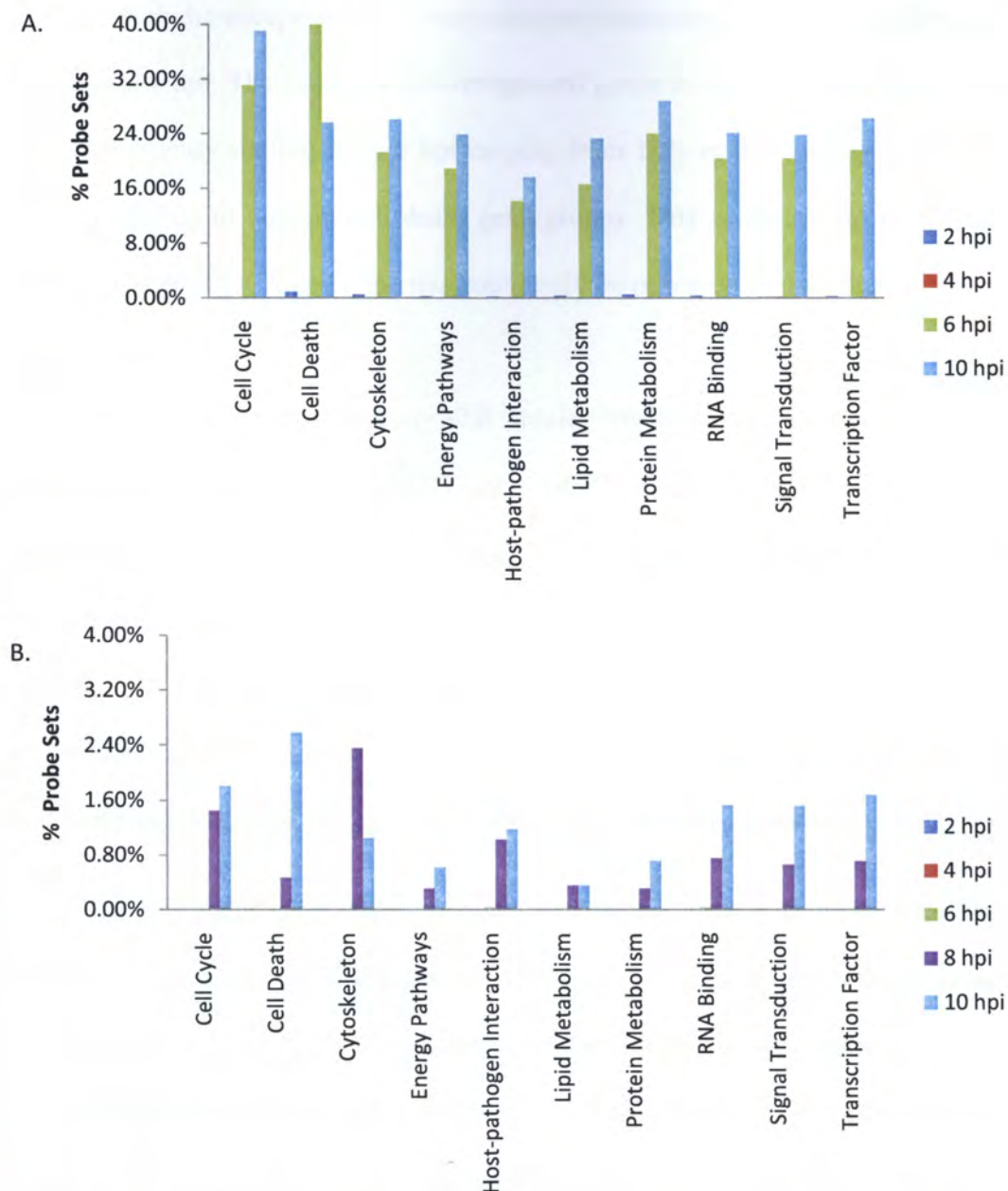


Fig 5.3 The downregulated gene expression of MDCK cells infected with H1N1 (A) and H9N2 (B) over time, grouped based on the gene function. Note the different scaling between the two graphs. (p-value < 0.05, FDR < 0.05, n=3)

The comparison of the downregulated gene grouping in percentage is shown in Fig. 5.3. Generally, most of the gene groups described had already shown a small amount of downregulation in H1N1-infected MDCK cells in as early as 2 hpi. While in H9N2 infected MDCK cells, most of the gene groups were only able to be detected

at 8 hpi, with the exception of the host-pathogen interaction and RNA binding protein which is at 6 hpi. The number of downregulated genes in H1N1-infected MDCK cells rose significantly starting from 6 hpi ranging from 15% in host pathogen interaction gene groups up to 40% in cell death gene groups. This continued up to 10 hpi. In H9N2-infected MDCK cells, the rise could only be observed by less than 2% starting from 8 hpi.

Most of the gene groups exhibit similar trends of the increased number of downregulated genes in both H1N1 and H9N2-infected MDCK cells. It is also interesting to note that the cell death gene groups in H1N1-infected MDCK cells peaked at 6 hpi by 40%, and lowered down to 25% at 10 hpi. The H9N2-infected MDCK cells however, showed a significant increase from approximately 0.4% at 8 hpi, to approximately 2.5% at 10 hpi. In both H1N1 and H9N2-infected MDCK cells, cell death and cell cycle gene groups showed the most downregulated genes.

The unchanged gene expression pattern of MDCK cells infected with H1N1 and H9N2 virus was shown in Fig 5.4. Generally, in all gene groups selected, H9N2-infected MDCK cells had more percentage of unchanged genes compared to H1N1-infected MDCK cells. In H1N1-infected MDCK cells, protein metabolism and energy pathways group of genes had the highest percentage of unchanged genes detected. In H9N2-infected MDCK cells, protein metabolism, energy pathways, cell death and cell cycle gene groups had the most unchanged genes detected.

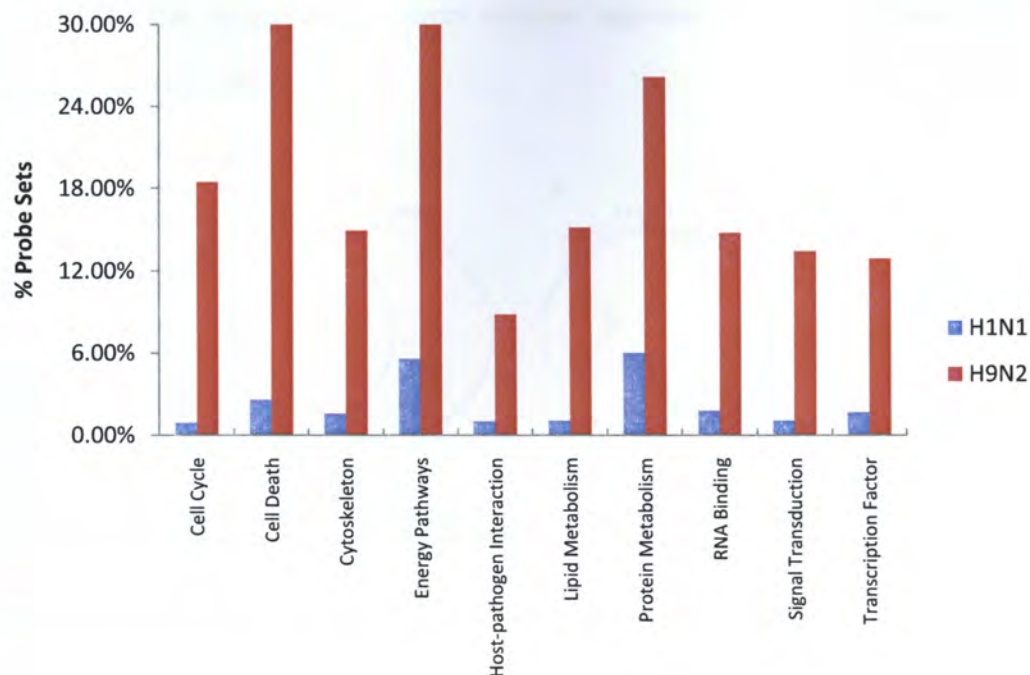


Fig 5.4 The unchanged gene expression of MDCK cells infected with H1N1 and H9N2 over time, grouped based on the gene function. (p-value < 0.05, FDR < 0.05, n=3)

Although it is known that many of the cellular mRNAs are downregulated upon influenza A virus infection, it is interesting to observe the genes that are upregulated as of host response identification. Here, We examined the upregulation of both H1N1 and H9N2-infected MDCK cells at 10 hpi in order study gene profiling of the infected cells related to the virus replication. The representative of which is shown in Fig. 5.5. In this analysis, the observation was focused on which probe sets were common to both virus, and which were unique. The result of those was tabulated in Table 5.1. Then Venn Diagram was classified into cytokine and innate immune response/antiviral gene groups, and cell death gene groups. In the cytokine gene groups, both H1N1 and H9N2 shared similar upregulated genes, which are CCL5 and CXCL10. In the antiviral gene groups, there were 5 upregulated probe sets in H1N1 and H9N2-infected cells, which comprised of interferon induced proteins, Mx1 and RSAD2 genes. It can also be seen that both H1N1 and H9N2 upregulates specific interferon induced protein

in infected cells, suggesting different cellular response towards infection of both viruses in MDCK cells.

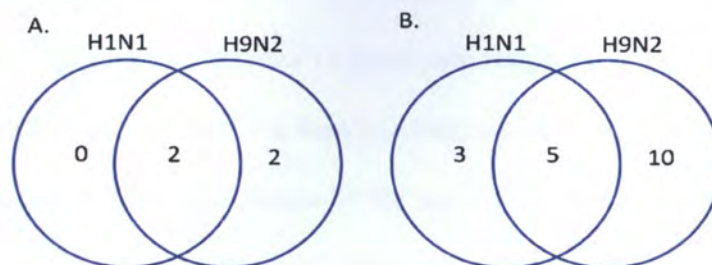


Fig. 5.5 The Venn Diagram of the amount of upregulated genes in H1N1 and H9N2 infected MDCK cells in cytokine genes (A), antiviral/innate immune related genes (B)

Table 5.1 List of upregulated cytokine, antiviral/innate immune related genes in MDCK cells

Cytokine					
GeneBank	Gene Symbol	Description	H1N1	H9N2	H1N1 and H9N2
CO676693	CCL4	chemokine (C-C motif) ligand 4	A	P	A
NM_001003010	CCL5	chemokine (C-C motif) ligand 5	P	P	P
pmma10679	LOC483406	similar to Interferon regulatory factor 7 (IRF-7)	A	P	A
BU748818	CXCL10	chemokine (C-X-C motif) ligand 10	P	P	P
pmma11883	LOC482905	toll-like receptor 3	A	P	A
Antiviral					
GeneBank	Gene Symbol	Description	H1N1	H9N2	H1N1 and H9N2
BU745815	OAS1	2',5'-oligoadenylate synthetase 1, 40/46kDa	P	P	P
pmma13997	OAS2	2'-5'-oligoadenylate synthetase 2, 69/71kDa	A	P	A
pmma16356	OASL	2'-5'-oligoadenylate synthetase-like	A	P	A
DN268079	LOC490198	interferon-induced protein 44	P	A	A
DN267574	LOC479980	interferon-induced protein 44-like	P	P	P
pmma15021	LOC488947	interferon-induced protein with tetratricopeptide repeats 1	P	P	P
pmma15018	LOC479183	interferon-induced protein with tetratricopeptide repeats 2	P	A	A
DN272024	LOC479575	ISG15 ubiquitin-like modifier	P	A	A
CO694611	LOC609006	LIM domain only 2 (rhombotin-like 1)	A	P	A
pmma15820	MX1	myxovirus (influenza virus) resistance 1	P	P	P
NM_001003133	MX2	myxovirus (influenza virus) resistance 2 (mouse)	A	P	A
	RSAD2	radical S-adenosyl methionine domain containing 2	P	P	P
pmma26752	LOC490461	S100 calcium binding protein A8	A	P	A
pmma19510	LOC606875	similar to immunity-related GTPase family, cinema 1	A	P	A
pmma1605	LOC481471	similar to interferon gamma inducible protein 47	A	P	A
CN002479	LOC478170	similar to interferon induced 6-16 protein isoform a	A	P	A
CO585250	LOC477402	similar to Nuclear autoantigen Sp-100	A	P	A
pmma1603	LOC478406	SON DNA binding protein	A	P	A

Note :

P : gene is upregulated

A : gene is not upregulated

Furthermore, we studied the upregulation pattern of the cytokine gene groups of the H9N2 and H1N1 infected cells, which was shown in Fig. 5.6. In this experiment, although the period of life-cycle in both viruses are different, we chose up to 10 hpi with 2 hpi interval in order to cover one single cycle of infection from the initial step of infection until the virus budding step, which is up to 10 hpi, as shown in immunofluorescence assay. The reason of the same time point usage, rather than the equivalent time points is to monitor gene expression difference in the same time point, which later could explain the more rapid replication of H1N1 WSN than H9N2. It is interesting to observe that Toll – like receptor 3 is not significantly upregulated in H1N1-infected MDCK cells. Toll – like receptor 3 recognizes dsRNA molecular pattern associated with viral infection, which leads to the activation of NF- κ B and type I interferon (Alexopoulou *et al.*, 2001). Both IRF1 and IRF7 genes was not upregulated in H1N1, but IRF7 gene upregulated slightly in H9N2. The antiviral genes MX1, OAS1 and OAS2 genes were detected in H1N1 as early as 6 hpi, whereas in H9N2, most of them were only detected at 10 hpi. The MX1, and OAS genes functions have been discussed in detail in Section 1.6.1.1, and 1.6.1.2, respectively. It could also be observed that H1N1 infected cells can upregulate these genes with higher fold change of these antiviral genes than H9N2-infected cells.

The expression of CCL5/RANTES in H9N2-infected cells was much higher compared to that in H1N1. Furthermore, it could be detected as early as 2 hpi in H9N2-infected cells. CCL5/RANTES is initiated after the cells detected dsRNA of the virus, and the downstream activation depends on the activation of PKR and RIG-I genes, which can be inhibited by NS1 protein of influenza virus. It is possible that NS1 protein of H1N1 is more potent of inhibiting the chemokine production of

CCL5/RANTES than H9N2. It also can be observed that the RSAD2 was expressed as early as 4 hpi in H1N1-infected cells, and can only be found in H9N2-infected cells in 10 hpi. The delayed expression in H9N2 might be due to lower interferon response. But in the end, the RSAD2 expression of both H1N1 and H9N2 cells were similar.

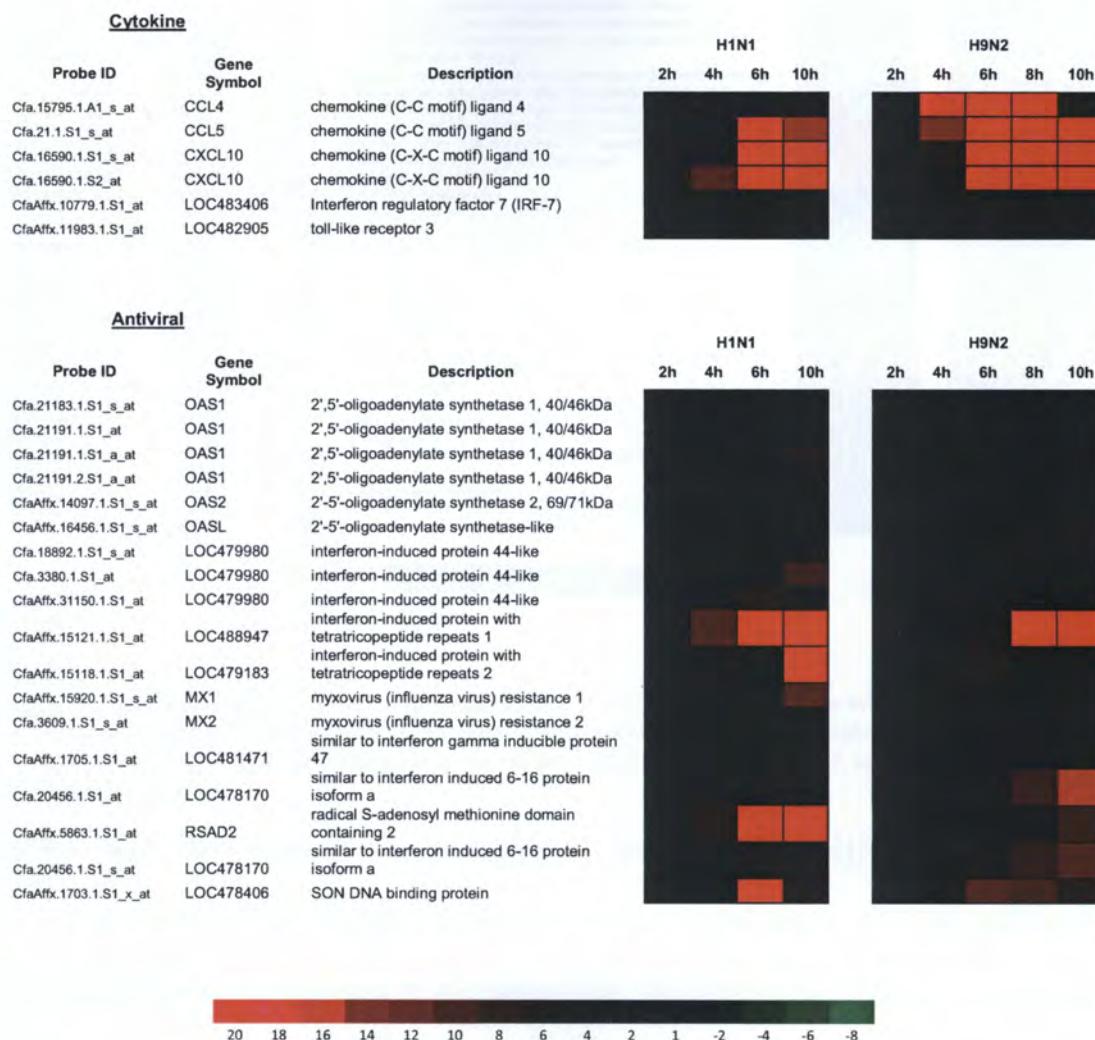


Fig. 5.6 The heatmap of the host-gene response in H1N1 and H9N2 infected MDCK cells. The heatmap scale bar represents fold change value from -8 to 20. (p-value < 0.05, FDR < 0.05, n=3)

Generally the H1N1-infected MDCK cells are prone to downregulate more genes in cholesterol metabolism pathway than H9N2-infected MDCK cells (Fig. 5.7). From the heatmap shown, the downregulation pattern was apparent from as early as 6 hpi in H1N1-infected cells, while H9N2-infected cells only showed 2 downregulated

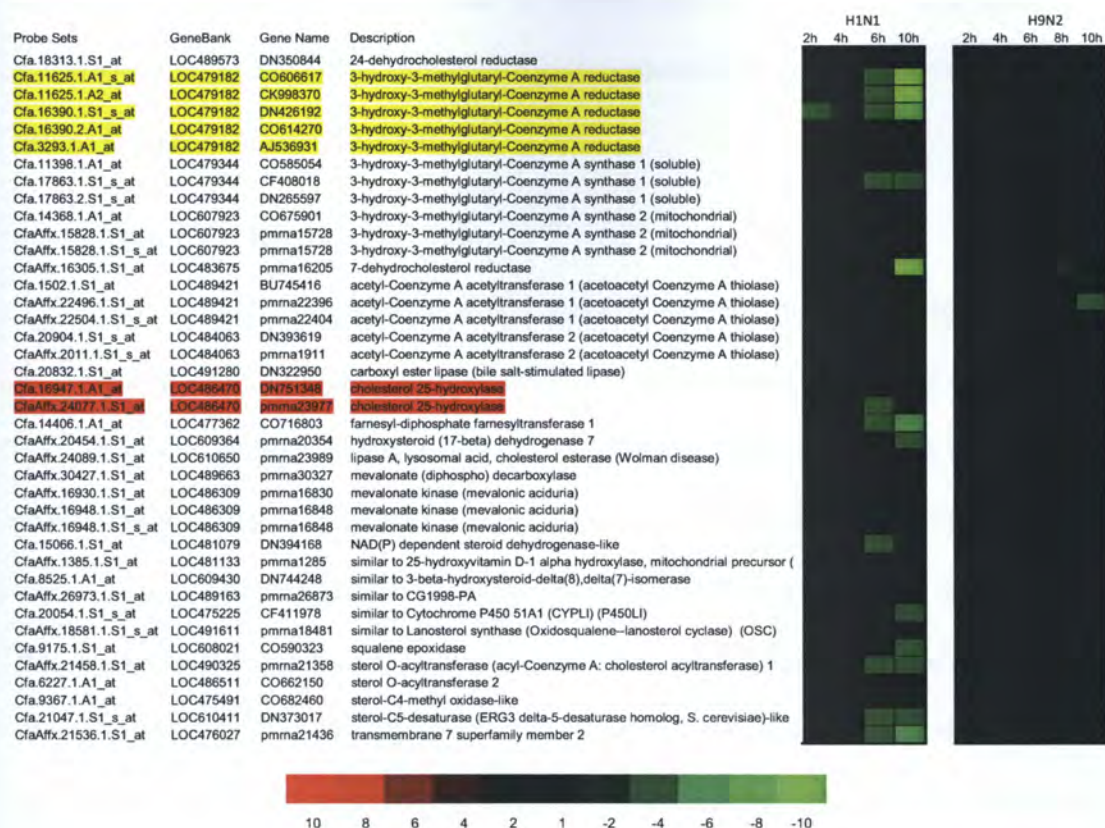


Fig. 5.7 Heatmap on Cholesterol Metabolism related genes in H1N1 and H9N2 infected MDCK cells. Highlighted in yellow is 3-hydroxyl-3-methylglutaryl-Coenzyme A reductase (HMGCR), and highlighted in red is cholesterol 25-hydroxylase (C25H). The heatmap scale bar represents fold change value from -10 to 10. (p-value < 0.05, FDR < 0.05, n=3)

probe sets. To examine the activity of the HMGCR, H1N1-infected cells downregulated the gene for approximately more than 8 fold, while H9N2 did not show any significant downregulated. In the experiment, the cholesterol 25-hydroxylase only showed slight downregulation at 6 hpi in H1N1-infected cells, and there was no downregulation of the gene in H9N2-infected cells. It is known that the decrease of cellular cholesterol will increase viral budding, but with lower infectious viral particles (Barman and Nayak, 2007). It is also known that RSAD2 protein interacts with farnesyl diphosphate farnesyl transferase (FPPS) in antagonistic way (Wang *et al.*, 2007) In Fig 5.6, it is shown that H1N1-infected MDCK cells upregulates RSAD2

more than H9N2-infected cells. Consistent with Wang *et al.* (2007) finding, the downregulation of FPPS is greater in H1N1-infected cells. To conclude, the downregulation of the cholesterol metabolism pathway is controlled by the host to reduce the infection rate of H1N1.

5.2 Host Cells Response in CEF

The amount of upregulated, downregulated and unchanged probe sets in H1N1 and H9N2-infected CEF cells is shown in Fig. 5.8. This result is contrary to what has been observed in MDCK-infected cells. In addition, there were more upregulated probe sets in H1N1 infected CEF cells compared to H9N2 infected CEF cells. There were also more downregulated probe sets in H9N2 infected CEF cells compared to H1N1-infected CEF cells. In H1N1-infected CEF cells, increase of the quantity of upregulated probe sets were gradual, starting from approximately 18 probe sets at 2 hpi, which then rose to approximately 60 probe sets at 8 hpi. The rise then increased dramatically to 140 probe sets at 10 hpi. In H9N2 infected CEF cells, the rise started from approximately 8 probe sets at 2 hpi, and rose steadily until the number of upregulated genes reached 60 probe sets at 6 hpi.

No downregulated genes were observed at 2 hpi and 4 hpi in both H1N1 and H9N2 infected CEF cells. At 6 hpi, both H1N1 and H9N2 infected CEF cells only showed less than 100 probe sets of downregulated genes. The dramatic rise of downregulated probe sets were observed for both H1N1 and H9N2 infected CEF cells at 8 hpi onwards, and increased steadily from 8 hpi to 10 hpi. The H9N2 infected CEF cells showed slight decrease from 8 hpi to 10 hpi. The number of downregulated probe sets in H9N2 reached as high as approximately 2,250 probe sets at 10 hpi, whereas H1N1 almost reached 1,000 probe sets at 8 hpi, which then decreased to

approximately 650 probe sets at 10 hpi. Based from these result, it could be concluded that CEF cells have a better antiviral defence mechanism against H1N1 infection better than H9N2. At the same time, the H9N2 replicated better in CEF cells. To relate the result shown in Section 4.1.2, where H1N1 did not show any significant fluorescent signal until 6 hpi and H9N2 had shown signal as early as 4 hpi, this indicates the faster rate of replication of H9N2 than H1N1 in CEF cells, which in turn degrades more cellular mRNA.

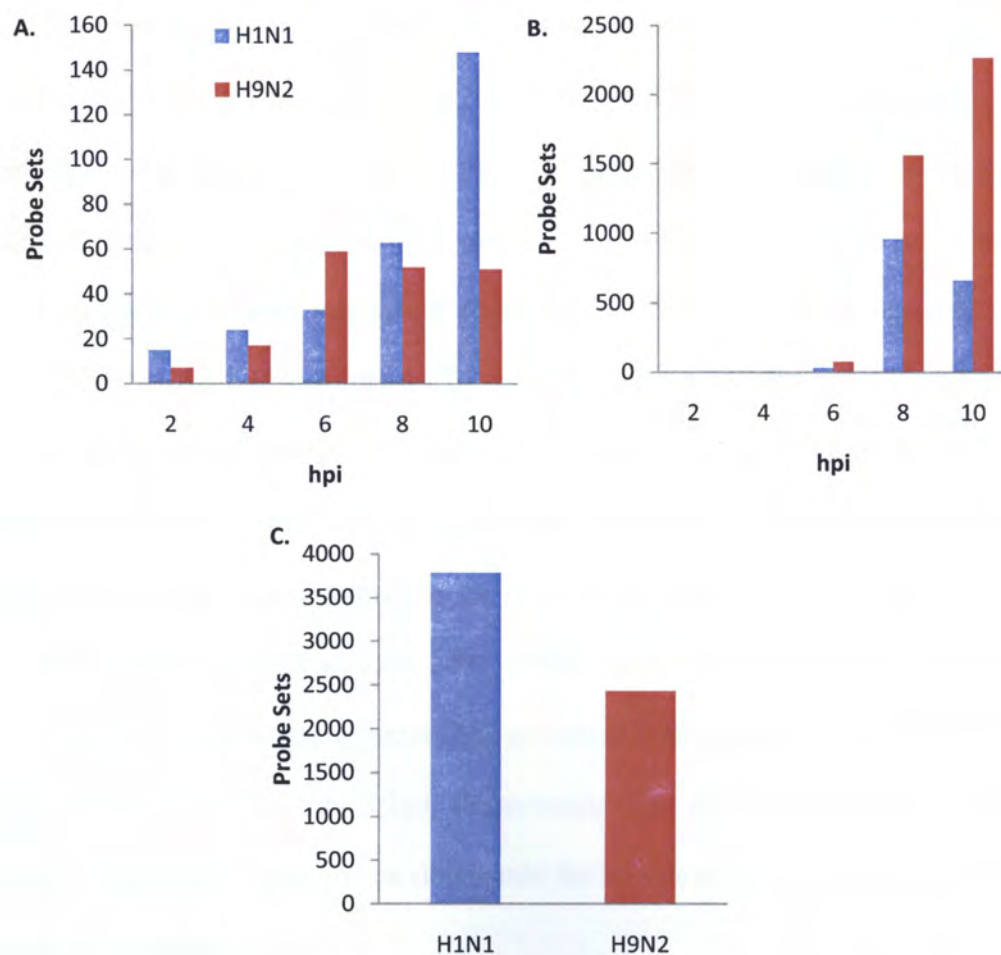


Fig. 5.8 The amount of upregulated (A), downregulated (B) and unchanged (C) probe sets in CEF infected with H1N1 and H9N2 isolate. (p-value < 0.05, FDR < 0.05, n=3)

The number of unchanged genes was higher in H1N1-infected CEF cells than H9N2-infected CEF cells, which was approximately 3,700 and 2,500 probe sets in H1N1 and H9N2-infected cells, respectively. Consistent with the result shown in Chapter 5, the slower growth of H1N1-infected CEF cells may be attributed to higher amount of intact mRNAs, as compared to H9N2-infected CEF cells.

The upregulated gene groups in CEF infected with H1N1 and H9N2 is shown in Fig. 5.9. In H1N1-infected CEF cells, there was a steady increase of almost all gene groups up to 8 hpi with the exception of cell cycle, cytoskeleton and energy pathways. The cell cycle and energy pathways were only detected at 10 hpi. There were no cytoskeleton gene groups detected in H1N1-infected CEF cells. Most of the genes showed a sharp rise from 8 hpi to 10 hpi in upregulated gene groups of cell death, host-pathogen interaction, and lipid metabolism and transcription factor. The cell death and host pathogen interaction gene groups dominated the upregulated genes profile. In contrast, H9N2-infected CEF cells, the amount of upregulated gene groups did not show steady rise with the increase of infection time as observed in H1N1-infected CEF cells. However, host-pathogen interaction, protein metabolism and transcription factor gene groups can be detected as early as 2 hpi. There were no cytoskeleton and energy pathways gene groups being upregulated in H9N2 infected CEF cells. Cell death and cell cycles gene groups were only detected in H9N2-infected CEF cell lines at 6 hpi and 8 hpi, respectively. The protein metabolism and host pathogen interaction gene groups dominated the upregulated genes profile in H9N2-infected CEF cells.

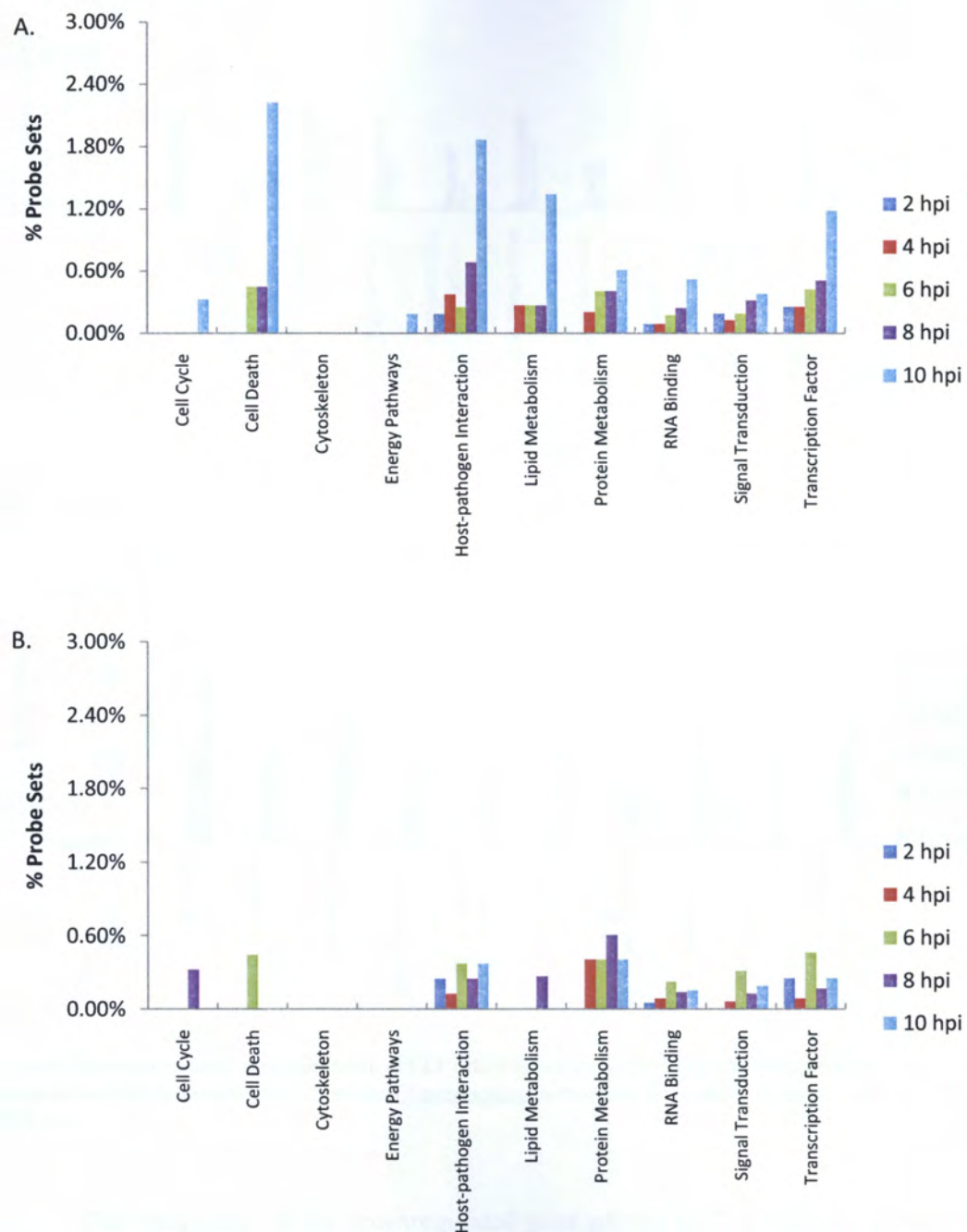


Fig 5.9 The upregulated gene expression of CEF cells infected with H1N1 (A) and H9N2 (B) over time, grouped based on the gene function. (p-value < 0.05, FDR < 0.05, n=3)

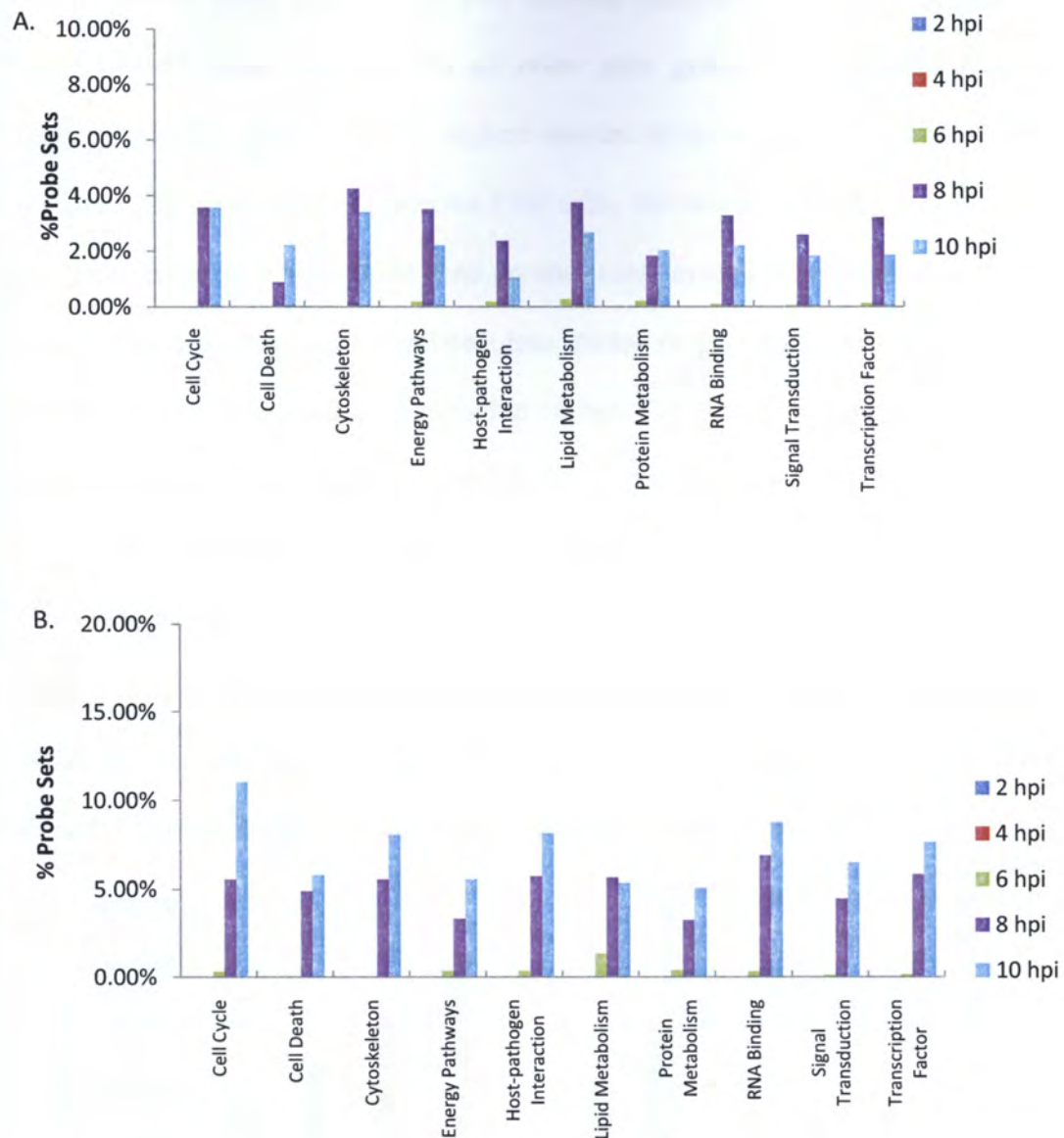


Fig 5.10 The downregulated gene expression of CEF cells infected with H1N1 (A) and H9N2 (B) over time, grouped based on the gene function. Note the different scaling between the two graphs. (p-value < 0.05, FDR < 0.05, n=3)

The comparison of the downregulated gene groups in CEF infected with H1N1 and H9N2 is shown in Fig. 5.10. For CEF infected with both H1N1 and H9N2, all the downregulation gene groups were observed at 6 hpi except for cytoskeleton and cell death. In H1N1 infected CEF cells, the downregulated gene groups were observed at 6 hpi, rose significantly at 8 hpi, and decreased slightly at 10 hpi. Cytoskeleton, cell

death and cell cycle gene groups only showed significant rise at 6 hpi, but with approximately equal amount with all other gene groups. Cytoskeleton and lipid metabolism gene groups had the highest amount of downregulated genes in H1N1 infected CEF cells. In H9N2 infected CEF cells, the downregulated genes were only be able to be seen at 6 hpi in all gene groups except cytoskeleton and cell death gene groups. The amount of downregulated gene started rising significantly from 8 hpi for all gene groups, and steadily increased in 10 hpi. The cell cycle gene groups showed highest amount of downregulated genes in H9N2 infected CEF cells.

The comparison of unchanged gene groups between H1N1 and H9N2 infected CEF cells is shown in Fig 5.11. It could be seen that for both H1N1 and H9N2 infected CEF cells, protein metabolism and energy pathways gene groups had the highest percentage of unchanged genes. Generally, H9N2 infected CEF cells had higher amount of unchanged genes as compared to H1N1 infected CEF cells.

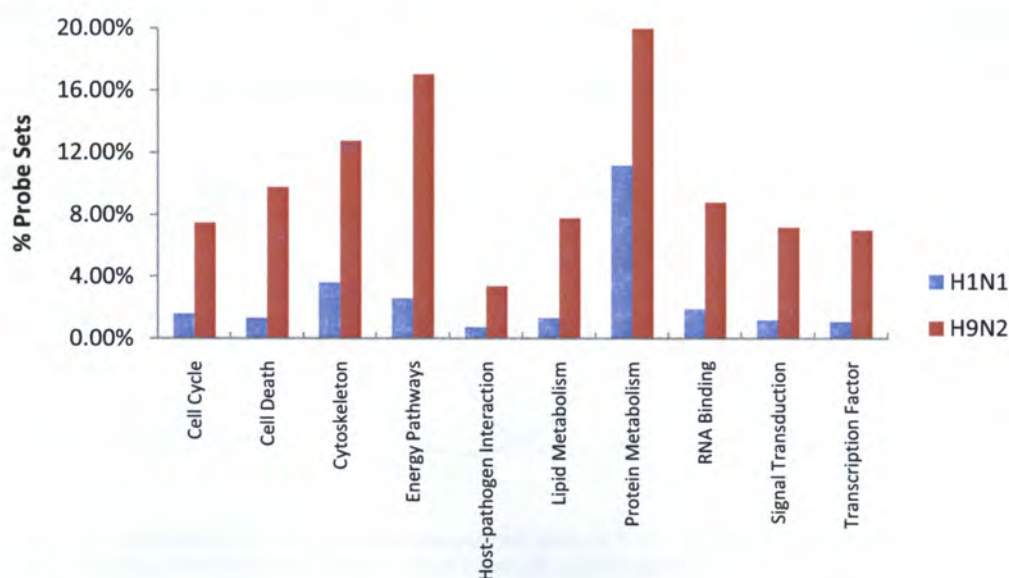


Fig 5.11 The unchanged gene expression of CEF cells infected with H1N1 and H9N2 over time, grouped based on the gene function. (p-value < 0.05, FDR < 0.05, n=3)

Three classes of probe sets were selected for grouping in the CEF infected with H1N1 and H9N2, and the result is shown in Fig. 5.12. The groupings consist of cytokine gene groups, antiviral/innate immune gene groups and cell death gene groups. The complete list of the genes is listed in Table 5.2. From the cytokine gene groups, it can be seen that H9N2 only upregulated 3 probe sets which was also upregulated in H1N1, and these are TLR3 IRF1 and IRF7. The genes that were upregulated only in H1N1 infected CEF cells were IRF genes, and IL8. Similarly, in the antiviral/innate immune gene groups, H1N1 upregulates more probe sets than H9N2. There were only 8 probe sets that were upregulated in both H9N2 and H1N1 infected CEF cells, and these are Mx1, OASL, and mature cGMF gene. The antiviral/innate immune genes expressed exclusively in H1N1 infected CEF cells are mostly interferon induced genes. In the cell death genes, the H1N1 upregulated 4 probe sets while H9N2 does not have upregulated probe set. To relate with the finding in Chapter 4, it can be seen that the H9N2, which is shown to replicate better in CEF cells, upregulates less cytokine and antiviral/innate immune related genes and cell death genes.

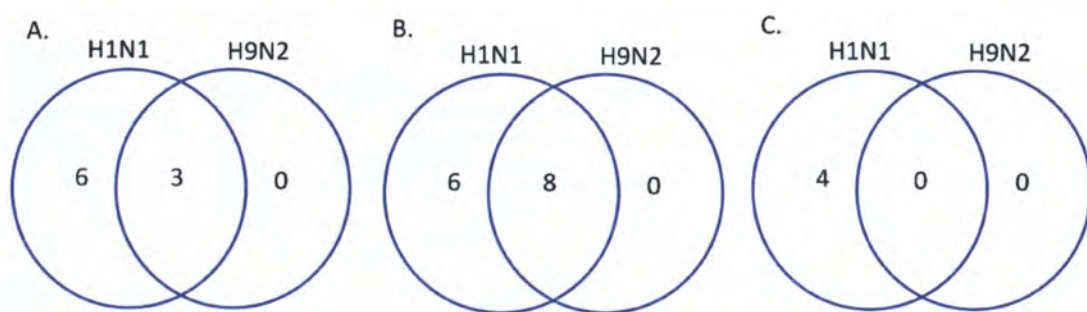


Fig. 5.12 The Venn Diagram of the amount of upregulated genes in H1N1 and H9N2 infected CEF cells in cytokine genes (A), antiviral/innate immune related genes (B) and cell death (C)

Table 5.2 List of upregulated cytokine, antiviral/innate immune, and cell death related genes in CEF cells

Cytokine

GeneBank	Gene Symbol	Description	H1N1	H9N2	H1N1 and H9N2
ENSGALT00000018067	IFIH1	interferon induced with helicase C domain 1	P	A	A
NM_205415	IRF1	interferon regulatory factor 1	P	P	P
NM_204558	IRF10	interferon regulatory factor 10	P	A	A
NM_205372	IRF7	interferon regulatory factor 7	P	P	P
NM_204524	IL1B	interleukin 1, beta	P	A	A
AJ564201	IL12B	interleukin 12B	P	A	A
NM_204628	IL6	interleukin 6 (interferon, beta 2)	P	A	A
M16199	IL8	interleukin 8	P	A	A
ENSGALT00000021950	TLR3	toll-like receptor 3	P	P	P

Antiviral

GeneBank	Gene Symbol	Description	H1N1	H9N2	H1N1 and H9N2
NM_204487	EIF2AK2	eukaryotic translation initiation factor 2-alpha kinase 2	P	A	A
NM_205018	K60	K60 protein	P	P	P
NM_205279	LOC396216	mature cMGF	P	P	P
BU120914	LOC417053	similar to class I alpha chain	P	A	A
AY257166	LOC417055	similar to MHC Rfp-Y class I alpha chain	P	P	P
ENSGALT00000015431	LOC420559	similar to KIAA2005 protein	P	A	A
ENSGALT00000010311	LOC423790	similar to Interferon-induced protein with tetratricopeptide repeats 5 (IFIT-5)	P	P	P
ENSGALT00000005376	LOC424402	similar to E-selectin precursor (Endothelial leukocyte adhesion molecule 1)	P	A	A
NM_204775	LY6E	lymphocyte antigen 6 complex, locus E	P	P	P
NM_204609	MX	Mx protein	P	P	P
NM_205041	OASL	2'-5'-oligoadenylate synthetase-like	P	P	P
ENSGALT00000012390	STAT4	signal transducer and activator of transcription 4	P	P	P
BU351319	VCAM1	vascular cell adhesion molecule 1	P	A	A
CR389298	ZC3HAV1	zinc finger CCCH-type, antiviral 1	P	A	A

Cell Death

GeneBank	Gene Symbol	Description	H1N1	H9N2	H1N1 and H9N2
ENSGALT00000024241	LOC427224	similar to programmed cell death 1 ligand 1	P	A	A
BU246920	LOC421684	similar to Tumor necrosis factor, alpha-induced protein 3	P	A	A
BU313956	SOCS1	suppressor of cytokine signaling 1	P	A	A
BU426375	TNFSF15	tumor necrosis factor (ligand) superfamily, member 15	P	A	A

Note :

P denotes the gene is upregulated

A denotes the gene is not upregulated

The host interferon response gene expression in CEF infected cells is shown in Fig. 5.13. Generally, the responses in H1N1-infected cells could be detected as early as 2 hpi, whereas for H9N2-infected cells, some of the genes actually became less

upregulated, and for the antiviral Mx1 and OASL gene expression, it could be seen that H1N1 infected CEF cells upregulates in much higher amount than H9N2 infected CEF cells. This similar trend was also observed in the EIK2AK2/PKR, TLR3, IRF1, IRF7 and STAT4. Furthermore in H1N1-infected cells, most of the gene expression continued to peak until 10 hpi, whereas in H9N2-infected cells, most of them peak only until 6 hpi and then steadily decline. The IRF7 gene in H9N2-infected cells did not show upregulation anymore at 8 hpi. This pattern of expression explained the ability of H9N2 to counter with CEF cells antiviral defence mechanism better than H1N1. This result is also consistent with the viral kinetics experiment, where H9N2 was found to be more efficient in replication and transcription in CEF cells compared to H1N1.

In the cell death group, the expression of SOCS1 in H1N1 was apparent at 10 hpi. However, the SOCS1 expression was downregulated in H9N2 infected cells. Suppressor of cytokine signalling (SOCS) is a pivotal negative regulator for cytokine signalling (Krebs and Hilton, 2001). Pothlichet *et al.* (2008) demonstrated that SOCS1 and SOCS3 up-regulation requires a TLR3-independent, RIG-I/MAVS/IFNAR1-dependent pathway. Further, they also revealed that the molecules inhibit antiviral responses. This observation suggests that the upregulation of SOCS1 in H1N1 could be a result from the high expression of all interferon related genes. In H9N2, the interferon-related genes were not expressed as high, and this probably explains the absence of the SOCS1. Similar experiment was conducted by Xing *et al.*, 2008, where they conducted microarray experiment on H9N2 and H6N2 viruses on chicken macrophages, they found that In H9N2 virus-infected chicken macrophages, Toll-like receptor 7 responded to infection and mediated the cytokine responses. Many of the pro-inflammatory cytokines were largely upregulated such as IRF3 and IRF7.

Interestingly, they also found that the interferon (IFN) response was fairly weak, but with the differentially regulated of IFN-inducible gene, which was similar to the expe-

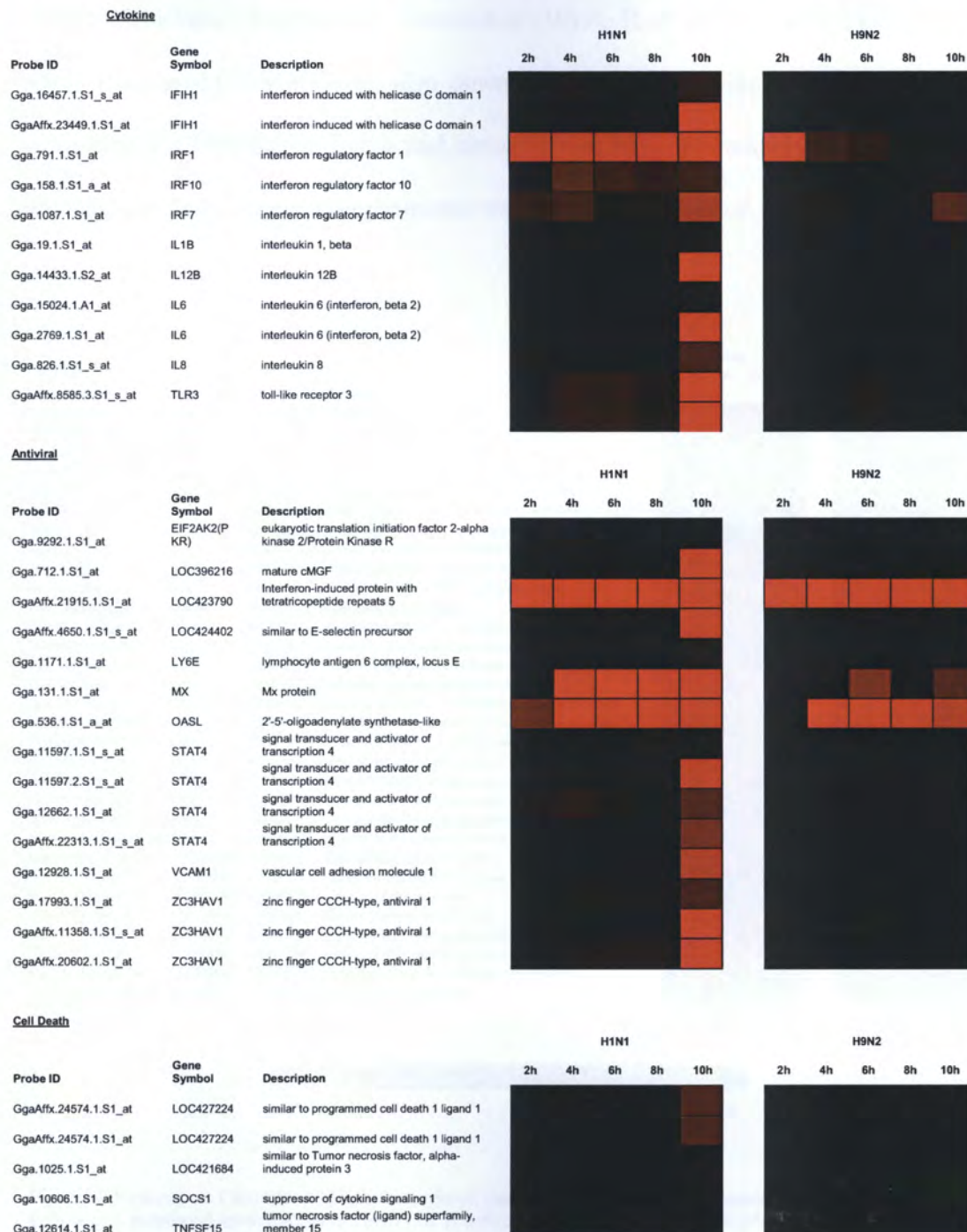


Fig. 5.13 The heatmap of the host-gene response in H1N1 and H9N2 infected CEF cells. The heatmap scale bars denotes the fold change value from -8 to 20. (p-value < 0.05, FDR < 0.05, n=3)

riment conducted. Among the regulated genes, major histocompatibility complex (MHC) antigens II were downregulated, which also occurred in the lungs of H9N2-infected chickens. Additionally, interleukin (IL)-4, IL-4 receptor and CD74 (MHC class II invariant chain) were also downregulated, all of which are pivotal in the activation of CD4⁺ helper T cells and humoral immunity. Remarkably, in H9N2 virus-infected chickens, the antibody response was severely suppressed.

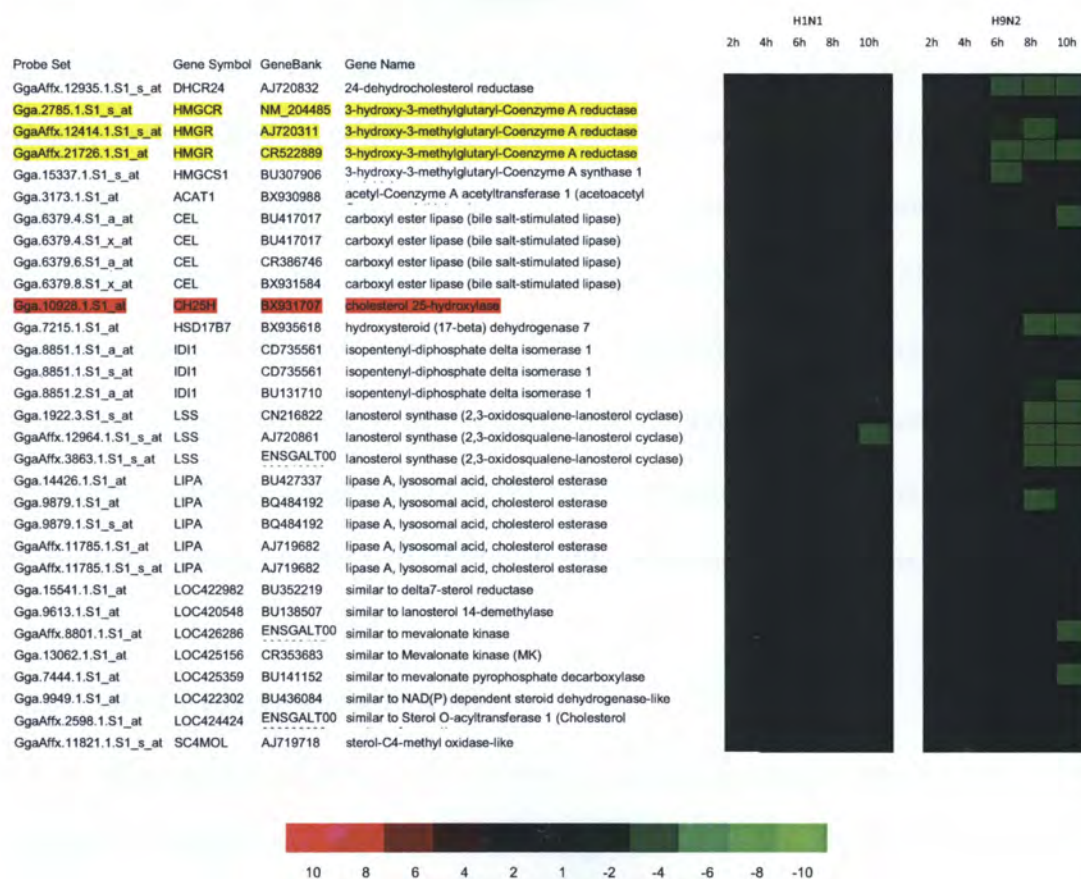


Fig. 5.14 Heatmap on Cholesterol Metabolism related genes in H1N1 and H9N2 infected CEF cells. Highlighted in yellow is 3-hydroxy-3-methylglutaryl-Coenzyme A reductase (HMGCR), and highlighted in red is cholesterol 25-hydroxylase (C25H). The heatmap scale bars denotes the fold change value from -10 to 10. (p-value < 0.05, FDR < 0.05, n=3)

The list of cholesterol metabolism pathways gene of H1N1 and H9N2 infected CEF cells are shown in Fig. 5.14. The H1N1 infected CEF cells did not show any significant downregulation even until 10 hpi. The H9N2 infected CEF cells showed downregulation in approximately 50% of the genes responsible in the cholesterol pathways from 6 hpi onwards. This finding correlates with both the HMGCR and CH25H gene profiling. In H1N1 infected CEF cells, there were no downregulation of the HMGCR gene, while there was slight increase of CH25H gene at 10 hpi by approximately 2 fold. In H9N2 infected cells, HMGCR was downregulated by approximately 5 fold at 6 hpi and it progressed up to 10 hpi. There was no significant change in the CH25H gene profiling. It has been documented that CH25H can inhibit the cholesterol biosynthesis, and the influenza virus exhibits better budding in cholesterol depleted cells. This finding suggests that the upregulation of CH25H gene in H1N1 infected CEF cells is the virus attempt to reduce the cholesterol amount in the cells due to their inability to downregulate the cholesterol biosynthesis. The H9N2 infection in CEF cells, however, does not require an upregulation of the CH25H gene, as the virus itself is capable to downregulate the cholesterol biosynthesis.

5.3 Host Cells Response in A549

The number of upregulated, downregulated and unchanged probe sets of A549 infected with H1N1 and H9N2 is shown in Fig. 5.15. In H1N1-infected A549 cells, the increase in the upregulated genes could be observed as early as 2 hpi and steadily increased until up to 10 hpi, which reached approximately 70 probe sets. The amount of upregulated probe in H9N2-infected cells, however, showed a very different profile. There were not many upregulated probe sets detected until up to 4 hpi. At 6 hpi, the amount of upregulated probe sets increased significantly exceeding 100 probe sets.

The amount of upregulated probe sets continued to rise significantly until more than 200 and 300 probe sets at 8 hpi and 10 hpi respectively. The upregulation profile clearly shows higher response in H9N2 infected A549 cells.

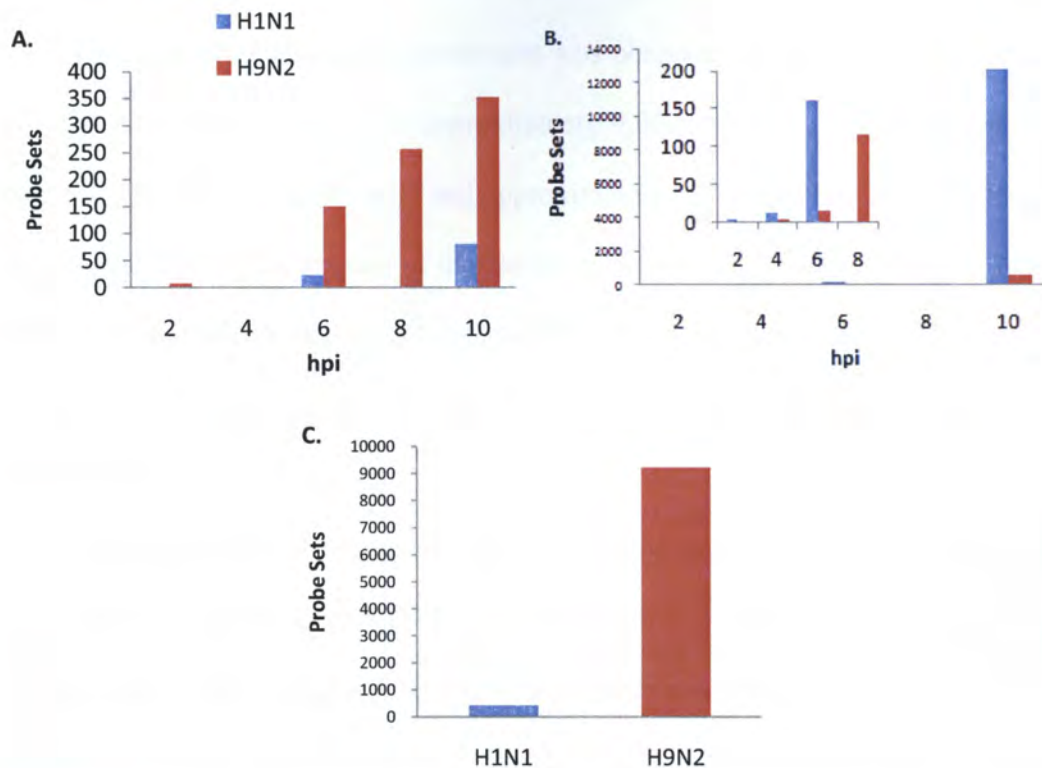


Fig 5.15. The amount of upregulated (A), downregulated (B) and unchanged (C) probe sets in A549 infected with A/Duck/Malaysia/01 (H9N2). (Note that there is **no 8 hpi** for for H1N1). The inset in the graph (B) denotes the smaller scale of the probe sets. (p-value < 0.05, FDR < 0.05, n=3)

There were only a few of downregulated probe sets detected in H1N1 infected A549 cells until 4 hpi. The amount rose by almost 200 probe sets at 6 hpi. However, at 10 hpi, the number of downregulated probe sets increased dramatically reaching more than 12,000 probe sets. The increase of the amount of downregulated probe sets in H9N2-infected A549 cells was much slower as compared to H1N1. Only a few of downregulated probe sets were observed in H9N2-infected A549 cells until 6 hpi. The

amount rose up by approximately 100 probe sets at 8 hpi to 600 probe sets at 10 hpi. As discussed previously in Section 5.1 and 5.2, the much lower amount of downregulated probe sets in H9N2 suggests that the amount of cellular mRNAs degradation was less in H9N2-infected A549 cells, which in turn also showed the lower replication activity of H9N2 in A549 cells.

The amount of unchanged probe sets was observed in higher amount in H9N2-infected A549 cells. There were approximately 9,000 probe sets of unchanged probe sets in H9N2-infected A549 cells and approximately 600 probe sets in H1N1 infected A549 cells. The higher amount of unchanged probe sets in H9N2 infected A549 cells shows that the mRNA degradation rate in H9N2 infected A549 cells is much less than that of H1N1 infected A549 cells, which can be correlated into lower virus yield in H9N2 infected A549 cells.

The percentage of upregulated gene grouping were compared between A549 cells infected with H1N1 and H9N2, and the result is shown in Fig. 5.16. In H1N1-infected A549 cells, there were no changes in genes associated with lipid metabolism groups and energy pathways from 6 hpi up to 10 hpi. Most of the genes were also upregulated starting from 6 hpi onwards, with the exception of energy pathways gene groups, which was only observed in 4 hpi. The rise pattern of all gene groups was gradual starting from 6 hpi up to 10 hpi, and the host pathogen interaction showed the most significant increase in the number of upregulated gene groups. The highest percentage of increased upregulated genes in H1N1-infected A549 cells were the cell death and host pathogen interaction gene groups. In H9N2-infected A549 cells, the upregulation patterns were observed as early as 4 hpi with steady increase up to 10 hpi in all genes. The early rise of the number of upregulated probe sets can be observed in transcription factor, signal transduction, RNA binding, cell death and cell cycle gene

groups. A significant rise in the number of upregulated gene groups was observed starting from 6 hpi and this continued to 10 hpi. This pattern is observed in all gene groups listed with the exception of RNA binding gene groups where the significant rise was only observed at 10 hpi. Both host pathogen interaction and cell death gene groups had the most percentage of genes being upregulated in both H1N1 and H9N2-infected A549 cells.

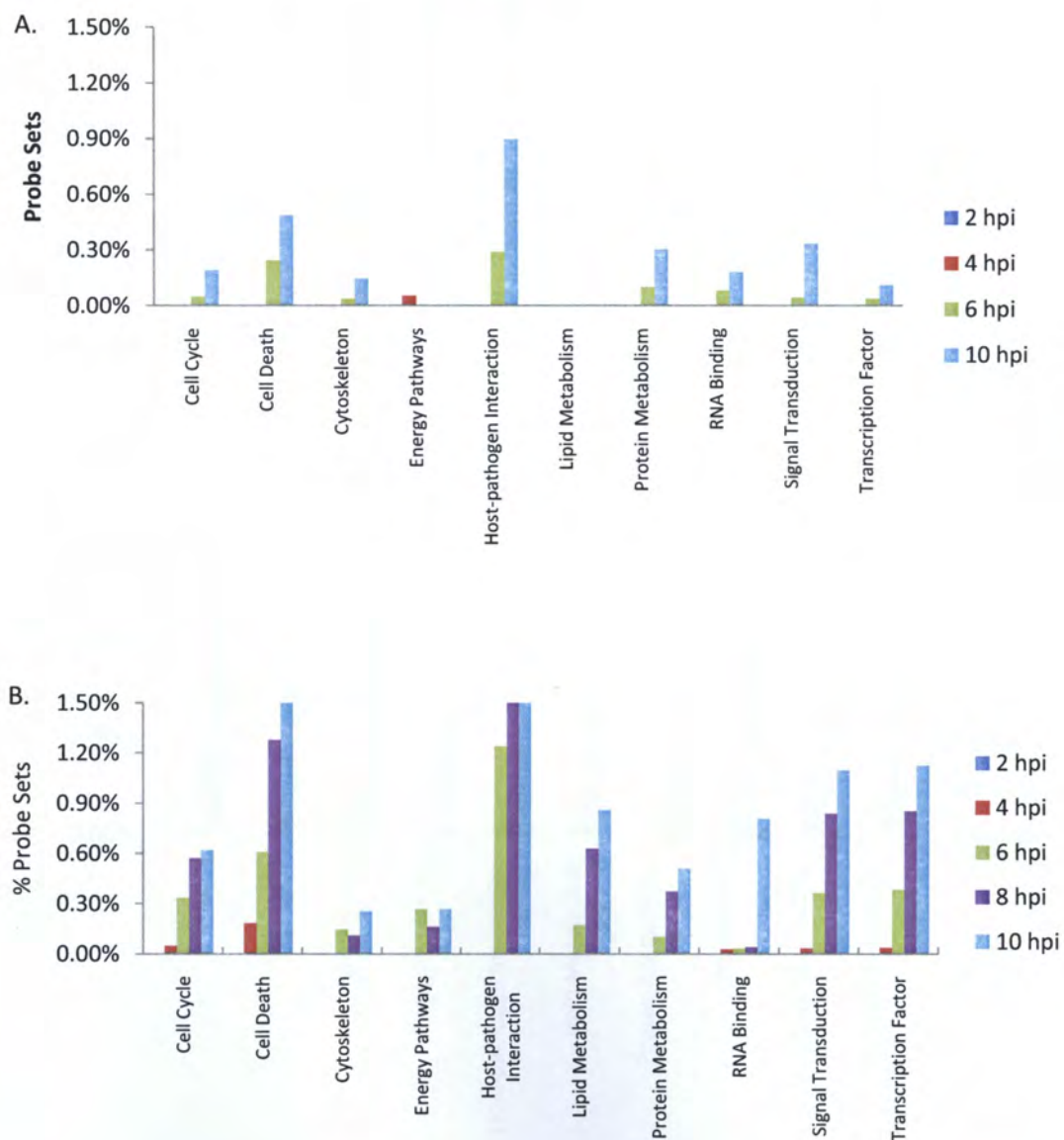


Fig 5.16. The upregulated gene expression of A549 cells infected with H1N1(A) and H9N2 (B), grouped based on the gene function. (p-value < 0.05, FDR < 0.05, n=3)

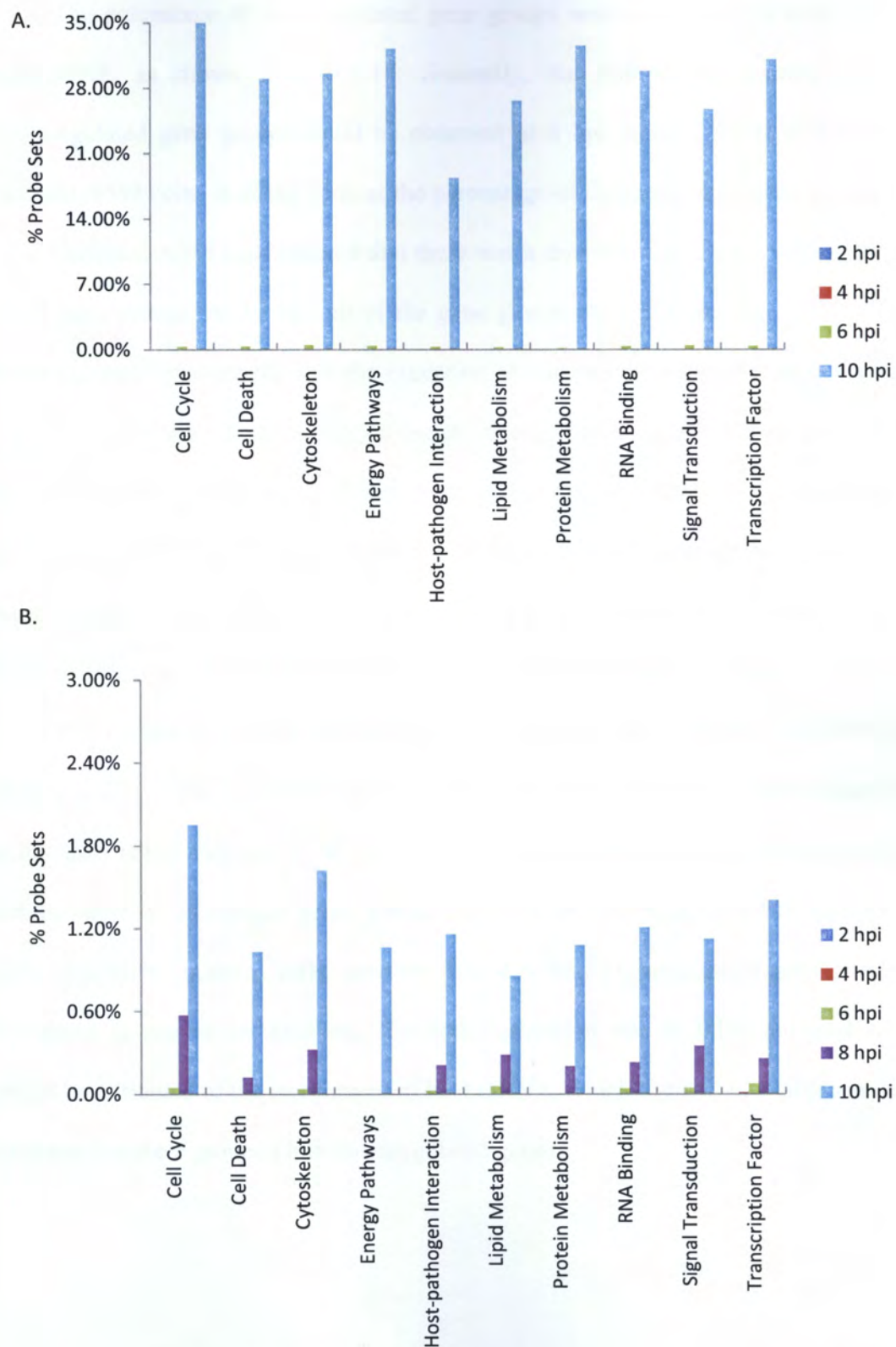


Fig 5.17 The upregulated gene expression of A549 cells infected with H1N1 (**A**) and H9N2 (**B**), grouped based on the gene function. Note the different scaling between the two graphs. (p-value < 0.05, FDR < 0.05, n=3)

The percentage of downregulated gene groups were compared for both H1N1 and H9N2, as shown in Fig 5.17. Generally, the rise in the amount of the downregulated gene groups could be observed at 6 hpi in both H1N1 and H9N2-infected A549 cells. A closer look at the percentage of downregulated gene groups in H1N1-infected A549 cells showed that there was a dramatic rise from 6 hpi to 10 hpi in all gene groups. At 10 hpi, all of the gene groups showed more than 20% in the downregulated gene groups with the exception of host-pathogen interaction. In H9N2-infected A549 cells, the transcription factor gene groups showed a rise as early as 4 hpi. Furthermore, the energy pathway gene groups did not show any downregulated probe sets until 10 hpi. The significant rise of the number of downregulated probe sets were observed from 8 hpi to 10 hpi. Similar to H1N1-infected A549 cells, the cell cycle gene groups showed the most amount of downregulated gene groups.

The comparison of the unchanged gene grouping between H1N1 and H9N2 is shown in Fig. 5.18. In H1N1-infected A549 cells, there were much less unchanged genes than H9N2-infected A549 cells. H9N2-infected A549 cells had approximately similar level of unchanged genes among different groups, which were around 16 – 20%. The H1N1-infected cells, however, had less than 4% unchanged genes, except for genes in protein metabolism. The high replication rate in H1N1-infected cells might be attributed to the recruitment of host mRNA, which resulted in a large amount of genes that were grouped into downregulated genes.

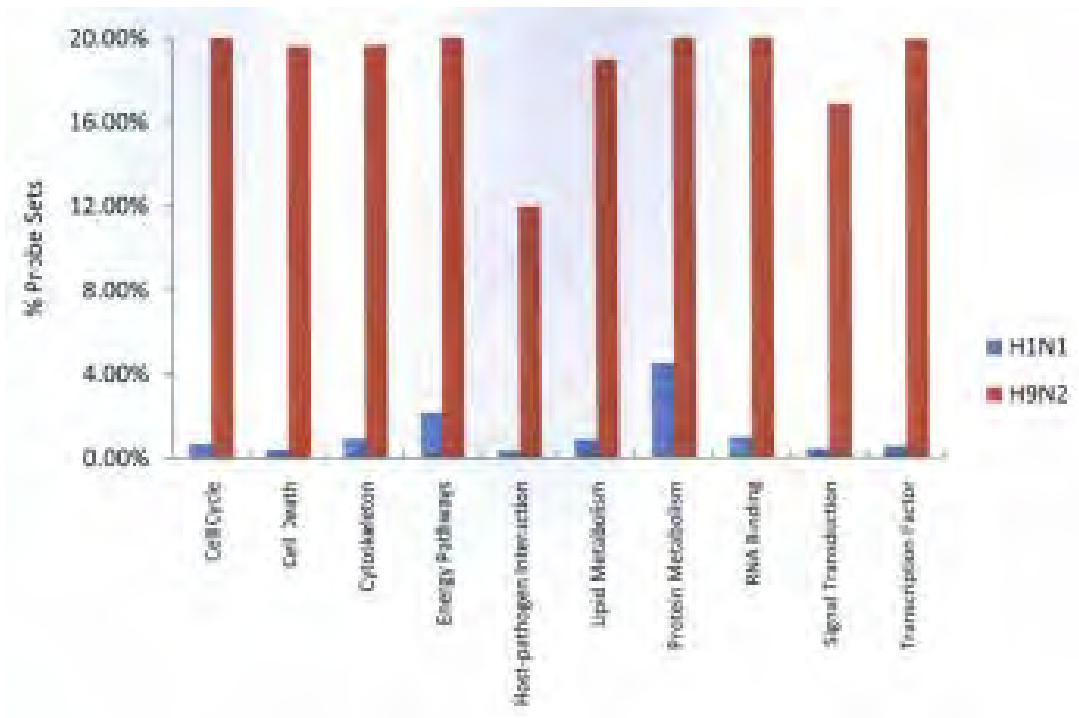


Fig 5.18 The unchanged gene expression of A549 cells infected with H1N1 and H9N2 over time, grouped based on the gene function. (p-value < 0.05, FDR < 0.05, n=3)

The grouping of the 3 classes probe sets of the A549 infected with H1N1 and H9N2 is shown in Fig. 5.19. The groupings consist of cytokine gene groups, antiviral/innate immune gene groups and cell death gene groups. The complete list of the genes is shown in Table 5.3.

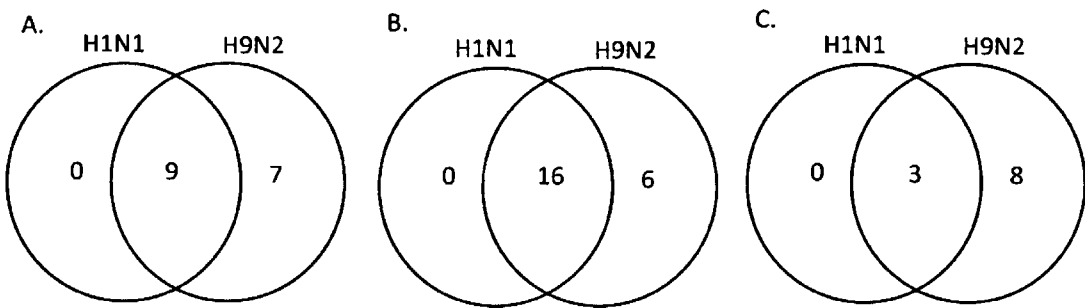


Fig. 5.19 The Venn Diagram of the amount of upregulated genes in H1N1 and H9N2 infected A549 cells in cytokine genes (A), antiviral/innate immune related genes (B) and cell death

Table 5.3 List of upregulated cytokine, antiviral/innate immune, and cell death related genes in A549 cells

Cytokine			H1N1	H9N2	H1N1 and H9N2
GeneBank	Gene Symbol	Description			
M21121	CCL5	chemokine (C-C motif) ligand 5	P	P	P
NM_001565	CXCL10	chemokine (C-X-C motif) ligand 10	P	P	P
AF030514	CXCL11	chemokine (C-X-C motif) ligand 11	P	P	P
NM_005101	G1P2	interferon, alpha-inducible protein (clone IFI-15K)	P	P	P
NM_022873	G1P3	interferon, alpha-inducible protein (clone IFI-6-16)	P	P	P
NM_005532	IFI27	interferon, alpha-inducible protein 27	P	P	P
NM_002176	IFNB1	interferon, beta 1, fibroblast	A	P	A
NM_022147	IFRG28	28kD interferon responsive protein	A	P	A
NM_172139	IL28A	interleukin 28A (interferon, lambda 2)	P	P	P
NM_172140	IL29	interleukin 29 (interferon, lambda 1)	P	P	P
NM_000880	IL7	interleukin 7	A	P	A
U88964	ISG20	interferon stimulated exonuclease gene 20kDa	A	P	A
BC002704	STAT1	signal transducer and activator of transcription 1, 91kDa	A	P	A
AW474434	TNFSF10	tumor necrosis factor (ligand) superfamily, member 10	P	P	P
AF134715	TNFSF13B	tumor necrosis factor (ligand) superfamily, member 13b	A	P	A
NM_003265	TLR3	toll-like receptor 3	A	P	A
Antiviral			H1N1	H9N2	H1N1 and H9N2
GeneBank	Gene Symbol	Description			
NM_014314	DDX58 (RIG-I)	DEAD (Asp-Glu-Ala-Asp) box polypeptide 58	P	P	P
NM_005531	IFIH6	interferon, gamma-inducible protein 16	P	P	P
NM_005532	IFI27	interferon, alpha-inducible protein 27	P	P	P
BE049439	IFI44	Interferon-induced protein 44	A	P	A
NM_006820	IFI44L	interferon-induced protein 44-like	P	P	P
NM_022168	IFIH1	interferon induced with helicase C domain 1	P	P	P
NM_001548	IFIT1	interferon-induced protein with tetratricopeptide repeats 1	P	P	P
AA131041	IFIT2	interferon-induced protein with tetratricopeptide repeats 2	P	P	P
AI075407	IFIT3	interferon-induced protein with tetratricopeptide repeats 3	P	P	P
N47725	IFIT5	interferon-induced protein with tetratricopeptide repeats 5	A	P	A
NM_003641	IFITM1	interferon induced transmembrane protein 1 (9-27)	P	P	P
M34455	INDO	indoleamine-pyrrole 2,3 dioxygenase	A	P	A
NM_242863	MX1	myxovirus (influenza virus) resistance 1	P	P	P
NM_002463	MX2	myxovirus (influenza virus) resistance 2 (mouse)	A	P	A
NM_002534	OAS1	2',5'-oligoadenylate synthetase 1, 40/46kDa	P	P	P
AI651594	OAS2	2'-5'-oligoadenylate synthetase 2, 69/71kDa	P	P	P
AF063612	OASL	2'-5'-oligoadenylate synthetase-like	P	P	P
AI608902	PDCD1LG1	CD274 antigen	P	P	P
AW189843	RSAD2	radical S-adenosyl methionine domain containing 2	P	P	P
AB005043	SOCS1	suppressor of cytokine signaling 1	A	P	A
AA286940	SP100	nuclear antigen Sp100	A	P	A
AF280095	SP110	SP110 nuclear body protein	P	P	P
Cell Death			H1N1	H9N2	H1N1 and H9N2
GeneBank	Gene Symbol	Description			
NM_016109	ANGPTL4	angiopoietin-like 4	A	P	A
AI43782	BIRC4BP (XIAP)	XIAP associated factor-1	A	P	A
NM_052889	CASP1	caspase 1, apoptosis-related cysteine peptidase (interleukin 1, beta, convertase)	A	P	A
T81422	CD38	CD38 antigen (p45)	A	P	A
AB005043	SOCS1	suppressor of cytokine signaling 1	A	P	A
AI244908	SOCS3	suppressor of cytokine signaling 3	A	P	A
AL136607	THAP2	THAP domain containing, apoptosis associated protein 2	P	P	P
NM_006290	TNFAIP3	tumor necrosis factor, alpha-induced protein 3	A	P	A
NM_007115	TNFAIP6	tumor necrosis factor, alpha-induced protein 6	A	P	A
U57059	TNFSF10	tumor necrosis factor (ligand) superfamily, member 10	P	P	P
AF114012	TNFSF13	tumor necrosis factor (ligand) superfamily, member 13	A	A	A
AF134715	TNFSF13B	tumor necrosis factor (ligand) superfamily, member 13b	P	P	P

Note :

P denotes the gene is upregulated

A denotes the gene is not upregulated

The Venn Diagram in Fig. 5.18 shows that there were no exclusively upregulated genes in H1N1-infected A549 cells in all three groups at 10 hpi. H9N2-infected A549 cells upregulated more genes in the same groups, suggesting that H9N2-infected A549 cells expressed a variety of interleukins and chemokines than H1N1-infected A549 cells. The H9N2-infected cells also upregulated a more diverse group of interferon induced genes, antiviral genes, and cell death gene groups. To relate with the finding in Chapter 4 where H1N1 is shown to replicate better in A549 cells, it is apparent that the A549 cells exhibit better antiviral defence mechanism against H9N2 infection by upregulating more cytokine, antiviral and cell death gene groups.

The host cell interferon response in infected A549 cells is shown in Fig. 5.20. Generally, most of the interferon related genes in H9N2 are expressed from as early as 6 hpi. In H1N1-infected cells, many of those genes are either upregulated at 10 hpi, or not significantly upregulated. The upregulated genes in H1N1-infected cells at 10 hpi are mostly the interferon downstream pathways which mostly are antiviral response (Mx, RSAD2 and OAS family). The interferon upstream pathways (TLR3, IRF1, IRF2 and IRF7) are mostly found not significantly upregulated in H1N1. The low response of the interferon in H1N1 also explains why both SOCS1 and SOCS3 are not significantly upregulated. The BIRC4BP protein is not significantly upregulated in H1N1, but upregulated significantly in H9N2. BIRC4BP protein has been reported to stop apoptotic cell death induced either by viral infection or by overproduction of caspases, such as caspase 3, 7 and 9 (Deveraux and Reed, 1999). Further, Wurzer *et al.* (2003) found that caspase 3 is essential for efficient influenza virus propagation. This suggests that the expression of BIRC4BP will inhibit the replication of virus. This finding explains the low replication rate of H9N2 in A549 cells. Our finding is also consistent with gene expression study using microarray experiment was conducted by

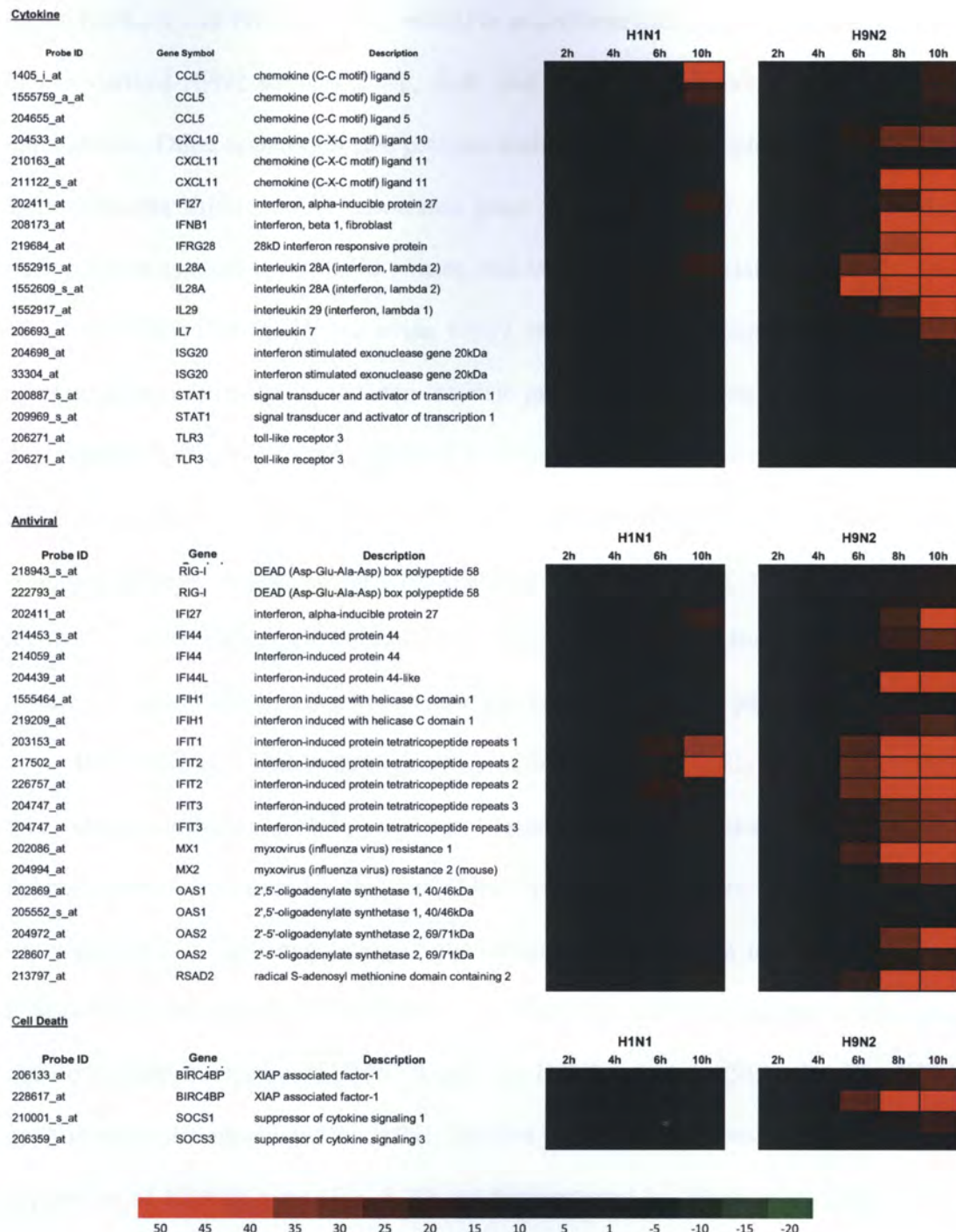


Fig. 5.20. The heatmap of the host-gene response in H1N1 and H9N2 infected A549 cells. The scale bar denotes the fold change range from -20 to 50. (p-value < 0.05, FDR < 0.05, n=3)

Xing *et al.*, 2011 to measure the host immune response on avian-H9N2 strain and human-H9N2 strain infection, they found that IFN-beta was the prominent antiviral

component, whereas interferon gamma-induced protein IP-10, chemokine (C-C motif) ligand (CCL)-5 and TNF- α may be critical in proinflammatory responses especially in human derived-H9N2 strains. IL-1 β , IL-8, and even IL-6 did not show significant upregulation. Other antiviral related proteins such as Toll-like receptor TLR-3, TLR-7, and melanoma differentiation-associated gene 5 (MDA-5) also contributed to the innate immunity against the H9N2 viruses, and MDA-5 was important in the induction of IFN- β . They also found that avian H9N2 strains induced apoptosis through the mitochondria/cytochrome c-mediated intrinsic pathway, in addition to the caspase 8-mediated extrinsic pathway, as evidenced by the cytosolic presence of active caspase 9 and cytochrome c, independent of truncated BH3 interacting domain death agonist (Bid) activation. Further, FLICE-like inhibitory protein (FLIP), an apoptotic dual regulator, and the p53-dependent Bcl-2 family members, Bax and Bcl-x(s), was shown to be involved in the regulation of extrinsic and intrinsic apoptotic pathways.

The cholesterol metabolism pathway of infected A549 cells is shown in Fig. 5.21. The downregulation of the cholesterol metabolism pathway is apparent in H1N1-infected A549 cells from 10 hpi. The H9N2 infected A549 cells, however, did not show any apparent downregulation on the cholesterol metabolism related genes. This is also consistent with the downregulation of HMGCR on H1N1-infected A549 cells, and no significant change of HMGCR gene on H9N2-infected A549 cells. The FPPS gene is more downregulated in H1N1 infected cells, which reversely related to the expression of RSAD2 gene (Fig. 5.20), as demonstrated by Wang *et al.* (2007). The CH25H gene, however, showed high increase in H9N2-infected A549 cells starting from as early as 2 hpi, which suggests an attempt of the cells to halt the downregulation of the cholesterol metabolism pathway to enhance the virus replication. This pattern is absent in H1N1-infected A549 cells.



Fig 5.21 Heatmap on Cholesterol Metabolism related genes in H1N1 and H9N2 infected A549 cells. Highlighted in yellow is 3-hydroxy - 3 - methylglutaryl-Coenzyme A reductase (HMGCR), and highlighted in red is cholesterol 25-hydroxylase (C25H). The scale bar denotes the fold change range from -10 to 10. (p-value < 0.05, FDR < 0.05, n=3)

5.4 Validation of cDNA microarray result

5.4.1 qRT-PCR

The value of the fold change obtained in the cDNA microarray analysis was based on the hybridized host mRNA on the chip. In order to confirm the consistency of the value, the quantitative RT-PCR is used to validate the result obtained in cDNA microarray data. Quantitative RT-PCR calculates the amount of fold change based on the detection threshold (C_T) value on the PCR amplified mRNA product. The value obtained for microarray value is shown at Table 5.4, 5.5, and 5.6 for A549, MDCK and CEF, respectively. The qPCR graphs are also shown for A549 (Fig. 5.22), MDCK (Fig. 5.23), and CEF (Fig. 5.24).

Based from the data above, the fold change value obtained between cDNA microarray analysis and qRT-PCR analysis is different. It should be noted that the difference in values was not due to the variability among different measurements. This is due to two different methods employed in order to obtain the fold changes. The cDNA microarrays collect the data based on hybridization, and qRT-PCR fold-change calculated is based on threshold point detected from PCR amplification. Despite such differences, there is a consistency in comparison in most the measurement. The higher fold change in H1N1 infected virus in cDNA microarray measurement as compared to H9N2 is also indicated similarly in the qRT-PCR measurement.

Table 5.4 Fold change value of genes on A549, to be compared with qPCR result.

Gene	GenBank Accession	H1N1	H9N2
		10h ^a	10h ^a
MX1	NM_002462	8.3 (0.003)	84.9 (0.000)
OAS1	NM_016816	NC	13.3 (0.001)
	NM_002534	2.3 (0.010)	11.4 (0.000)
OAS2	NM_016817	8.9 (0.005)	49.3 (0.003)
	AI651594	7.8 (0.050)	22.3 (0.018)
RSAD2	AW189843	6.5 (0.001)	147 (0.002)
	AA142842	NC	242 (0.013)
BIRC4BP	NM_017523	NC	27.6 (0.004)
	AI859280	NC	3.4 (0.011)
	NM_002176	NC	104.0 (0.001)

Note :
number in brackets : p-value of designated genes
NC : No change
a : Number in parenthesis denotes p-value

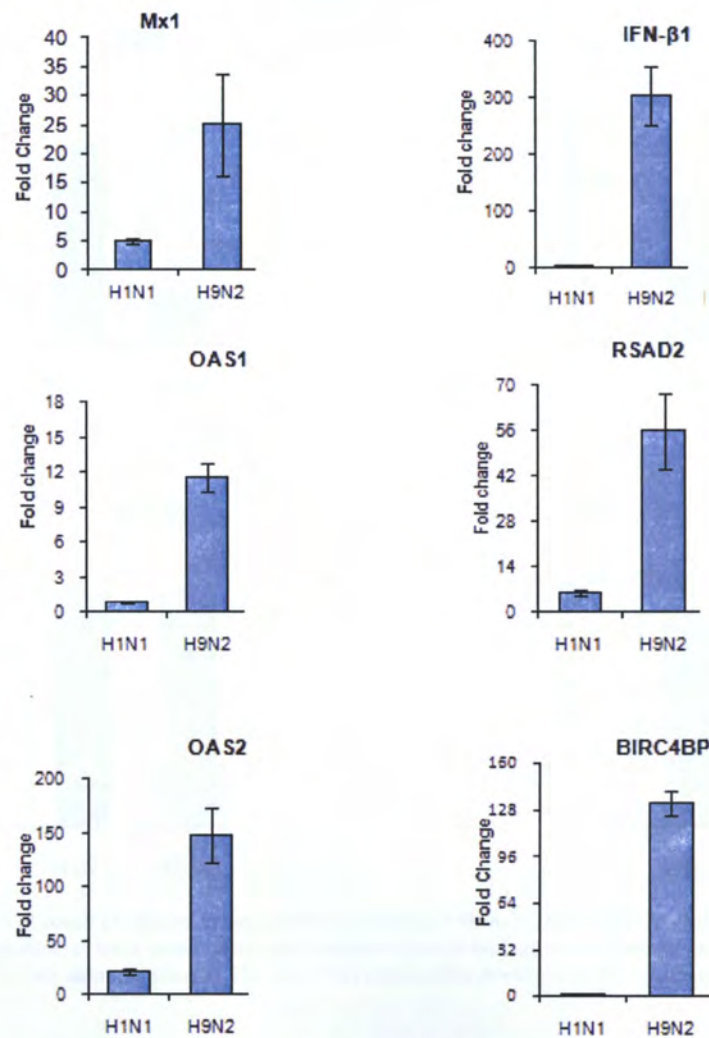


Fig. 5.22. The qPCR result of various genes in A549 infected with A/WSN/33 (H1N1) and A/Duck/Malaysia/01 (H9N2). The experiments were based on six replicates (n=6) with the bars as the average value, and error bars and the standard deviations among replicates. The error bars denotes the deviation of the measurement (n=6)

Table 5.5 Fold change value of genes on MDCK, to be compared with qPCR result

Gene	GenBank Accession	H1N1 10h ^a	H9N2 10h ^a
MX1	pmma15820	10.9 (0.001)	5.4 (0.049)
OAS1	BU745815	4.4 (0.006)	2.1 (0.042)
	DN744143	5.7 (0.003)	2.1 (0.031)
RSAD2	pmma5763	19.5 (0.002)	8.6 (0.034)
IFN- β 1	pmma2761	NC	NC

Note :
number in brackets : p-value of designated genes
NC : No change
a : Number in parenthesis denotes p-value

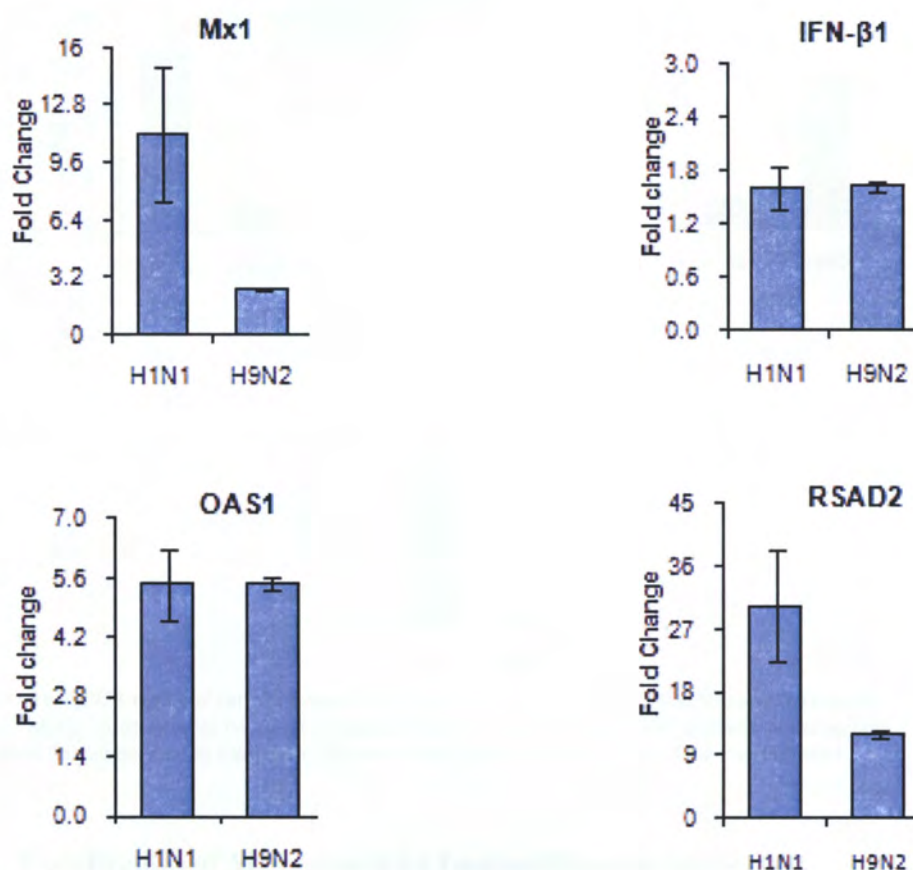


Fig. 5.23 The qPCR result of various genes in MDCK infected with A/WSN/33 (H1N1) and A/Duck/Malaysia/01 (H9N2). The experiments were based on six replicates (n=6) with the bars as the average value, and error bars and the standard deviations among replicates. The error bars denotes the deviation of the measurement

Table 5.6 Fold change value of genes on CEF, to be compared with qPCR result

Gene	GenBank Accession	H1N1 10h ^a	H9N2 10h ^a
MX1	NM_204609	193 (0.012)	11.0 (0.022)
OASL	NM_205041	144 (0.000)	15.4 (0.009)
IFN- β 1	NM_227573	NC	NC

Note :
number in brackets : p-value of designated genes
NC : No change
a : Number in parenthesis denotes p-value

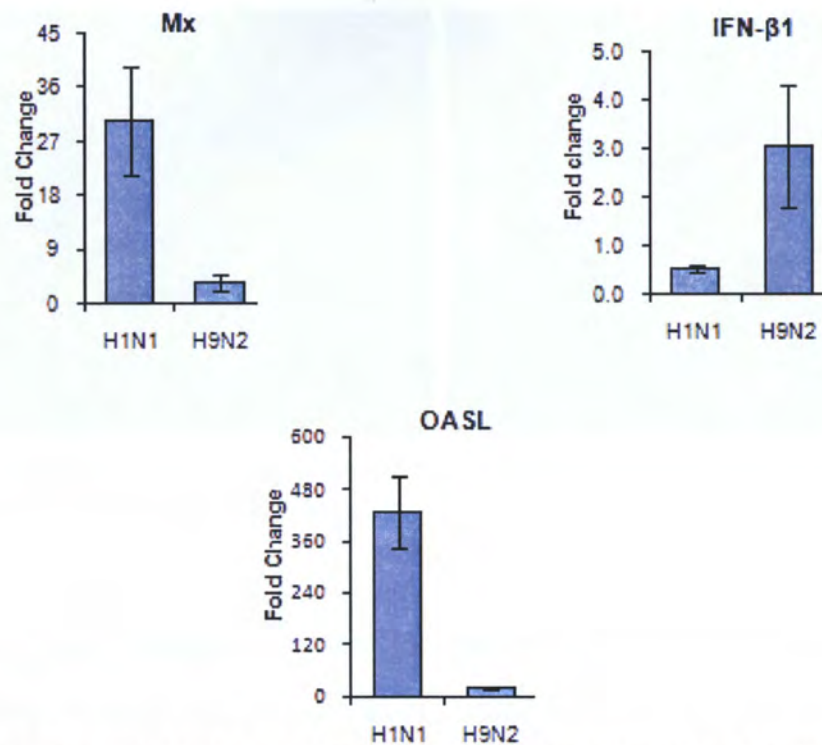


Fig. 5.24 The qPCR result of various genes in CEF infected with A/WSN/33 (H1N1) and A/Duck/Malaysia/01 (H9N2). The experiments were based on six replicates (n=6) with the bars as the average value, and error bars and the standard deviations among replicates. The error bars denotes the deviation of the measurement

5.4.2 Localization of Mx1 protein by Immunofluorescence Assay

Further, we would like to ascertain if the antiviral response genes were able to be verified in the immunofluorescence assay and to detect its presence in the protein level. In this experiment, we chose Mx, as the antibody was available. The Mx stained cells was shown to be cytoplasmic staining (Ditmann *et al.*, 2008). Initially, the infection was carried at 10 hpi, but the signal was too weak to make any comparison.



Fig 5.25. The staining pattern of Mx1 protein in Mock, H1N1 and H9N2 infected A549 cells at 24 hpi (moi =3), with enlarged view of the Mx1 staining in inset.

It was only notably stronger at 24 hpi. The localization Mx1 protein in mock-infected, H1N1 infected and H9N2 infected A549 cells is shown in Fig 5.25. There was no signal observed in mock-infected cells. After virus infection, fluorescing signals were observed in both H1N1 and H9N2 infected cells. The signal pattern was a diffused cellular cytoplasmic staining without any nuclear staining. Furthermore, it could be observed that H9N2 infected cells generally had more spread of the signals with almost all of the cells stained. In H1N1 infected cells, only approximately 20% of the total cells possessed distinctive staining. This result is consistent with our findings in microarray result. Dittmann *et al.* (2008) conducted Mx1 protein effect on various strains of influenza virus infected cells, and observed that various virus strains reacted

differently. For example, they found that human pandemic 1918 was not susceptible to Mx1, while avian HPAI H5N1 virus was susceptible. Similar with Mx1 expression study, our finding suggests that the Mx1 proteins exerted higher effect on the unadapted strains of influenza virus.

5.4.3 Detection of MAP Kinase Related Protein by Western Blotting

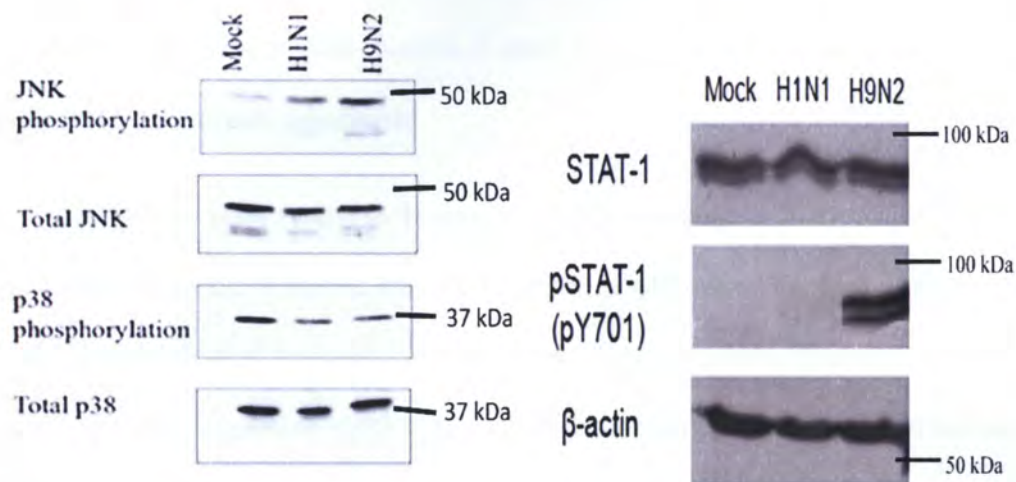


Fig 5.26. The Western Blot result of total JNK, phosphorylated JNK, total p38, phosphorylated 38, total STAT1, phosphorylated STAT1 and β -actin as a control in A/WSN/33 (H1N1) and A/duck/Malaysia/01 (H9N2) infected A549 cells at 16 hpi (moi =3). β -actin was used as control protein for the measurement.

The host cells can detect the presence of viral 5'-phosphorylated, single stranded and double stranded RNA, which in turn release interferons and interleukins. The JAK-receptor will bind these interferons and phosphorylate the JNK. The phosphorylation of JNK results in the activation of STAT proteins. The phosphorylated STAT will then translocate to the nucleus to initiate transcription of immunological response related genes (Darnell *et al.*, 1994; Levy *et al.*, 2001). Similarly, p38 MAPK is also critical for immunological response against viral infection by inducing expression of STAT1 (Sumbayev and Yakinska, 2006). The western blotting result of total and phosphorylated JNK, total and phosphorylated 38, total and phosphorylated STAT1 of the H1N1 and H9N2 infected A549 cells at 16 hpi is shown in Fig. 5.26. It could be observed that both STAT1 and JNK were

phosphorylated at greater amount in H9N2 infected A549 cells compared to H1N1 cells. The phosphorylation of p38 protein is similar on H1N1 and mock infected cells, but higher on H9N2 infected cells. It is known that influenza virus evades immunological response by binding of NS1 protein to PKR, thus preventing the activation of NF- κ B and induction of alpha/beta interferon. This finding suggests that the H1N1 virus were able to evade the immunological response in A549 cells better than H9N2. In this experiment, β -actin is used as a control to show equal amount of sample were used in this experiment.

5.5 Host-virus Interaction in Mouse Lung Macrophage

The utilization of mouse lung macrophage in addition to the host model cells is useful to determine host response because macrophages are primary source of cytokine production which expresses more cytokine proteins than epithelial cells (Julkunen *et al.*, 2001). To demonstrate the ability of H1N1 and H9N2 to infect mouse lung macrophage, the immunofluorescence image of H1N1 and H9N2-infected mouse lung macrophage with moi of 5 at 16 hpi is shown in Fig. 5.27. It is apparent that based on the fluorescence signal, H1N1 is more capable to replicate in mouse lung macrophage than H9N2.

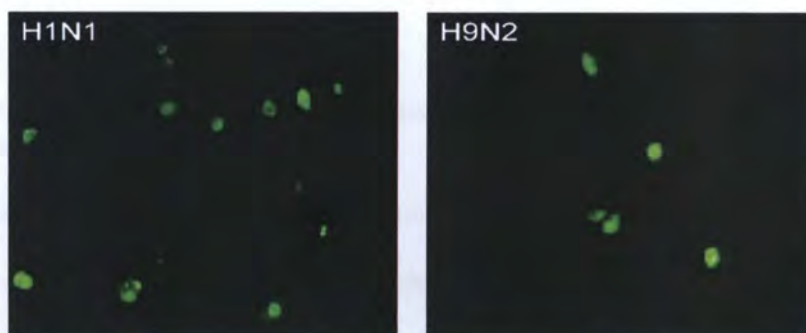


Fig 5.27 The immunofluorescence image of mouse lung macrophages infected with A/WSN/33 (H1N1) (**left**) and A/Duck/Malaysia/01 (H9N2) (**right**) with moi of 5 at 16 hpi, using monoclonal anti-NP antibody.

5.5.1 Viral kinetics in mouse lung macrophage

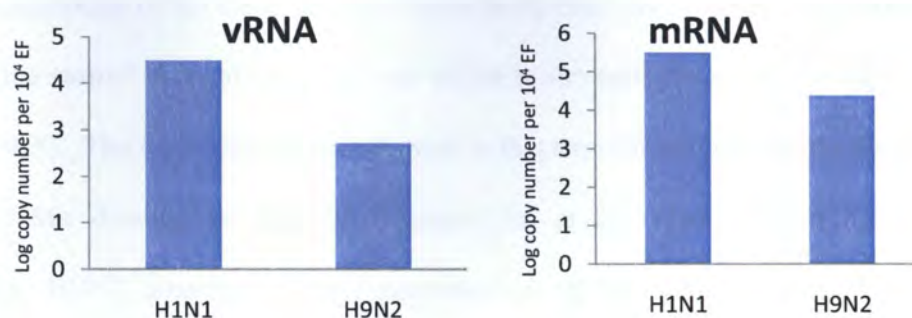


Fig 5.28 The replication (vRNA) and transcription (mRNA) rate of A/WSN/33(H1N1) and A / Duck / Malaysia /01 (H9N2) infected mouse lung macrophage (moi=3) at **16 hpi**. The experiments were based on six replicates (n=6)

In both replication and transcription of the lung macrophage at 24 hpi is shown in Fig. 5.28, it was observed that the H1N1-infected macrophages had a higher rate of replication and transcription than H9N2-infected macrophages by 2 logs and 1 log, respectively. Dendritic cells and macrophages are located together with the epithelium of the respiratory organs and these cells can be targeted by influenza viruses for infection. From the epithelial cells, influenza viruses will further spread and infect dendritic cells and macrophages which will in turn induce innate immune response against the virus (Seo *et al.*, 2004). The H9N2 isolate were not passaged in mice before, hence no adaptation to mice host. But from the result, it is shown that both of the viruses are capable of undergoing replication and translation inside mouse lung macrophage.

5.5.2 Measurement of Antiviral Proteins Response in Infected Mouse Lung Macrophage

The antiviral host response of mouse lung macrophage against H1N1 and H9N2 infections measured using qPCR is shown at Fig. 5.29. It could be observed that H1N1 infected cells induced higher level of OASL and IFN- β 1 proteins. To correlate with the result seen in Fig. 5.27, it is obvious that the higher cytokine response in

H1N1-infected mouse lung macrophages was not able to inhibit both the replication and transcription of the virus. It is also more likely that this cytokine overproduction or “cytokine storm” brought more adverse effect to the cells than to the virus (Yap and Ada, 1978). The Mx1 was not investigated in this experiment because the Balb/c mice possess Mx deletion on the chromosome (Jin *et al.*, 1998). Based on sequence analysis, H9N2 possesses avian signatures in all of the segments. This might contribute to the specificity of the host of the H9N2 isolate. However, there is an evidence of very low LD₅₀ of A/WSN/33(H1N1) capable of killing mice even without adaptation due to cytokine overproduction (Yap and Ada, 1978).

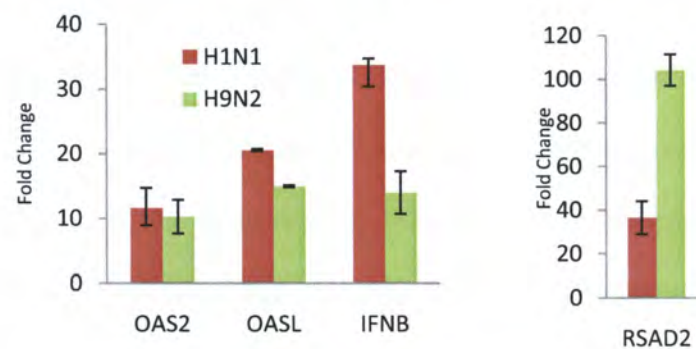


Fig 5.29 The antiviral host response in A/WSN/33(H1N1) (red bar) and A/Duck/Malaysia/01(H9N2) (green bar) infected mouse lung macrophage (moi =3) at **16 hpi**. The experiments were based on six replicates (n=6) with the bars as the average value, and error bars and the standard deviations among replicates.

5.5.3 Cytokine profiling of mouse lung macrophage

In previous sub-section, MDCK, CEF and A549 cells were used as a basis of the host cells for the influenza virus infection. While the measurement of the transcriptional level of the cytokine gene mRNA could be done, it is not possible to measure the amount of secreted cytokine protein, because those cells secreted very low amount of cytokines, and only some strongly expresses cytokines would be detectable with ELISA method, such as RANTES, MCP-1 and IL-8 (Ronni *et al.*, 1997; Sareneva *et al.*, 1998). Therefore, mouse lung macrophages were used to assess the amount of

secreted cytokines, which is indicative to the virus ability to activate immune system through immune cells. Since completely different cell origins (mouse as opposed to canine, chicken and human) and cell types (immune cells as opposed to epithelial and fibroblast cells) were used, direct correlations may not be deduced directly. However, the higher cytokine excreted by the mouse lung macrophage is closely related to the severity of the viral pathogenicity (Heinrich *et al.*, 2003), which could only be observed in immune cells from the amount of cytokine excretion. The measurement of the excreted cytokine in mouse lung macrophage was carried out using the 23-plex Bioplex[®] kit from Biorad. In this experiment, there were 20 cytokines detected during the measurement (Fig. 5.30). The cytokine measurement experiment was based on two measurements done in two independent experiments, with total of 4 replicates. The bars shown in Fig. 5.30 are the average of each cytokine measurement, and the error bars are the deviates of the measurement. From the result, generally the cytokine amount decreased in 4 hpi and 8 hpi, and rose in 20 hpi. The H1N1 infected mouse lung macrophage showed higher expression of IL-1 α , IL-1 β , IL-6, and G-SCF, while the H9N2 infected cells showed higher expression of IL-13, MIP-1 β , MCP-1 and RANTES. There were no significant differences detected in the expression of Eotaxin, IFN- γ , KC and MIP-1 α . It is obvious that H1N1 induced more cytokine responses compared to H9N2, which include proinflammatory response proteins (IL-1 α , IL-1 β , IL-6), allergic inflammation pathways related proteins (IL-17) and chemoattractant (G-SCF). The H9N2 infected cells only induced more MCP-1 and MIP-1 β , which are chemoattractants. This suggests that the H1N1 virus has more capability to induce “cytokine storm” in mouse lung macrophages. This type of cytokine production upon viral infection has been described before in mouse models (Dinarrelo, 1994)

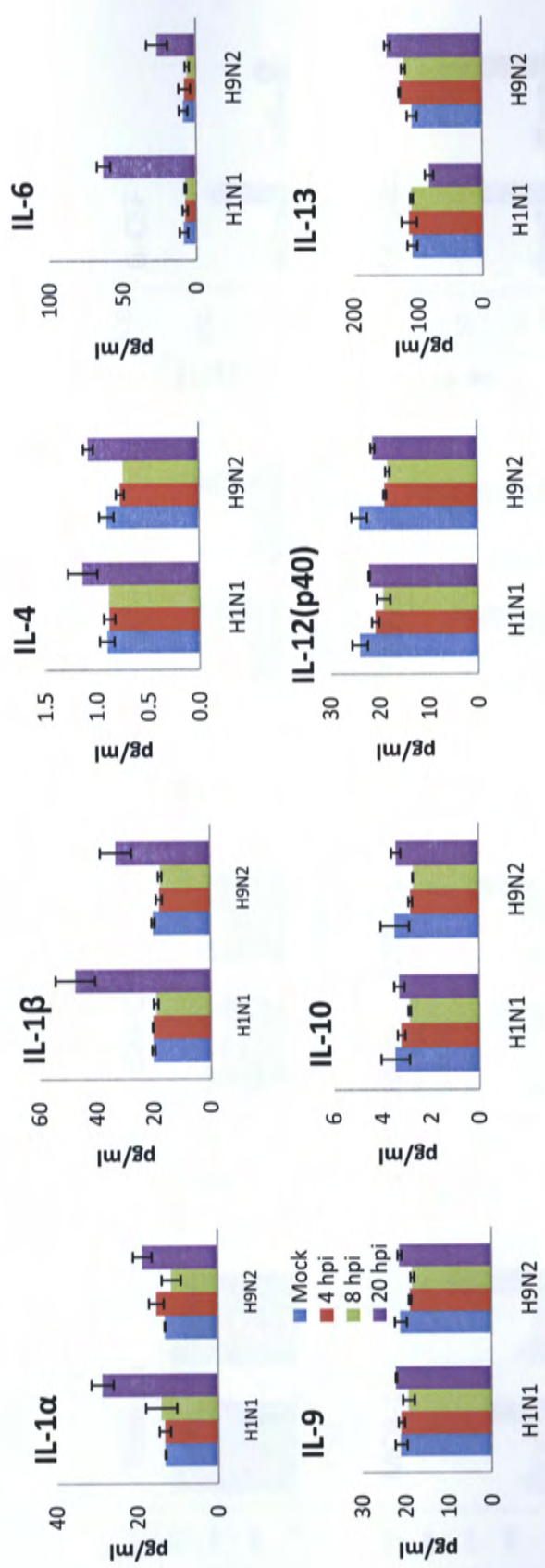


Fig 5.30 The cytokine profiling of H1N1 and H9N2 infected mouse lung macrophages. The bar color represents infection time, starting from Non-Infected/Mock (blue), 4 hpi (red), 8 hpi (green) and 20 hpi (purple). The error bars denotes the deviation among 4 replicates (n=4)

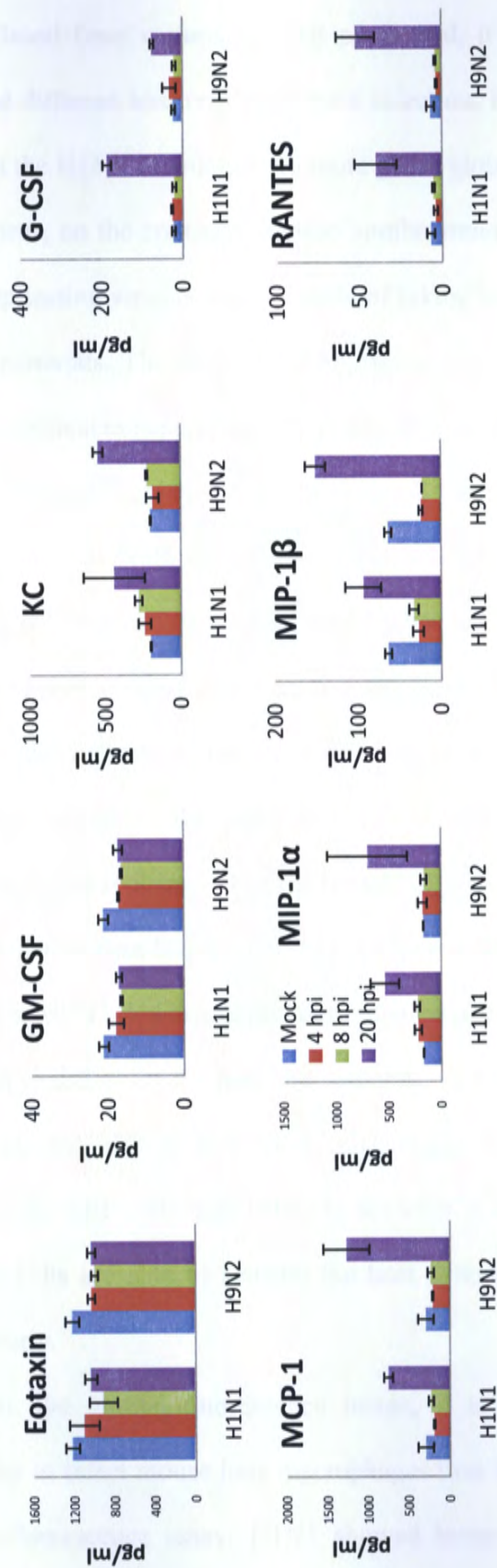


Fig 5.30 (Cont.) The cytokine profiling of H1N1 and H9N2 infected mouse lung macrophages. The bar color represents infection time, starting from Non-Infected/Mock (), 4 hpi (), 8 hpi () and 20 hpi (). The error bars denotes the deviation among 4 replicates (n=4)

5.6 Conclusion

Based from various analysis performed, it can be seen that both the viruses exhibited different host responses upon infection. From the microarray data, it can be seen that the H1N1 downregulated more genes globally in MDCK and A549 cells. The H9N2 virus, on the contrary, showed similar trend in CEF cells. This shows that the better replicating virus is more capable of taking host-cell mRNAs to produce its own genetic materials. The ability of the virus to counter host-cell defense mechanism is also very critical in supporting this observation, as explained below.

H9N2-infected A549 and MDCK cells upregulated higher number of cytokine, antiviral and cell death related genes. However, H1N1 upregulated higher number of cytokine, antiviral and cell death related genes in CEF cells. Furthermore, the heatmap also shows that H9N2-infected A549 cells showed higher expression of all the selected cytokine and antiviral genes in A549 cells. On the contrary, H1N1 showed higher expression of all of the selected cytokine and antiviral genes in CEF cells. In cholesterol metabolism, H1N1-infected MDCK and A549 cells showed more downregulation than H9N2-infected MDCK and A549 cells. On the contrary, in the CEF cells, H9N2 downregulated more cholesterol pathway related genes than H1N1. The high induction of the host cell response, as seen in H1N1 infected CEF cells and H9N2 infected MDCK and A549 cells, might explain the lower replication of the H1N1 in the CEF cells, and H9N2 in the MDCK and A549 cells. This shows that if the host cells are able to activate the host defence mechanism, the virus will grow more poorly.

In the immunofluorescence image, it is shown that the H1N1 has better capability to infect mouse lung macrophages than H9N2. Consistent with the result in immunofluorescence assay, H1N1 showed better replication than H9N2 in qPCR

assay, although H1N1 generally induced more immune response genes in qPCR. It is shown that although the influenza virus is attenuated or not replicating well, it still has the potential to induce comparable cytokine response in macrophages, such as TNF- α , IL-6 and IFNs, if compared with the wild type and better replicating influenza virus (Rekstin *et al.*, 2006). Similarly, in cytokine assay, H1N1 also induced more proinflammatory, allergic, and chemoattractant proteins as compared to H9N2, although H9N2 had lower replication rate. This also suggests that the induction of immune response genes and antiviral genes does not affect the virus replication.

Chapter Six. Characterization of 2009 Pandemic Influenza Virus Isolated From Patients in Singapore

In this decade, HPAI H5N1 influenza virus and 2009 pandemic strains are drawing attentions for its pandemic potentials. There are various factors contributing to the influenza virus pandemic potentials. The ability of the current 2009 pandemic strains to cause significant illness and high airborne transmissibility are several very critical properties of potentially pandemic influenza strains (Webby and Webster, 2003; Viboud *et al.*, 2006; Tumpey and Belser, 2009; Neumann *et al.*, 2009). The phylogenetic analysis done by Garten *et al.*, 2009 and Smith *et al.*, 2009 shows that the pandemic influenza was resulted from quadruple reassortants between triple reassortant swine influenza virus and avian-derived influenza virus, with came from swine, human and avian hosts.

Understanding the virus kinetics and host-cell interaction in different cell lines is critical in assessing the virus characteristics and preference in different hosts. We employed similar strategy to characterize the viruses as discussed in previous chapters. We explored the growth kinetics, host – virus interactions and immunological response study of the swine influenza virus in different hosts. We used canine, chicken and human based cell lines for these experiments. The ability of the virus to grow in different type of host was assessed. For cytokine profiling, primary mouse lung macrophage model was used.

To characterize the 2009 H1N1 swine influenza viruses isolated in Singapore, several sample collections from the suspected Singapore patients were collected by nasal swabs. From the patients sample collection, four positive 2009 pandemic strains isolates were obtained and named A/Singapore/276/2009 (H1N1), A/Singapore/471/2009 (H1N1), A/Singapore/478/2009 (H1N1) and

A/Singapore/527/2009 (H1N1). In the graphs, they were labelled 276, 471, 478 and 527, respectively. A positive control for swine influenza virus was used, A/California/7/2009(H1N1). It was labeled “Cal” in the graph. Two laboratory strains, A/WSN/33 (H1N1) and A/PR/8/34 (H1N1) were also used, and they were labeled “WSN” and “PR8” for A/WSN/33 (H1N1) and A/PR/8/34 (H1N1) in the graph, respectively.

6.1 Genetic Analysis of Strains

The full genome of four circulating 2009 pandemic strains isolates from Singapore was sequenced in order to determine their genetic characteristics. In the genetic characterization, sequence similarity, phylogenetic tree and the drug resistance sites were assessed in order to gain insight of the nature of the 2009 pandemic strains isolates. All of the isolates were sequenced from amplified PCR products, and analyzed using LASER-gene[®]. ClustalX[®] was used to root phylogenetic tree of each virus segment with bootstrap of 1000 replicates, with 2009 pandemic strains, control strains and seasonal strains as the members of the each tree.

The sequence similarity comparison is useful to assess the similarity of the four circulating 2009 pandemic strains isolates, and at the same time to compare with other 2009 pandemic strains isolates and laboratory strain. Any differences revealed from this comparison will indicate the rate of mutation of the virus. The sequence similarity comparison is shown at Table 6.1. Among all 4 strains isolated, there were high similarity (>99%) of nucleotide sequences, even compared to the two control strains, A/California/7/2009(H1N1) and A/Singapore/ON132/2009(H1N1) or National Public Health Library (NPHL) strain. All the strains, however, have low similarity when compared to laboratory strain (<80%). This suggests that the swine influenza virus currently circulating in Singapore had not developed significant variation and the high

similarity with A/California/7/2009 further suggest that the currently circulating swine flu in Singapore might originate from one origin.

Table 6.1 Sequence similarity among 2009 Singapore swine influenza virus isolates, control strains and laboratory strains. Top left corner denotes the gene segment compared. Comparison is performed with column vs. row basis with the indicated value in the middle.

HA	276	471	478	527	Cal	NPHL	PR8	WSN	NA	276	471	478	527	Cal	NPHL	PR8	WSN
276		100.00%	99.70%	99.90%	99.50%	99.70%	79.70%	80.00%	276		100.00%	100.00%	100.00%	99.70%	99.90%	77.50%	76.90%
471	100.00%		99.70%	99.90%	99.50%	99.70%	79.70%	80.00%	471	100.00%		100.00%	100.00%	99.70%	99.90%	77.50%	76.90%
478	99.70%	99.70%		99.60%	99.20%	99.40%	79.50%	79.90%	478	100.00%	100.00%		100.00%	99.70%	99.90%	77.50%	76.90%
527	99.90%	99.90%	99.60%		99.40%	99.60%	79.80%	80.10%	527	100.00%	100.00%	100.00%		99.70%	99.90%	77.50%	76.90%
Cal	99.50%	99.50%	99.20%	99.40%		99.20%	79.60%	80.00%	Cal	99.70%	99.70%	99.70%	99.70%		99.70%	77.30%	76.70%
NPHL	99.70%	99.70%	99.40%	99.60%	99.20%		79.40%	79.80%	NPHL	99.90%	99.90%	99.90%	99.90%	99.70%		77.50%	76.90%
PR8	79.70%	79.70%	79.50%	79.80%	79.60%	79.40%		95.90%	PR8	77.50%	77.50%	77.50%	77.50%	77.30%	77.50%		94.70%
WSN	80.00%	80.00%	79.90%	80.10%	80.00%	79.80%	95.90%		WSN	76.90%	76.90%	76.90%	76.90%	76.70%	76.90%	94.70%	
M	276	471	478	527	Cal	NPHL	PR8	WSN	NS	276	471	478	527	Cal	NPHL	PR8	WSN
276		99.90%	99.90%	99.90%	99.80%	99.60%	89.90%	90.10%	276		99.70%	99.60%	99.70%	99.70%	99.70%	84.40%	84.80%
471	99.90%		100.00%	99.90%	99.70%	99.70%	90.00%	90.20%	471	99.70%		99.60%	100.00%	99.70%	99.70%	84.40%	84.60%
478	99.90%	100.00%		99.90%	99.70%	99.70%	90.00%	90.20%	478	99.60%	99.60%		99.60%	99.60%	99.60%	84.10%	84.40%
527	99.80%	99.90%	99.90%		99.60%	99.60%	89.90%	90.10%	527	99.70%	100.00%	99.60%		99.70%	99.70%	84.40%	84.60%
Cal	99.60%	99.70%	99.70%	99.60%		99.80%	89.90%	90.10%	Cal	99.70%	99.70%	99.60%	99.70%		100.00%	84.40%	84.80%
NPHL	99.60%	99.70%	99.70%	99.60%	99.80%		89.70%	89.90%	NPHL	99.70%	99.70%	99.60%	99.70%	100.00%		84.40%	84.80%
PR8	89.90%	90.00%	90.00%	89.90%	89.90%	89.70%		96.60%	PR8	84.40%	84.40%	84.10%	84.40%	84.40%	84.40%		96.00%
WSN	90.10%	90.20%	90.20%	90.10%	90.10%	89.90%	96.60%		WSN	84.80%	84.60%	84.40%	84.60%	84.80%	84.80%	96.00%	
NP	276	471	478	527	Cal	NPHL	PR8	WSN	PA	276	471	478	527	Cal	NPHL	PR8	WSN
276		99.50%	99.70%	99.80%	99.60%	99.80%	86.00%	85.60%	276		100%	99.90%	99.80%	99.60%	99.60%	88.90%	86.10%
471	99.50%		99.30%	99.40%	99.20%	99.40%	85.60%	85.20%	471	100%		100.00%	99.90%	99.70%	99.70%	89.00%	90.20%
478	99.70%	99.30%		99.70%	99.40%	99.60%	85.80%	85.50%	478	99.90%	100.00%		99.90%	99.70%	99.70%	89.10%	90.20%
527	99.80%	99.40%	99.70%		99.50%	99.70%	85.90%	85.50%	527	99.80%	99.90%	99.90%		99.60%	99.90%	89.90%	90.10%
Cal	99.60%	99.20%	99.40%	99.50%		99.60%	85.90%	85.50%	Cal	99.60%	99.70%	99.70%	99.90%		99.80%	89.90%	90.10%
NPHL	99.80%	99.40%	99.60%	99.70%	99.60%		86.00%	85.60%	NPHL	99.60%	99.70%	99.70%	99.60%	99.80%		89.70%	89.90%
PR8	86.00%	85.60%	85.80%	85.90%	85.90%	86.00%		95.90%	PR8	88.90%	89.00%	89.10%	89.90%	89.90%	89.70%		96.60%
WSN	85.60%	85.20%	85.50%	85.50%	85.50%	85.60%	95.90%		WSN	86.10%	90.20%	90.20%	90.10%	90.10%	89.90%	96.60%	
PB1	276	471	478	527	Cal	NPHL	PR8	WSN	PB2	276	471	478	527	Cal	NPHL	PR8	WSN
276		99.00%	98.60%	98.60%	99.10%	98.40%	79.10%	79.10%	276		98.60%	99.20%	99.60%	99.30%	99.20%	84.60%	85.70%
471	99.00%		99.40%	99.20%	99.30%	98.50%	79.00%	79.10%	471	98.60%		99.40%	99.20%	99.70%	99.70%	84.40%	84.60%
478	98.60%	99.40%		99.70%	98.90%	99.00%	79.40%	79.40%	478	99.20%	99.40%		99.20%	99.60%	99.60%	84.00%	83.60%
527	98.60%	99.20%	99.70%		99.00%	99.10%	79.50%	79.50%	527	99.60%	99.20%	99.20%		99.10%	99.20%	84.10%	83.20%
Cal	99.10%	99.30%	98.90%	99.00%		99.10%	79.50%	79.60%	Cal	99.30%	99.70%	99.60%	99.10%		98.30%	83.70%	83.40%
NPHL	98.40%	98.50%	99.00%	99.10%	99.10%		80.00%	80.10%	NPHL	99.20%	99.70%	99.60%	99.20%	98.30%		85.30%	84.90%
PR8	79.10%	79.00%	79.40%	79.50%	79.50%	80.00%		97.40%	PR8	84.60%	84.40%	84.00%	84.10%	83.70%	85.30%		96.20%
WSN	79.10%	79.10%	79.40%	79.50%	79.60%	80.10%	97.40%		WSN	85.70%	84.60%	83.60%	83.20%	83.40%	84.90%	96.20%	

Furthermore, the clustering pattern of the four 2009 pandemic strains isolates, together with the control 2009 pandemic strains isolates and laboratory strains with other 2009 pandemic strains isolates sequenced on other regions were accessed in the phylogenetic tree analysis in order to see indication of reassortments and divergences (Fig 6.1 – Fig 6.8). The accession number of the all of the four isolate genes is shown in Appendix 7. As a comparison, seasonal influenza strains and 2009 pandemic strains

derived from various regions in the world were used. The information of the clustering pattern of the 2009 pandemic strains isolates is useful to determine if the swine flu viruses have evolved to form clades, as observed in the global H5N1 spread (CDC, 2008). The phylogenetic tree analysis of the virus surface glycoprotein, HA and NA genes pose the most critical genes, as they revealed the predicted virus epitope site based on sequence information. The pattern of the virus spread can be observed in the analysis and therefore the vaccine development and prevention strategy can be assessed and established. Nelson *et al.* (2009) did the clustering using whole genome sequencing of the pandemic swine flu viruses from representative regions of the world. They discovered particular clades forming from currently circulating pandemic swine influenza virus. They showed indication that the pandemic influenza were starting to diverge into 7 clades.

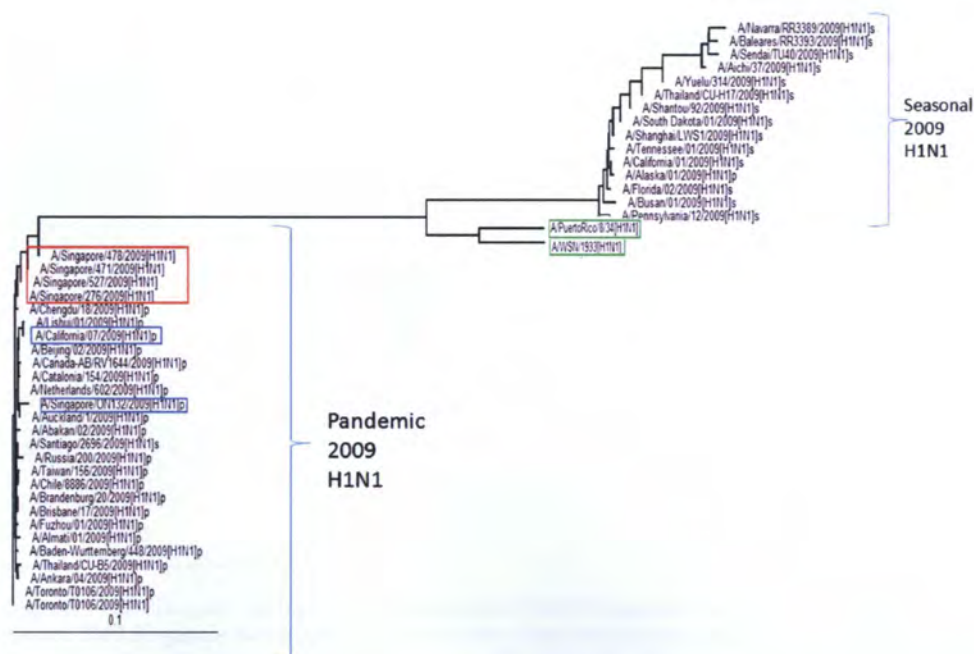


Fig. 6.1 The HA gene phylogenetic tree analysis of 2009 Singapore swine influenza virus isolates. Red box denotes 2009 Singapore swine influenza virus isolates. Blue box denotes control swine influenza virus used in this experiment. Green box denotes the lab strain. The 0.1 with a line beneath denotes 10% nucleotide difference per line length.

The phylogenetic tree of HA gene is shown above (Fig. 6.1). It can be seen that all 2009 pandemic strains isolates used in this experiment were clustered together with all the rest of 2009 pandemic strains from other regions of the world. The seasonal influenza strains and laboratory strains fall on other distinct clusters from 2009 pandemic strains. Within the 2009 pandemic strains, no particular sub-clustering are observed in the HA gene phylogenetic tree. Whereas for the seasonal strains, there is an indication clustering formation. This indicates that the HA gene of the Singapore 2009 pandemic strains isolates have not formed any distinct clades from the rest of the 2009 pandemic strains isolates from the rest of the world.

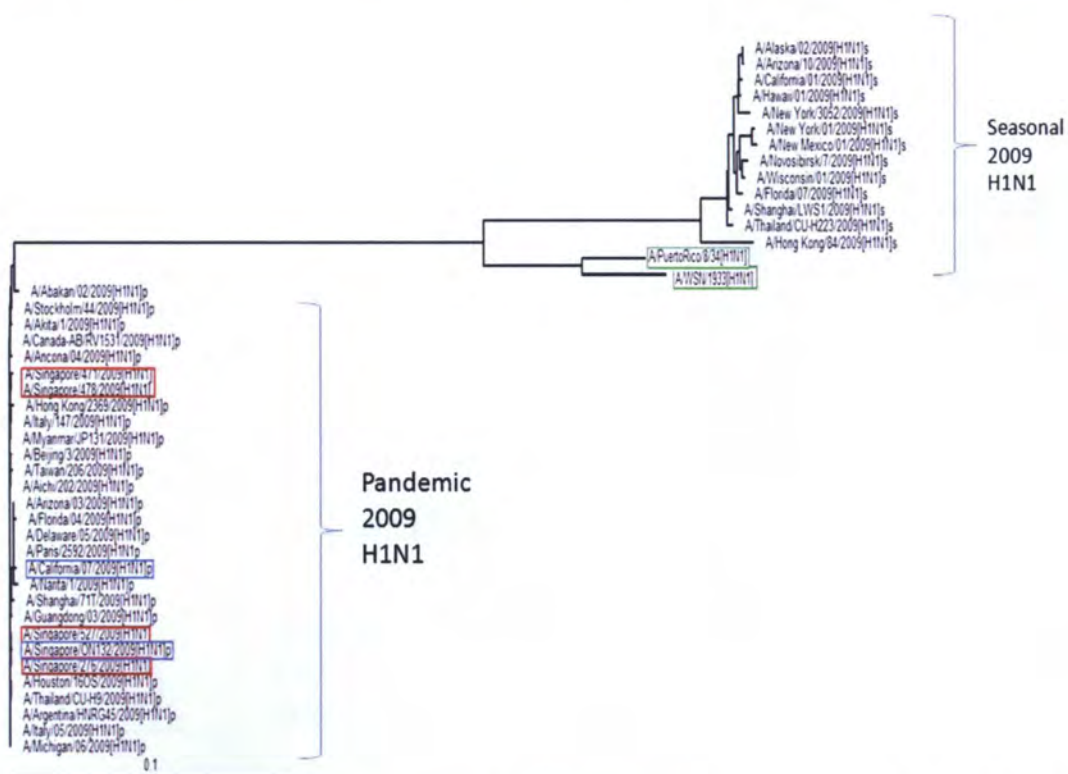


Fig. 6.2. The NA gene phylogenetic tree analysis of 2009 Singapore swine influenza virus isolates. Red box denotes 2009 Singapore swine influenza virus isolates. Blue box denotes control swine influenza virus used in this experiment. Green box denotes the laboratory strain. The 0.1 with a line beneath denotes 10% nucleotide difference per line length.

The phylogenetic tree analysis of the NA gene is shown in Fig. 6.2. It can be seen that 2009 pandemic strains, laboratory virus strains and seasonal influenza strains

clustered very differently. Among the pandemic influenza strains shown above, there is no indication of the subclustering formation among 2009 pandemic strains, which indicates that the NA gene of the 2009 pandemic strains comparison from different regions of the world do not show any clear indication of developing distinct clades. This demonstrates that there is no obvious diversification of the NA gene formed among the 2009 pandemic strains yet. In the seasonal influenza strains, however, distinct clades started to form among the strains, which show that the seasonal influenza strains could be evolved from different strains of seasonal strains.

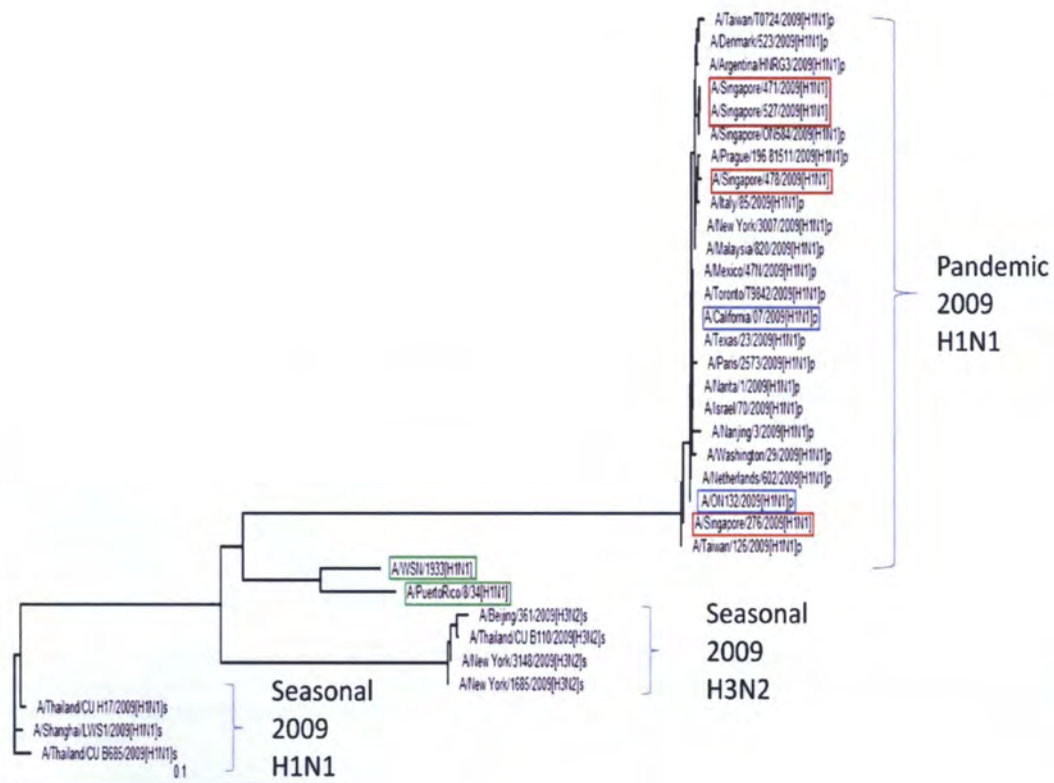


Fig. 6.3. The NS gene phylogenetic tree analysis of 2009 Singapore swine influenza virus isolates. Red box denotes 2009 Singapore swine influenza virus isolates. Blue box denotes control swine influenza virus used in this experiment. Green box denotes the laboratory strain. The 0.1 with a line beneath denotes 10% nucleotide difference per line length.

The phylogenetic tree of NS gene is shown in Fig. 6.3. All 2009 pandemic strains from various regions of the world form distinct cluster from seasonal flu H1N1, seasonal influenza virus H3N2 and laboratory strains. No sub- clustering is formed among the 2009 pandemic strains, which shows that the NS gene of the 2009 pandemic strains isolates have not showed any indication of forming distinct clades as well. There is only a few genes sequence information available at the GeneBank for both seasonal flu H1N1 and H3N2.

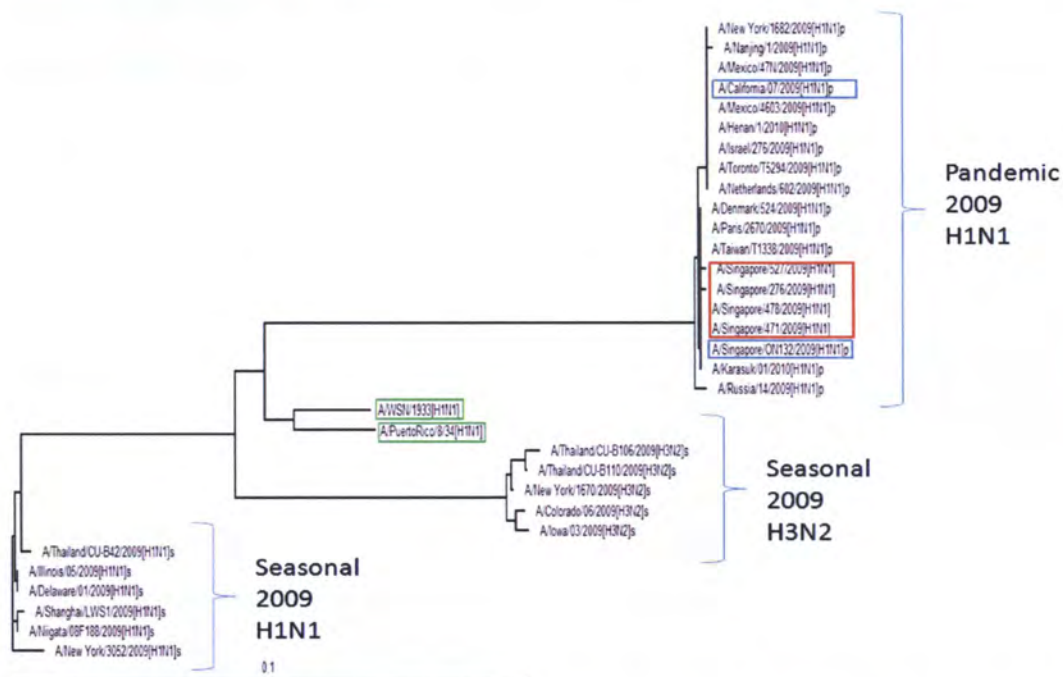


Fig. 6.4. The M gene phylogenetic tree analysis of 2009 Singapore swine influenza virus isolates. Red box denotes 2009 Singapore swine influenza virus isolates. Blue box denotes control swine influenza virus used in this experiment. Green box denotes the laboratory strain. The 0.1 with a line beneath denotes 10% nucleotide difference per line length.

The phylogenetic analysis of the M gene is shown above (Fig. 6.4). It clearly shows that all 2009 pandemic strains, seasonal influenza strains and laboratory strains formed distinct clustering among themselves. Within the 2009 pandemic strains, no distinct pattern of clustering among the isolates is observed, which suggests that the M gene of 2009 pandemic strains isolates from all over the world have not developed any

distinct clades. The M segment from the 2009 pandemic H1N1 influenza virus was originated from avian host, which then reassorted into swine in 1979. Later, the M segment of this avian-derived swine influenza virus was then reassorted to form the current 2009 pandemic H1N1 influenza virus strain (Smith *et al.*, 2009; Kowalczyk and Markowska-Daniel, 2010). It can be concluded that the M gene of all 2009 pandemic strains from various regions of the world continue to share very high similarity among themselves. In the seasonal strains, however, the sub-clustering pattern can be observed within the seasonal flu H1N1 and H3N2, suggesting that the seasonal influenza viruses are developing distinctive clades from the 2009 pandemic strains.

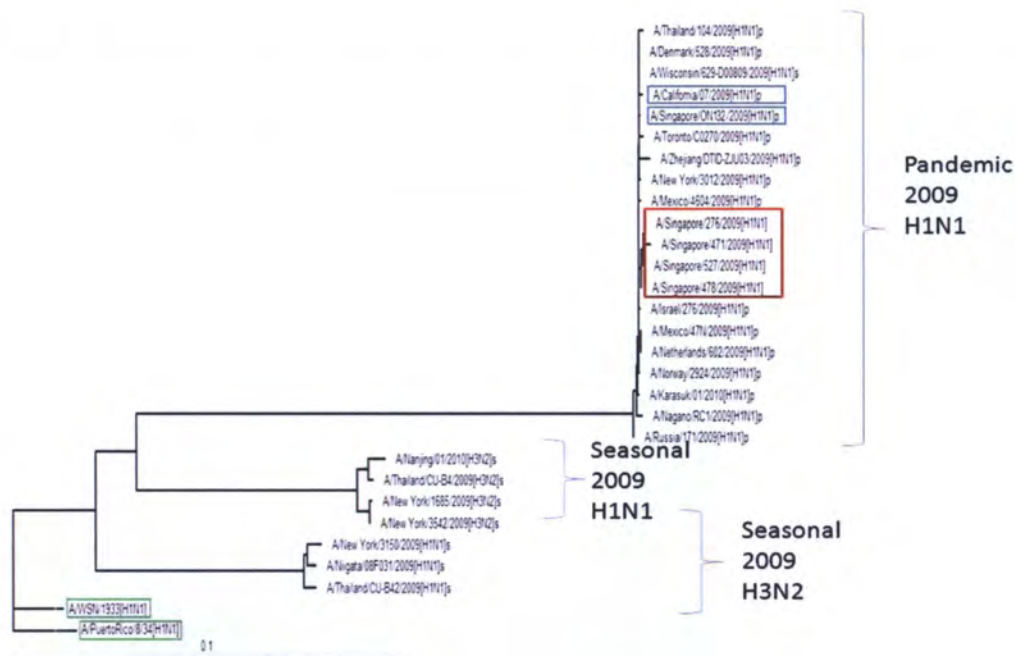


Fig. 6.5 The NP gene phylogenetic tree analysis of 2009 Singapore swine influenza virus isolates. Red box denotes 2009 Singapore swine influenza virus isolates. Blue box denotes control swine influenza virus used in this experiment. Green box denotes the laboratory strain. The 0.1 with a line beneath denotes 10% nucleotide difference per line length.

The phylogenetic tree of the NP gene is shown above (Fig. 6.5). The seasonal influenza virus H1N1, and seasonal influenza virus H3N2 clustering is different from that of the 2009 pandemic strains isolates. Within the pandemic flu strains from

various regions of the world, no distinct clustering has been observed. This suggests that there is no distinct pattern of evolution observed in the NP gene among the pandemic strains. Although both the seasonal flu H1N1 and H3N2 showed distinct clades, the distance gap of the NP gene among the clustering is closer than those of other genes, which shows that both seasonal flu H1N1 and H3N2 have higher degree of NP gene similarity.

The phylogenetic tree of PA gene is shown below (Fig. 6.6). There is distinct clustering among 2009 pandemic strains, seasonal H1N1 strains and seasonal H3N2 strains. Among the 2009 pandemic strains from various regions of the world, there is no indication of the formation of distinct clades among the swine flu strains, which shows that the PA gene from the currently isolated and sequenced 2009 pandemic strains have high degree of similarity. It also demonstrates that there is no distinct sub-clustering within the 2009 pandemic strains.

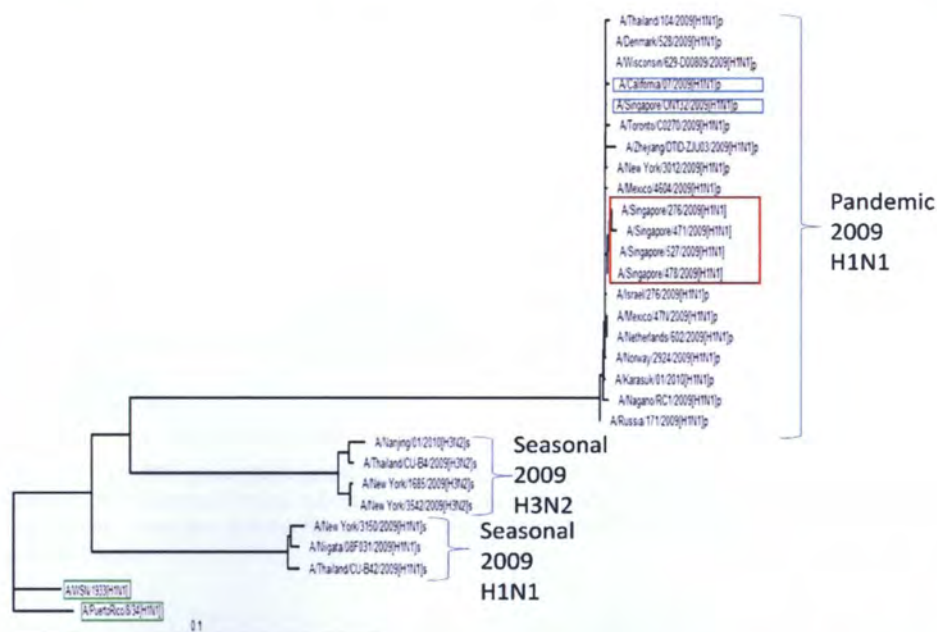


Fig. 6.6 The PA gene phylogenetic tree analysis of 2009 Singapore swine influenza virus isolates. Red box denotes 2009 Singapore swine influenza virus isolates. Blue box denotes control swine influenza virus used in this experiment. Green box denotes the laboratory strain. The 0.1 with a line beneath denotes 10% nucleotide difference per line length.

The phylogenetic tree of the PB1 gene is shown below (Fig. 6.7). The 2009 pandemic strains, seasonal H1N1 and H3N2 strains showed distinct clustering. However, there are no distances between the seasonal H3N2 and the 2009 pandemic strains isolates observed in the tree. This demonstrates that the PB1 gene of the 2009 pandemic strains isolates are very similar with that of the seasonal flu H3N2, which has been reported by Garten *et al.* (2009). Within the 2009 pandemic strains isolates, there was no distinct sub-clustering was not observed among the different regions of the 2009 pandemic strains isolates, which shows that the PB1 gene sequence of the 2009 pandemic strains isolates from different regions of the world are very similar.

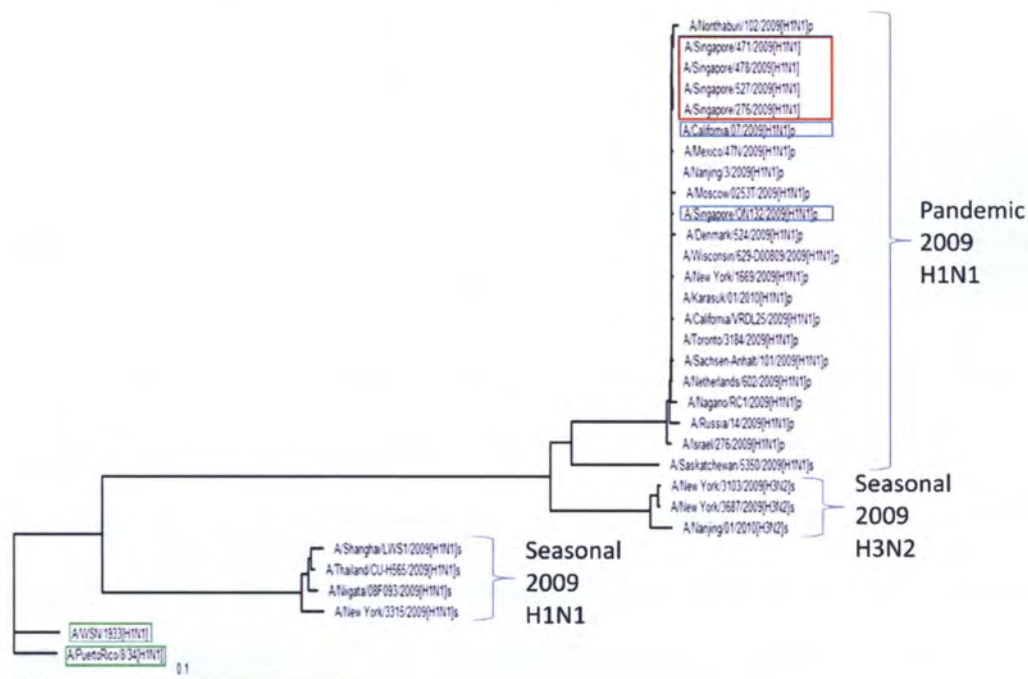


Fig. 6.7 The PB1 gene phylogenetic tree analysis of 2009 Singapore swine influenza virus isolates. Red box denotes 2009 Singapore swine influenza virus isolates. Blue box denotes control swine influenza virus used in this experiment. Green box denotes the laboratory strain. The 0.1 with a line beneath denotes 10% nucleotide difference per line length.

The phylogenetic analysis of the PB2 gene is shown in Fig. 6.8. Similar with the rest of the genes, the pandemic H1N1, seasonal H3N2, seasonal H1N1 strains form

very distinct clustering. Among the 2009 pandemic strains, no distinct sub-clustering pattern is observed, which demonstrates that the PB2 sequence of the circulating 2009 pandemic strains are very similar.

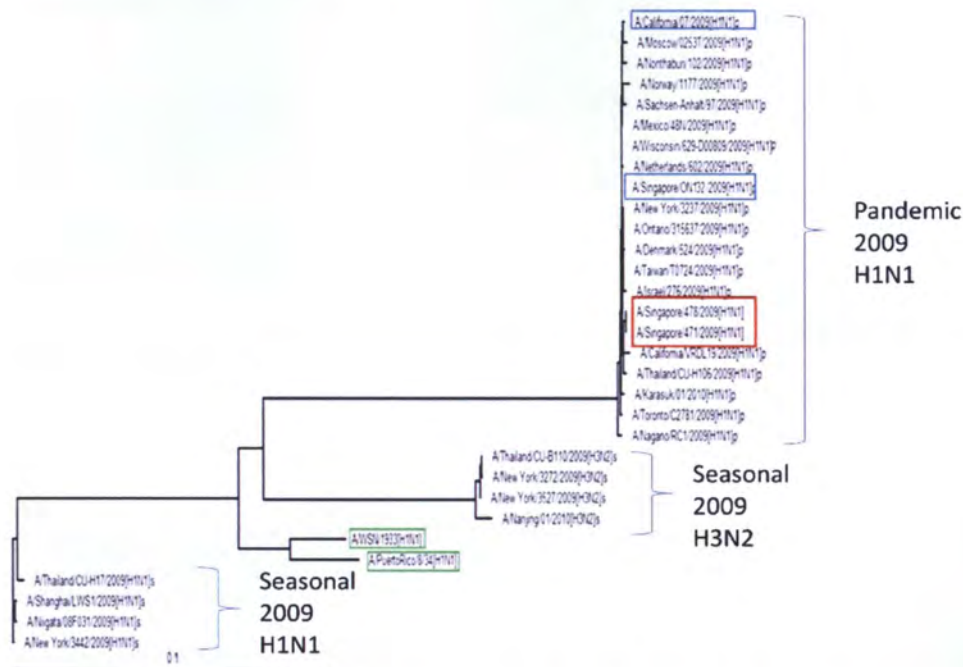


Fig. 6.8. The PB2 gene phylogenetic tree analysis of 2009 Singapore swine influenza virus isolates. Red box denotes 2009 Singapore swine influenza virus isolates. Blue box denotes control swine influenza virus used in this experiment. Green box denotes the laboratory strain. The 0.1 with a line beneath denotes 10% nucleotide difference per line length.

Further, drug resistance mutation among the 2009 pandemic strains was highlighted. The amino acid sequence of M2 and NA are shown in Fig. 6.9 and Fig. 6.10 respectively. The critical points of mutation at amino acids V27A and S31N in the M protein has been shown to develop amantadine resistance among influenza virus (Sugrue and Hay, 1991; Pinto *et al.*, 1992; Suzuki *et al.*, 2003). All 2009 pandemic strains have a S31N mutation. It showed that Singapore isolated swine flu strains are resistant to amantadine.

The amino acid residue of H275Y is responsible for oseltamivir resistance in the N1 strain (Gubareva *et al.*, 2000; Zambon and Haiden, 2001; McKimm-Breschkin *et al.*, 2000). Several reports have shown emergence of oseltamivir resistance of 2009

pandemic influenza virus in America (CDC, 2009), Canada (FluWatch, 2009) Hong Kong and China (Chen *et al.*, 2009), and Europe (ECDC, 2009). Singapore 2009 pandemic strains isolates had H in position 275, which confers susceptibility to oseltamivir.

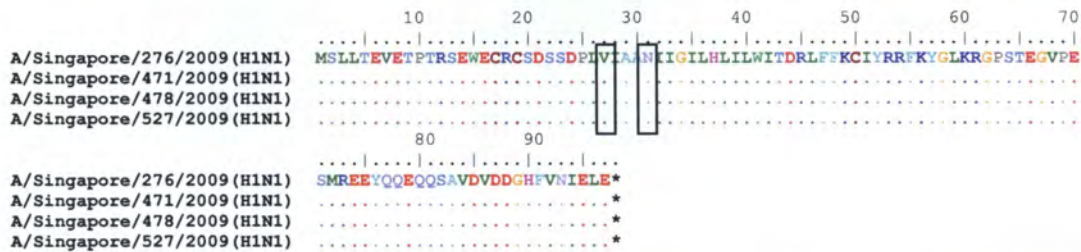


Fig. 6.9 Amino Acid Sequence of M2 in 2009 pandemic strains isolates. The amantadine resistance mutations are shown in black boxes

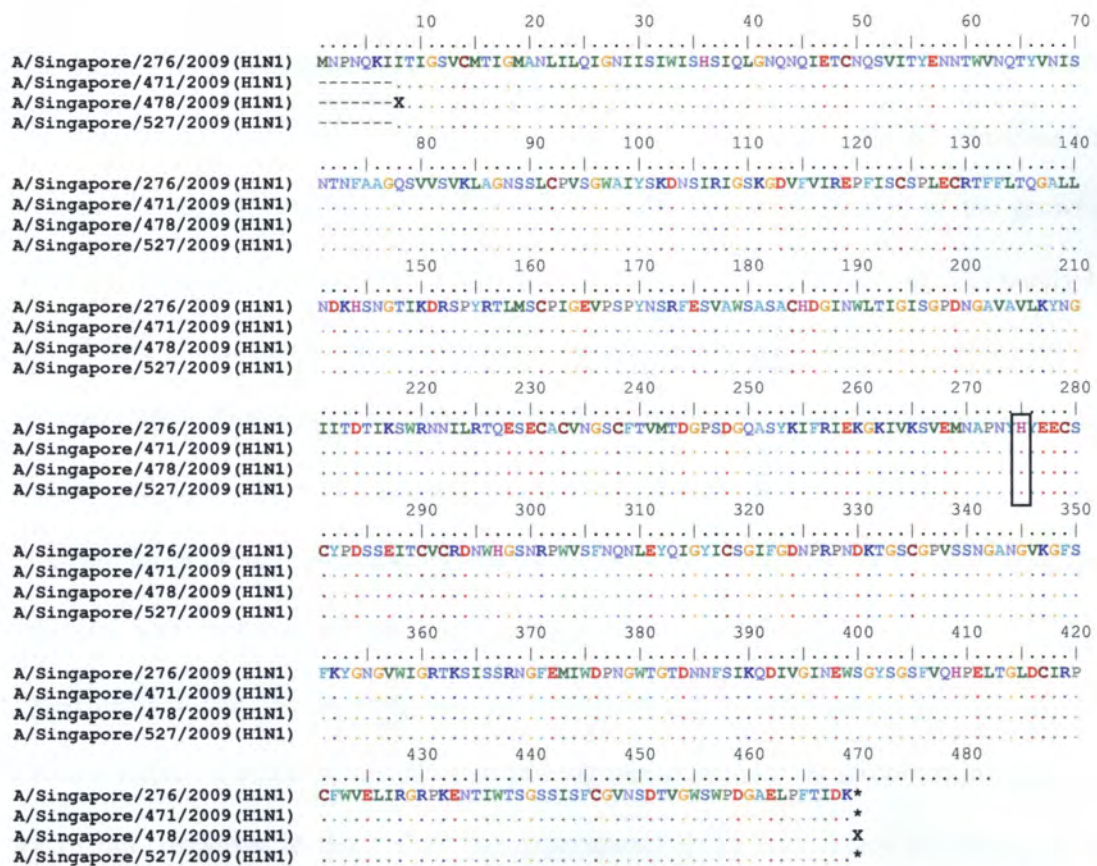


Fig. 6.10 Amino Acid Sequence of NA in 2009 pandemic strains isolates. Note the amino acid sequence marked with black box

6.2 Growth Characteristics

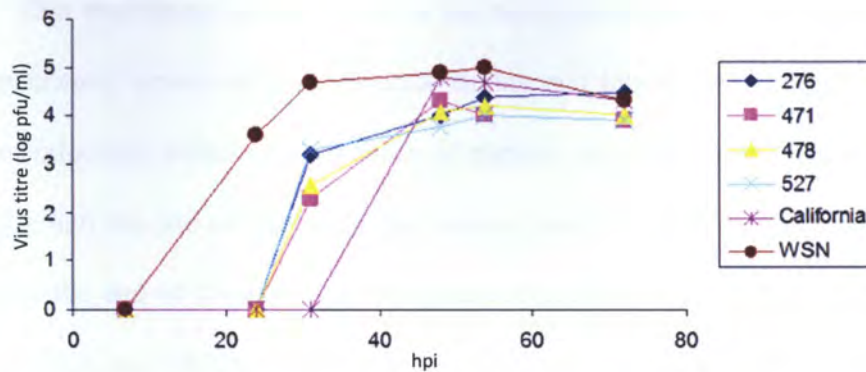


Fig. 6.11. The growth curve of the 2009 pandemic strains isolates grown in MDCK cells with moi of 0.1 at specific hours post infection (hpi).

The growth curve of the swine flu viruses is shown in Fig. 6.11. All four 2009 pandemic strains used in the study shows similar pattern of growth in MDCK cells. The cells were infected with the 2009 pandemic strains and A/WSN/33 (H1N1) with the moi of 0.1, and virus titers were measured every 12 hpi, with the presence of trypsin to support multiple cycle of infection. The logarithmic phase of the growth could be observed starting from approximately 30 hpi with difference approximately 1 log among the isolates. The California strain however, showed logarithmic phase approximately 20 hpi later than the rest of the isolates, but from 50 hpi onwards, the amount of virus titer of California virus detected was similar with the rest of the isolates. From 30 hpi onwards, replication endpoint was reached where no significant titre rise was observed, which reached at approximately 10^5 pfu/ml at the end of the experiment. It can also be seen that the laboratory strain WSN showed better growth characteristics, marked by distinct rise and log phase of the viral growth from as early as 10 hpi. However in the end of the experiment, all of the viruses showed similar amount of virus titre.

6.3 Viral Kinetics in host-cell lines

This experiment aims to observe the replication and transcription rate of each 2009 pandemic strains with the control strains and laboratory strains within single cycle of infection, without the presence of trypsin. All of the cells were infected with moi of 3, and the rate of replication and transcription was measured every 2 hpi with 10 hpi as the end of measurement. The measurements were based on the amount of matrix vRNA and mRNA amplification, and normalized against 10^4 copy of EF. The result of which is shown in Fig 6.12, and the tabulated form is shown in Table 6.2. all Singapore swine strain influenza viruses, and California strain generally have lower replication and transcription level of expression over time as compared to WSN and PR8 in all cell lines. Both laboratory strains WSN and PR8 reached stationary phase earlier compared to 2009 pandemic strains in all cell lines observed.

In MDCK cell lines, the laboratory strains PR8 and WSN reached stationary phase at 6 hpi in both vRNA and mRNA kinetics. All 2009 pandemic strains behaved similarly for both vRNA and mRNA kinetics. The rise of the vRNA and mRNA copies could only be observed after 6 hpi for the vRNA and 8 hpi for the mRNA. At 10 hpi, both WSN and PR8 had significantly more copy numbers of both vRNA and mRNA produced than those of swine influenza virus strain. The difference is approximately 4 log of copy number. This suggests that all strains of swine influenza virus used in this experiment replicated less efficiently than the laboratory strain in canine based cell lines. To correlate this result with the in the mRNA (Fig. 4.9) and vRNA (Fig. 4.11) of H1N1 in Chapter 4, it could be observed that the vRNA of the M gene and most of the genes peaked around 5-6 hpi in all cells, which is consistent with this experiment. Further, the trend of the 2009 pandemic strains were similar with that of the mRNA and vRNA of avian H9N2 isolate in MDCK cells (Fig. 4.13), where it could be

observed that the rise of both replication and transcription were generally steady up to 8 hpi. However, the H9N2 isolate showed much lower replication and transcription rate than 2009 pandemic strains in A549 cells. This is expected because the H9N2 isolate used in this experiment possesses avian signature in all of its segments, while 2009 pandemic strains contain human-derived segment in PB1, which explains the better ability of the 2009 pandemic strains to grow in A549 cells.

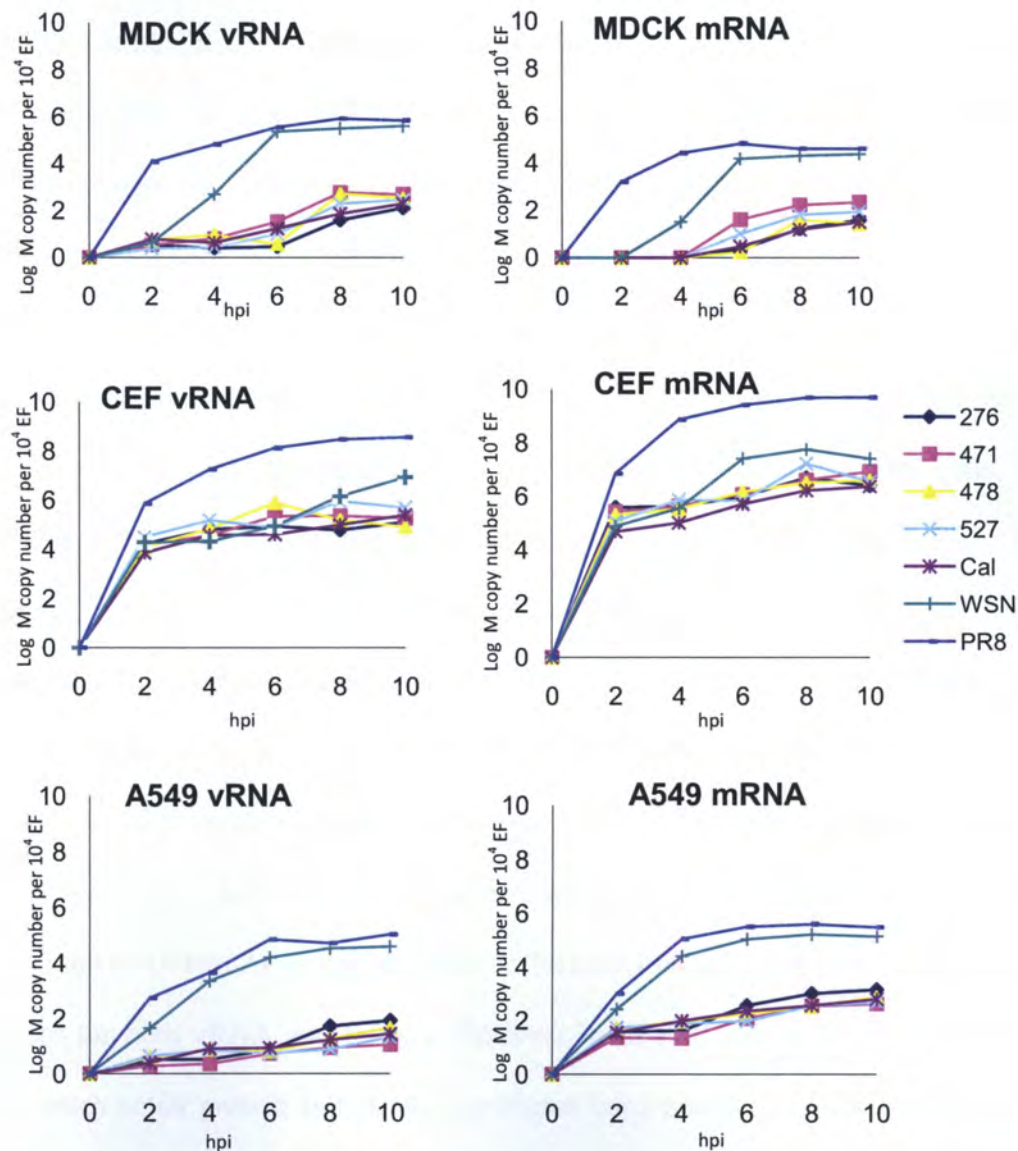


Fig 6.12 Replication (vRNA) and Transcription (mRNA) rate of 2009 pandemic strains isolates as compared to A/WSN/33(H1N1) and A/PR/8/34(H1N1) in MDCK, CEF and A549 cells with the moi of 3. The result shown above was based on the copy number of the M segment per 10⁴ EF.

Table 6.2 Tabulated copy number of 2009 pandemic strains, WSN and PR8 infected MDCK, CEF and A549 cells at 10 hpi, as shown in Fig 6.12. The result shown was based on the copy number of the M segment per 10^4 EF.

	MDCK		CEF		A549	
	vRNA	mRNA	vRNA	mRNA	vRNA	mRNA
276	1.29×10^2	3.95×10^1	1.27×10^5	2.50×10^6	8.38×10^1	1.44×10^3
471	4.86×10^2	2.26×10^2	1.84×10^5	8.58×10^6	1.15×10^1	4.26×10^2
478	3.39×10^2	2.81×10^1	8.25×10^4	3.95×10^6	4.68×10^1	7.68×10^2
527	2.91×10^2	8.94×10^1	5.04×10^5	3.58×10^6	2.11×10^1	5.00×10^2
Cal	2.00×10^2	3.23×10^1	2.48×10^5	2.36×10^6	2.80×10^1	6.46×10^2
WSN	4.10×10^5	2.47×10^4	8.64×10^6	2.60×10^7	3.92×10^4	1.41×10^5
PR8	6.99×10^5	4.18×10^4	3.70×10^8	4.97×10^9	1.09×10^5	3.06×10^5

The vRNA and mRNA of all 2009 pandemic strains show a similar trend with the WSN strain in CEF cell lines at early time point up to 8 hpi. At 10 hpi, the replication and transcription rate of WSN continued to rise, while the vRNA and mRNA of swine influenza virus strains were stagnant. All of the virus strains exhibited a rise on both vRNA and mRNA as early as 2 hpi. The PR8 strain had the most rapid rate of both replication and transcription. At 10 hpi, PR8 strain could produce 3 more logs in copy number as compared to the rest. It can be deduced that the swine influenza viruses are replicating as efficient as the WSN strain in CEF cells. To correlate with the replication and transcription rate of avian H9N2 isolate in CEF cells (Fig. 4.13), it can be observed that the avian H9N2 cells reached plateau at 5 hpi, while the 2009 pandemic strains were as early as 2 hpi, which showed the indication of earlier replication and transcription endpoint for the pandemic strains.

The 2009 pandemic strains growth in A549 is able to be compared to that in MDCK cell lines. Both vRNA and mRNA were shown to increase slowly starting from 2 hpi to 10 hpi. At 10 hpi, all swine influenza virus have similar amount of copy number for both vRNA and mRNA. However, both PR8 and WSN were shown to have much better growth as indicated by higher copy number of vRNA and mRNA. From the result, it can be observed that swine influenza virus have poor growth in human lung cell lines as compared to WSN and PR8. The 2009 pandemic strains

showed very low copy number of vRNA ($\sim 10^1$ copies/ 10^4 EF) and mRNA ($\sim 10^2$ copies/ 10^4 EF), which could also be observed in avian H9N2 isolate (Fig. 4.13).

It can also be observed that 2009 pandemic strains have poor ability to replicate in MDCK and A549 cell lines, but moderate ability to replicate in CEF. It has been reported that PB2 and PA segments from the swine influenza virus were originated directly from avian lineage, and both the NA and M segments were originated from avian-like swine lineage (Garten *et al.*, 2009). This might explain the higher ability of the 2009 pandemic strains to replicate better in avian based cell lines. Similar characterization was done by Itoh *et al.*, 2010, where they found that the growth curve of the 2009 pandemic strains is comparable with other contemporary H1N1 viruses in canine based (MDCK) and human based cells (Human Airway Epithelial (HAE)). In our experiment, it is shown that both WSN and PR8 strains, which are two classical human strains, replicated at higher rate than the 2009 pandemic strains, which suggests that the evolutionary basis of these older strains may be attributed to the higher replication in both cells.

6.4 Cell response in host-cell lines

In this experiment, the host-cells response to 2009 pandemic strains infection was monitored in order to explain the difference in replication and transcription rate. The experiments were done in MDCK, CEF and A549 cells. The selected antiviral genes based on the result obtained in Chapter 5 were taken as the basis of the measurement of the host response to counteract the virus infection. The selected genes for antiviral response of the MDCK cell line is shown in Fig. 6.13. The infection was carried at moi 3, and measured at 10 hpi. Two different sets of experiments with triplicate measurement were conducted for reproducibility ($n=6$). The error bars shown

below denotes the variability of the measurement among replicates. All of the 2009 pandemic strains, induced approximately similar level of RSAD2, which ranged from 6 fold change observed in strain 276 to 13 fold change observed in strain 527. The WSN strain showed slightly higher upregulation of the RSAD2 gene than 2009 pandemic strains, at approximately 13 fold change. The PR8 strain showed higher upregulation of the RSAD2 gene which reached approximately 250 fold change. In the Mx1 gene, the upregulation of the PR8 strain showed the highest upregulation, reaching up to 60 fold change. All of the 2009 pandemic strains showed approximately similar upregulation, which were about 8 fold changes. WSN strain showed slightly higher upregulation of the Mx1 gene at approximately 8 fold change. There were no significant change in the IFN- β 1 and OAS1 in term of fold change observed in all isolates in MDCK cells. Although the expression of both RSAD2 and Mx1 showed higher upregulation in WSN and PR8 infected cells, they exerted much higher virus replication (Table 6.1). These findings suggest that the intensity of antiviral gene expression may not affect the rate of replication and transcription of the viruses, as shown in Fig 6.11 and Fig 6.12. It is possible that both WSN and PR8 strains were able to counteract the expression of the antiviral genes. It should be noted that only WSN strain was used as laboratory control strain in Fig. 6.11. The low copy numbers observed in Fig. 6.12 might result from the low compatibility of the virus gene segments that give rise to inefficient replication in the pandemic strains. There is also a possibility that WSN strain produced higher viral genetic materials to induce higher innate response, as demonstrated by Pothlichet et al., 2008.

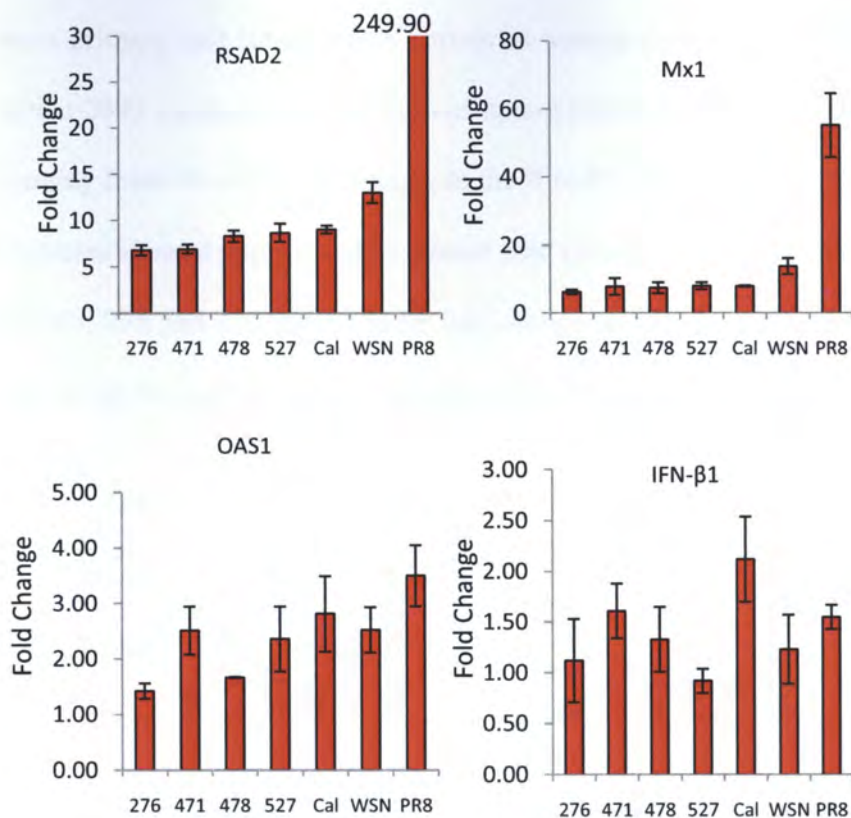


Fig 6.13 Relative quantification of mRNA expression of selected genes expressed in virus infected MDCK cells denotes fold change with comparison with mock-infected cells at 10 hpi with moi 3. The experiments were based on six replicates (n=6) with the bars as the average value, and error bars and the standard deviations among replicates.

Selected genes for antiviral response of the CEF cell line is shown in Fig. 6.14. In the OASL gene, it can be observed that PR8 strain showed the lowest compared to the rest. The WSN strain showed the highest upregulation of the OASL gene at 400 fold change. Most of the 2009 pandemic strains showed similar upregulation of the OASL gene, ranging from approximately 90 fold change to 180 fold change. In the Mx1 gene, the PR8 strain showed the least upregulated as compared to the rest of the isolates. The WSN strain showed the highest upregulated Mx1 gene at approximately 350 fold change. The rise of both the Mx1 gene expression of the WSN strain in this experiment was considerably more than that of in Fig. 5.24. This might be due to differences in the characteristics and conditions of CEF cells harvested, since CEF

cells were primary cell lines, where variations among embryos were highly likely. Most of the 2009 pandemic strains showed approximately similar upregulation of the gene, ranging from 40 to 60 fold change. In the IFN- β 1 gene, all of the 2009 pandemic strains isolates showed approximately similar fold change, ranging from 6 fold change in California, 276 and 478 strains to 10 fold change in 471 and 527 strain. The WSN strain did not show significant upregulation of the IFN- β 1 gene.

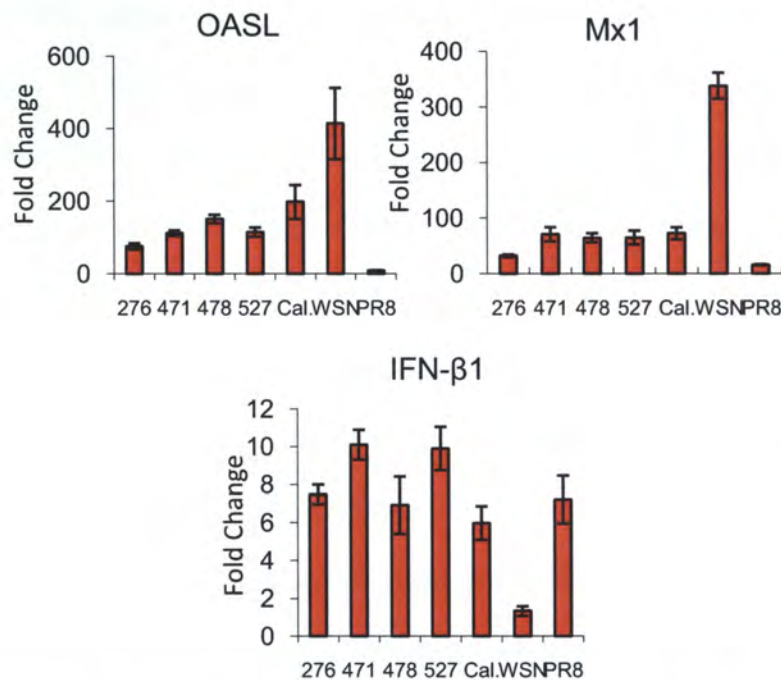


Fig 6.14 Relative quantification of mRNA expression of selected genes expressed in virus infected CEF cells denotes fold change with comparison with mock-infected cells at 10 hpi (moi 3). The experiments were based on six replicates (n=6) with the bars as the average value, and error bars and the standard deviations among replicates.

The host response in A549 cell line is shown in Fig. 6.15. In the IFN- β 1 gene, both the WSN and PR8 strains did not show any significant upregulation of the gene. The 2009 pandemic strains, however showed approximately similar upregulation, which ranged from approximately 6 fold change observed in 276 and 527 strain up to 10 fold change observed in 471 strains. In the OAS1 gene, the WSN strain showed the least upregulated pattern, followed by PR8 strain at 50 fold change. The 2009

pandemic strains upregulates the OAS1 gene up to approximately 200 fold change as observed in 478 strain. The 276 strain showed the lowest which was approximately 110 fold change. In the OAS2 gene, both the WSN and PR8 strains showed the lowest upregulation at 40 fold change. All of the 2009 pandemic strains showed approximately similar upregulation profile, from 60 to 80 fold change. In the Mx1 gene, WSN showed the lowest upregulation at approximately 5 fold change. All the 2009 pandemic strains and PR8 showed similar upregulation, which were approximately 10 fold change. In the RSAD2 gene, both WSN and PR8 strains showed the lowest upregulation. Most of the 2009 pandemic strains showed varied upregulation pattern, which ranged from 60 fold change in strain 276 to 140 fold change in 527 strain. To correlate the result of the WSN strain found in Fig. 5.22, unlike CEF cells, it can be observed that the fold change value of all the genes in A549 cells is similar. The nature of the cell line and higher controlled conditions may explain the more consistent result in A549 cells.

Based solely on the finding described above, there are variations in antiviral mRNA quantifications among swine influenza virus, WSN and PR8 in MDCK and CEF cells. However, it was more consistent on A549 cells, where all of the antiviral genes showed a similar trend, with swine influenza viruses generally having higher responses than WSN and PR8 strains. It is known that the NS1 protein plays a central role to evade immunological response (Fernandez-Sesma, 2001), but the NS1 protein from 2009 pandemic strains were not as potent as other human-derived strains in human cell lines (Hale *et al.*, 2010), which explain the higher response in A549 cells. It can be concluded that the viruses have various ability to evade the induction of immunological response in different cell lines with different extent.

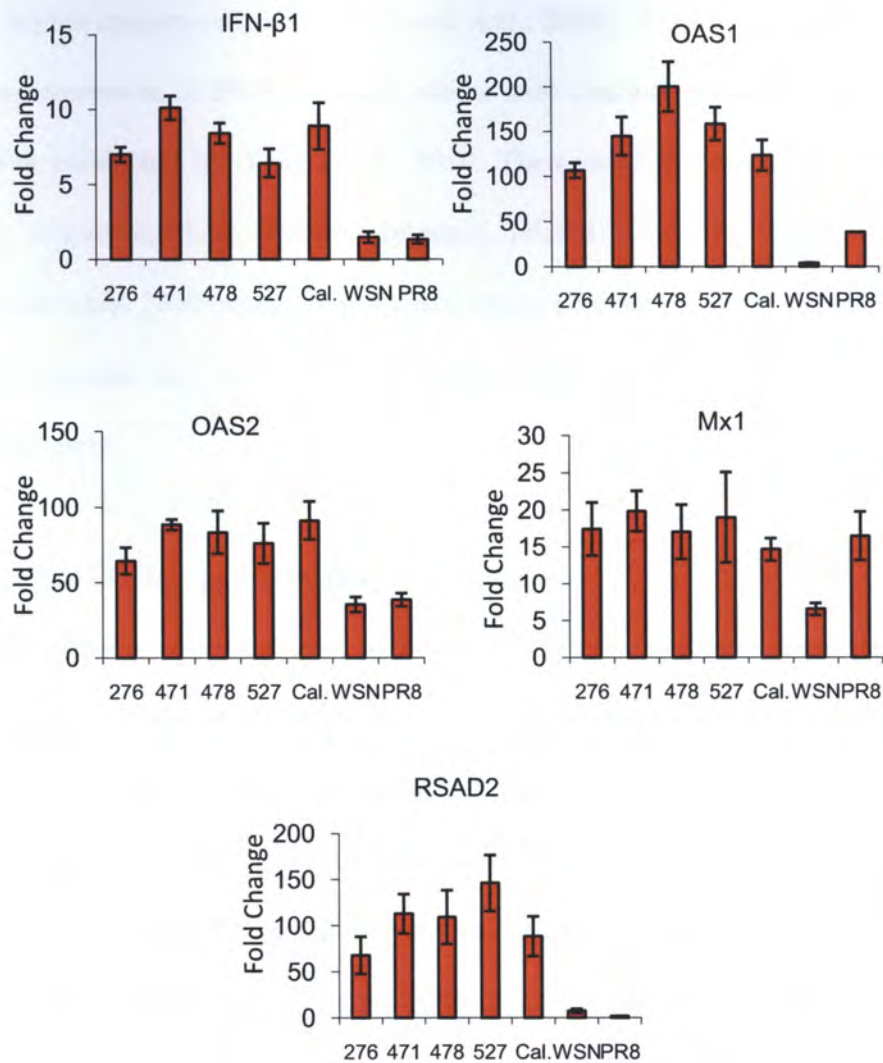


Fig 6.15 Relative quantification of mRNA expression of selected genes expressed in virus infected A549 cells denotes fold change with comparison with mock-infected cells 10 hpi (moi 3). The experiments were based on six replicates (n=6) with the bars as the average value, and error bars and the standard deviations among replicates.

The 2009 pandemic strains are quadruple reassortants viruses originated from human, avian and swine hosts (Garten *et al.*, 2009), which also confer to the ability of the 2009 pandemic strains to adapt and grow efficiently in different hosts. The interaction of the different polymerase genes may correlate to low replication and transcription rates, as compatibility among polymerase genes and nucleoprotein is critical for replication (Naffakh *et al.*, 2000; Labadie *et al.*, 2007; Rameix-Welti *et al.*, 2008). Furthermore, higher replicating viruses can produce more 5'-capped RNA to

induce higher immune response (Pothlichet et al., 2008). Microarray study to compare the gene expression of 2009 pandemic strains with seasonal influenza strains in A549 cells was conducted by Yang *et al.*, 2010. Their result indicated that both of the viruses suppressed host immune response related pathways including cytokine production while 2009 pandemic influenza strains showed weaker suppression of host immune response than seasonal H1N1 strains, which is also similar to the finding in this experiment.

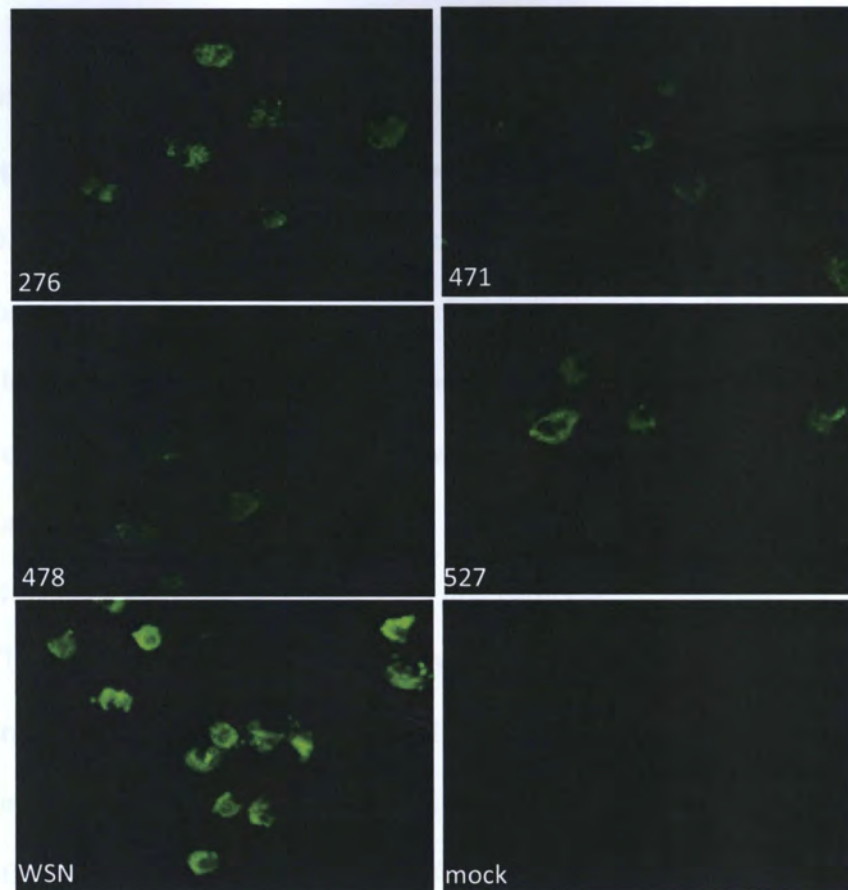
6.5 Viral kinetics in mouse lung macrophage

In order to assess the virus ability to induce immunological response, we used mouse lung macrophage. Initially, we set up the optimal time of the moi used and the infection time. Later, the experiment was verified using immunofluorescence assay in order to predict optimal amount of time and moi needed to achieve good infection in 2009 pandemic virus. The result is shown below Fig. 6.16(A). It could be observed that the 2009 pandemic strains and WSN strains were able to infect mouse lung macrophage. However, even at moi of 5, only ~30% of the cells were infected by 2009 pandemic virus strains. The WSN strain, however, showed ~70% infection. This shows that WSN strain has better infectivity in mouse lung macrophage. This also suggests that 24 hpi, rather than 10 hpi, was required to observe more immunological response.

The measurement of replication and transcription of the swine influenza viruses in mouse lung macrophage are shown in Fig. 6.16(B), and they were generally lower than WSN. The WSN strain produced approximately 5 log and 4 log higher for vRNA and mRNA, respectively, at 24 and 48 hpi. All of the swine influenza viruses had significantly lower expression levels of vRNA and mRNA, exhibiting only up to 2

logs and 3 logs of M copy number, respectively. Unlike epithelial cells, macrophages generally excrete more cytokine and chemoattractant proteins to counteract infection,

A.



B.

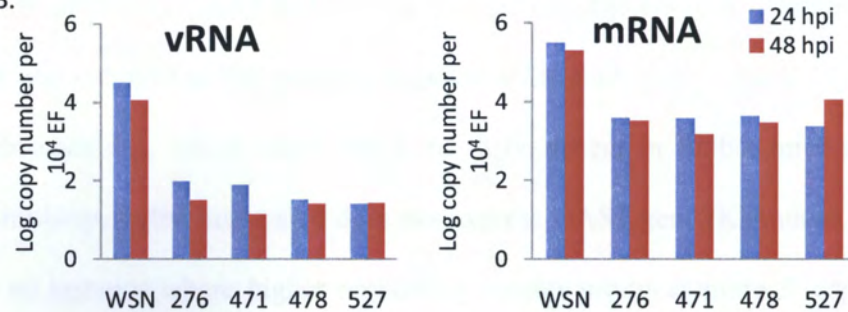


Fig 6.16 (A) The immunofluorescence image of 2009 pandemic flu infected and WSN infected mouse lung macrophage with the moi of 5 at 24 hpi, stained using anti-NP antibody (B) Replication (vRNA) and Transcription (mRNA) Rate of 2009 pandemic strains isolates as compared to A/WSN/33(H1N1) in mouse lung macrophages.

and virus pathogenicity. The ability of different strains of influenza virus to counteract this activity from the NS1 gene might contribute to different level of replication and transcription rate. From this experiment, WSN strain is shown to be able to grow and replicate better in mouse lung macrophage, which is also shown in other reports (Mak *et al.*, 1984; Noble and Dimmock, 1995). Unlike in host-cell models, we used 24 hpi and 48 hpi in mouse lung macrophage instead, based on the cytokine studies shown in Fig. 5.30. It could be observed that there was no increase of cytokine excretion found up to 8 hpi, which signifies that the mouse lung macrophage might not exert optimal stage of host defense mechanism. Further, we were unable to compare this result with growth curve experiment because no virus was detected in the medium for mouse lung macrophage infection at 24 hpi.

6.6 Host gene response in mouse lung macrophage

The selected antiviral genes in mouse lung macrophage against 2009 pandemic swine strains are shown in Fig. 6.17. All of the swine influenza viruses exhibited almost similar levels of OASL, OAS2 and IFN- β 1 at 24 hpi and 48 hpi. There were slight differences observed among the 2009 pandemic strains. It did not show any increase of the all gene response at 48 hpi. The WSN strain had generally exhibit higher level of OASL, OAS2 and IFN- β 1 compared to the all of the pandemic strains. The Mx1 was not used in this experiment because the Balb/c mice contain Mx deletion on the chromosome, which cause Mx gene to be absent in Balb/c mice (Jin *et al.*, 1998). Similarly, Balb/c mice also does not express OAS1 gene (Kakuta *et al.*, 2004). There is an instance where higher replicating viruses produces more 5'-capped RNA to induce higher immune response (Pothlichet *et al.*, 2008). From the result shown, it is clear that the WSN strain did not show any inhibition of the immunological

response of the lung macrophage. But at the same time, it is also obvious that the antiviral genes show little effect on the WSN replication and transcription rate.

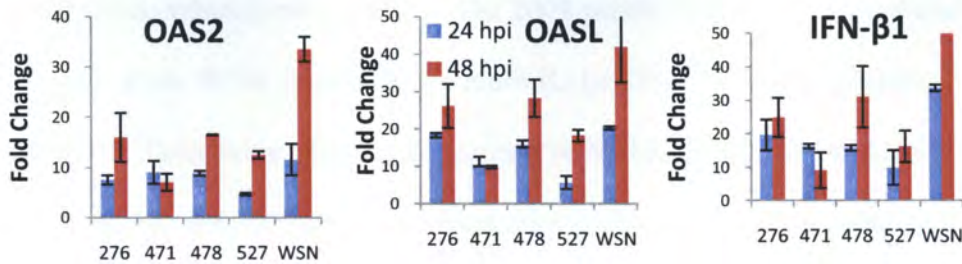


Fig 6.17 Relative quantification of mRNA expression of selected genes expressed in virus infected mouse lung macrophage cells denotes fold change with comparison with non-infected cells, for infection time of 24 hpi (■) and 48 hpi (■). The experiments were based on six replicates (n=6) with the bars as the average value, and error bars and the standard deviations among replicates.

6.7 Cytokine profiling in mouse lung macrophage

Similar with experiment done in Section 5.5.3, this experiment was conducted in order to detect secreted cytokine in the 2009 pandemic strains. However, it should be noted that 24 hpi and 48 hpi were used instead, because earlier time point, 4 hpi and 8 hpi as indicated in Fig. 5.30, did not show any significant change of cytokine excretion compared to the uninfected macrophages. The statistical significance was assessed by conducting two separated harvesting, and measurements were done in duplicates each (n=4). The collection of cytokine profiling graphs is shown in Fig. 6.18. It should be noted that the value of the secreted cytokine in WSN strain shown in Fig. 5.30 and Fig 6.18 are different, because two separated experiments with different period of cell harvesting were done. Therefore, variances in the amount of cytokine excreted were expected. The ability of the 2009 pandemic strains to infect mouse lung macrophages has also been demonstrated by Woo *et al.*, 2010, and Itoh *et al.*, 2010. In the 2009 pandemic strains infection, several macrophage related cytokines were detected, which are IL-1 α , IL-1 β , IL-6, IL-13, KC, MIP-1 α , MIP-1 β , G-CSF, GM-CSF, Eotaxin, MCP-1, TNF- α , and RANTES. The 2009 pandemic strains did not increase

the excretion of IL-6, IL-13, MIP-1 β , Eotaxin and G-CSF, while WSN strain generally triggered an increase in all cytokine observed with the exception of IL-6, as compared to the mock-infected macrophages. The 2009 pandemic strains only induced more IL-12(p40), while WSN strain induced more IL-1 α , IL-13, MIP-1 β , Eotaxin, G-CSF and RANTES. There were comparable increase of IL-1 β , IL-6, MIP-1 α , KC and GM-CSF. IL-1 α , IL-1 β , and IL-6 are proinflammatory pathways and act as precursor to induce immunological response (Dinarrelo, 1994; Kaufman *et al.*, 2001; Heinrich *et al.*, 2003). From the results, it is shown that pandemic 2009 pandemic strains did not induce much of the proinflammatory responses as compared to WSN, and this results in lower response on antiviral genes. chemoattractant and chemotactic proteins such as MCP-1, Eotaxin, MIP-1 α , MIP-1 β were induced higher in WSN strain, which was indication of more severe immunological response (Julkunen *et al.*, 2001; Heinrich *et al.*, 2003).

The infection of mouse both *in-vitro* (lung macrophages) and *in-vivo* (Balb/c mice) with 2009 pandemic strains has also been done by other groups (Woo *et al.*, 2010; Itoh *et al.*, 2010), where they found that generally 2009 pandemic influenza virus strains generally exhibited comparable amount of cytokines with the seasonal strains, which suggests that the 2009 pandemic strains may have similar severity with the seasonal strains. However, in our experiment, the WSN strain generally induced higher cytokine response than 2009 pandemic strains. This suggests that the 2009 pandemic swine influenza strains caused lower immunological response in mouse lung macrophage than WSN strain. The 2009 pandemic viruses also caused less severe immunological responses than WSN strain to macrophages due to lower cytokine expression, as high cytokine response are very closely related to pathogenicity due to the cytokine overexpression (Heinrich *et al.*, 2003). The higher level of both mRNA

and vRNA kinetics in WSN-infected macrophages showed that the immune response exhibited by macrophages was ineffective to reduce the replication rate.

To correlate with other studies, an *in vivo* model using mice has also been conducted to compare the cytokine production upon infection of 2009 pandemic strains and H5N1 high pathogenic avian influenza virus (Woo *et al.*, 2010). They found that the cytokine response of 2009 pandemic influenza viruses were generally much less compared to that of H5N1 high pathogenic avian influenza virus infection, which has also been shown by other groups (Osterlund *et al.*, 2010; Woo *et al.*, 2010).

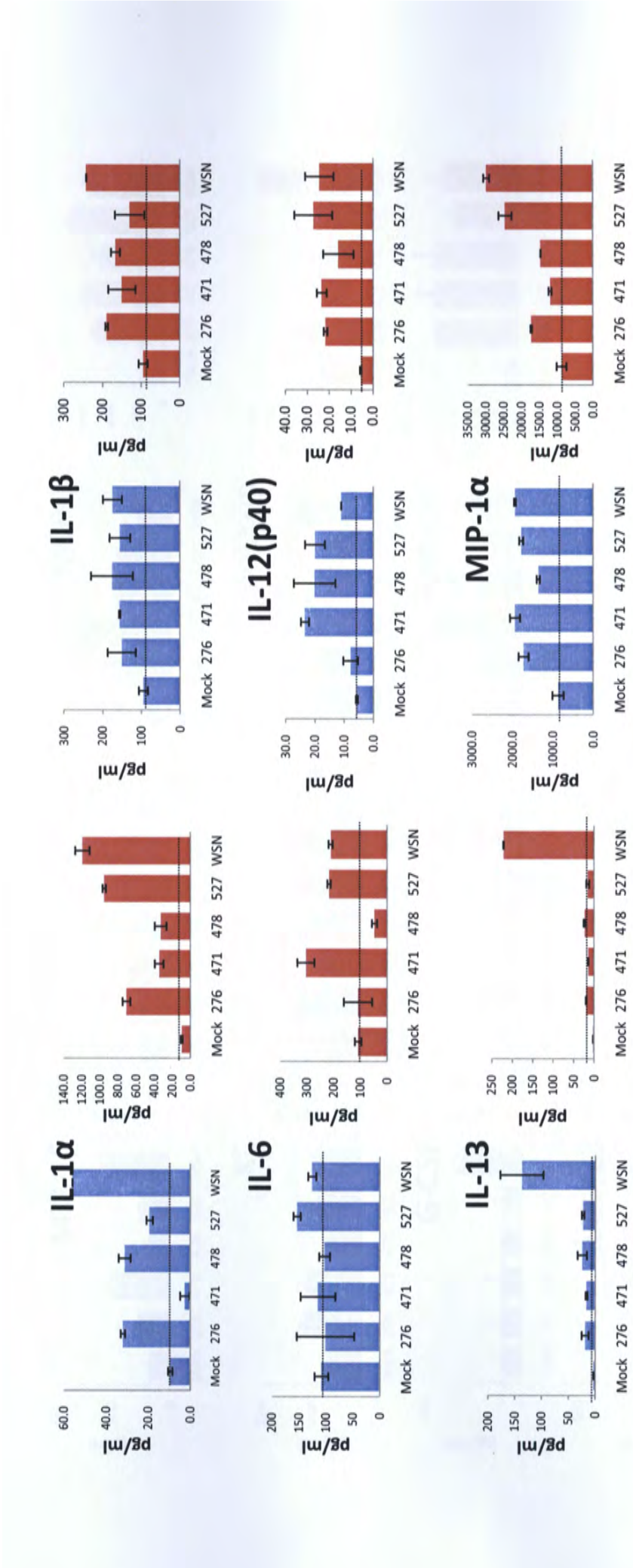


Fig 6.18 Cytokine profiling of 2009 pandemic strains-infected mouse lung macrophage for infection time of 24 hpi (■) and 48 hpi (■), with dotted line as mock baseline. The result shown above is based on two experiments with two measurements (n=4)

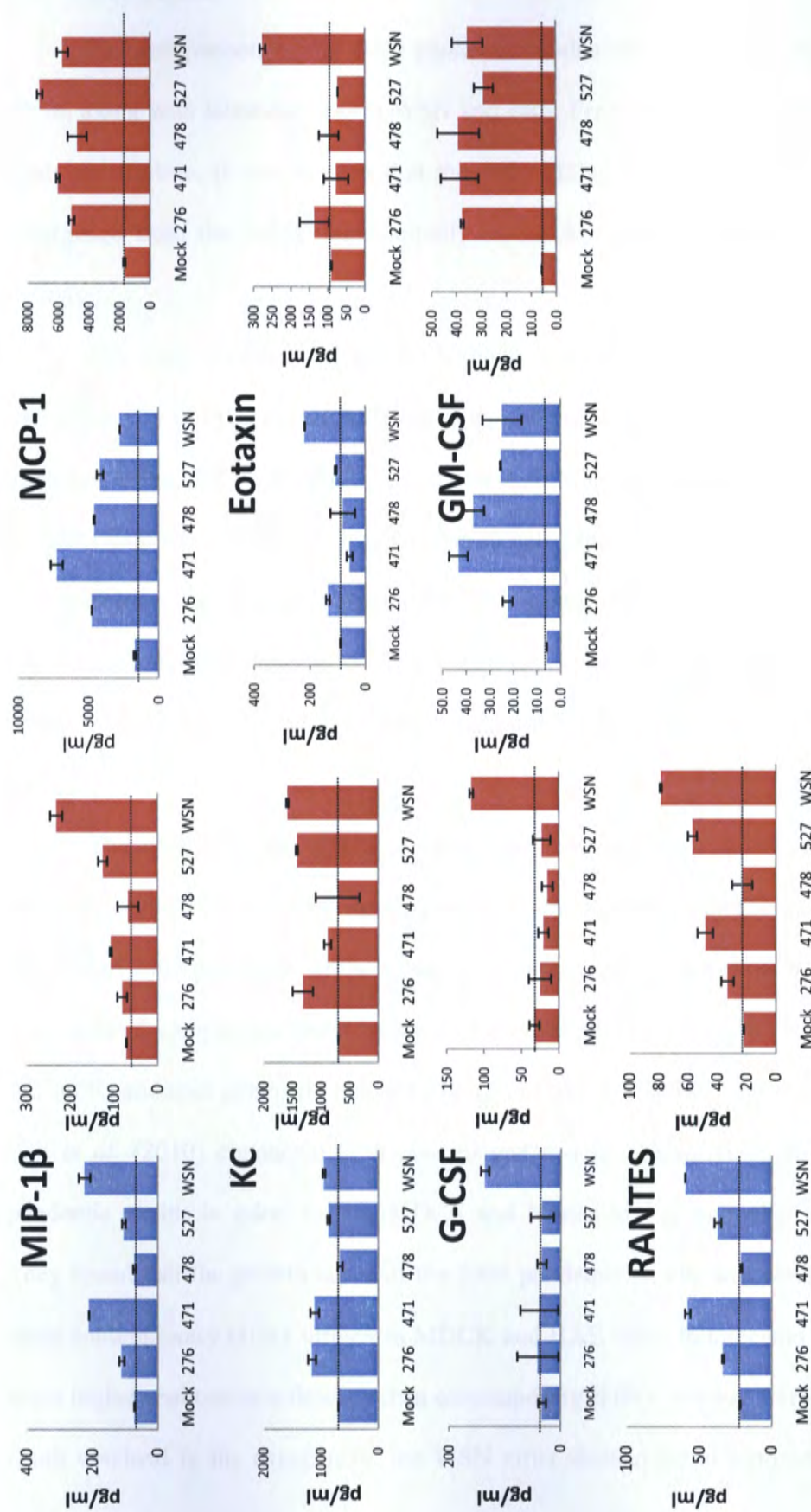


Fig 6.18 (Cont.) Cytokine profiling of 2009 pandemic strains-infected mouse lung macrophage for infection time of 24 hpi (■) and 48 hpi (■) with dotted line as mock baseline.

6.8 Conclusion

The comparison of the 2009 pandemic strains was made with the California strain, along with laboratory strain WSN and PR8. From the sequence analysis in the phylogenetic tree, it can be seen that the 2009 H1N1 isolates have not shown any divergence from the strain found initially in the American continent, and the other regions.

The virus kinetic analysis also showed that the 2009 pandemic strains grew less efficiently in MDCK and A549 cells, and only comparable to WSN in CEF cells, as shown in the qRT-PCR result. This shows that the 2009 pandemic strains were able to infect canine-, chicken- and human-based cell lines. From the comparison of the three cell lines, the pandemic strains showed highest virus yield in the chicken-based cell lines, from the amount of the copy numbers generated. This might be due to the origin of PB2, PA, NA and M gene segments which came originally from avian lineage.

The qRT-PCR on several antiviral response genes in A549 indicates that generally both WSN and PR8 induced much lower upregulation of antiviral response genes than 2009 pandemic strains isolates. However, the qPCR results in MDCK and CEF showed comparable result, with the exception of PR8. It can be concluded that the 2009 pandemic strains do not replicate efficiently in MDCK, CEF and A549 cells. Itoh *et al.* (2010) conducted both *in-vitro* and *in-vivo* characterization of the 2009 pandemic strains in mice, ferrets, MDCK and human airway epithelial (HAE) cells. They found that the growth curve of the 2009 pandemic strains was comparable with other contemporary H1N1 viruses in MDCK and HAE cells. In mice and ferrets, they show higher replication efficiency than contemporary H1N1 viruses. To relate with the result obtained in the experiment, the WSN virus showed better replication than the

2009 pandemic strains, from the higher copy number of vRNA and mRNA generated in WSN strain. This is due to the adaptive nature of the WSN strain in mouse cells, hence the result showed higher replication in mouse lung macrophages.

In mouse lung macrophage, the 2009 pandemic strains showed much lower replication rate compared to WSN strain. However, the WSN strain showed higher immunological response compared to the 2009 H1N1 swine influenza virus isolates both in qRT-PCR and cytokine profiling. The 2009 pandemic strains generally induced lower expression of cytokines than WSN strain, notably IL-1 α , IL-13, MIP-1 β , Eotaxin, G-CSF and RANTES, while only IL-12(p40) was higher in the 2009 pandemic strains. Woo *et al.* (2010) conducted cytokine profiling on the the 2009 pandemic to compare H1N1 swine influenza virus, H5N1 and several H1N1 seasonal influenza virus strains, and they found that the 2009 pandemic strains induced proinflammatory cytokines (IL-2, IL-6, MIP-1 α , MIP-1 β , RANTES, and MCP-1) to be secreted in similar level with the H1N1 seasonal influenza virus, which is shown to have lower replication rate (Itoh *et al.*, 2010). To relate with the result obtained in this experiment, the cytokine profiling shows that generally the 2009 pandemic strains secreted lower cytokines than WSN strain, which has higher replication rate. It can be concluded that higher immune response in lung macrophages in WSN strains does not necessary to inhibit viral replication.

Chapter Seven. Conclusion

Based on the sequence analysis, the isolate A/Duck/Malaysia/01 (H9N2) is shown to be most similar with Asian origin, with the exception of NP and NS genes, which are more similar with European origin. This finding also confirms the dominance of H9N2 in Asian continent (Guo *et al.*, 2000), with some have the ability to infect humans (Matrosovich *et al.*, 2001). This finding is consistent in both sequence similarity and phylogenetic tree clustering. The A/Duck/Malaysia/01 (H9N2) isolate also contains amantadine resistance signature in the M2 protein, which is already prevalent (Shiraishi *et al.*, 2003; Cheng *et al.*, 2010). However, there is no indication of oseltamivir resistance signature. It has been documented that oseltamivir is effective against H9N2 infection (Leneva *et al.*, 2000; Govorkova *et al.*, 2001). Until recently, there is no evidence of development in oseltamivir resistant H9N2 strain. In term of pathogenicity, the A/Duck/Malaysia/01 (H9N2) HA protein isolate possesses single basic cleavage site, which classifies it as LPAI. All host sequence signature of A/Duck/Malaysia/01 (H9N2) belongs to avian signature. The human isolates of H9N2 possess some human signatures in their proteins, except PB1 and M1, which confer to the ability to adapt to human host, although inefficiently (Uyeki *et al.*, 2002; Butt *et al.*, 2005).

A/Duck/Malaysia/01 (H9N2) has been shown to replicate poorly in MDCK, and A549 cells, but efficiently in CEF cells. It has been demonstrated that both human and avian influenza viruses grow well in MDCK cell lines (Murakami *et al.*, 1988) and immortalized chick embryo cell lines (Smith *et al.*, 2008). These findings are also similarly observed in our experiment by the ability to replicate, although with different rate of replication. Recently, it has been found that H9N2 lineage G1 replicated

efficiently in A549 cells due to its H5N1-like internal genes (Lee *et al.*, 2010). On the other hand, the H9N2 lineage Y280, and H9N2 lineage Y439 replicated poorly in A549 cells (Lee *et al.*, 2010). The A/Duck/Malaysia/01 (H9N2) belongs to Y439 lineage, and it is expected to replicate inefficiently in non-avian cell lines.

Gene expression profiling using cDNA microarrays and qRT-PCR shows that the H9N2 upregulated more host immune response in CEF cells than in MDCK and A549 cells. It has been reported that the more virulent strains of influenza virus in suitable host had better ability to suppress interferon and antiviral responses (Wang *et al.*, 2000; Solorzano *et al.*, 2005; Cauthen *et al.*, 2007; Hayman *et al.*, 2007; Kochs *et al.*, 2009; Li *et al.*, 2010). Based on these findings, it can be concluded that A/Duck/Malaysia/01 (H9N2) is less virulent in MDCK and A549 cells. Further, Wang *et al.*, 2008 compared the gene expression profiling of human influenza viruses and highly pathogenic influenza viruses in mice. They found that the highly pathogenic strain showed considerably higher expression of cytokine involving in activation of T-cells and macrophages. Consistently, in our experiment, A/WSN/33 (H1N1) strain, which is shown to be highly virulent in mice (Aronsson *et al.*, 2003; Abed *et al.*, 2010), induced generally higher cytokine responses than A/Duck/Malaysia/01 (H9N2).

Based on the experiments, it is shown that A/Duck/Malaysia/01 (H9N2) did not replicate efficiently in human, which may also mean that A/Duck/Malaysia/01 (H9N2) is not likely to pose problem in human health. However, mutations and reassortments with other strains may alter the pathogenicity and infectivity of this strain in human, as occurred in H9N2 strains in China (Guo *et al.*, 1999; Peiris *et al.*, 1999), or with internal genes from H5N1 LPAI (Butt *et al.*, 2005; Wang *et al.*, 2007).

All of the 2009 pandemic strains collected in Singapore showed very high similarity in all segments, which confirms the finding by Nelson *et al.* (2009). They

found that the nucleotide sequence of the 2009 pandemic strains isolates started to diverge into 7 clades, but overall, the sequences are still very similar. The HA and NA gene in 2009 pandemic strains is shown to be the most unstable and more prone to changes (Lu *et al.*, 2009). However, in our experiment, >99% genes are similar in sequences, and we did not observe any higher dissimilarities in both HA and NA genes. To compare the replication and transcription rate, the 2009 pandemic strains generally had less growth in all cell lines used as compared to laboratory strain A/WSN/33(H1N1) and A/PR/8/34 (H1N1). An experiment has been done elsewhere to compare the replication of the 2009 pandemic strains, seasonal influenza virus and H5N1 high pathogenic influenza virus in human lung tissues (Zhang *et al.*, 2010). It is shown that the 2009 pandemic strains was able to replicate better than seasonal influenza virus, but still slower than H5N1 high pathogenic influenza virus. It can be inferred that the triple reassortment might be beneficial to assist the better replication of 2009 pandemic strains. Further, in A549 cells lines, 2009 pandemic strains generally showed lower expression of immune response and antiviral related genes than A/WSN/33 (H1N1) and PR8, which shows that the 2009 pandemic strains induced less innate immune responses. However, there were various results observed in MDCK and CEF cells. It has been shown that the cultures of human cells did not show any significant differences upon 2009 pandemic strains and seasonal influenza strains infection (Chan *et al.*, 2010). In cytokine profiling, the 2009 pandemic strains generally showed weak cytokine profiling compared to A/WSN/33 (H1N1) strain. This finding has also been demonstrated elsewhere (Osterlund *et al.*, 2010; Woo *et al.*, 2010). To further prove this, an *in vivo* model using mice has also been conducted to compare the cytokine production upon infection of 2009 pandemic strains and H5N1 high pathogenic avian influenza virus (Woo *et al.*, 2010). Based on the result, the

cytokine response of 2009 pandemic strains is generally much less compared to that of H5N1 high pathogenic avian influenza virus infection.

References

- Abdel-Haq NM, Asmar BI. 2011. Novel swine--origin influenza A: the 2009 H1N1 influenza virus. *Indian J Pediatr* 78:74-80.
- Abed Y, Simon P, Boivin G. 2010. Prophylactic activity of intramuscular peramivir in mice infected with a recombinant influenza A/WSN/33 (H1N1) virus containing the H274Y neuraminidase mutation. *Antimicrob Agents Chemother* 54:2819-2822.
- Abusugra IA, Linné T, Klingeborn B. 1987. The provenance of the Swedish swine influenza H1N1 virus of 1983. 1987. *Zentralbl Veterinarmed B*. 34:566-72.
- Adachi M, Matsukura S, Tokunaga H, Kokubu F. 1997. Expression of cytokines on human bronchial epithelial cells induced by influenza virus A. *Int Arch Allergy Immunol*. 113(1-3):307-11.
- Air G, Els M, Brown L, Laver W, Webster R. 1985. Location of antigenic sites on the three-dimensional structure of the Influenza N2 virus neuraminidase. *Virology* 145:237-248.
- Air G, Laver W, Webster R, Els M, Luo M. 1989. Antibody recognition of the influenza virus neuraminidase. *Cold Spring Harb. Symp. Quant. Biol.* 54:247-255.
- Air GM, Webster RG, Colman PM, Laver WG. 1987. Distribution of sequence differences in influenza N9 neuraminidase of tern and whale viruses and crystallization of the whale neuraminidase complexed with antibodies. *Virology*. 160(2):346-54.
- Akarsu H, Burmeister WP, Petosa C, Petit I, Muller CW, Ruigrok RW & Baudin F. 2003. Crystal structure of the M1 protein-binding domain of the influenza A virus nuclear export protein (NEP/NS2). *EMBO J* 22:4646-4655.
- Akkina RK, Chambers TM, Londo DR, Nayak DP. 1987. Intracellular localization of the viral polymerase proteins in cells infected with influenza virus and cells expressing PB1 protein from cloned cDNA. *J Virol*. 61(7):2217-24.
- Akkina RK, Richardson JC, Aguilera MC, Yang CM., 1991. Heterogeneous forms of polymerase proteins exist in influenza A virus-infected cells. *Virus Res*. 19(1):17-30.
- Alberts AW, Lovastatin and simvastatin--inhibitors of HMG CoA reductase and cholesterol biosynthesis. 1990. *Cardiology* 77 Suppl 4: 14-21.
- Albo C, Valencia A, Portela A. 1995. Identification of an RNA binding region within the N-terminal third of the influenza A virus nucleoprotein. *J. Virol*. 69:3799-3806
- Alexander DJ. Highly pathogenic avian influenza. 2000. In: World Organisation for Animal Health OIE, ed. *OIE Manual of Standards for Diagnostic Tests and Vaccines*. Paris: 212-220.
- Alexopoulou L, Holt AC, Medzhitov R, Flavell RA. 2001. Recognition of double-stranded RNA and activation of NF-kappaB by Toll-like receptor 3. *Nature*. 413(6857):732-8.
- Aronsson F, Robertson B, Ljunggren HG, Kristensson K. 2003. Invasion and persistence of the neuroadapted influenza virus A/WSN/33 in the mouse olfactory system. *Viral Immunol* 16:415-423.
- Arzt S, Baudin F, Barge A, Timmins P, Burmeister WP, Ruigrok RW. 2001. Combined results from solution studies on intact influenza virus M1 protein and from a new crystal form of its N-terminal domain show that M1 is an elongated monomer. *Virology*. 279(2):439-46.
- Avalos RT, Zhong Y, Nayak DP. 1998. Association of Influenza Virus NP and M1 Proteins with Cellular Cytoskeletal Elements in Influenza Virus-Infected Cells, *J. Virol* 71(4):2947-2958
- Baggiolini M. 1998. Chemokines and leukocyte traffic. *Nature*. 392(6676):565-8.

- Banet-Noach C, Panshin A, Golender N, Simanov L, Rozenblut E, Pokamunski S, Pirak M, Tendler Y, García M, Gelman B, Pasternak R, Perk S. 2007. Genetic analysis of nonstructural genes (NS1 and NS2) of H9N2 and H5N1 viruses recently isolated in Israel. *Virus Genes*.(2):157-68.
- Barbey-Martin C, Gigant B, Bizebard T, Calder LJ, Wharton SA, Skehel JJ, Knossow M. 2002. An antibody that prevents the hemagglutinin low pH fusogenic transition. *Virology* 294:70-74.
- Barman S, Adhikary L, Chakrabarti AK, Bernas C, Kawaoka Y, Nayak DP. 2004. Role of transmembrane domain and cytoplasmic tail amino acid sequences of influenza A virus neuraminidase in raft association and virus budding. *J Virol* 78:5258-5269.
- Barman S, Ali A, Hui EK, Adhikary L, Nayak DP. 2001. Transport of viral proteins to the apical membranes and interaction of matrix protein with glycoproteins in the assembly of influenza viruses. *Virus Res.* 77(1):61-9.
- Barman S, Nayak DP. 2000. Analysis of the transmembrane domain of influenza virus neuraminidase, a type II transmembrane glycoprotein, for apical sorting and raft association. *J Virol.* 74(14):6538-45.
- Barman S, Nayak DP. 2007. Lipid raft disruption by cholesterol depletion enhances influenza A virus budding from MDCK cells. *J Virol* 81:12169-12178.
- Barrett T, Wolstenholme AJ, Mahy BW. 1979. Transcription and replication of influenza virus RNA. *Virology* 98(1):211-25.
- Baskin CR, García-Sastre A, Tumpey TM, Bielefeldt-Ohmann H, Carter VS, Nistal-Villán E, Katze MG. 2004. Integration of clinical data, pathology, and cDNA microarrays in influenza virus-infected pigtailed macaques (*Macaca nemestrina*). *J Virol.* 78(19):10420-32.
- Baudin F, Bach C, Cusack S, Ruigrok RW. 1994. Structure of influenza virus RNP. I. Influenza virus nucleoprotein melts secondary structure in panhandle RNA and exposes the bases to the solvent, *EMBO J.* 13(13):3158-65
- Baudin F, Petit I, Weissenhorn W, Ruigrok RW. 2001. In vitro dissection of the membrane and RNP binding activities of influenza virus M1 protein. *Virology* 281(1):102-8.
- Bean WJ, Cox NJ, Kendal AP. 1980. Recombination of human influenza A viruses in nature. *Nature* 1980 284:638-40.
- Beaton AR, Krug RM. 1981. Selected host cell capped RNA fragments prime influenza viral RNA transcription in vivo. *Nucleic Acids Res* 9(17):4423-4436
- Beaton AR, Krug RM. 1986. Transcription antitermination during influenza viral template RNA synthesis requires the nucleocapsid protein and the absence of a 5' capped end. *Proc Natl Acad Sci U S A.* 83(17):6282-6.
- Beaven SW. 2006. Tontonoz P. Nuclear receptors in lipid metabolism: targeting the heart of dyslipidemia. *Annu Rev Med* 57: 313-329.
- Bender A, Amann U, Jäger R, Nain M, Gerns D. 1993. Effect of granulocyte/macrophage colony-stimulating factor on human monocytes infected with influenza A virus. Enhancement of virus replication, cytokine release, and cytotoxicity. *J Immunol.* 151(10):5416-24.
- Biddison WE, Doherty PC, Webster RG. 1977. Antibody to influenza virus matrix protein detects a common antigen on the surface of cells infected with type A influenza viruses. *J Exp Med.* 146(3):690-7.
- Bikour MH, Frost EH, Deslandes S, Talbot B, Elazhary Y. 1995. Persistence of a 1930 swine influenza A (H1N1) virus in Quebec. *J Gen Virol.* 76 (Pt 10):2539-47.
- Bilsel P, Castrucci MR, Kawaoka Y. 1993. Mutations in the cytoplasmic tail of influenza A virus neuraminidase affect incorporation into virions. *J Virol* 67:6762-6767.
- Biswas S, Yin SR, Blank PS, Zimmerberg J. 2008. Cholesterol promotes hemifusion and pore widening in membrane fusion induced by influenza hemagglutinin. *J Gen Physiol* 131:503-513.

- Biswas SK, Boutz PL, Nayak DP. 1998. Influenza virus nucleoprotein interacts with influenza virus polymerase proteins. *J Virol.* 72(7):5493-501.
- Biswas SK, Nayak DP. 1994. Mutational analysis of the conserved motifs of influenza A virus polymerase basic protein 1. *J Virol.* 68(3):1819-26.
- Biswas SK, Nayak DP. 1996. Influenza virus polymerase basic protein 1 interacts with influenza virus polymerase basic protein 2 at multiple sites. *J Virol.* 70(10):6716-22
- Biswas SK., Boutz PL, Nayak DP. 1998. Influenza virus nucleoprotein interacts with influenza virus polymerase proteins. *J. Virol.* 72:5493-5501
- Blaas D, Patzelt E, Kuechler E. 1982. Identification of the cap binding protein of influenza virus. *Nucleic Acids Res.* 10(15):4803-12.
- Blok J, Air GM. 1982. Variation in the membrane-insertion and "stalk" sequences in eight subtypes of influenza type A virus neuraminidase. *Biochemistry* 21:4001-4007.
- Boudinot P, Riffault S, Salhi S, Carrat C, Sedlik C, Mahmoudi N, Charley B, Benmansour A. 2000. Vesicular stomatitis virus and pseudorabies virus induce a *vig1/cig5* homologue in mouse dendritic cells via different pathways. *J Gen Virol.* 81(Pt 11):2675-82.
- Boulon S, Akarsu H, Ruigrok RW, Baudin F. 2007. Nuclear traffic of influenza virus proteins and ribonucleoprotein complexes. *Virus Res.* 124(1-2):12-21.
- Braam J, Ulmanen I, Krug RM. 1983. Molecular model of a eucaryotic transcription complex: functions and movements of influenza P proteins during capped RNA-primed transcription. *Cell.* 34(2):609-18.
- Brown EG. 1990. Increased virulence of a mouse-adapted variant of influenza A/FM/1/47 virus is controlled by mutations in genome segments 4, 5, 7, and 8. *J Virol.* 64(9):4523-33.
- Brown F, Redfern PH. 1976. Studies on the mechanism of action of amantadine. *Br J Pharmacol* 58:561-567.
- Brown IH. 2000. The epidemiology and evolution of influenza viruses in pigs. *Vet Microbiol.* 74(1-2):29-46.
- Brown MS, Goldstein JL. 1997. The SREBP pathway: regulation of cholesterol metabolism by proteolysis of a membrane-bound transcription factor. *Cell* 89: 331-340.
- Brydon EW, Morris SJ, Sweet C. 2005. Role of apoptosis and cytokines in influenza virus morbidity, *FEMS Microbiol Rev.* 29(4):837-50
- Bukrinskaya AG, Vorkunova NK, Komilayeva GV, Narmanbetova RA, Vorkunova GK.. 1982. Influenza virus uncoating in infected cells and effect of rimantadine. 60(Pt 1):49-59.
- Bullough PA, Hughson FM, Skehel JJ, Wiley DC. 1994. Structure of influenza haemagglutinin at the pH of membrane fusion. *Nature* 371:37-43.
- Bullough PA, Hughson FM, Skehel JJ, Wiley DC. Structure of influenza haemagglutinin at the pH of membrane fusion. *Nature.* 1994 Sep 1;371(6492):37-43.
- Bush RM, Bender CA, Subbarao K, Cox NJ, Fitch WM. 1999. Predicting the evolution of human influenza A. *Science.* 286(5446):1921-5.
- Butt KM, Smith GJ, Chen H, Zhang LJ, Leung YH, Xu KM, Lim W, Webster RG, Yuen KY, Peiris JS, Guan Y. 2005. Human infection with an avian H9N2 influenza A virus in Hong Kong in 2003. *J Clin Microbiol.* 43(11):5760-7.
- Butt KM, Smith GJ, Chen H, Zhang LJ, Leung YH, Xu KM, Lim W, Webster RG, Yuen KY, Peiris JS, Guan Y. 2005. Human infection with an avian H9N2 influenza A virus in Hong Kong in 2003. *J Clin Microbiol* 43:5760-5767.

- Cady SD, Hong M. 2008. Amantadine-induced conformational and dynamical changes of the influenza M2 transmembrane proton channel. *Proc Natl Acad Sci U S A* 105:1483-1488.
- Cady SD, Schmidt-Rohr K, Wang J, Soto CS, Degrado WF, Hong M. 2010. Structure of the amantadine binding site of influenza M2 proton channels in lipid bilayers. *Nature* 463:689-692.
- Cameron CM, Cameron MJ, Bermejo-Martin JF, Ran L, Xu L, Turner PV, Ran R, Danesh A, Fang Y, Chan PK, Mytle N, Sullivan TJ, Collins TL, Johnson MG, Medina JC, Rowe T, Kelvin DJ. 2008. Gene expression analysis of host innate immune responses during Lethal H5N1 infection in ferrets. *J Virol*. 82(22):11308-17.
- Capua I, Alexander DJ. 2004. Avian influenza: recent developments. *Avian Pathol* 33:393-404
- Carr CM, Chaudhry C, Kim PS. 1997. Influenza hemagglutinin is spring-loaded by a metastable native conformation. *Proc Natl Acad Sci U S A* 94:14306-14313.
- Castrucci MR, Donatelli I, Sidoli L, Barigazzi G, Kawaoka Y, Webster RG. 1993. Genetic reassortment between avian and human influenza A viruses in Italian pigs. *Virology*.193(1):503-6.
- Castrucci MR, Kawaoka Y. 1993. Biologic importance of neuraminidase stalk length in influenza A virus, *J. Virol*. 67(2):759-764
- Caton AJ, Brownlee GG, Yewdell JW, Gerhard W. 1982. The antigenic structure of the influenza virus A/PR/8/34 hemagglutinin (H1 subtype). *Cell*. 31(2 Pt 1):417-27.
- Caton AJ, Brownlee GG, Yewdell JW, Gerhard W. 1982. The antigenic structure of the influenza virus A/PR/8/34 hemagglutinin (H1 subtype). *Cell* 31:417-427.
- Cauthen AN, Swayne DE, Sekellick MJ, Marcus PI, Suarez DL. 2007. Amelioration of influenza virus pathogenesis in chickens attributed to the enhanced interferon-inducing capacity of a virus with a truncated NS1 gene. *J Virol* 81:1838-1847.
- CDC .2008.Toward a Unified Nomenclature System for Highly Pathogenic Avian Influenza Virus (H5N1), http://www.who.int/csr/disease/avian_influenza/guidelines/nomenclature/en/index.html, accessed at 1st March 2010
- CDC .2010. <http://www.cdc.gov/flu/2010/keyfacts.htm>, Accessed at 15 Feb 2011.
- CDC.2009. <http://www.cdc.gov/flu/2009/keyfacts.htm>, Accessed at 15 Dec 2009.
- Chambers TM, Hinshaw VS, Kawaoka Y, Easterday BC, Webster RG. 1991. Influenza viral infection of swine in the United States 1988-1989. *Arch Virol*. 116(1-4):261-5.
- Chan MC, Chan RW, Yu WC, Ho CC, Yuen KM, Fong JH, Tang LL, Lai WW, Lo AC, Chui WH, Sihoe AD, Kwong DL, Wong DS, Tsao GS, Poon LL, Guan Y, Nicholls JM, Peiris JS. 2010. Tropism and innate host responses of the 2009 pandemic H1N1 influenza virus in ex vivo and in vitro cultures of human conjunctiva and respiratory tract. *Am J Pathol* 176:1828-1840.
- Chang TY, Limanek JS. 1980. Regulation of cytosolic acetoacetyl coenzyme A thiolase, 3-hydroxy-3-methylglutaryl coenzyme A synthase, 3-hydroxy-3-methylglutaryl coenzyme A reductase, and mevalonate kinase by low density lipoprotein and by 25-hydroxycholesterol in Chinese hamster ovary cells. *J Biol Chem* (255):7787-7795.
- Chatterjee PK, Eng CH, Kielian M. 2002. Novel mutations that control the sphingolipid and cholesterol dependence of the Semliki Forest virus fusion protein. *J Virol* (76):12712-12722.
- Chatterjee PK, Vashishtha M, Kielian M. 2000. Biochemical consequences of a mutation that controls the cholesterol dependence of Semliki Forest virus fusion. *J Virol* (74):1623-1631.

- Chen BJ, Takeda M, Lamb RA. 2005. Influenza virus hemagglutinin (H3 subtype) requires palmitoylation of its cytoplasmic tail for assembly: M1 proteins of two subtypes differ in their ability to support assembly. *J Virol.* 79(21):13673-84.
- Chen GW, Chang SC, Mok CK, Lo YL, Kung YN, Huang JH, Shih YH, Wang JY, Chiang C, Chen CJ, Shih SR. 2006. Genomic signatures of human versus avian influenza A viruses. *Emerg Infect Dis.* 12(9):1353-60.
- Chen H, Deng G, Li Z, Tian G, Li Y, Jiao P, Zhang L, Liu Z, Webster RG, Yu K.. 2004. The evolution of H5N1 influenza viruses in ducks in southern China. *Proc Natl Acad Sci U S A.* 101(28):10452-7.
- Chen J, Skehel JJ, Wiley DC. 1999. N- and C-terminal residues combine in the fusion-pH influenza hemagglutinin HA(2) subunit to form an N cap that terminates the triple-stranded coiled coil. *Proc Natl Acad Sci U S A* 96:8967-8972.
- Chen W, Calvo PA, Malide D, Gibbs J, Schubert U, Bacik I, Basta S, O'Neill R, Schickli J, Palese P, Henklein P, Bennis JR, Yewdell JW. 2001. A novel influenza A virus mitochondrial protein that induces cell death. *Nat Med.* 2001 7(12):1286-8.
- Chen, Z, Li Y, Krug RM. 1999. Influenza A virus NS1 protein targets poly(A)-binding protein II of the cellular 3'-end processing machinery, *EMBO J.* 18(8):2273-83
- Cheng PK, To AP, Leung TW, Leung PC, Lee CW, Lim WW. 2010. Oseltamivir- and amantadine-resistant influenza virus A (H1N1). *Emerg Infect Dis* 16:155-156.
- Cheung CY, Poon LL, Lau AS, Luk W, Lau YL, Shortridge KF, Gordon S, Guan Y, Peiris JS. 2002. Induction of proinflammatory cytokines in human macrophages by influenza A (H5N1) viruses: a mechanism for the unusual severity of human disease? *Lancet* 360(9348):1831-7.
- Chin KC, Cresswell P. 2001. Viperin (cig5), an IFN-inducible antiviral protein directly induced by human cytomegalovirus. *Proc Natl Acad Sci U S A.* 98(26):15125-30.
- Choi AM, Knobil K, Otterbein SL, Eastman DA, Jacoby DB. 1996. Oxidant stress responses in influenza virus pneumonia: gene expression and transcription factor activation. *Am J Physiol.* 271(3 Pt 1):L383-91.
- Chu CM, Dawson IM, Eford WJ. 1949. Filamentous forms associated with newly isolated influenza virus. *Lancet.* 1(6554):602.
- Chu WM., Ostertag D, Li ZW., Chang L, Chen Y, Hu Y, Williams B, Perrault J, Karin M, 1999. JNK2 and IKKbeta are required for activating the innate response to viral infection. *Immunity* 11, 721-731.
- Claas EC, Kawaoka Y, de Jong JC, Masurel N, Webster RG. 1994. Infection of children with avian-human reassortant influenza virus from pigs in Europe. *Virology* 204:453-457.
- Cole JL, Carroll SS, Kuo LC. 1996. Stoichiometry of 2',5'-oligoadenylate-induced dimerization of ribonuclease L. A sedimentation equilibrium study. *J Biol Chem.* 271(8):3979-81.
- Colman PM, Varghese JN, Laver WG. 1983. Structure of the catalytic and antigenic sites in influenza virus neuraminidase. *Nature* 303:41-44.
- Compans RW, Content J, Duesberg PH. 1972. Structure of the ribonucleoprotein of influenza virus. *J Virol* 10(4):795-800.
- Compans RW, Meier-Ewert H, Palese P. 1974. Assembly of lipid-containing viruses. *J Supramol Struct* 2(2-4):496-511.
- Conenello GM, Zamarin D, Perrone LA, Tumpey T, Palese P. 2007. A single mutation in the PB1-F2 of H5N1 (HK/97) and 1918 influenza A viruses contributes to increased virulence. *PLoS Pathog.* 3(10):1414-21
- Conner SD, Schmid SL. 2003. Regulated portals of entry into the cell. *422(6927):37-44*

- Couceiro JN, Paulson JC, Baum LG. 1993. Influenza virus strains selectively recognize sialyloligosaccharides on human respiratory epithelium, the role of the host cell in selection of hemagglutinin receptor specificity, *Virus Res.* 29(2):155-65
- Cox NJ, Subbarao K.. 2000. Global epidemiology of influenza: Past and present. *Annu. Rev. Med.* 51: 407-421
- Cros JF, García-Sastre A, Palese P. 2005. An unconventional NLS is critical for the nuclear import of the influenza A virus nucleoprotein and ribonucleoprotein. *Traffic.* 6(3):205-13.
- Cros JF, Palese P. 2003. Trafficking of viral genomic RNA into and out of the nucleus: influenza, Thogoto and Borna disease viruses. *Virus Res* 95(1-2):3-12
- Cross KJ, Burleigh LM, Steinhauer, DA. 2001. Mechanisms of cell entry by influenza virus. *Expert Rev Mol Med.* 3:1-18
- Daniels RS, Downie JC, Hay AJ, Knossow M, Skehel JJ, Wang ML, Wiley DC. 1985. Fusion mutants of the influenza virus hemagglutinin glycoprotein. *Cell.* 40(2):431-9.
- Darnell JE Jr, Kerr IM, Stark GR. 1994. Jak-STAT pathways and transcriptional activation in response to IFNs and other extracellular signaling proteins. *Science* 264(5164):1415-21.
- Das KP, Mallick BB, Da, K. 1981. Note on the prevalence of influenza antibodies in swine. *Indian J. Anim. Sci.* 51:907-908.
- Davenport FM, Dowdle WR, St. Groth S, Fukumi F, Kilbourne FM, Schild ED, Schulman DF, Sohler JL, Soloviev R, Tumova VD, Webster RG, Zakstel'skaja L, Ja Zdanov WM. 1972. A Revised System of Influenza Virus Nomenclature
- de la Luna, S., Fortes, P., Beloso, A. & Ortin, J. 1995. Influenza virus NS1 protein enhances the rate of translation initiation of viral mRNAs. *J Virol* 69:2427-2433.
- Decker A. 2006. Cytokines. <http://users.ipfw.edu/Blumenth/Immunology/Cytokines.htm>.
- Deng T, Engelhardt OG, Thomas B, Akoulitchiev AV, Brownlee GG, Fodor E. 2006. Role of Ran Binding Protein 5 in Nuclear Import and Assembly of the Influenza Virus RNA Polymerase Complex, *J. Virol* 80(24):11911-11919
- Deng T, Vreede FT, Brownlee GG. 2006. Different de novo initiation strategies are used by influenza virus RNA polymerase on its cRNA and viral RNA promoters during viral RNA replication. *J Virol* 80(5):2337-2348.
- Desselberger U, Nakajima K, Alfino P, Pedersen FS, Haseltine WA, Hannoun C, Palese P. 1978. Biochemical evidence that "new" influenza virus strains in nature may arise by recombination (reassortment). *Proc Natl Acad Sci U S A.* 75(7):3341-5.
- Desselberger U, Racaniello VR, Zazra JJ, Palese P. 1980. The 3' and 5'-terminal sequences of influenza A, B and C virus RNA segments are highly conserved and show partial inverted complementarity. *Gene* 8:315-328.
- Deveraux QL, Reed JC. 1999. IAP family proteins--suppressors of apoptosis. *Genes Dev.* 13(3):239-52.
- Dias A, Bouvier D, Crépin T, McCarthy AA, Hart DJ, Baudin F, Cusack S, Ruigrok RW. 2009. The cap-snatching endonuclease of influenza virus polymerase resides in the PA subunit. *Nature.* 458(7240):914-8.
- Diaz-Mitoma F, Alvarez-Maya I, Dabrowski A, Jaffey J, Frost R, Aucoin S, Kryworuchko M, Lapner M, Tadesse H, Giulivi A. 2004. Transcriptional analysis of human peripheral blood mononuclear cells after influenza immunization. *J Clin Virol.* 31(2):100-12.
- Dinareello CA. 1994. The interleukin-1 family: 10 years of discovery. *FASEB J.* 8(15):1314-25.
- Dittmann J, Stertz S, Grimm D, Steel J, García-Sastre A, Haller O, Kochs G. 2008. Influenza A virus strains differ in sensitivity to the antiviral action of Mx-GTPase. *J Virol.* 82(7):3624-31.

- Donelan NR, Basler CF, García-Sastre A. 2003. A recombinant influenza A virus expressing an RNA-binding-defective NS1 protein induces high levels of beta interferon and is attenuated in mice. *J Virol*. 77(24):13257-66.
- Dong B, Silverman RH. 1995. 2-5A-dependent RNase molecules dimerize during activation by 2-5A. *J Biol Chem*. 270(8):4133-7.
- Dunham EJ, Dugan VG, Kaser EK, Perkins SE, Brown IH, Holmes EC, Taubenberger JK. 2009. Different evolutionary trajectories of European avian-like and classical swine H1N1 influenza A viruses. *J Virol* 83:5485-5494.
- Easterday BC, 1980. Animals in the influenza world. *Philos. Trans. R. Soc., London* 12:433-437
- Ehrhardt C, Wolff T, Pleschka S, Planz O, Beermann W, Bode JG, Schmolke M, Ludwig S. 2007. Apoptosis and pathogenesis of avian influenza A (H5N1) virus in humans, *Emerg Infect Dis*. 13(5):708-12
- Eisen MB, Sabesan S, Skehel JJ, Wiley DC. 1997. Binding of the influenza A virus to cell-surface receptors: structures of five hemagglutinin-sialyloligosaccharide complexes determined by X-ray crystallography. *Virology*. 232(1):19-31.
- Elbers AR, Bouma A, Stegeman JA. 2002. Quantitative assessment of clinical signs for the detection of classical swine fever outbreaks during an epidemic, *Vet. Microbiol*. 85:323-332.
- Elder KT, Bye JM, Skehel JJ, Waterfield MD, Smith AE. 1979. In vitro synthesis, glycosylation, and membrane insertion of influenza virus haemagglutinin. *Virology*. 95(2):343-50.
- Ellis JS, Alvarez-Aguero A, Gregory V, Lin YP, Hay A, Zambon MC. 2003. Influenza AH1N2 viruses, United Kingdom, 2001-02 influenza season. *Emerg Infect Dis*. 9:304-310.
- Elton D, Medcalf L, Bishop K, Harrison D, and Digard P. 1999. Identification of amino acid residues of influenza virus nucleoprotein essential for RNA binding. *J. Virol*. 73:7357-7367
- Elton D, Simpson-Holley M, Archer K, Medcalf L, Hallam R, McCauley J, Digard P. 2001. Interaction of the Influenza Virus Nucleoprotein with the Cellular CRM1-Mediated nuclear Export Pathway, *J. Virol* 75(1):408-419
- Emtage JS, Catlin GH, Carey NH. 1979. Polyadenylation and reverse transcription of influenza viral RNA. *Nucleic Acids Res* 6:1221-1239.
- Enami M, Sharma G, Benham C, Palese P. 1991. An influenza virus containing nine different RNA segments. *Virology*. 185(1):291-8.
- Engelhardt OG, Smith M, Fodor E. 2005. Association of the influenza A virus RNA-dependent RNA polymerase with cellular RNA polymerase II. *J Virol*. 79(9):5812-8.
- Ertl H, Ada GL. 1981. Roles of influenza virus infectivity and glycosylation of viral antigen for recognition of target cells by cytolytic T lymphocytes. *Immunobiology* 158:239-253.
- Eskildsen S, Hartmann R, Kjeldgaard NO, Justesen J. 2002. Gene structure of the murine 2'-5'-oligoadenylate synthetase family. *Cell Mol Life Sci*. 2002 Jul;59(7):1212-22.
- Etkind PR, Krug RM. 1974. Influenza viral messenger RNA. *Virology*. 62(1):38-45.
- Falcon AM, Fortes P, Marion RM, Beloso A, Ortin J. 1999. Interaction of influenza virus NS1 protein and the human homologue of Staufen in vivo and in vitro, *Nuc. Acid. Res*. 27(11):2241-2247
- Falcon AM, Marion RM, Zurcher T, Gomez P, Portela A, Nieto A, Ortin J. 2004. Defective RNA replication and late gene expression in temperature-sensitive influenza viruses expressing deleted forms of the NS1 protein. *J Virol* 78:3880-3888.
- Fanning TG, Reid AH, Taubenberger JK. 2000. Influenza A virus neuraminidase: regions of the protein potentially involved in virus-host interactions. *Virology*. 276(2):417-23.

- Favier ML, Remesy C, Moundras C, Demigne C. 1995. Effect of cyclodextrin on plasma lipids and cholesterol metabolism in the rat. *Metabolism* 44:200-206.
- Feldmann M. 2008. Many cytokines are very useful therapeutic targets in disease. *J Clin Invest*. 118(11):3533-6.
- Fernandez-Sesma A. 2007. The influenza virus NS1 protein: inhibitor of innate and adaptive immunity. *Infect Disord Drug Targets*. 7(4):336-43.
- Flory E, Kunz M, Scheller C, Jassoy C, Stauber R, Rapp UR, Ludwig S. 2000. Influenza virus-induced NF-kappaB-dependent gene expression is mediated by overexpression of viral proteins and involves oxidative radicals and activation of IkappaB kinase. *J Biol Chem*. 275(12):8307-14.
- Floyd-Smith G, Slattey E, Lengyel P. 1981. Interferon action: RNA cleavage pattern of a (2'-5') oligoadenylate--dependent endonuclease. *Science*. 212(4498):1030-2.
- Fodor E, Mingay LJ, Crow M, Deng T, Brownlee GG. A single amino acid mutation in the PA subunit of the influenza virus RNA polymerase promotes the generation of defective interfering RNAs. *J Virol* 2003(77):5017-5020.
- Fodor E, Smith M. 2004. The PA subunit is required for efficient nuclear accumulation of the PB1 subunit of the influenza A virus RNA polymerase complex. *J Virol* 78:9144-9153.
- Fornek JL, Korth MJ, Katze MG. 2007. Use of functional genomics to understand influenza-host interactions. *Adv Virus Res*. 70:81-100
- Fouchier RA, Munster V, Wallensten A, Bestebroer TM, Herfst S, Smith D, Rimmelzwaan GF, Olsen B, Osterhaus AD. 2005. Characterization of a novel influenza A virus hemagglutinin subtype (H16) obtained from black-headed gulls, *J Virol*. 79(5):2814-22
- Fouchier RA, Schneeberger PM, Rozendaal FW, Broekman JM, Kemink SA, Munster V, Kuiken T, Rimmelzwaan GF, Schutten M, Van Doornum GJ, Koch G, Bosman A, Koopmans M, Osterhaus AD. 2004. Avian influenza A virus (H7N7) associated with human conjunctivitis and a fatal case of acute respiratory distress syndrome. *Proc Natl Acad Sci U S A*. 101(5):1356-61.
- Francis SA., Kelly JM., McCormack J, Rogers RA, Lai J, Schneeberger EE., Lynch R. 1999. Rapid reduction of MDCK cell cholesterol by methyl-beta-cyclodextrin alters steady state transepithelial electrical resistance. *Eur J Cell Biol* 78, 473-484.
- Fraser C, Donnelly CA, Cauchemez S, Hanage WP, Van Kerkhove MD, Hollingsworth TD, Griffin J, Baggaley RF, Jenkins HE, Lyons EJ, Jombart T, Hinsley WR, Grassly NC, Balloux F, Ghani AC, Ferguson NM, Rambaut A, Pybus OG, Lopez-Gatell H, Alpuche-Aranda CM, Chapela IB, Zavala EP, Guevara DM, Checchi F, Garcia E, Hugonnet S, Roth C. 2009. WHO Rapid Pandemic Assessment Collaboration. Pandemic potential of a strain of influenza A (H1N1): early findings. *Science*. 324(5934):1557-61.
- Frishman WH, Rapier RC. 1979. Lovastatin: an HMG-CoA reductase inhibitor for lowering cholesterol. *Med Clin North Am* 73:437-448.
- Fritzemeier J, Teuffert J, Greiser-Wilke I, Staubach, Schluter H, Moennig V. 2000. Epidemiology of classical swine fever in Germany in the 1990s, *Vet. Microbiol*. 77 (2000):29-41.
- Fujiyoshi Y, Kume NP, Sakata K, Sato SB. 1994. Fine structure of influenza A virus observed by electron cryo-microscopy. *EMBO J*. 13(2):318-26.
- Furuse Y, Suzuki A, Oshitani H. 2010. Reassortment between swine influenza A viruses increased their adaptation to humans in pandemic H1N1/09. *Infect Genet Evol*. 201:455-69
- Gabriel G, Abram M, Keiner B, Wagner R, Klenk HD, Stech J. 2007. Differential polymerase activity in avian and mammalian cells determines host range of influenza virus. *J Virol*. 81(17):9601-4.

- Gabriel G, Dauber B, Wolff T, Planz O, Klenk HD, Stech J. 2005. The viral polymerase mediates adaptation of an avian influenza virus to a mammalian host. *Proc Natl Acad Sci U S A*. 102(51):18590-5.
- Gabriel G, Herwig A, Klenk HD. 2008. Interaction of polymerase subunit PB2 and NP with importin alpha1 is a determinant of host range of influenza A virus. *PLoS Pathog*. 4(2):e11.
- Gambaryan A, Webster R, Matrosovich M. 2002. Differences between influenza virus receptors on target cells of duck and chicken. *Arch Virol*. 147(6):197-208.
- Gambaryan AS, Robertson JS, Matrosovich MN. 1999. Effects of Egg-Adaptation on the Receptor Binding Properties of Human Influenza A and B Viruses, *Virology* 258:232-239
- Gambotto A, Barratt-Boyes SM, de Jong MD, Neumann G, Kawaoka Y. 2008. Human infection with highly pathogenic H5N1 influenza virus. *Lancet*. 371(9622):1464-75.
- Gao Y, Zhang Y, Shinya K, Deng G, Jiang Y, Li Z, Guan Y, Tian G, Li Y, Shi J, Liu L, Zeng X, Bu Z, Xia X, Kawaoka Y, Chen H. 2009. Identification of amino acids in HA and PB2 critical for the transmission of H5N1 avian influenza viruses in a mammalian host. *PLoS Pathog*. 5(12):e1000709.
- Garcia-Robles I, Akarsu H, Muller CW, Ruigrok RWH, Baudin F. 2004. Interaction of influenza virus proteins with nucleosomes, *Virology* 332: 329-336
- Garten RJ, Davis CT, Russell CA, Shu B, Lindstrom S, Balish A, Sessions WM, Xu X, Skepner E, Deyde V, Okomo-Adhiambo M, Gubareva L, Barnes J, Smith CB, Emery SL, Hillman MJ, Rivallier P, Smagala J, de Graaf M, Burke DF, Fouchier RA, Pappas C, Alpuche-Aranda CM, López-Gatell H, Olivera H, López I, Myers CA, Faix D, Blair PJ, Yu C, Keene KM, Dotson PD Jr, Boxrud D, Sambol AR, Abid SH, St George K, Bannerman T, Moore AL, Stringer DJ, Blevins P, Demmler-Harrison GJ, Ginsberg M, Kriner P, Waterman S, Smole S, Guevara HF, Belongia EA, Clark PA, Beatrice ST, Donis R, Katz J, Finelli L, Bridges CB, Shaw M, Jernigan DB, Uyeki TM, Smith DJ, Klimov AI, Cox NJ. 2009. Antigenic and genetic characteristics of swine-origin 2009 A(H1N1) influenza viruses circulating in humans. *Science*. 2009 Jul 10;325(5937):197-201.
- Garten W, Klenk HD. 1999. Understanding influenza virus pathogenicity, *Trends Microbiol*. 7:99-100
- Geiss GK, An MC, Bumgarner RE, Hammersmark E, Cunningham D, Katze MG. 2001. Global impact of influenza virus on cellular pathways is mediated by both replication-dependent and -independent events. *J Virol* 75(9):4321-31.
- Geiss GK, Salvatore M, Tumpey TM, Carter VS, Wang X, Basler CF, Taubenberger JK, Bumgarner RE, Palese P, Katze MG, Garcia-Sastre A. 2002. Cellular transcriptional profiling in influenza A virus-infected lung epithelial cells: the role of the nonstructural NS1 protein in the evasion of the host innate defense and its potential contribution to pandemic influenza. *Proc Natl Acad Sci U S A*. 99(16):10736-41.
- Gerhard W, Yewdell J, Frankel ME, Webster R. 1981. Antigenic structure of influenza virus haemagglutinin defined by hybridoma antibodies. *Nature* 290:713-717.
- Ginzinger DG. 2002. Gene quantification using real-time quantitative PCR: an emerging technology hits the mainstream. *Exp Hematol*. 30(6):503-12.
- Gitelman AK, Kaverin NV, Kharitonov IG, Rudneva IA, Sklyanskaya EL, Zhdanov VM. 1986. Dissociation of the haemagglutination inhibition and the infectivity neutralization in the reactions of influenza A/USSR/90/77 (H1N1) virus variants with monoclonal antibodies. *J Gen Virol*. 67 (Pt 10):2247-51.
- Gitelman AK, Kaverin NV, Kharitonov IG, Rudneva IA, Zhdanov VM. 1984. Changes in the antigenic specificity of influenza hemagglutinin in the course of adaptation to mice. *Virology*. 134(1):230-2.
- Godley L, Pfeifer J, Steinhauer D, Ely B, Shaw G, Kaufmann R, Suchanek E, Pabo C, Skehel JJ, Wiley DC, et al. 1992. Introduction of intersubunit disulfide bonds in the membrane-distal region of the influenza hemagglutinin abolishes membrane fusion activity. *Cell* 68:635-645.
- Goldstein JL, DeBose-Boyd RA, Brown MS. 2006. Protein sensors for membrane sterols. *Cell* (124):35-46.

- Gong JH, Sprenger H, Hinder F, Bender A, Schmidt A, Horch S, Nain M, Gemsa D. 1991. Influenza A virus infection of macrophages. Enhanced tumor necrosis factor- α (TNF- α) gene expression and lipopolysaccharide-triggered TNF- α release. *J Immunol.* 147(10):3507-13.
- González S, Ortín J. 1999. Characterization of influenza virus PB1 protein binding to viral RNA: two separate regions of the protein contribute to the interaction domain. *J Virol.* 73(1):631-7.
- Görlich D, Mattaj JW. 1996. Nucleocytoplasmic transport. *Science.* 271(5255):1513-8.
- Gorman OT, Bean WJ, Kawaoka Y, Donatelli I, Guo YJ, Webster RG. 1991. Evolution of influenza A virus nucleoprotein genes: implications for the origins of H1N1 human and classical swine viruses. *J Virol* 65:3704-3714.
- Gorman OT, Bean WJ, Kawaoka Y, Donatelli I, Guo YJ, Webster RG. 1991. Evolution of influenza A virus nucleoprotein genes: implications for the origins of H1N1 human and classical swine viruses, *J. Virol.* 65(7):3704-14
- Gottschalk A. 1958. The influenza virus neuraminidase. *Nature.* 181(4606):377-8.
- Govorkova EA, Leneva IA, Golubeva OG, Bush K, Webster RG. 2001. Comparison of efficacies of RWJ-270201, zanamivir, and oseltamivir against H5N1, H9N2, and other avian influenza viruses. *Antimicrob Agents Chemother* 45:2723-2732.
- Gregory V, Bennett M, Orkhan MH, Al Hajjar S, Varsano N, Mendelson E, Zambon M, Ellis J, Hay A, Lin YP. 2002. Emergence of influenza A H1N2 reassortant viruses in the human population during 2001. *Virology.* 300(1):1-7.
- Grewal TS, Genever PG, Brabbs AC, Birch M, Skerry TM. 2000. Best5: a novel interferon-inducible gene expressed during bone formation. *FASEB J.* 3:523-531
- Guan Y, Shortridge KF, Krauss S, Li PH, Kawaoka Y, Webster RG. 1996. Emergence of avian H1N1 influenza viruses in pigs in China. *J Virol* 70:8041-8046.
- Guan Y, Shortridge KF, Krauss S, Webster RG. 1999. Molecular characterization of H9N2 influenza viruses: were they the donors of the "internal" genes of H5N1 viruses in Hong Kong? *Proc Natl Acad Sci U S A.* 96(16):9363-7.
- Guan Z, Liu D, Mi S, Zhang J, Ye Q, Wang M, Gao GF, Yan J. 2010. Interaction of Hsp40 with influenza virus M2 protein: implications for PKR signaling pathway. *Protein Cell* 1:944-955.
- Gubareva LV, Kaiser V, Hayden FG. 2000. Influenza virus neuraminidase inhibitors, *Lancet* 355:827–835
- Guilligay D, Tarendeau F, Resa-Infante P, Coloma R, Crepin T, Sehr P, Lewis J, Ruigrok RW, Ortín J, Hart DJ, Cusack S. 2008. The structural basis for cap binding by influenza virus polymerase subunit PB2. *Nat Struct Mol Biol.* 15(5):500-6.
- Guillot L, Le Goffic R, Bloch S, Escriou N, Akira S, Chignard M, Si-Tahar M. 2005. Involvement of toll-like receptor 3 in the immune response of lung epithelial cells to double-stranded RNA and influenza A virus. *J Biol Chem.* 280(7):5571-80.
- Guo Y, Jin F, Wang P, Wang M, Zhu J.M. 1983. "Isolation of Influenza C Virus from Pigs and Experimental Infection of Pigs with Influenza C Virus". *Journal of General Virology* 64: 177–82
- Guo Y, Wang M, Kawaoka Y, Gorman O, Ito T, Saito T, Webster RG. 1992. Characterization of a new avian-like influenza A virus from horses in China. *Virology.* 188(1):245-55.
- Guo YJ, Krauss S, Senne DA, Mo IP, Lo KS, Xiong XP, Norwood M, Shortridge KF, Webster RG, Guan Y. 2000. Characterization of the pathogenicity of members of the newly established H9N2 influenza virus lineages in Asia. *Virology* 267:279-288.
- Guo YJ, Xu X, Cox NJ. 1992. Human influenza A (H1N2) viruses isolated from China. *J Gen Virol* 73:383–8.

- Ha Y, Stevens DJ, Skehel JJ, Wiley DC. 2002. H5 avian and H9 swine influenza virus haemagglutinin structures: possible origin of influenza subtypes. *EMBO J.* 21(5): 865–875.
- Hagen M, Chung TD, Butcher JA, Krystal M. 1994. Recombinant influenza virus polymerase: requirement of both 5' and 3' viral ends for endonuclease activity. *J Virol.* 68(3):1509-15
- Hale BG, Batty IH, Downes CP, Randall RE. 2008. Binding of influenza A virus NS1 protein to the inter-SH2 domain of p85 suggests a novel mechanism for phosphoinositide 3-kinase activation, *J Biol Chem.* 283(3):1372-80
- Hale BG, Randall RE, Ortin J, Jackson D. 2008. The multifunctional NS1 protein of influenza A viruses. *J Gen Virol.* 89(10):2359-76.
- Hale BG, Steel J, Medina RA, Manicassamy B, Ye J, Hickman D, Hai R, Schmolke M, Lowen AC, Perez DR, Garcia-Sastre A. 2010. Inefficient control of host gene expression by the 2009 pandemic H1N1 influenza A virus NS1 protein. *J Virol* 84:6909-6922.
- Haller O, Arnheiter H, Gresser I, Lindenmann J. 1981. Virus-specific interferon action. Protection of newborn Mx carriers against lethal infection with influenza virus. *J Exp Med.* 154(1):199-203.
- Haller O, Frese M, Kochs G. 1998. Mx proteins: mediators of innate resistance to RNA viruses. *Rev Sci Tech.* 1998 Apr;17(1):220-30.
- Haller O, Staeheli P, Kochs G. 2007. Interferon-induced Mx proteins in antiviral host defense. *Biochimie.* 89(6-7):812-8.
- Haller O, Stertz S, Kochs G. 2007. The Mx GTPase family of interferon-induced antiviral proteins. *Microbes Infect.* 2007 Nov-Dec;9(14-15):1636-43.
- Hara K, Schmidt FI, Crow M, Brownlee GG. 2006. Amino acid residues in the N-terminal region of the PA subunit of influenza A virus RNA polymerase play a critical role in protein stability, endonuclease activity, cap binding, and virion RNA promoter binding. *J Virol.* 80(16):7789-98
- Harada H, Fujita T, Miyamoto M, Kimura Y, Maruyama M, Furia A, Miyata T, Taniguchi T. 1989. Structurally similar but functionally distinct factors, IRF-1 and IRF-2, bind to the same regulatory elements of IFN and IFN-inducible genes. *Cell.* 58(4):729-39.
- Harris A, Cardone G, Winkler DC, Heymann JB, Brecher M, White JM. 2006. Steven AC. Influenza virus pleiomorphy characterized by cryoelectron tomography. *Proc. Natl. Acad. Sci. U S A.* 103:19123–19127
- Hatada E, Fukuda R. 1992. Binding of influenza A virus NS1 protein to dsRNA in vitro. *J Gen Virol.* 73 (12):3325-9.
- Hatada E, Takizawa T, Fukuda R. 1992. Specific binding of influenza A virus NS1 protein to the virus minus-sense RNA in vitro. *J Gen Virol.* 73 (Pt 1):17-25.
- Hatakeyama S, Sakai-Tagawa Y, Kiso M, Goto H, Kawakami C, Mitamura K, Sugaya N, Suzuki Y, Kawaoka Y. 2005.Enhanced expression of an alpha2,6-linked sialic acid on MDCK cells improves isolation of human influenza viruses and evaluation of their sensitivity to a neuraminidase inhibitor. *J Clin Microbiol.* 2005 Aug;43(8):4139–46.
- Hatta M, Gao P, Halfmann P, Kawaoka Y. 2001. Molecular basis for high virulence of Hong Kong H5N1 influenza A viruses, *Science* 293(5536):1840-2
- Hay AJ, Gregory V, Douglas AR, Lin YP. 2001. The evolution of human influenza viruses. *Philos Trans R Soc Lond B Biol Sci.* 356(1416):1861-70.
- Hay AJ, Kennedy NC, Skehel JJ, Appleyard G. 1979. The matrix protein gene determines amantadine-sensitivity of influenza viruses. *J Gen Virol* 42:189-191.
- Hay AJ, Lomniczi B, Bellamy AR, Skehel JJ. 1977. Transcription of the influenza virus genome. *Virology.* 83(2):337-55.

- Hay AJ, Zambon MC, Wolstenholme AJ, Skehel JJ, Smith MH. 1986. Molecular basis of resistance of influenza A viruses to amantadine. *J Antimicrob Chemother* 18 Suppl B 1986:19-29.
- Hay AJ, Kennedy NC., Skehel JJ., Appleyard G. 1979. The matrix protein gene determines amantadine-sensitivity of influenza viruses. *J Gen Virol* 42:189-191.
- Haye K, Burmakina S, Moran T, García-Sastre A, Fernandez-Sesma A. 2009. The NS1 protein of a human influenza virus inhibits type I interferon production and the induction of antiviral responses in primary human dendritic and respiratory epithelial cells. *J Virol*. 83(13):6849-62.
- Hayman A, Comely S, Lackenby A, Hartgroves LC, Goodbourn S, McCauley JW, Barclay WS. 2007. NS1 proteins of avian influenza A viruses can act as antagonists of the human alpha/beta interferon response. *J Virol* 81:2318-2327.
- He X, Zhou J, Bartlam M, Zhang R, Ma J, Lou Z, Li X, Li J, Joachimiak A, Zeng Z, Ge R, Rao Z, Liu Y. 2008. Crystal structure of the polymerase PA(C)-PB1(N) complex from an avian influenza H5N1 virus. *Nature* 454:1123-1126.
- Heinrich PC, Behrmann I, Haan S, Hermanns HM, Müller-Newen G, Schaper F. 2003. Principles of interleukin (IL)-6-type cytokine signalling and its regulation. *Biochem J*. 374(Pt 1):1-20.
- Herrler G, Dürkop I, Becht H, Klenk HD. 1988. The glycoprotein of influenza C virus is the haemagglutinin, esterase and fusion factor. *J Gen Virol*. 69 (4):839-46.
- Hinshaw VS, Alexander DJ, Aymard M, Bachmann PA, Easterday BC, Hannoun C, Kida H, Lipkind M, Mackenzie JS, Nerome K, Schild GC, Scholtissek C, Senne DA, Shortridge KF, Skehel JJ, Webster RG. 1984. Antigenic comparisons of swine-influenzalike H1N1 isolates from pigs, birds and humans: an international collaborative study. *Bull World Health Organ* 62: 871-878
- Hinshaw VS, Bean WJ Jr, Webster RG, Easterday BC. 1978. The prevalence of influenza viruses in swine and the antigenic and genetic relatedness of influenza viruses from man and swine. *Virology* 84:51-62.
- Hinshaw VS., Webster RG, Turner B. 1978. Novel influenza A viruses isolated from Canadian feral ducks: including strains antigenically related to swine influenza (HswIN1) viruses. *J. Gen. Virol.* 41:115-127.
- Hoffmann E, Stech J, Guan Y, Webster RG, Perez DR. 2001. Universal primer set for the full-length amplification of all influenza A viruses. *Arch Virol*. 146(12):2275-89.
- Hofmann P, Sprenger H, Kaufmann A, Bender A, Hasse C, Nain M, Gerns D. 1997. Susceptibility of mononuclear phagocytes to influenza A virus infection and possible role in the antiviral response. *J Leukoc Biol*. 61(4):408-14.
- Holsinger LJ, Shaughnessy MA, Micko A, Pinto LH, Lamb RA. 1995. Analysis of the posttranslational modifications of the influenza virus M2 protein. *J Virol*. 69(2):1219-25.
- Homme PJ, Easterday BC. 1970. Avian influenza virus infections. IV. Response of pheasants, ducks, and geese to influenza A-turkey-Wisconsin-1966 virus. *Avian Dis*. 14(2):285-90.
- Honda A, Takuto O, Ishihama A. 2007. Host Factor Ebp1: Selective inhibitor of influenza virus transcriptase, *Genes. Cells*. 12:133-142
- Horimoto T, Kawaoka Y. 1995. Molecular changes in virulent mutants arising from avirulent avian influenza viruses during replication in 14-day-old embryonated eggs. *Virology* 206:755-759.
- Horimoto T, Kawaoka Y. 2005. Influenza: lessons from past pandemics, warnings from current incidents. *Nat Rev Microbiol* 3:591-600.
- Horisberger MA, Wathlet M, Szpirer J, Szpirer C, Islam Q, Levan G, Huez G, Content J. 1988. cDNA Cloning and assignment to chromosome 21 of IFI-78K gene, the human equivalent of murine Mx gene, *Somatic Cell Mol. Genet.* 1988(14):123-131.

- Horisberger MA. 1980. The large P proteins of influenza A viruses are composed of one acidic and two basic polypeptides. *Virology*. 107(1):302-5.
- Hovanessian AG, Justesen J. 2007. The human 2'-5'oligoadenylate synthetase family: unique interferon-inducible enzymes catalyzing 2'-5' instead of 3'-5' phosphodiester bond formation. *Biochimie*. 89(6-7):779-88.
- Hovnanian A, Rebouillat D, Mattei MG, Levy ER, Marié I, Monaco AP, Hovanessian AG. 1998. The human 2',5'-oligoadenylate synthetase locus is composed of three distinct genes clustered on chromosome 12q24.2 encoding the 100-, 69-, and 40-kDa forms. *Genomics*. 52(3):267-77.
- Hsu MT, Parvin JD, Gupta S, Krystal M, Palese P. 1987. Genomic RNAs of influenza viruses are held in a circular conformation in virions and in infected cells by a terminal panhandle. *Proc Natl Acad Sci U S A*. 84(22):8140-4.
- Hu J, Asbury T, Achuthan S, Li C, Bertram R, Quine JR, Fu R, Cross TA. 2007. Backbone structure of the amantadine-blocked trans-membrane domain M2 proton channel from Influenza A virus. *Biophys J* 92:4335-4343.
- Huarte M, Sanz-Ezquerro JJ, Roncal F, Ortin J, Nieto A. 2001. PA Subunit from Influenza Virus Polymerase Complex Interacts with a Cellular Protein with Homology to a Family of Transcriptional Activators, *J. Virol*. 75(18):8597-8604
- Huet S, Avilov S, Ferbitz L, Daigle N, Cusack S, Ellenberg J. 2009. Nuclear import and assembly of the influenza A virus RNA polymerase studied in live cells by Fluorescence Cross Correlation Spectroscopy. *J Virol*. 294:1992-2006
- Hughey PG, Roberts PC, Holsinger LJ, Zebedee SL, Lamb RA, Compans RW. 1995. Effects of antibody to the influenza A virus M2 protein on M2 surface expression and virus assembly. *Virology*. 212(2):411-21.
- Hull JD, Gilmore R, Lamb RA. 1988. Integration of a small integral membrane protein, M2, of influenza virus into the endoplasmic reticulum: analysis of the internal signal-anchor domain of a protein with an ectoplasmic NH2 terminus. *J Cell Biol*. 106(5):1489-98.
- Hurt AC, Holien JK, Parker M, Kelso A, Barr IG. 2009. Zanamivir-resistant influenza viruses with a novel neuraminidase mutation. *J Virol* 83:10366-10373.
- Ikonen E. 2008. Cellular cholesterol trafficking and compartmentalization. *Nat Rev Mol Cell Biol* 9:125-138.
- Imada K, Leonard WJ. 2000. The Jak-STAT pathway. *Mol Immunol*. 37(1-2):1-11.
- Inglis SC, Almond JW. 1980. An influenza virus gene encoding two different proteins. *Philos Trans R Soc Lond B Biol Sci*. 288(1029):375-81.
- Inglis SC, Barrett T, Brown CM, Almond JW. 1979. The smallest genome RNA segment of influenza virus contains two genes that may overlap. *Proc Natl Acad Sci U S A*. 76(8):3790-4.
- Iqbal M, Yaqub T, Reddy K, McCauley JW. 2009. Novel genotypes of H9N2 influenza A viruses isolated from poultry in Pakistan containing NS genes similar to highly pathogenic H7N3 and H5N1 viruses. *PLoS One*. 4(6):e5788.
- Ito T, Couceiro JN, Kelm S, Baum LG, Krauss S, Castrucci MR, Donatelli I, Kida H, Paulson JC, Webster RG, Kawaoka Y. 1998. Molecular basis for the generation in pigs of influenza A viruses with pandemic potential. *J Virol*. 72(9):7367-73.
- Ito T, Kobayashi Y, Morita T, Horimoto T, Kawaoka Y. 2002. Virulent influenza A viruses induce apoptosis in chickens. *Virus Res*. 84(1-2):27-35.
- Itoh Y, Shinya K, Kiso M, Watanabe T, Sakoda Y, Hatta M, Muramoto Y, Tamura D, Sakai-Tagawa Y, Noda T, Sakabe S, Imai M, Hatta Y, Watanabe S, Li C, Yamada S, Fujii K, Murakami S, Imai H, Kakugawa S, Ito M, Takano R, Iwatsuki-Horimoto K, Shimojima M, Horimoto T, Goto H, Takahashi K, Makino A, Ishigaki H, Nakayama M, Okamatsu M, Takahashi K, Warshauer D, Shult PA, Saito R, Suzuki H, Furuta Y, Yamashita M, Mitamura K, Nakano K, Nakamura M, Brockman-Schneider R, Mitamura H, Yamazaki M, Sugaya N, Suresh M,

- Ozawa M, Neumann G, Gern J, Kida H, Ogasawara K, Kawaoka Y. 2009. In vitro and in vivo characterization of new swine-origin H1N1 influenza viruses. *Nature*. 460(7258):1021-5.
- Jenkins KA, Bean AG, Lowenthal JW. 2007. Avian genomics and the innate immune response to viruses. *Cytogenet Genome Res*. 117(1-4):207-12.
- Jin H, Leser GP, Zhang J, Lamb RA. 1997. Influenza virus hemagglutinin and neuraminidase cytoplasmic tails control particle shape. *EMBO J*. 16(6):1236-47.
- Jin HK, Yamashita T, Ochiai K, Haller O, Watanabe T.1998. Characterization and expression of the Mx1 gene in wild mouse species. *Biochem Genet*. 36(9-10):311-22.
- Jones IM, Reay PA, Philpott KL. 2001. Nuclear location of all three influenza polymerase proteins and a nuclear signal in polymerase PB2. *EMBO Rep*. 2(4):313-317
- Julkunen I, Sareneva T, Pirhonen J, Ronni T, Melén K, Matikainen S. 2001. Molecular pathogenesis of influenza A virus infection and virus-induced regulation of cytokine gene expression, *Cytokine Growth Factor Rev*. 12(2-3):171-80
- Justesen J, Hartmann R, Kjeldgaard NO. 2000. Gene structure and function of the 2'-5'-oligoadenylate synthetase family. *Cell Mol Life Sci*. 57(11):1593-612.
- Kakuta S, Shibata S, Iwakura Y. 2002. Genomic structure of the mouse 2',5'-oligoadenylate synthetase gene family. *J Interferon Cytokine Res*. 22(9):981-93.
- Kash JC, Tumpey TM, Prohl SC, Carter V, Perwitasari O, Thomas MJ, Basler CF, Palese P, Taubenberger JK, García-Sastre A, Swayne DE, Katze MG. 2006. Genomic analysis of increased host immune and cell death responses induced by 1918 influenza virus. *Nature*. 443(7111):578-81.
- Kaufmann A, Salentin R, Meyer RG, Bussfeld D, Pauligk C, Fesq H, Hofmann P, Nain M, Gerns D, Sprenger H. 2001. Defense against influenza A virus infection: essential role of the chemokine system. *Immunobiology*. 204(5):603-13.
- Kaverin NV, Finskaya NN, Rudneva IA, Gitelman AK, Kharitonov IG, Smirnov YA. 1989. Studies on the genetic basis of human influenza A virus adaptation to mice: degrees of virulence of reassortants with defined genetic content. *Arch Virol*. 105(1-2):29-37.
- Kaverin NV, Rudneva IA, Ilyushina NA, Lipatov AS, Krauss S, Webster RG. 2004. Structural differences among hemagglutinins of influenza A virus subtypes are reflected in their antigenic architecture: analysis of H9 escape mutants. *J Virol*. 78(1):240-9.
- Kawaguchi A, Kyosuke N. 2007. De novo replication of the influenza virus RNA genome is regulated by DNA replicative helicase, MCM, *EMBO J*. 26:4566-4575
- Kawakami K, Mizumoto K, Ishihama A, Shinozaki-Yamaguchi K, Miura K. 1985. Activation of influenza virus-associated RNA polymerase by cap-1 structure (m7GpppNm). *J Biochem*. 97(2):655-61.
- Kawaoka Y, Chambers TM, Sladen WL, Webster RG. 1988. Is the gene pool of influenza viruses in shorebirds and gulls different from that in wild ducks? *Virology*. 163(1):247-50.
- Kawaoka Y, Gorman OT, Ito T, Wells K, Donis RO, Castrucci MR, Donatelli I, Webster RG. 1998. Influence of host species on the evolution of the nonstructural (NS) gene of influenza A viruses. *Virus Res*. 55(2):143-56.
- Keeler CL Jr, Bliss TW, Lavric M, Maughan MN. 2007. A functional genomics approach to the study of avian innate immunity. *Cytogenet Genome Res*. 117(1-4):139-45.
- Keller P, Simons K. 1998. Cholesterol is required for surface transport of influenza virus hemagglutinin. *J Cell Biol* 140: 1357-1367.

- Kemble GW, Bodian DL, Rose J, Wilson IA, White JM. 1992. Intermonomer disulfide bonds impair the fusion activity of influenza virus hemagglutinin. *J Virol* 66:4940-4950.
- Kida H, Ito T, Yasuda J, Shimizu Y, Itakura C, Shortridge KF, Kawaoka Y, Webster RG. 1993. Potential for transmission of avian influenza viruses to pigs, *J Gen Virol* 75 (9):2183-8
- Kielian MC, Helenius A. 1984. Role of cholesterol in fusion of Semliki Forest virus with membranes. *J Virol* 98: 281-283.
- Kingsbury DW, Jones IM, Murti KG, 1987. Assembly of influenza ribonucleoprotein in vitro using recombinant nucleoprotein, *Virology*. 156(2):396-403
- Kiso M, Mitamura K, Sakai-Tagawa Y, Shiraishi K, Kawakami C, Kimura K, Hayden FG, Sugaya N, Kawaoka Y. 2004. Resistant influenza A viruses in children treated with oseltamivir: descriptive study. *Lancet*. 364(9436):733-4.
- Klein D. 2002. Quantification using real-time PCR technology: applications and limitations. *Trends Mol Med*. 8(6):257-60.
- Klenk HD, Rott R, Orlich M. 1977. Further studies on the activation of influenza virus by proteolytic cleavage of the haemagglutinin. *J Gen Virol*. 36(1):151-61.
- Knossow M, Gaudier M, Douglas A, Barrère B, Bizebard T, Barbey C, Gigant B, Skehel JJ. 2002. Mechanism of neutralization of influenza virus infectivity by antibodies. *Virology*. 302(2):294-8.
- Kobasa D, Jones SM, Shinya K, Kash JC, Copps J, Ebihara H, Hatta Y, Kim JH, Halfmann P, Hatta M, Feldmann F, Alimonti JB, Fernando L, Li Y, Katze MG, Feldmann H, Kawaoka Y. 2007. Aberrant innate immune response in lethal infection of macaques with the 1918 influenza virus. *Nature*. 445(7125):319-23
- Kobasa D, Kodihalli S, Luo M, Castrucci MR, Donatelli I, Suzuki Y, Suzuki T, Kawaoka Y. 1999. Amino acid residues contributing to the substrate specificity of the influenza A virus neuraminidase. *J Virol* 73:6743-6751.
- Kobasa D, Wells K, Kawaoka Y. 2001. Amino acids responsible for the absolute sialidase activity of the influenza A virus neuraminidase: relationship to growth in the duck intestine. *J Virol* 75:11773-11780.
- Kobayashi M, Toyoda T, Adyshev DM, Azuma Y, Ishihama A. 1994. Molecular dissection of influenza virus nucleoprotein: deletion mapping of the RNA binding domain. *J. Virol*. 68:8433-8436
- Kochs G, García-Sastre A, Martínez-Sobrido L. 2007. Multiple anti-interferon actions of the influenza A virus NS1 protein, *J Virol*. 81(13):7011-21
- Kochs G, Martinez-Sobrido L, Lienenklaus S, Weiss S, Garcia-Sastre A, Staeheli P. 2009. Strong interferon-inducing capacity of a highly virulent variant of influenza A virus strain PR8 with deletions in the NS1 gene. *J Gen Virol* 90:2990-2994.
- Kogure T, Suzuki T, Takahashi T, Miyamoto D, Hidari KI, Guo CT, Ito T, Kawaoka Y, Suzuki Y. 2006. Human trachea primary epithelial cells express both sialyl(alpha2-3)Gal receptor for human parainfluenza virus type 1 and avian influenza viruses, and sialyl(alpha2-6)Gal receptor for human influenza viruses. *Glycoconj J*. 23(1-2):101-6.
- Koopmans M, Wilbrink B, Conyn M, Natrop G, van der Nat H, Vennema H, Meijer A, van Steenbergen J, Fouchier R, Osterhaus A, Bosman A. 2004. Transmission of H7N7 avian influenza A virus to human beings during a large outbreak in commercial poultry farms in the Netherlands. *Lancet*. 363(9409):587-93.
- Korth MJ, Kash JC, Baskin CR, Katze MG. 2006. Insights into influenza virus-host interactions through global gene expression profiling: cell culture systems to animal models, in *Influenza Virology:Current Topics*, edited by Kawaoka, Y, Caister Academic Press, England
- Korth MJ, Katze MG. 2002. Unlocking the mysteries of virus-host interactions: does functional genomics hold the key? *Ann N Y Acad Sci*. 975:160-8.

- Kou Z, Lei FM, Yu J, Fan ZJ, Yin ZH, Jia CX, Xiong KJ, Sun YH, Zhang XW, Wu XM, Gao XB, Li TX. 2005. New genotype of avian influenza H5N1 viruses isolated from tree sparrows in China. *J Virol.* 79(24):15460-6.
- Kowalczyk A, Markowska-Daniel I. 2010. Phylogenetic evolution of swine-origin human influenza virus: a pandemic H1N1 2009. *Pol J Vet Sci* 13:491-500.
- Krebs DL, Hilton DJ. 2001. SOCS proteins: negative regulators of cytokine signaling. *Stem Cells.* 19(5):378-87.
- Krug RM, Shaw M, Broni B, Shapiro G, Haller O. 1985. Inhibition of influenza viral mRNA synthesis in cells expressing the interferon-induced Mx gene product. *J Virol.* 56(1):201-6.
- Krug RM, Soeiro R. 1975. Studies on the intranuclear localization of influenza virus-specific proteins. *Virology.* 64(2):378-87.
- Kujime K, Hashimoto S, Gon Y, Shimizu K, Horie T. 2000. p38 mitogen-activated protein kinase and c-jun-NH2-terminal kinase regulate RANTES production by influenza virus-infected human bronchial epithelial cells. *J Immunol.* 164(6):3222-8.
- Kumar A, Yang YL, Flati V, Der S, Kadereit S, Deb A, Haque J, Reis L, Weissmann C, Williams BR. 1997. Deficient cytokine signaling in mouse embryo fibroblasts with a targeted deletion in the PKR gene: role of IRF-1 and NF-kappaB. *EMBO J.* 16(2):406-16.
- Kwon JS, Lee HJ, Lee DH, Lee YJ, Mo IP, Nahm SS, Kim MJ, Lee JB, Park SY, Choi IS, Song CS. 2008. Immune responses and pathogenesis in immunocompromised chickens in response to infection with the H9N2 low pathogenic avian influenza virus. *Virus Res.* 133(2):187-94.
- Labadie K, Dos Santos Afonso E, Rameix-Welti MA, van der Werf S, Naffakh N. 2007. Host-range determinants on the PB2 protein of influenza A viruses control the interaction between the viral polymerase and nucleoprotein in human cells. *Virology.* 362(2):271-82.
- Lam WY, Tang JW, Yeung AC, Chiu LC, Sung JJ, Chan PK. 2008. Avian influenza virus A/HK/483/97(H5N1) NS1 protein induces apoptosis in human airway epithelial cells, *J Virol.* 82(6):2741-51
- Lamb RA, Choppin PW. 1976. Synthesis of influenza virus proteins in infected cells: translation of viral polypeptides, including three P polypeptides, from RNA produced by primary transcription. *Virology.* 74(2):504-19.
- Lamb RA, Choppin PW. 1981. Identification of a second protein (M2) encoded by RNA segment 7 of influenza virus. *Virology.* 112(2):729-37.
- Lamb RA, Krug RM. 2001. *Orthomyxoviridae : The viruses and their replication.* In *Fields of Virology* (B.N Fields, D.M Knipe, P.M. Howley, Eds.), Lippincott-Raven, Philadelphia
- Lamb RA, Lai CJ. 1981. Conservation of the influenza virus membrane protein (M1) amino acid sequence and an open reading frame of RNA segment 7 encoding a second protein (M2) in H1N1 and H3N2 strains. *Virology.* 112(2):746-51.
- Lamb RA, Lai CJ. 1982. Spliced and unspliced messenger RNAs synthesized from cloned influenza virus M DNA in an SV40 vector: expression of the influenza virus membrane protein (M1). *Virology* 123(2):237-256.
- Lamb RA, Lai CJ. 1984. Expression of unspliced NS1 mRNA, spliced NS2 mRNA, and a spliced chimera mRNA from cloned influenza virus NS DNA in an SV40 vector. *Virology* 135(1):139-147.
- Lee DC., Mok CK, Law AH, Peiris M, Lau AS. 2010. Differential replication of avian influenza H9N2 viruses in human alveolar epithelial A549 cells. *Virol J* 2010(7): 71-80.
- Lee TG, Tang N, Thompson S, Miller J, Katze MG. 1994. The 58,000-dalton cellular inhibitor of the interferon-induced double-stranded RNA-activated protein kinase (PKR) is a member of the tetratricopeptide repeat family of proteins. *Mol Cell Biol.* 4:2331-42.

- Leneva IA, Roberts N, Govorkova EA, Goloubeva OG, Webster RG. 2000. The neuraminidase inhibitor GS4104 (oseltamivir phosphate) is efficacious against A/Hong Kong/156/97 (H5N1) and A/Hong Kong/1074/99 (H9N2) influenza viruses. *Antiviral Res* 2000(48):101-115.
- Leser GP, Lamb RA. 2005. Influenza virus assembly and budding in raft-derived microdomains: a quantitative analysis of the surface distribution of HA, NA and M2 proteins. *Virology*. 342(2):215-27.
- Levy DE, García-Sastre A. 2001. The virus battles: IFN induction of the antiviral state and mechanisms of viral evasion. *Cytokine Growth Factor Rev.* 12(2-3):143-56.
- Li CJ, Yu KZ, Tian GB, Yu DD, Liu L, Jing B, Ping JH, Chen HL. 2005. Evolution of H9N2 influenza viruses from domestic poultry in Mainland China. *Virology* 340:70-83
- Li KS, Guan Y, Wang J, Smith GJ, Xu KM, Duan L, Rahardjo AP, Puthavathana P, Buranathai C, Nguyen TD, Estoepongastie AT, Chaisingh A, Auewarakul P, Long HT, Hanh NT, Webby RJ, Poon LL, Chen H, Shortridge KF, Yuen KY, Webster RG, Peiris JS. 2004. Genesis of a highly pathogenic and potentially pandemic H5N1 influenza virus in Eastern Asia. *Nature*. 430(6996):209-13..
- Li S, Min JY, Krug RM, Sen GC. 2006. Binding of the influenza A virus NS1 protein to PKR mediates the inhibition of its activation by either PACT or double-stranded RNA, *Virology*. 349(1):13-21
- Li W, Wang G, Zhang H, Xin G, Zhang D, Zeng J, Chen X, Xu Y, Cui Y, Li K. Effects of NS1 variants of H5N1 influenza virus on interferon induction, TNF α response and p53 activity. *Cell Mol Immunol* 2010, (7):235-242.
- Li X, Palese P. 1994. Characterization of the polyadenylation signal of influenza virus RNA. *J Virol*. 68(2):1245-9.
- Li XL, Blackford JA, Hassel BA. 1998. RNase L mediates the antiviral effect of interferon through a selective reduction in viral RNA during encephalomyocarditis virus infection. *J Virol*. 72(4):2752-9.
- Li Z, Watanabe T, Hatta M, Watanabe S, Nanbo A, Ozawa M, Kakugawa S, Shimojima M, Yamada S, Neumann G, Kawaoka Y. 2009. Mutational analysis of conserved amino acids in the influenza A virus nucleoprotein *J Virol*. 83(9):4153-62
- Liao Z, Cimasky LM, Hampton R, Nguyen DH, Hildreth JE. 2001. Lipid rafts and HIV pathogenesis: host membrane cholesterol is required for infection by HIV type 1. *AIDS Res Hum Retroviruses* 17:1009-1019.
- Liao Z, Graham DR, Hildreth JE. 2003. Lipid rafts and HIV pathogenesis: virion-associated cholesterol is required for fusion and infection of susceptible cells. *AIDS Res Hum Retroviruses* 19:675-687.
- Lin YP, Gregory V, Bennett M, Hay A. 2004. Recent changes among human influenza viruses. *Virus Res*. 103(1-2):47-52.
- Lin YP, Shaw M, Gregory V, Cameron K, Lim W, Klimov A, Subbarao K, Guan Y, Krauss S, Shortridge K, Webster R, Cox N, Hay A. 2000. Avian-to-human transmission of H9N2 subtype influenza A viruses: relationship between H9N2 and H5N1 human isolates. *Proc Natl Acad Sci U S A*. 97(17):9654-8.
- Lindstrom SE, Cox NJ, Klimov A. 2004. Genetic analysis of human H2N2 and early H3N2 influenza viruses, 1957-1972: evidence for genetic divergence and multiple reassortment events. *Virology*. 328(1):101-19.
- Livak KJ, Schmittgen TD. 2001. Analysis of relative gene expression data using real-time quantitative PCR and the 2(-Delta Delta C(T)) Method. *Methods*. 25(4):402-8.
- Long JX, Peng DX, Liu YL, Wu YT, Liu XF. 2008. Virulence of H5N1 avian influenza virus enhanced by a 15-nucleotide deletion in the viral nonstructural gene. *Virus Genes*. 36(3):471-8.
- Loucaides EM, von Kirchbach JC, Foeglein A, Sharps J, Fodor E, Digard P. 2009. Nuclear dynamics of influenza A virus ribonucleoproteins revealed by live-cell imaging studies. *Virology* 394(1):154-63.
- Lu J, Liu D, Liu W, Shi T, Tong Y, Cao W. 2009. Genetic stability and linkage analysis of the 2009 Influenza A(H1N1) virus based on sequence homology. *Arch Virol* 154:1883-1890.

- Lu Y, Wambach M, Katze MG, Krug RM. 1995. Binding of the influenza virus NS1 protein to double-stranded RNA inhibits the activation of the protein kinase that phosphorylates the eIF-2 translation initiation factor. *Virology*. 214(1):222-8.
- Ludwig S, Schultz U, Mandler J, Fitch WM, Scholtissek C. 1991. Phylogenetic relationship of the nonstructural (NS) genes of influenza A viruses. *Virology*. 183(2):566-77.
- Luo G, Chung J, Palese P. 1993. Alterations of the stalk of the influenza virus neuraminidase: deletions and insertions. *Virus Res* 29:141-153.
- Luo GX, Luytjes W, Enami M, Palese P. 1991. The polyadenylation signal of influenza virus RNA involves a stretch of uridines followed by the RNA duplex of the panhandle structure. *J Virol*. 65(6):2861-7.
- Macdonald RD, Yamamoto T, Fedorak P. 1977. Statistical prediction of the number of cells surviving infection by an autointerfering virus using the Poisson distribution. *J Theor Biol* 68:355-363.
- Mahy BW, Barrett T, Briedis DJ, Brownson JM, Wolstenholme AJ. 1980. Influence of the host cell on influenza virus replication. *Philos Trans R Soc Lond B Biol Sci* 288:349-357.
- Mahy BW, Hastie ND, Armstrong SJ. 1972. Inhibition of influenza virus replication by -amanitin: mode of action. *Proc Natl Acad Sci U S A*. 1972 Jun;69(6):1421-4.
- Maines TR, Jayaraman A, Belser JA, Wadford DA, Pappas C, Zeng H, Gustin KM, Pearce MB, Viswanathan K, Shriver ZH, Raman R, Cox NJ, Sasisekharan R, Katz JM, Tumpey TM. 2009. Transmission and pathogenesis of swine-origin 2009 A(H1N1) influenza viruses in ferrets and mice. *Science*. 325(5939):484-7
- Mak NK, Sweet C, Ada GL, Tannock GA. 1984. The sensitization of mice with a wild-type and cold-adapted variant of influenza A virus. II. Secondary cytotoxic T cell responses. *Immunology* 51:407-416.
- Mamane Y, Heylbroeck C, Génin P, Algarté M, Servant M.J, LePage C, DeLuca C, Kwon H, Lin R, Hiscott J., 1999. Interferon regulatory factors: the next generation, *Gene*. 237(1):1-14
- Marié I, Durbin JE, Levy DE, 1998. Differential viral induction of distinct interferon-alpha genes by positive feedback through interferon regulatory factor-7. *EMBO J*. 17(22):6660-9.
- Marsh GA, Rabadán R, Levine AJ, Palese P. 2008. Highly conserved regions of influenza A virus polymerase gene segments are critical for efficient viral RNA packaging. *J Virol*. 82(5):2295-304.
- Martin K, Helenius A. 1991. Nuclear transport of influenza virus ribonucleoproteins: the viral matrix protein (M1) promotes export and inhibits import. *Cell* 67:117-130.
- Martin K, Helenius A. 1991. Transport of incoming influenza virus nucleocapsids into the nucleus. *J Virol*. 65(1):232-44.
- Martín-Benito J, Area E, Ortega J, Llorca O, Valpuesta JM, Carrascosa JL, Ortín J. Three-dimensional reconstruction of a recombinant influenza virus ribonucleoprotein particle. *EMBO J* 1986;5(9):2371-2376
- Mashimo T, Glaser P, Lucas M, Simon-Chazottes D, Ceccaldi PE, Montagutelli X, Desprès P, Guénet JL. 2003. Structural and functional genomics and evolutionary relationships in the cluster of genes encoding murine 2',5'-oligoadenylate synthetases. *Genomics*. 82(5):537-52.
- Masurel N, de Boer GF, Anker WJ, Huffels AD. 1983. Prevalence of influenza viruses A-H1N1 and A-H3N2 in swine in the Netherlands. *Comp Immunol Microbiol Infect Dis*. 6(2):141-9.
- Matikainen S, Pirhonen J, Miettinen M, Lehtonen A, Govenius-Vintola C, Sareneva T, Julkunen I. 2000. Influenza A and sendai viruses induce differential chemokine gene expression and transcription factor activation in human macrophages. *Virology*. 276(1):138-47.
- Matlin KS, Reggio H, Helenius A, Simon K. 1981. Infectious entry pathway of influenza virus in a canine kidney cell line, *J. Cell. Biol* 91:601-613

- Matrosovich M, Matrosovich T, Garten W, Klenk HD. 2006. New low-viscosity overlay medium for viral plaque assays. *Virology* 3:63.
- Matrosovich M, Tuzikov A, Bovin N, Gambaryan A, Klimov A, Castrucci MR, Donatelli I, Kawaoka Y. 2000. Early alterations of the receptor-binding properties of H1, H2, and H3 avian influenza virus hemagglutinins after their introduction into mammals. *J Virol*. 74(18):8502-12.
- Matrosovich M, Zhou N, Kawaoka Y, Webster R. 1999. The surface glycoproteins of H5 influenza viruses isolated from humans, chickens, and wild aquatic birds have distinguishable properties. *J. Virol*. 73, 1145–1146.
- Matrosovich MN, Gambaryan AS, Teneberg S, Piskarev VE, Yamnikova SS, Lvov DK, Robertson JS, Karlsson KA. 1997. Avian influenza A viruses differ from human viruses by recognition of sialyloligosaccharides and gangliosides and by a higher conservation of the HA receptor-binding site. *Virology*. 233(1):224-34.
- Matrosovich MN, Krauss S, Webster RG. 2001. H9N2 influenza A viruses from poultry in Asia have human virus-like receptor specificity. *Virology* 281:156-162.
- Matsukura S, Kokubu F, Noda H, Tokunaga H, Adachi M. 1996. Expression of IL-6, IL-8, and RANTES on human bronchial epithelial cells, NCI-H292, induced by influenza virus A. *J Allergy Clin Immunol*. 98(6 Pt 1):1080-7.
- Matsuoka Y, Swayne DE, Thomas C, Rameix-Welti MA, Naffakh N, Warnes C, Altholtz M, Donis R, Subbarao K. 2009. Neuraminidase stalk length and additional glycosylation of the hemagglutinin influence the virulence of influenza H5N1 viruses for mice. *J Virol* 83:4704-4708.
- Mazur I, Anhlén D, Mltzner D, Wixler L, Schubert U, Ludwid S. 2008. The proapoptotic influenza virus protein PB1-F2 regulates viral polymerase activity by interaction with the PB1 protein, *Cell. Microbiol*. 10(5):1140-1151
- McAuley JL, Hornung F, Boyd KL, Smith AM, McKeon R, Bennink J, Yewdell JW, McCullers, J.A. 2007. Expression of the 1918 influenza A virus PB1-F2 enhances the pathogenesis of viral and secondary bacterial pneumonia, *Cell Host & Microbe* 2:240–249
- Medcalf L, Poole E, Elton D, Digard P. 1999. Temperature-sensitive lesions in two influenza A viruses defective for replicative transcription disrupt RNA binding by the nucleoprotein. *J Virol*. 73(9):7349-56.
- Melen K, Fagerlund R, Franke J, Kohler M, Kinnunen L, Julkunen I. 2003. Importin alpha nuclear localization signal binding sites for STAT1, STAT2, and influenza A virus nucleoprotein. *J Biol Chem*. 278(30):28193-200.
- Metcalf D. 1985. The granulocyte-macrophage colony-stimulating factors. *Science*. 229(4708):16-22.
- Michaelis M, Doerr HW, Cinatl J Jr. 2009. Novel swine-origin influenza A virus in humans: another pandemic knocking at the door. *Med Microbiol Immunol*. 198(3):175-83.
- Mitnaul LJ, Castrucci MR, Murti KG, Kawaoka Y. 1996. The cytoplasmic tail of influenza A virus neuraminidase (NA) affects NA incorporation into virions, virion morphology, and virulence in mice but is not essential for virus replication. *J Virol* 70:873-879.
- Momose F, Basler CF, O'Neill RE, Iwamatsu A, Palese P, Nagata K. 2001. Cellular Splicing Factor RAF-2p48/NPI-5/BAT1/UAP56 interacts with the influenza virus nucleoprotein and enhances Viral RNA synthesis, *75(4): 1899-1908*
- Momose F, Naito T, Yano K, Sugimoto S, Morikawa Y, Nagata K. 2002. Identification of Hsp90 as a stimulatory host factor involved in influenza virus RNA synthesis, *J. Biol. Chem*. 277(47):45306-45314
- Morin M, Phaneuf JB., Sauvageau R, DiFranco F, Marsolais G, Boudreault A. 1981. An epizootic of swine influenza in Quebec. *Can. Vet. J*. 22: 204–205.
- Moser B, Clark-Lewis I, Zwahlen R, Baggiolini M. 1990.. Neutrophil-activating properties of the melanoma growth-stimulatory activity. *J Exp Med*. 171(5):1797-802.

- Mukaigawa J, Nayak DP. 1991. Two signals mediate nuclear localization of influenza virus (A/WSN/33) polymerase basic protein 2. *J Virol*. 65(1):245-53.
- Munier S, Larcher T, Cormier-Aline F, Soubieux D, Su B, Guigand L, Labrosse B, Cherel Y, Quere P, Marc D, Naffakh N. 2010. A genetically engineered waterfowl influenza virus with a deletion in the stalk of the neuraminidase has increased virulence for chickens. *J Virol* 84:940-952.
- Munster VJ, de Wit E, van Riel D, Beyer WE, Rimmelzwaan GF, Osterhaus AD, Kuiken T, Fouchier RA. 2007. The molecular basis of the pathogenicity of the Dutch highly pathogenic human influenza A H7N7 viruses. *J Infect Dis*. 196(2):258-65.
- Murakami Y, Nerome K, Yoshioka Y, Mizuno S, Oya A. 1988. Difference in growth behavior of human, swine, equine, and avian influenza viruses at a high temperature. *Arch Virol* 100:231-244.
- Murayama R, Harada Y, Shibata T, Kuroda K, Hayakawa S, Shimizu K, Tanaka T. 2007. Influenza A virus non-structural protein 1 (NS1) interacts with cellular multifunctional protein nucleolin during infection, *Biochem. Biophys. Res. Comm* 362:880-885
- Murray PJ. 2007. The JAK-STAT signaling pathway: input and output integration. *J Immunol*. 178(5):2623-9.
- Murti KG, Brown PS, Bean WJ Jr, Webster RG. 1992. Composition of the helical internal components of influenza virus as revealed by immunogold labeling/electron microscopy. *Virology*. 186(1):294-9.
- Muster T, Rajtarova J, Sachet M, Unger H, Fleischhacker R, Romirer I, Grassauer A, Url A, Garcia-Sastre A, Wolff K, Pehamberger H, Bergmann M. 2004. Interferon resistance promotes oncolysis by influenza virus NS1-deletion mutants. *Int J Cancer* 110:15-21.
- Nachamkin I, Shadomy SV, Moran AP, Cox N, Fitzgerald C, Ung H, Corcoran AT, Iskander JK, Schonberger LB, Chen RT. 2008. Anti-ganglioside antibody induction by swine (A/NJ/1976/H1N1) and other influenza vaccines: insights into vaccine-associated Guillain-Barré syndrome. *J Infect Dis* 198:226–233
- Naffakh N, Massin P, Escriou N, Crescenzo-Chaigne B, van der Werf S. 2000. Genetic analysis of the compatibility between polymerase proteins from human and avian strains of influenza A viruses. *J Gen Virol*. 81(Pt 5):1283-91.
- Nain M, Hinder F, Gong JH, Schmidt A, Bender A, Sprenger H, Gerns D. 1990. Tumor necrosis factor- α production of influenza A virus-infected macrophages and potentiating effect of lipopolysaccharides. *J Immunol*. 145(6):1921-8.
- Naito T, Momose F, Kawaguchi A, Nagata K. 2007. Involvement of Hsp90 in Assembly and Nuclear Import of Influenza Virus RNA Polymerase Subunits, *J. Virol* 81(3): 1339-1349
- Nakagawa Y, Kimura N, Toyoda T, Mizumoto K, Ishihama A, Oda K, Nakada S. 1995. The RNA polymerase PB2 subunit is not required for replication of the influenza virus genome but is involved in capped mRNA synthesis. *J Virol*. 69(2):728-33.
- Nakagawa Y, Oda K, Nakada S. 1996. The PB1 subunit alone can catalyze cRNA synthesis, and the PA subunit in addition to the PB1 subunit is required for viral RNA synthesis in replication of the influenza virus genome. *J Virol*. 70(9):6390-4.
- Nakamura K, Compans RW. 1978. Effects of glucosamine, 2-deoxyglucose, and tunicamycin on glycosylation, sulfation, and assembly of influenza viral proteins. *Virology* 84:303-319.
- Nardelli L, Pascucci S, Gualandi GL, Loda P. 1976. Outbreaks of classical swine influenza in Italy in 1976. *Zentralblatt fuer Veterinaermedizin B25*:853-857.
- Nayak DP, Hui EK, Barman S. 2004. Assembly and budding of influenza virus. *Virus Res*. 106(2):147-65.

- Nelson M, Spiro D, Wentworth D, Beck E, Fan J, Ghedin E, Halpin R, Bera J, Hine E, Proudfoot K, Stockwell T, Lin X, Griesemer S, Kumar S, Bose M, Viboud C, Holmes E, Henrickson K. 2009. The early diversification of influenza A/H1N1pdm. *PLoS Curr Influenza*. RRN1126.
- Nemeroff ME, Barabino SML, Li Y, Keller W, Krug RM. 1998. Influenza Virus NS1 Protein Interacts with the Cellular 30 kDa Subunit of CPSF and Inhibits 3' End Formation of Cellular pre-mRNAs, *Molec. Cell*. 1:991-1000
- Neumann G, Castrucci MR, Kawaoka Y. 1997. Nuclear import and export of influenza virus nucleoprotein. *J Virol*. 71(12):9690-700.
- Neumann G, Hughes MT, Kawaoka Y. *J Gen Virol*. 2000. Influenza A virus NS2 protein mediates vRNP nuclear export through NES-independent interaction with hCRM1. *EMBO J*. 19(24):6751-8.
- Neumann G, Kawaoka Y. 2006. Host Range Restriction and Pathogenicity in the Context of Influenza Pandemics, *Emerg. Infect. Dis*. 12(6):881-886
- Neumann G, Noda T, Kawaoka Y. 2009. Emergence and pandemic potential of swine-origin H1N1 influenza virus. *Nature*. 459(7249):931-9.
- Neumeier E, Meier-Ewert H, Cox NJ. 1994. Genetic relatedness between influenza A (H1N1) viruses isolated from humans and pigs. *J Gen Virol* 75 (Pt 8):2103-2107.
- Newcomb LL, Kuo RL, Ye Q, Jiang Y, Tao YJ, Krug RM. 2009. Interaction of the influenza A virus nucleocapsid protein with the viral RNA polymerase potentiates unprimed viral RNA replication. *J Virol*. 83(1):29-36.
- NIAID (2009) The Flu Types – Seasonal, Pandemic, Avian, Swine.
<http://www3.niaid.nih.gov/topics/Flu/understandingFlu/definitionsOverview.htm>, Accessed at 15 Dec 2009.
- Nieto A, de la Luna S, Bárcena J, Portela A, Ortín J. 1994. Complex structure of the nuclear translocation signal of influenza virus polymerase PA subunit. *J Gen Virol*. 75 (Pt 1):29-36.
- Nishikawa F, Sugiyama T. Direct isolation of H1N2 recombinant virus from a throat swab of a patient simultaneously infected with H1N1 and H3N2 influenza A viruses. *J Clin Microbiol* 18:425–7.
- Noble S, Dimmock NJ. 1995. Characterization of putative defective interfering (DI) A/WSN RNAs isolated from the lungs of mice protected from an otherwise lethal respiratory infection with influenza virus A/WSN (H1N1): a subset of the inoculum DI RNAs. *Virology* 210:9-19.
- Nobusawa E, Aoyama T, Kato H, Suzuki Y, Tateno Y, Nakajima K. 1991. Comparison of complete amino acid sequences and receptor-binding properties among 13 serotypes of hemagglutinins of influenza A viruses. *Virology*. 182(2):475-85.
- Noda T, Sagara H, Yen A, Takada A, Kida H, Cheng RH, Kawaoka Y. 2006. Architecture of ribonucleoprotein complexes in influenza A virus particles. *Nature*. 439(7075):490-2.
- Noton SL, Medcalf E, Fisher D, Mullin AE, Elton D, Digard P. 2007. Identification of the domains of the influenza A virus M1 matrix protein required for NP binding, oligomerization and incorporation into virions. *Gen Virol*. 88(Pt 8):2280-90.
- Novel Swine-Origin Influenza A (H1N1) Virus Investigation Team, Dawood FS, Jain S, Finelli L, Shaw MW, Lindstrom S, Garten RJ, Gubareva LV, Xu X, Bridges CB, Uyeki TM. 2009. Emergence of a novel swine-origin influenza A (H1N1) virus in humans. *N Engl J Med*. 360(25):2605-15.
- Nussbaum O, Rott R, Loyter A. 1992. Fusion of influenza virus particles with liposomes: requirement for cholesterol and virus receptors to allow fusion with and lysis of neutral but not of negatively charged liposomes. *J Gen Virol* 73 (11):2831-2837.
- O'Neill RE, Palese P. 1995. NPI-1, The Human Homolog of SRP-1, interacts with influenza virus nucleoprotein, *Virol*. 206:116-125

- O'Neill, Talon RE, Palese P. 1998. The influenza virus NEP (NS2 protein) mediates the nuclear export of viral ribonucleoproteins, *Embo J.* 17(1):288-296
- Obayashi E, Yoshida H, Kawai F, Shibayama N, Kawaguchi A, Nagata K, Tame JR, Park SY. 2008. The structural basis for an essential subunit interaction in influenza virus RNA polymerase. *Nature.* 454(7208):1127-31.
- Okada J, Ohshima N, Kubota-Koketsu R, Ota S, Takase W, Azuma M, Iba Y, Nakagawa N, Yoshikawa T, Nakajima Y, Ishikawa T, Asano Y, Okuno Y, Kurosawa Y. 2009. Monoclonal antibodies in man that neutralized H3N2 influenza viruses were classified into three groups with distinct strain specificity: 1968-1973, 1977-1993 and 1997-2003. *Virology.* 162:1093-1104
- Okazaki K, Kawaoka Y, Webster RG. 1989. Evolutionary pathways of the PA genes of influenza A viruses. *Virology* 172:601-608.
- O'Neill, R. E., Talon, J. & Palese, P. 1998. The influenza virus NEP (NS2 protein) mediates the nuclear export of viral ribonucleoproteins. *EMBO J* 17:288-296.
- Onomoto K, Yoneyama M, Fujita T, 2007, Regulation of antiviral innate immune responses by RIG-I family of RNA helicases, *Curr Top Microbiol Immunol.* 316:193-205
- Osterhaus AD, Rimmelzwaan GF, Martina BE, Bestebroer TM, Fouchier RA. 2000. Influenza B virus in seals. *Science.* 288 (5468): 1051-3
- Osterlund P, Pirhonen J, Ikonen N, Ronkko E, Strengell M, Makela SM, Broman M, Hamming OJ, Hartmann R, Ziegler T, Julkunen I. 2010. Pandemic H1N1 2009 influenza A virus induces weak cytokine responses in human macrophages and dendritic cells and is highly sensitive to the antiviral actions of interferons. *J Virol* 84:1414-1422.
- Paget WJ, Meerhoff TJ, Goddard NL. 2002. Mild to moderate influenza activity in Europe and the detection of novel A(H1N2) and B viruses during the winter of 2001-02. *Euro Surveill.* 7:147-157.
- Pahl HL, Baeuerle PA. 1995. Expression of influenza virus hemagglutinin activates transcription factor NF-kappa B. *J Virol.* 69(3):1480-4.
- Palese P, Racaniello VR, Desselberger U, Young J, Baez M. 1980. Genetic structure and genetic variation of influenza viruses. *Philos Trans R Soc Lond B Biol Sci* 288:299-305.
- Palese P, Schulman JL. 1976. Differences in RNA patterns of influenza A viruses. *J Virol.* 17(3):876-84.
- Palese P. 1977. The genes of influenza virus. *Cell* 10(1):1-10
- Palese P. 1980. New biochemical techniques for the characterization of viruses to assist the epidemiologist. *J Infect Dis* 142(4):633-635.
- Palm M, Leroy M, Thomas A, Linden A, Desmecht D. 2007. Differential anti-influenza activity among allelic variants at the *Sus scrofa* Mx1 locus, *J. Interferon Cytokine Res.* 2007(27): 147-155.
- Park YW, Wilusz J, Katze MG. 1999. Regulation of eukaryotic protein synthesis: Selective influenza viral mRNA translation is mediated by the nuclear RNA-binding protein GRSF-1, *Proc. Natl. Acad. Sci. USA* 96:6694-6699
- Patterson S, Gross J, Oxford JS. 1988. The intracellular distribution of influenza matrix protein and nucleoprotein in infected cells and their relationship to haemagglutinin in the plasma membrane, *J. Gen. Virol.* 69:1859-1872
- Pavlovic J, Haller O, Staeheli P. 1992. Human and mouse Mx proteins inhibit different steps of the influenza virus multiplication cycle. *J Virol.* 66(4):2564-9.
- Pearce J. 1971. Mechanism of action of amantadine. *Br Med J* 3:529.
- Peiris M, Yuen KY, Leung CW, Chan KH, Ip PL, Lai RW, Orr WK, Shortridge KF. 1999. Human infection with influenza H9N2. *Lancet* 354:916-917.

- Pensaert M, Ottis K, Vandeputte J, Kaplan MM, Bachmann PA. 1981. Evidence for the natural transmission of influenza A virus from wild ducts to swine and its potential importance for man. *Bull World Health Organ* 59:75-78.
- Perales B, de la Luna S, Palacios I, Ortín J. 1996. Mutational analysis identifies functional domains in the influenza A virus PB2 polymerase subunit. *J Virol*. 70(3):1678-86.
- Perez DR, Webby RJ, Hoffmann E, Webster RG. 2003. Land-based birds as potential disseminators of avian mammalian reassortant influenza A viruses. *Avian Dis*. 47(3 Suppl):1114-7.
- Pielak RM, Schnell JR, Chou JJ. 2009. Mechanism of drug inhibition and drug resistance of influenza A M2 channel. *Proc Natl Acad Sci U S A* 106:7379-7384.
- Pinto LH, Holsinger LJ, Lamb RA. 1992. Influenza virus M2 protein has ion channel activity. *Cell*. 69(3):517-528.
- Pirhonen J, Sareneva T, Kurimoto M, Julkunen I, Matikainen S. 1999. Virus infection activates IL-1 beta and IL-18 production in human macrophages by a caspase-1-dependent pathway. *J Immunol*. 162(12):7322-9.
- Plotch SJ, Bouloy M, Ulmanen I, Krug RM. 1981. A unique cap(m7GpppXm)-dependent influenza virion endonuclease cleaves capped RNAs to generate the primers that initiate viral RNA transcription. *Cell*. 23(3):847-58.]
- Poch O, Sauvaget I, Delarue M, Tordo N. 1989. Identification of four conserved motifs among the RNA-dependent polymerase encoding elements. *EMBO J*. 8(12):3867-74
- Poole E, Elton D, Medcalf L, Digard P. 2004. Functional domains of the influenza A virus PB2 protein: identification of NP- and PB1-binding sites. *Virology*. 321(1):120-33.
- Poon LL, Pritlove DC, Fodor E, Brownlee GG. 1999. Direct evidence that the poly(A) tail of influenza A virus mRNA is synthesized by reiterative copying of a U track in the virion RNA template. *J Virol*. 73(4):3473-6.
- Portela A, Digard P. 2002. The influenza virus nucleoprotein: a multifunctional RNA-binding protein pivotal to virus replication. *J Gen Virol* 83:723-734.
- Pothlichet J, Chignard M, Si-Tahar M. 2008. Cutting edge: innate immune response triggered by influenza A virus is negatively regulated by SOCS1 and SOCS3 through a RIG-I/IFNAR1-dependent pathway. *J Immunol*. 180(4):2034-8.
- Puerta-Guardo H, Mosso C, Medina F, Liprandi F, Ludert JE, del Angel RM. 2010. Antibody-dependent enhancement of dengue virus infection in U937 cells requires cholesterol-rich membrane microdomains. *J Gen Virol* 91:394-403.
- Puthavathana P, Auewarakul P, Charoenying P.C, Sangsiriwut K, Pooruk P, Boonnak K, Khanyok R, Thawachsupha P, Kijphati R, Sawanpanyalert P. 2005. Molecular characterization of the complete genome of human influenza H5N1 virus isolates from Thailand, *J Gen Virol*. 86(Pt 2):423-33
- Qiu Y, Nemeroff M, Krug RM. 1995. The influenza virus NS1 protein binds to a specific region in human U6 snRNA and inhibits U6-U2 and U6-U4 snRNA interactions during splicing. *RNA*. 1(3):304-16.
- Rabadan R, Levine AJ, Krasnitz M. 2008. Non-random reassortment in human influenza A viruses. *Influenza Other Respi Viruses*. 2008 Jan;2(1):9-22.
- Racaniello, 2009, <http://www.virology.ws/2009/05/04/influenza-virus-attachment-to-cells/>. Accessed at 1st Jan 2010.
- Rameix-Welti MA, Tomoiu A, Dos Santos Afonso E, van der Werf S, Naffakh N. 2009. Avian Influenza A virus polymerase association with nucleoprotein, but not polymerase assembly, is impaired in human cells during the course of infection. *J Virol*. 83(3):1320-31.

- Reading PC., Tate MD, Pickett DL., Brooks AG. 2007. Glycosylation as a target for recognition of influenza viruses by the innate immune system. *Adv. Exp. Med. Biol.* 598:279–292.
- Rebouillat D, Hovanessian AG. 1999. The human 2',5'-oligoadenylate synthetase family: interferon-induced proteins with unique enzymatic properties. *J Interferon Cytokine Res.* 1999 19(4):295-308.
- Reemers SS, Groot Koerkamp MJ, Holstege FC, van Eden W, Vervelde L. 2009. Cellular host transcriptional responses to influenza A virus in chicken tracheal organ cultures differ from responses in in vivo infected trachea. *Vet Immunol Immunopathol.*
- Renauld JC, Houssiau F, Louahed J, Vink A, Van Snick J, Uyttenhove C. 1993. Interleukin-9. *Adv Immunol.* 54:79-97.
- Richardson JC, Akkina RK. 1991. NS2 protein of influenza virus is found in purified virus and phosphorylated in infected cells. *Arch Virol* 116(14):69-80
- Robb NC, Smith M, Vreede FT, Fodor E. 2009. NS2/NEP protein regulates transcription and replication of the influenza virus RNA genome. *J Gen Virol.* 90(Pt 6):1398-407.
- Roberts DH, Cartwright SF, Wibberley G. 1987. Outbreaks of classical swine influenza in pigs in England in 1986. *Vet Rec.* 1987 Jul 18;121(3):53-5.
- Roberts PC, Lamb RA, Compans RW. 1998. The M1 and M2 proteins of influenza A virus are important determinants in filamentous particle formation. *Virology.* 240(1):127-37.
- Robertson JS, Schubert M, Lazzarini RA. 1981. Polyadenylation sites for influenza virus mRNA. *J Virol.* 38(1):157-63.
- Rodriguez A, Perez-Gonzalez A, Nieto A. 2007. Influenza Virus Infection Causes Specific Degradation of the Largest Subunit of Cellular RNA Polymerase II. *J. Virol* 81(10):5315-5324
- Rogers GN, Paulson JC. 1983. Receptor determinants of human and animal influenza virus isolates: differences in receptor specificity of the H3 hemagglutinin based on species of origin, *Virology.* 127(2):361-73
- Ronni T, Matikainen S, Sareneva T, Melén K, Pirhonen J, Keskinen P, Julkunen I. 1997. Regulation of IFN- α /beta, MxA, 2',5'-oligoadenylate synthetase, and HLA gene expression in influenza A-infected human lung epithelial cells. *J Immunol.* 158(5):2363-74.
- Ronni T, Sareneva T, Pirhonen J, Julkunen I. 1995. Activation of IFN- α , IFN- γ , MxA, and IFN regulatory factor 1 genes in influenza A virus-infected human peripheral blood mononuclear cells. *J Immunol.* 154(6):2764-74.
- Rossman JS, Jing X, Leser GP, Balannik V, Pinto LH, Lamb RA. 2010. Influenza Virus M2 Ion Channel Protein is Necessary for Filamentous Virion Formation. *J Virol.* 32(2):2344-56
- Rothwell C, Lebreton A, Young Ng C, Lim JY, Liu W, Vasudevan S, Labow M, Gu F, Gaither LA. 2009. Cholesterol biosynthesis modulation regulates dengue viral replication. *Virology* 389:8-19.
- Russell CA, Jones TC, Barr IG, Cox NJ, Garten RJ, Gregory V, Gust ID, Hampson AW, Hay AJ, Hurt AC, de Jong JC, Kelso A, Klimov AI, Kageyama T, Komadina N, Lapedes AS, Lin YP, Mosterin A, Obuchi M, Odagiri T, Osterhaus AD, Rimmelzwaan GF, Shaw MW, Skepner E, Stohr K, Tashiro M, Fouchier RA, Smith DJ. 2008. The global circulation of seasonal influenza A (H3N2) viruses. *Science.* 320(5874):340-6.
- Rutherford MN, Hannigan GE, Williams BR. 1988. Interferon-induced binding of nuclear factors to promoter elements of the 2-5A synthetase gene. *EMBO J.* 7(3):751-9.
- Salomon R, Staeheli P, Kochs G, Yen HL, Franks J, Rehge JE, Webster RG, Hoffmann E. 2007. Mx1 gene protects mice against the highly lethal human H5N1 influenza virus. *Cell Cycle.* 6(19):2417-21

- Sarmiento L, Afonso CL, Estevez C, Wasilenko J, Pantin-Jackwood M. 2008. Differential host gene expression in cells infected with highly pathogenic H5N1 avian influenza viruses. *Vet Immunol Immunopathol.* 125(3-4):291-302.
- Sato M, Hata N, Asagiri M, Nakaya T, Taniguchi T, Tanaka N. 1998. Positive feedback regulation of type I IFN genes by the IFN-inducible transcription factor IRF-7. *FEBS Lett.* 441(1):106-10.
- Schmidt MF. 1982. Acylation of viral spike glycoproteins: a feature of enveloped RNA viruses. *Virology.* 116(1):327-38.
- Schmitt AP, Lamb RA. 2005. Influenza virus assembly and budding at the viral budzone. *Adv Virus Res.* 64:383-416.
- Scholtissek C, Bürger H, Bachmann PA, Hannoun C. 1983. Genetic relatedness of hemagglutinins of the H1 subtype of influenza A viruses isolated from swine and birds. *Virology.* 129(2):521-3.
- Scholtissek C, Stech J, Krauss S, Webster RG. 2002. Cooperation between the hemagglutinin of avian viruses and the matrix protein of human influenza A viruses. *J Virol.* 76(4):1781-6
- Scholtissek C. 1997. Molecular epidemiology of influenza. *Arch Virol Suppl.* 13:99-103.
- Schroeder C, Heider H, Moncke-Buchner E, Lin TI. 2005. The influenza virus ion channel and maturation cofactor M2 is a cholesterol-binding protein. *Eur Biophys.* 34:52-66.
- Sencer DJ, Millar JD. 2006. Reflections on the 1976 swine flu vaccination program. *Emerg Infect Dis* 12:29-33
- Seo SH, Webby R, Webster RG. 2004. No apoptotic deaths and different levels of inductions of inflammatory cytokines in alveolar macrophages infected with influenza viruses. *Virology* 329:270-279.
- Seo SH, Hoffmann E, Webster RG. 2002. Lethal H5N1 influenza viruses escape host anti-viral cytokine responses. *Nat Med.* 8(9):950-4
- Seo SH, Hoffmann E, Webster RG. 2004. The NS1 gene of H5N1 influenza viruses circumvents the host anti-viral cytokine responses. *Virus Res.* 103(1-2):107-13.
- Seyama T, Ko JH, Ohe M, Sasaoka N, Okada A, Gomi H, Yoneda A, Ueda J, Nishibori M, Okamoto S, Maeda Y, Watanabe T. 2006. Population research of genetic polymorphism at amino acid position 631 in chicken Mx protein with differential antiviral activity. *Biochem. Genet.* 44: 437-448.
- Sha B, Luo M. 1997. Structure of a bifunctional membrane-RNA binding protein, influenza virus matrix protein M1. *Nat Struct Biol.* 1997 Mar;4(3):239-44.
- Shangguan T, Siegel DP, Lear JD, Axelsen PH, Alford D, Bentz J. 1998. Morphological changes and fusogenic activity of influenza virus hemagglutinin. *Biophys J.* 74(1):54-62.
- Shapira SD, Gat-Viks I, Shum BO, Dricot A, de Grace MM, Wu L, Gupta PB, Hao T, Silver SJ, Root DE, Hill DE, Regev A, Hacohen N. 2009. A physical and regulatory map of host-influenza interactions reveals pathways in H1N1 infection. *Cell.* 2009 139(7):1255-67.
- Shapiro GI, Krug RM. 1988. Influenza virus RNA replication in vitro: synthesis of viral template RNAs and virion RNAs in the absence of an added primer. *J Virol.* 62(7):2285-90.
- Shaw M, Cooper L, Xu X, Thompson W, Krauss S, Guan Y, Zhou N, Klimov A, Cox N, Webster R, Lim W, Shortridge K, Subbarao K. 2002. Molecular changes associated with the transmission of avian influenza a H5N1 and H9N2 viruses to humans. *J Med Virol* 66:107-114.
- Shaw M, Cooper L, Xu X, Thompson W, Krauss S, Guan Y, Zhou N, Klimov A, Cox N, Webster R, Lim W, Shortridge K, Subbarao K. 2002. Molecular changes associated with the transmission of avian influenza a H5N1 and H9N2 viruses to humans. *J Med Virol.* 66(1):107-14.

- Shaw MW, Choppin PW, Lamb RA. 1983. A previously unrecognized influenza B virus glycoprotein from a bicistronic mRNA that also encodes the viral neuraminidase. *Proc Natl Acad Sci U S A* 80(16):4879-4883.
- Shaw MW, Lamb RA. 1984. A specific sub-set of host-cell mRNAs prime influenza virus mRNA synthesis. *Virus Res* 1(6):455-467
- Sheng M, Sala C.2001. PDZ domains and the organization of supramolecular complexes. *Annu. Rev. Neurosci.* 24, 1 - 29
- Shinya K, Ebina M, Yamada S, Ono M, Kasai N, Kawaoka Y. 2006. Avian flu: influenza virus receptors in the human airway. *Nature.* 440(7083):435-6.
- Shiraishi K, Mitamura K, Sakai-Tagawa Y, Goto H, Sugaya N, Kawaoka Y. 2003. High frequency of resistant viruses harboring different mutations in amantadine-treated children with influenza. *J Infect Dis* 188:57-61.
- Shogomori H, Futerman AH. 2001. Cholesterol depletion by methyl-beta-cyclodextrin blocks cholera toxin transport from endosomes to the Golgi apparatus in hippocampal neurons. *J Neurochem* 2001(78):991-999.
- Shope RE. 1931. Swine influenza. III. Filtration experiments and etiology. *J Exp Med* 1931;373-380
- Shortridge KF, Zhou NN, Guan Y, Gao P, Ito T, Kawaoka Y, Kodihalli S, Krauss S, Markwell D, Murti KG, Norwood M, Senne D, Sims L, Takada A, Webster RG. 1998. Characterization of avian H5N1 influenza viruses from poultry in Hong Kong. *Virology.* 252(2):331-42.
- Shortridge, K.F. and Webster, R.G., 1979. Geographical distribution of swine (Hsw1N1) and Hong Kong (H3N2) influenza virus variants in pigs in southeast Asia. *Intervirology* 11: 9-15.
- Sieczkarski SB, Whittaker GR. 2002. Influenza virus can enter and infect cells in the absence of clathrin-mediated endocytosis. *J Virol.* 76(20):10455-64.
- Sims LD, Domenech J, Benigno C, Kahn S, Kamata A, Lubroth J, Martin V, Roeder P. 2005. Origin and evolution of highly pathogenic H5N1 avian influenza in Asia. *Vet Rec.* 157(6):159-64.
- Skehel JJ, Hay AJ, Armstrong JA. 1978. On the mechanism of inhibition of influenza virus replication by amantadine hydrochloride. *J Gen Virol* 38:97-110.
- Skehel JJ, Stevens DJ, Daniels RS, Douglas AR, Knossow M, Wilson IA, Wiley DC. 1984. A carbohydrate side chain on hemagglutinins of Hong Kong influenza viruses inhibits recognition by a monoclonal antibody. *Proc Natl Acad Sci U S A.* 81(6):1779-83.
- Skehel JJ, Waterfield MD, McCauley JW, Elder K, Wiley DC. 1980. Studies on the structure of the haemagglutinin. *Philos Trans R Soc Lond B Biol Sci.* 288(1029):335-9.
- Skehel JJ, Wiley DC. 2000. Receptor binding and membrane fusion in virus entry, the influenza hemagglutinin. *Annu Rev Biochemistry.* 69:531-569
- Smith DJ, Lapedes AS, de Jong JC, Bestebroer TM, Rimmelzwaan GF, Osterhaus AD, Fouchier RA. 2004. Mapping the antigenic and genetic evolution of influenza virus. *Science.* 305(5682):371-6.
- Smith GJ, Vijaykrishna D, Bahl J, Lycett SJ, Worobey M, Pybus OG, Ma SK, Cheung CL, Raghvani J, Bhatt S, Peiris JS, Guan Y, Rambaut A. 2009. Origins and evolutionary genomics of the 2009 swine-origin H1N1 influenza A epidemic. *Nature* 459:1122-1125.
- Smith GJ, Vijaykrishna D, Bahl J, Lycett SJ, Worobey M, Pybus OG, Ma SK, Cheung CL, Raghvani J, Bhatt S, Peiris JS, Guan Y, Rambaut A. 2009. Origins and evolutionary genomics of the 2009 swine-origin H1N1 influenza A epidemic. *Nature* 459(7250):1122-5.
- Smith KA, Colvin CJ, Weber PS, Spatz SJ, Coussens PM. 2008. High titer growth of human and avian influenza viruses in an immortalized chick embryo cell line without the need for exogenous proteases. *Vaccine* 26:3778-3782.

Snyder MH, London WT, Maassab HF, Chanock RM, Murphy BR. 1990. A 36 nucleotide deletion mutation in the coding region of the NS1 gene of an influenza A virus RNA segment 8 specifies a temperature-dependent host range phenotype. *Virus Res* 15:69-83.

Solorzano A, Webby RJ, Lager KM, Janke BH, Garcia-Sastre A, Richt JA. 2005. Mutations in the NS1 protein of swine influenza virus impair anti-interferon activity and confer attenuation in pigs. *J Virol* (79):7535-7543.

Sprenger H, Meyer RG, Kaufmann A, Bussfeld D, Rischkowsky E, Gerns D. 1996. Selective induction of monocyte and not neutrophil-attracting chemokines after influenza A virus infection. *J Exp Med*. 184(3):1191-1196.

Steel J, Lowen AC, Pena L, Angel M, Solórzano A, Albrecht R, Perez DR, García-Sastre A, Palese P. 2009. Live attenuated influenza viruses containing NS1 truncations as vaccine candidates against H5N1 highly pathogenic avian influenza. *J Virol*. 83(4):1742-53.

Stetson DB, Medzhitov R. 2006. Type I interferons in host defense. *Immunity*. 25(3):373-81.

Stevens J, Corper AL, Basler CF, Taubenberger JK, Palese P, Wilson IA. 2004. Structure of the uncleaved human H1 hemagglutinin from the extinct 1918 influenza virus. *Science*. 303(5665):1866-70.

Stieneke-Gröber A, Vey M, Anglikar H, Shaw E, Thomas G, Roberts C, Klenk HD, Garten W. 1992. Influenza virus hemagglutinin with multibasic cleavage site is activated by furin, a subtilisin-like endoprotease. *EMBO J*. 11(7):2407-14.

Sturm-Ramirez KM, Ellis T, Bousfield B, Bissett L, Dyrting K, Rehg JE, Poon L, Guan Y, Peiris M, Webster RG. 2004. Reemerging H5N1 influenza viruses in Hong Kong in 2002 are highly pathogenic to ducks. *J Virol*. 78(9):4892-901.

Suarez DL, Perdue ML, Cox N, Rowe T, Bender C, Huang J, Swayne DE. 1998. Comparisons of highly virulent H5N1 influenza A viruses isolated from humans and chickens from Hong Kong. *J Virol*. 72(8):6678-88.

Suarez DL, Perdue ML. 1998. Multiple alignment comparison of the non-structural genes of influenza A viruses. *Virus Res*. 54(1):59-69.

Subbarao K, Klimov A, Katz J, Regnery H, Lim W, Hall H, Perdue M, Swayne D, Bender C, Huang J, Hemphill M, Rowe T, Shaw M, Xu X, Fukuda K, Cox N. 1998. Characterization of an avian influenza A (H5N1) virus isolated from a child with a fatal respiratory illness. *Science*. 279(5349):393-6.

Sugrue RJ, Belshe RB, Hay AJ. 1990. Palmitoylation of the influenza A virus M2 protein. *Virology*. 179(1):51-6.

Sugrue RJ, Hay AJ. 1991. Structural characteristics of the M2 protein of influenza A viruses: evidence that it forms a tetrameric channel. *Virology* 180:617-624.

Sui J, Hwang WC, Perez S, Wei G, Aird D, Chen LM, Santelli E, Stec B, Cadwell G, Ali M, Wan H, Murakami A, Yammanuru A, Han T, Cox NJ, Bankston LA, Donis RO, Liddington RC, Marasco WA. 2009. Structural and functional bases for broad-spectrum neutralization of avian and human influenza A viruses. *Nat Struct Mol Biol*. 16(3):265-73. Epub 2009 Feb 22.

Sumbayev VV, Yasinska IM. 2006. Role of MAP kinase-dependent apoptotic pathway in innate immune responses and viral infection. *Scand J Immunol*. 63(6):391-400.

Sun BJ, Nie P. 2004. Molecular cloning of the viperin gene and its promoter region from the mandarin fish *Siniperca chuatsi*. *Vet Immunol Immunopathol*. 101(3-4):161-70.

Sun L, Hemgard GV, Susanto SA, Wirth M. 2010. Caveolin-1 influences human influenza A virus (H1N1) multiplication in cell culture. *Virol J* 7:108.

Sun X, Whittaker GR. 2003. Role for influenza virus envelope cholesterol in virus entry and infection. *J Virol* 77:12543-12551.

- Sun Y, Qin K, Wang J, Pu J, Tang Q, Hu Y, Bi Y, Zhao X, Yang H, Shu Y, Liu J. 2011. High genetic compatibility and increased pathogenicity of reassortants derived from avian H9N2 and pandemic H1N1/2009 influenza viruses. *Proc Natl Acad Sci U S A*.
- Suzuki H, Saito R, Masuda H, Oshitani H, Sato M, Sato I. 2003. Emergence of amantadine-resistant influenza A viruses: epidemiological study. *J. Infect. Chemother.* 9:195–200.
- Suzuki T, Takahashi T, Saito T, Guo CT, Hidari KI, Miyamoto D, Suzuki Y. 2004. Evolutional analysis of human influenza A virus N2 neuraminidase genes based on the transition of the low-pH stability of sialidase activity. *FEBS Lett.* 557(1-3):228-32.
- Suzuki Y, Nei M. 2002. Origin and evolution of influenza virus hemagglutinin genes. *Mol Biol Evol.* 4:501-9.
- Szkopińska A, Plochocka D. 2005. Farnesyl diphosphate synthase; regulation of product specificity. *Acta Biochim Pol.* 52(1):45-55.
- Takahashi T, Suzuki Y, Nishinaka D, Kawase N, Kobayashi Y, Hidari KI, Miyamoto D, Guo CT, Shortridge KF, Suzuki T. 2001. Duck and human pandemic influenza A viruses retain sialidase activity under low pH conditions. *J. Biochem.* 130:279-283
- Takeda M, Leser GP, Russell CJ, Lamb RA. 2003. Influenza virus hemagglutinin concentrates in lipid raft microdomains for efficient viral fusion. *Proc Natl Acad Sci U S A.* 100(25):14610-7.
- Tanaka N, Nakanishi M, Kusakabe Y, Goto Y, Kitade Y, Nakamura KT. 2004. Structural basis for recognition of 2',5'-linked oligoadenylates by human ribonuclease L. *EMBO J.* 23(20):3929-38.
- Tarendeau F, Boudet J, Guilligay D, Mas PJ, Bougault CM, Boulo S, Baudin F, Ruigrok RW, Daigle N, Ellenberg J, Cusack S, Simorre JP, Hart DJ. 2007. Structure and nuclear import function of the C-terminal domain of influenza virus polymerase PB2 subunit. *Nat Struct Mol Biol.* 2007 Mar;14(3):229-33.
- Taubenberger JK, Morens DM. 2006. 1918 Influenza: the mother of all pandemics. *Emerg Infect Dis.* 2006 12(1):15-22.
- Taubenberger JK, Reid AH, Lourens RM, Wang R, Jin G, Fanning TG. 2007. Characterization of the 1918 influenza virus polymerase genes. *Nature* 437:889–893
- Thomas DB, Hodgson J, Riska PF, Graham CM. 1990. The role of the endoplasmic reticulum in antigen processing. N-glycosylation of influenza hemagglutinin abrogates CD4+ cytotoxic T cell recognition of endogenously processed antigen. *J Immunol* 144:2789-2794.
- Tomeczkowski J, Ludwig A, Kretzmer G. 1993. Effect of cholesterol addition on growth kinetics and shear stress sensitivity of adherent mammalian cells. *Enzyme Microb Technol* 15:849-853.
- Treanor JJ, Snyder MH, London WT, Murphy BR. 1989. The B allele of the NS gene of avian influenza viruses, but not the A allele, attenuates a human influenza A virus for squirrel monkeys. *Virology.* 1989 171(1):1-9.
- Tumpey TM, Belser JA. 2009. Resurrected pandemic influenza viruses. *Annu Rev Microbiol.* 63:79-98.
- Tumpey TM, Szretter KJ, Van Hoeven N, Katz JM, Kochs G, Haller O, García-Sastre A, Staeheli P. 2007. The Mx1 gene protects mice against the pandemic 1918 and highly lethal human H5N1 influenza viruses. *J Virol.* 81(19):10818-21.
- Uetani K, Hiroi M, Meguro T, Ogawa H, Kamisako T, Ohmori Y, Erzurum SC. 2008. Influenza A virus abrogates IFN-gamma response in respiratory epithelial cells by disruption of the Jak/Stat pathway. *Eur J Immunol.* 6:1559-73.
- Uyeki TM, Chong YH, Katz JM, Lim W, Ho YY, Wang SS, Tsang TH, Au WW, Chan SC, Rowe T, Hu-Primmer J, Bell JC, Thompson WW, Bridges CB, Cox NJ, Mak KH, Fukuda K. 2002. Lack of evidence for human-to-human transmission of avian influenza A (H9N2) viruses in Hong Kong, China 1999. *Emerg Infect Dis* 8:154-159.

- van Wielink R, Kant-Eenbergen HC, Harmsen MM, Martens DE, Wijffels RH, Coco-Martin JM. 2011. Adaptation of a Madin-Darby canine kidney cell line to suspension growth in serum-free media and comparison of its ability to produce avian influenza virus to Vero and BHK21 cell lines. *J Virol Methods* 171:53-60.
- Varghese JN, Laver WG, Colman PM. 1983. Structure of the influenza virus glycoprotein antigen neuraminidase at 2.9 Å resolution. *Nature* 303(5912):356-40.
- Veit M, Klenk HD, Kendal A, Rott R. 1991. The M2 protein of influenza A virus is acylated. *J Gen Virol.* 72 (Pt 6):1461-5.
- Veit M, Schmidt MF. 2006. Palmitoylation of influenza virus proteins. *Berl Munch Tierarztl Wochenschr.* 119(3-4):112-22.
- Viboud C, Tam T, Fleming D, Handel A, Miller MA, Simonsen L. 2006. Transmissibility and mortality impact of epidemic and pandemic influenza, with emphasis on the unusually deadly 1951 epidemic. *Vaccine.* 24(44-46):6701-7.
- Vines A, Wells K, Matrosovich M, Castrucci MR, Ito T, Kawaoka Y. 1998. The role of influenza A virus hemagglutinin residues 226 and 228 in receptor specificity and host range restriction. *J Virol.* 72(9):7626-31.
- Wagner E, Matrosovich M, Klenk H.D, 2002. Functional balance between hemagglutinin and neuraminidase in influenza virus infections. *Rev Med Virol* 12:159-166
- Wan H, Perez DR. 2007. Amino acid 226 in the hemagglutinin of H9N2 influenza viruses determines cell tropism and replication in human airway epithelial cells. *J Virol* 81:5181-5191.
- Wang P, Palese P, O'Neill RE. 1997. The NP1-1/NP1-3 (karyopherin alpha) binding site on the influenza A virus nucleoprotein NP is a nonconventional nuclear localization signal. *J Virol.* 71(3):1850-6.
- Wang W, Riedel K, Lynch P, Chien CY, Montelione GT, Krug RM. 1999. RNA binding by the novel helical domain of the influenza virus NS1 protein requires its dimer structure and a small number of specific basic amino acids. *RNA.* 5(2):195-205.
- Wang X, Hinson ER, Cresswell P. 2007. The interferon-inducible protein viperin inhibits influenza virus release by perturbing lipid rafts. *Cell Host Microbe.* 2(2):71-2.
- Wang X, Li M, Zheng H, Muster T, Palese P, Beg AA, Garcia-Sastre A.2002. Influenza A virus NS1 protein prevents activation of NF-kappaB and induction of alpha/beta interferon. *J Virol.* 74(24):11566-73.
- Ward AC, Castelli LA, Lucantoni AC, White JF, Azad AA, Macreadie IG. 1995. Expression and analysis of the NS2 protein of influenza A virus. *Arch Virol.* 140(11):2067-73.
- Watanabe M, Fukuda M, Yoshida M, Yanagida M, Nishida E. 1999. Involvement of CRM1, a nuclear export receptor, in mRNA export in mammalian cells and fission yeast. *Genes Cells.* 4(5):291-7.
- Wathelet MG, Lin CH, Parekh BS, Ronco LV, Howley PM, Maniatis T. 1998. Virus infection induces the assembly of coordinately activated transcription factors on the IFN-beta enhancer in vivo. *Mol Cell.* 1(4):507-18.
- Weaver BK, Kumar KP, Reich NC. 1998. Interferon regulatory factor 3 and CREB-binding protein/p300 are subunits of double-stranded RNA-activated transcription factor DRAF1. *Mol Cell Biol.* 1998 Mar;18(3):1359-68.
- Webby RJ, Swenson SL, Krauss SL, Gerrish PJ, Goyal SM, Webster RG. 2000. Evolution of swine H3N2 influenza viruses in the United States. *J Virol.* 74(18):8243-51.
- Webby RJ, Webster RG. 2003. Are we ready for pandemic influenza? *Science.* 302(5650):1519-22.
- Weber F, Kochs G, Gruber S, Haller O. 1998. A classical bipartite nuclear localization signal on hogoto and influenza A virus nucleoproteins. *Virology.* 250(1):9-18.

- Webster RG, Bean WJ, Gorman OT, Chambers TM, Kawaoka Y. 1992. Evolution and Ecology of Influenza A Viruses, *Microbiol. Rev.* 56 (1):152-179
- Webster RG, Brown LE, Laver WG. 1984. Antigenic and biological characterization of influenza virus neuraminidase (N2) with monoclonal antibodies. *Virology.* 135(1):30-42.
- Webster RG, Hinshaw VS, Bean WJ, Jr., Turner B, Shortridge KF. 1977. Influenza viruses from avian and porcine sources and their possible role in the origin of human pandemic strains. *Dev Biol Stand* 39:461-468
- Webster RG, Kawaoka Y. 1988. Avian influenza. *Crit Rev Poult Biol* 1:211-246
- Webster RG, Yakhno M, Hinshaw VS, Bean WJ, Murti KG. 1978. Intestinal influenza: replication and characterization of influenza viruses in ducks. *Virology* 84: 268-278.
- Weis WI, Cusack SC, Brown JH, Daniels RS, Skehel JJ, Wiley DC. 1990. The structure of a membrane fusion mutant of the influenza virus haemagglutinin. *EMBO J.* 9(1):17-24.
- Whelan JA, Russell NB, Whelan MA. 2003. A method for the absolute quantification of cDNA using real-time PCR. *J Immunol Methods.* 278(1-2):261-9.
- WHO. 2009. Pandemic (H1N1) 2009 – update 72. Accessed November 2, 2009.http://www.who.int/csr/don/2009_10_30/en/index.html.
- Wiley DC, Skehel JJ, Waterfield M. 1977. Evidence from studies with a cross-linking reagent that the haemagglutinin of influenza virus is a trimer. *Virology.* 79(2):446-8.
- Wiley DC, Skehel JJ. 1977. Crystallization and x-ray diffraction studies on the haemagglutinin glycoprotein from the membrane of influenza virus. *J Mol Biol.* 112(2):343-7.
- Wilson IA, Skehel JJ, Wiley DC. 1981. Structure of the haemagglutinin membrane glycoprotein of influenza virus at 3 Å resolution. *Nature* 289:366-373.
- Winter G, Fields S, Ratti G. 1981. The structure of two subgenomic RNAs from human influenza virus A/PR/8/34. *Nucleic Acids Res.* 9(24):6907-15.
- Woo PC, Tung ET, Chan KH, Lau CC, Lau SK, Yuen KY. 2010. J Infect Dis. Cytokine Profiles Induced by the Novel Swine-Origin Influenza A/H1N1 Virus: Implications for Treatment Strategies. *J. Infect. Dis.* 43:1033-45
- Wood GW, McCauley JW, Bashiruddin JB, Alexander DJ. 1993. Deduced amino acid sequences at the haemagglutinin cleavage site of avian influenza A viruses of H5 and H7 subtypes. *Arch Virol.* 130(1-2):209-17.
- Wood L, Brockman S, Harkness JW, Edwards S. 1988. Classical swine fever: virulence and tissue distribution of a 1986 English isolate in pigs. *Vet. Rec.* 122 : 391–394.
- Wreschner DH, McCauley JW, Skehel JJ, Kerr IM. 1981. Interferon action--sequence specificity of the ppp(A2'p)nA-dependent ribonuclease. *Nature.* 289(5796):414-7.
- Wu R, Sui ZW, Zhang HB, Chen QJ, Liang WW, Yang KL, Xiong ZL, Liu ZW, Chen Z, Xu DP. 2007. Characterization of a pathogenic H9N2 influenza A virus isolated from central China in 2007. *Arch. Virol.* 153:1549–1555
- Wu WW, Sun YH, Panté N. 2007. Nuclear import of influenza A viral ribonucleoprotein complexes is mediated by two nuclear localization sequences on viral nucleoprotein. *Virol J.* 4:4:49.
- Wurzer WJ, Planz O, Ehrhardt C, Giner M, Silberzahn T, Pleschka S, Ludwig S. 2003. Caspase 3 activation is essential for efficient influenza virus propagation. *EMBO J.* 22(11):2717-28.
- Xing Z, Cardona CJ, Li J, Dao N, Tran T, Andrada J. 2008. Modulation of the immune responses in chickens by low-pathogenicity avian influenza virus H9N2. *J Gen Virol* 89(Pt 5):1288-99.

- Xu KM, Smith GJ, Bahl J, Duan L, Tai H, Vijaykrishna D, Wang J, Zhang JX, Li KS, Fan XH, Webster RG, Chen H, Peiris JS, Guan Y. 2007. The Genesis and evolution of H9N2 influenza viruses in poultry from southern China, 2000–2005. *J. Virol.* 81:10389–10401
- Xu R, McBride R, Paulson JC, Basler CF, Wilson IA. 2010. Structure, receptor binding and antigenicity of influenza virus hemagglutinins from the 1957 H2N2 pandemic. *J Virol.* 45(8):545-51
- Xu R, Wilson IA. 2011. Structural characterization of an early fusion intermediate of influenza virus hemagglutinin. *J Virol.*
- Xu X, Rocha EP, Regnery HL, Kendal AP, Cox NJ. 1993. Genetic and antigenic analysis of influenza A (H1N1) viruses, 1986–1991. *Virus Res* 1993; 28:37–55.
- Yamada H, Chounan R, Higashi Y, Kurihara N, Kido H. 2004. Mitochondrial targeting sequence of the influenza A virus PB1-F2 protein and its function in mitochondria. *FEBS Lett.* 2004(578):331–336.
- Yamaguchi M, Danev R, Nishiyama K, Sugawara K, Nagayama K. 2007. Zernike phase contrast electron microscopy of ice-embedded influenza A virus. *J Struct Biol.* 162:271–276
- Yamanaka K, Ishihama A, Nagata K. 1990. Reconstitution of influenza virus RNA-nucleoprotein complexes structurally resembling native viral ribonucleoprotein cores, *J Biol Chem.* 265(19):11151-5
- Yamane N, Arikawa J, Odagiri T, Kumasaka M, Ishida N. 1978. Distribution of antibodies against swine and Hong Kong influenza viruses among pigs in 1977. *Tohoku J. Experimental Med.* 126: 199–200.
- Yamane N, Arikawa J, Odagiri T. 1978. Isolation of three different influenza A viruses from an individual after probable double infection with H3N2 and H1N1 viruses. *Jpn J Med Sci Biol* 31:431–4.
- Yang XX, Du N, Zhou JF, Li Z, Wang M, Guo JF, Wang DY, Shu YL. 2010. Gene expression profiles comparison between 2009 pandemic and seasonal H1N1 influenza viruses in A549 cells. *Biomed Environ Sci* 23:259-266.
- Yap KL, Ada GL. 1978. Cytotoxic T cells in the lungs of mice infected with an influenza A virus. *Scand J Immunol.* 7(1):73-80.
- Yasuda J, Nakada S, Kato A, Toyoda T, Ishihama A. 1993. Molecular assembly of influenza virus: association of the NS2 protein with virion matrix. *Virology.* 196(1):249-55.
- Yeo DS, Chan R, Brown G, Ying L, Sutejo R, Aitken J, Tan BH, Wenk MR, Sugrue RJ. 2009. Evidence that selective changes in the lipid composition of raft-membranes occur during respiratory syncytial virus infection. *Virology* 386:168-182.
- Yip, TKS. 1976. Serological survey on the influenza antibody status in pigs of the Takwuling pig breeding centre. *Agric. Hong Kong* 2: 446–458.
- Yoneyama M, Suhara W, Fukuhara Y, Fukuda M, Nishida E, Fujita T. 1998. Direct triggering of the type I interferon system by virus infection: activation of a transcription factor complex containing IRF-3 and CBP/p300. *EMBO J.* 17(4):1087-95.
- Yoshimura A, Kuroda K, Kawasaki K, Yamashina S, Maeda T, Ohnishi S. 1982. Infectious cell entry mechanism of influenza virus. *J Virol.* 43(1):284-93.
- Yuan P, Bartlam M, Lou Z, Chen S, Zhou J, He X, Lv Z, Ge R, Li X, Deng T, Fodor E, Rao Z, Liu Y. 2009. Crystal structure of an avian influenza polymerase PA(N) reveals an endonuclease active site. *Nature.* 458(7240):909-13.
- Zamarin D, Garcia-Sastre A, Xiao X, Wang R, Palese P. 2005. Influenza virus PB1-F2 protein induces cell death through mitochondrial ANT3 and VDAC1. *PLoS Pathog.* 20: 13211-24
- Zamarin D, Ortigoza MB, Palese P. 2006. Influenza A virus PB1-F2 protein contributes to viral pathogenesis in mice. *J Virol.* 80(16):7976-83

- Zambon M and Hayden FG. 2001. Position statement: global neuraminidase inhibitor susceptibility network, *Antiviral Res* 49 2001: 147–156.
- Zebedee SL, Richardson CD, Lamb RA. 1985. Characterization of the influenza virus M2 integral membrane protein and expression at the infected-cell surface from cloned cDNA. *J Virol*. 56(2):502-11.
- Zhang J, Zhang Z, Fan X, Liu Y, Wang J, Zheng Z, Chen R, Wang P, Song W, Chen H, Guan Y. 2010. 2009 pandemic H1N1 influenza virus replicates in human lung tissues. *J Infect Dis* 201:1522-1526.
- Zhang W, Li H, Cheng G, Hu S, Li Z, Bi D. 2008. Avian influenza virus infection induces differential expression of genes in chicken kidney. *Res Vet Sci*. 2008 Jun;84(3):374-81
- Zhang XM, Herbst W, Lange-Herbst H, Schliesser T. 1989. Seroprevalence of porcine and human influenza A virus antibodies in pigs between 1986 and 1988 in Hesse. *Zentralbl Veterinärmed B*. 36(10):765-70.
- Zheng H, Lee HA, Palese P, García-Sastre A. 1999. Influenza A virus RNA polymerase has the ability to stutter at the polyadenylation site of a viral RNA template during RNA replication. *J Virol*. 73(6):5240-3.
- Zhou A, Paranjape J, Brown TL, Nie H, Naik S, Dong B, Chang A, Trapp B, Fairchild R, Colmenares C, Silverman RH. 1997. Interferon action and apoptosis are defective in mice devoid of 2',5'-oligoadenylate-dependent RNase L. *EMBO J*. 16(21):6355-63.
- Zhou H, Yu Z, Hu Y, Tu J, Zou W, Peng Y, Zhu J, Li Y, Zhang A, Ye Z, Chen H, Jin M. 2009. The special neuraminidase stalk-motif responsible for increased virulence and pathogenesis of H5N1 influenza A virus. *PLoS One* 4:e6277.
- Zhu H, Cong JP, Shenk T. 1997. Use of differential display analysis to assess the effect of human cytomegalovirus infection on the accumulation of cellular RNAs: induction of interferon-responsive RNAs. *Proc Natl Acad Sci U S A*. 94(25):13985-90.
- Zlotnik A, Yoshie O. 2000. Chemokines: a new classification system and their role in immunity. *Immunity*. 12(2):121-7.

Publication List

Sutejo R* , Yeo DS*, Li L, Myint ZM, Tan BH; Sugrue RJ, Characterization of low pathogenic avian influenza A virus isolated in Singapore, 2011 (Submitted to PLoS Pathogen)

Sutejo R*, Ko DH* , Yeo DS, , Li L, Tan BH, Sugrue RJ, Characterization of 2009/H1N1 swine influenza A virus isolated in Singapore, 2011 (Manuscript in Preparation)

Yeo DS, **Sutejo R**, Li L, Sivalingam SP, Ruedl C, Tan BH, Sugrue, RJ, The host response to low pathogenic avian influenza virus infection in murine lung macrophages, 2011 (Submitted to Journal of General Virology)

*). Co-first author

Appendix

1. The Primer used for viral kinetics PCR Amplification and Sequencing (Hoffmann *et al.*, 2001)

Gene	Forward primer	Reverse primer
PB2	Ba-PB2-1: <u>TATTGGTCTCAGGGAGCGAAAGCAGGTC</u>	Ba-PB2-2341R: <u>ATATGGTCTCGTATTAGTAGAAACAAGGTCGTTT</u>
PB1	Bm-PB1-1: <u>TATTCGTCTCAGGGAGCGAAAGCAGGCA</u>	Bm-PB1-2341R: <u>ATATCGTCTCGTATTAGTAGAAACAAGGCATTT</u>
PA	Bm-PA-1: <u>TATTCGTCTCAGGGAGCGAAAGCAGGTAC</u>	Bm-PA-2233R: <u>ATATCGTCTCGTATTAGTAGAAACAAGGTACTT</u>
HA	Bm-HA-1: <u>TATTCGTCTCAGGGAGCAAAAGCAGGGG</u>	Bm-NS-890R: <u>ATATCGTCTCGTATTAGTAGAAACAAGGGTGTTTT</u>
NP	Bm-NP-1: <u>TATTCGTCTCAGGGAGCAAAAGCAGGGTA</u>	Bm-NP-1565R: <u>ATATCGTCTCGTATTAGTAGAAACAAGGGTATTTTT</u>
NA	Ba-NA-1: <u>TATTGGTCTCAGGGAGCAAAAGCAGGAGT</u>	Ba-NA-1413R: <u>ATATGGTCTCGTATTAGTAGAAACAAGGAGTTTTTT</u>
M	Bm-M-1: <u>TATTCGTCTCAGGGAGCAAAAGCAGGTAG</u>	Bm-M-1027R: <u>ATATCGTCTCGTATTAGTAGAAACAAGGTAGTTTTT</u>
NS	Bm-NS-1: <u>TATTCGTCTCAGGGAGCAAAAGCAGGGTG</u>	Bm-NS-890R: <u>ATATCGTCTCGTATTAGTAGAAACAAGGGTGTTTT</u>

Table 1a. Additional Primer used for H9N2 sequencing

Gene	Primer	Sequence
HA	H9-HA-328F	GGTCCTATATTGTCGAAAG
PA	H9-PA-528F	ACCCTTGATGAAGAGAGCAG
PB1	H9-PB1-586F	CACATTTCCAGAGAAAGA
	H9-PB1-739R	TCTTTCTGCATCCTTTATCAT
	H9-PB1-1736F	GCAGATTCAAACGAGAAGAT
	H9-PB1-1872R	TCAAGCAGACCTCCGGAATGTG
PB2	H9-PB2-88F	CGCACTCGCGAGATACTG
	H9-PB2-757R	TTCCTTGAGTCAAATGCAATA
	H9-PB2-1495F	GGGTGGATGAATATTCTA
	H9-PB2-1666R	CCGTTAATCTCCCACATCATA

2. The Primer used for viral kinetics qRT-PCR Analysis

2.a H1N1

Gene-Position	Sequence (5'3')	UPL Sequence (UPL #)
PB2 Forw.	TCCGCAGTTCTGAGAGGATT	CTGGGCAA (61)
PB2 Rev.	TGCTGGTCCATACTCCTGTC	
PB1 Forw.	GCTCCAATAATGTTCTCAAACAAA	ACTGGGAA (48)
PB1 Rev.	TCTTGCTCAAACATGTACCC	
PA Forw.	CGGAAAAGGCAATGAAAGAG	GGAGAGGA (55)
PA Rev.	CTGCAAATTTGTTTGTTCGAT	
HA Forw.	GCAAGGCCCAAAGTAAGAGA	GGAGGATG (88)
HA Rev.	TTGTGTCTCCGGTTCTAGC	
NP Forw.	TGGAATCAAGTACCCTTGAACCTG	GGACCAGA (93)
NP Rev.	GCCCTCTGTTGATTGGTGTT	
NA Forw.	ATGGAATGGGCTGGCTAAC	TCTGGTCC (93)
NA Rev.	ATACAGCCACTGCTCCATCA	
M Forw.	AGATGAGTCTTCTAACCAGAGGTCG	FAM-TCAGGCCCCCTCAAAGCCGA-TAMRA
M Rev.	TGCAAAAACATCTTCAAGTCTCTG	
NS Forw.	AGCACTCTCGGTCTGGACAT	CAGCCACC (83)
NS Rev.	CCGCTCCACTATTTGCTTTC	

2.b H9N2

Gene-Position	Sequence (5'3')	UPL Sequence (UPL #)
PB2 Forw.	ACAAAAACCACTGTGGACCAT	CTGCTCTC (108)
PB2 Rev.	CATTGCCATCATCCATTICA	
PB1 Forw.	CTTGAAGTGGGAATTGATGGA	CCAGGGCA (37)
PB1 Rev.	ATGGGTTCTGAGGATTGCAC	
PA Forw.	AAAGCGGACTACACCCTTGA	GAGAGCAG (108)
PA Rev.	AGTGAACAGCCTGGTTTGTGATT	
HA Forw.	TCTGCAAGATCCATTGGACA	GAAGGCAG (8)
HA Rev.	CCTCATCTCTCGTGCTTGC	
NP Forw.	CCCGAAGAAAACCTGGAGGTC	GAAGGAGG (134)
NP Rev.	TCAGCTCTCTCATCCATTICC	
NA Forw.	CGATGAGGAATTCTATCATGTATTGT	TGCTGTCC (56)
NA Rev.	TACCCTTGGGCAGGGAAC	
M Forw.	AGATGAGTCTTCTAACCAGAGGTCG	FAM-TCAGGCCCCCTCAAAGCCGA-TAMRA
M Rev.	TGCAAAAACATCTTCAAGTCTCTG	
NS Forw.	TGGTCTGGACATCGAAACAG	CTGGAGGA (65)
NS Rev.	TCATTCTAAGTGCCTCATCAGACT	

2.c Host Genes

Host	Gene	Sequence (5'-3')	Probe Sequence
Canine	Mx1 Fw	GTACATCCTTAAGCAGGAGACGA	GGTGGTGG (#77)
	Mx1 Rv	GCAATGTCCACGTTGCAG	
	OAS1 Fw	TGGGACGTGCTGGTAAAC	GGAGGAAG (#69)
	OAS1 Rv	CGCTGTGTAGAGGGGTTAGG	
	RSAD2 Fw	AAAGCGGACTACACCTTGA	TTGCCAG (#61)
	RSAD2 Rv	CTCTTTCAGAACCTCACCA	
	IFNB Fw	ATCGAGAAATCACGCCAGTT	GAAGGAGG (#134)
	IFNB Rv	CTGGAACATCTCATGGGTGA	
	HMGR Fw	GAGCCATTTTGCTCGAGTTT	AGAAGAAGA (#143)
	HMGR Rv	CTCTCTGAGTAACAGGATTTGGTTT	
	EF Fw	GCTGGAAGATGGTCCCAAG	GGATGCTG (#89)
	EF Rv	TGCCAGGAACCATATCAACA	
Chicken	Mx Fw	GTTTCGGACATGGGGAGTAA	TCTCCAGG (#80)
	Mx Rv	GCATACGATTCTTCAACTTTGG	
	OASL Fw	CCAGTACCGGGACATCTGTATT	CTTCTCCC (#7)
	OASL Rv	CACCGACCACTCATCCT	
	IFNB Fw	AAGAAGCAAGCAGCCATCAC	GGAGGATG (#88)
	IFNB Rv	TGGGCTGCTAAGCATGTTG	
	EF Fw	TGCACCATGAAGCCCTTAG	CTCTGCCT (#13)
	EF Rv	TCTTGACATTGAAGCCAACG	
Human	Mx1 Fw	TCCAGCCACCATTCCAAG	TTCTCCTG (#2)
	Mx1 Rv	CAACAAGTTAAATGGTATCACAGAGC	
	OAS1 Fw	GGTGGAGTTCGATGTGCTG	CCAGGGCA (#37)
	OAS1 Rv	AGGTTTATAGCCGCCAGTCA	
	OAS2 Fw	CCTGCCTTTAATGCACTGG	CTGGCTCC (#36)
	OAS2 Rv	ATGAGCCCTGCATAAACCTC	
	BIRC Fw	CCTGCCGATCCTAAATCAAC	CAGGAGAA (#2)
	BIRC Rv	TTTCCTTTTGATGAAGCTAACCA	
	HMGR Fw	GAGCCATTTTGCTCGAGTTT	AGAAGAAGA (#85)
	HMGR Rv	CTCTCTGAGTAACAGGATTTGGTTT	
	RSAD2 Fw	TGCTTTTGCTTAAGGAAGCTG	AGGTGGAG (#39)
	RSAD2 Rv	TCCCCGGTCTTGAAGAAAT	
	IFNB Fw	CTTTGCTATTTTCAGACAAGATTCA	CTGGCTGG (#20)
	IFNB Rv	GCCAGGAGGTTCTCAAGAAT	
	IL6 Fw	GATGAGTACAAAAGTCTGATCCA	GCCTGCTG (#40)
	IL6 Rv	CTGCAGCCACTGGTTCTGT	
	IL28 Fw	CCTGGTGGACGTCTTGGA	CTGGGAGA (#14)
	IL28 Rv	GTGGGCTGAGGCTGGATA	
	CCL5 Fw	ACACAGTGGCAAGTGCTC	CTGCTGGG (#3)
	CCL5 Rv	ACACACTGGCGGTTCTTTC	
	EF Fw	TGGGAGGGTTGCTTTGATTA	ACACTGGA (#47)
	EF Rv	TGACAGGCAATCAGCAACAT	
Mouse	OAS2 Fw	GGCCCAGGACTTGAGCTAC	CTCTGCCT (#13)
	OAS2 Rv	CCATCGTTGCTAGCTGGTCT	
	OASL Fw	GTGGGGAGACTGCATCCTTA	GGCAGAAG (#29)
	OASL Rv	GCAGGGAGATCCAGTTTACCT	
	IFNB Fw	CTGGCTTCCATCATGAACAA	TCCTGCTG (#18)
	IFNB Rv	AGAGGGCTGTGGTGGAGAA	
	HMGR Fw	CGTAAGCGCAGTTCCTTCC	GGCTGGAG (#19)
	HMGR Rv	TCTCAATGGAGGCCAAGC	
	EF Fw	ACACGTAGATTCCGGCAAGT	TGGTGGAA (#31)
	EF Rv	ACTTTTCGATGGTTCGCTTG	

3. Upregulation of probe sets in MDCK cells at 10 hpi

Cytokine

Gene Symbol	Description	H1N1	H9N2
CCL5	chemokine (C-C motif) ligand 5	14.9	141
CXCL10	chemokine (C-X-C motif) ligand 10	21.4	32.9
CXCL10	chemokine (C-X-C motif) ligand 10	16.5	49.6

Innate/Antiviral

Gene Symbol	Description	H1N1	H9N2
LOC477402	similar to Nuclear autoantigen Sp-100 (Speckled 100 kDa) (Nuclear dot-associated Sp100 protein) (Lysp100b)	-	2.4
LOC478170	similar to interferon induced 6-16 protein isoform a	-	10.4
LOC478170	similar to interferon induced 6-16 protein isoform a	-	15.4
LOC478406	SON DNA binding protein	-	6.8
LOC479183	interferon-induced protein with tetratricopeptide repeats 2	20.2	-
LOC479402	sperm autoantigenic protein 17	-	2.4
LOC479575	ISG15 ubiquitin-like modifier	16.5	4.2
LOC479575	ISG15 ubiquitin-like modifier	12.9	-
LOC479980	interferon-induced protein 44-like	4.9	2.5
LOC479980	interferon-induced protein 44-like	9.2	2.6
LOC479980	interferon-induced protein 44-like	-	2.9
LOC481471	similar to interferon gamma inducible protein 47	-	5.1
LOC483406	similar to Interferon regulatory factor 7 (IRF-7)	2.1	3.5
LOC488122	receptor (chemosensory) transporter protein 4	20.7	-
LOC488729	interferon stimulated exonuclease gene 20kDa	-	5.2
LOC488947	interferon-induced protein with tetratricopeptide repeats 1	20.9	29.2
LOC490198	interferon-induced protein 44	3.4	-
LOC490198	interferon-induced protein 44	4.5	-
LOC490461	S100 calcium binding protein A8	-	3.2
LOC490954	interferon-induced protein 35	-	2.1
LOC490954	interferon-induced protein 35	-	2.5
LOC490954	interferon-induced protein 35	-	3.0
LOC490954	interferon-induced protein 35	-	3.1
LOC606875	similar to immunity-related GTPase family, cinema 1	-	5.1
LOC609006	UIM domain only 2 (rhombotin-like 1)	-	4.2
MX1	myxovirus (influenza virus) resistance 1, interferon-inducible protein p78 (mouse)	10.9	5.4
MX2	myxovirus (influenza virus) resistance 2 (mouse)	-	5.2
RSAD2	similar to radical S-adenosine containing 2	19.5	8.6

4. Upregulation of probe sets in CEF cells at 10 hpi

Cytokine

Gene Symbol	Description	H1N1	H9N2
CCL20	chemokine (C-C motif) ligand 20	15.0	3.8
IL12B	interleukin 12B (natural killer cell stimulatory factor 2, cytotoxic lymphocyte maturation factor 2, p40)	19.3	-
IL1B	interleukin 1, beta	4.2	-
IL6	interleukin 6 (interferon, beta 2)	2.7	-
IL6	interleukin 6 (interferon, beta 2)	16.7	-
IL8	interleukin 8	10.6	2.2
IRF1	interferon regulatory factor 1	30.6	2.5
IRF10	interferon regulatory factor 10	9.9	-
IRF7	interferon regulatory factor 7	15.5	11.0
IRF8	interferon regulatory factor 8	4.0	-
K203	chemokine K203	9.1	-
LOC395551	Chemokine (C-C motif) ligand 3	4.7	-

Innate/Antiviral

Gene Symbol	Description	H1N1	H9N2
B2M	beta-2 microglobulin	3.5	-
EIF2AK2 (PKR)	eukaryotic translation initiation factor 2-alpha kinase 2	5.0	-
IFI35	interferon-induced protein 35	5.3	-
IFIH1	interferon induced with helicase C domain 1	8.1	-
IFIH1	interferon induced with helicase C domain 1	18.4	-
ISG12-2	putative ISG12-2 protein	55.5	3.2
K60	K60 protein	8.7	3.8
LOC396216	mature cMGF	24.0	3.0
LOC415651	similar to Small inducible cytokine A2 precursor (CCL2)	3.6	-
LOC417053	similar to class I alpha chain	3.4	-
LOC429220	similar to MHC Rfp-Y class I alpha chain	2.1	2.1
LOC420302	similar to prostate stem cell antigen	-	3.3
LOC420559	similar to KIAA2005 protein	41.2	-
IFIH-1	similar to interferon induced protein with tetratricopeptide repeat 1	651.0	-
LY6E	lymphocyte antigen 6 complex, locus E	5.7	-
MX	Mx protein	193.3	11.0
NFKBIZ	nuclear factor of kappa light polypeptide gene enhancer in B-cells inhibitor, zeta	4.0	-
OASL	2'-5'-oligoadenylate synthetase-like	143.8	15.8
PBEF1	pre-B-cell colony enhancing factor 1	4.0	-
SOCS1	suppressor of cytokine signaling 1	4.7	-

TLR3	toll-like receptor 3	19.1	3.8
VCAM1	vascular cell adhesion molecule 1	15.9	-
ZC3HAV1	zinc finger CCCH-type, antiviral 1	24.3	-
ZC3HAV1	zinc finger CCCH-type, antiviral 1	10.4	-
ZC3HAV1	zinc finger CCCH-type, antiviral 1	30.2	-

Cell Death

Gene Symbol	Description	H1N1	H9N2
LOC421684	similar to Tumor necrosis factor, alpha-induced protein 3 (Putative DNA binding protein A20) (Zinc finger protein A20)	2.9	5.0
LOC427122	similar to Adipocyte-derived leucine aminopeptidase precursor (A-LAP) (ARTS-1)	3.9	-
LOC427122	similar to Adipocyte-derived leucine aminopeptidase precursor (A-LAP) (ARTS-1)	3.4	-
LOC427224	similar to programmed cell death 1 ligand 1	10.9	-
TNFSF15	tumor necrosis factor (ligand) superfamily, member 15	3.6	-

5. Upregulation of probe sets in A549 cells at 10 hpi

Cytokine

Gene Symbol	Description	H1N1	H9N2
CCL5	chemokine (C-C motif) ligand 5 ; chemokine (C-C motif) ligand 5	5.8	13.9
CCL5	chemokine (C-C motif) ligand 5	23.4	20.6
CCL5	chemokine (C-C motif) ligand 5	49.6	21.5
CXCL10	chemokine (C-X-C motif) ligand 10	-	34.4
CXCL11	chemokine (C-X-C motif) ligand 11	2.4	10.0
CXCL11	chemokine (C-X-C motif) ligand 11	-	75.8
IFRG28	28kD interferon responsive protein	-	64.0
IL22RA1	interleukin 22 receptor, alpha 1	-	2.1
IL28A	interleukin 28A (interferon, lambda 2)	20.9	76.7
IL28A ; IL28B	interleukin 28A (interferon, lambda 2) ; interleukin 28B (interferon, lambda 3)	10.9	142.0
IL29	interleukin 29 (interferon, lambda 1)	7.4	48.1
IL6	interleukin 6 (interferon, beta 2)	-	5.7
IL7	interleukin 7	-	33.6
TLR3	toll-like receptor 3	-	10.8

Innate/Antiviral

Gene Symbol	Description	H1N1	H9N2
ACE2	angiotensin I converting enzyme (peptidyl-dipeptidase A) 2	-	11.8
BLNK	B-cell linker	-	9.2
BTG1	B-cell translocation gene 1, anti-proliferative	-	2.5
CD38	CD38 antigen (p45)	-	5.8
CEACAM1	carcinoembryonic antigen-related cell adhesion molecule 1 (biliary glycoprotein)	-	3.1
CEACAM1	carcinoembryonic antigen-related cell adhesion molecule 1 (biliary glycoprotein)	-	5.9
CEACAM1	carcinoembryonic antigen-related cell adhesion molecule 1 (biliary glycoprotein)	-	9.0
DDX58 (RIG-I)	DEAD (Asp-Glu-Ala-Asp) box polypeptide 58	-	6.9
DDX58 (RIG-I)	DEAD (Asp-Glu-Ala-Asp) box polypeptide 58	-	16.5
DDX58 (RIG-I)	DEAD (Asp-Glu-Ala-Asp) box polypeptide 58	2.9	16.1
ETS2	v-ets erythroblastosis virus E26 oncogene homolog 2 (avian)	-	2.1
G1P2	interferon, alpha-inducible protein (clone IFI-15K)	10.9	10.5
G1P3	interferon, alpha-inducible protein (clone IFI-6-16)	27.1	3.9
GBP1	guanylate binding protein 1, interferon-inducible, 67kDa ; guanylate binding protein 1, interferon-inducible, 67kDa	6.0	14.5
GBP1	guanylate binding protein 1, interferon-inducible, 67kDa	17.4	24.5
GBP1	guanylate binding protein 1, interferon-inducible, 67kDa ; guanylate binding protein 1, interferon-inducible, 67kDa	21.8	23.4
GBP2	guanylate binding protein 2, interferon-inducible	-	5.2

HLA-E	major histocompatibility complex, class I, E	-	2.6
IFI16	interferon, gamma-inducible protein 16	4.8	7.9
IFI16	interferon, gamma-inducible protein 16	3.9	10.7
IFI16	interferon, gamma-inducible protein 16	3.0	9.7
IFI27	interferon, alpha-inducible protein 27	19.4	46.6
IFI35	interferon-induced protein 35	-	3.9
IFI44	interferon-induced protein 44	4.3	29.5
IFI44	Interferon-induced protein 44	-	9.2
IFI44L	interferon-induced protein 44-like	-	158.0
IFIH1	Interferon induced with helicase C domain 1	-	4.6
IFIH1	Interferon induced with helicase C domain 1	-	4.6
IFIH1	interferon induced with helicase C domain 1	-	8.6
IFIH1	interferon induced with helicase C domain 1	-	8.6
IFIH1	interferon induced with helicase C domain 1	6.6	26.1
IFIH1	interferon induced with helicase C domain 1	6.6	26.1
IFIT1	interferon-induced protein with tetratricopeptide repeats 1	37.1	49.8
IFIT2	interferon-induced protein with tetratricopeptide repeats 2	86.1	79.8
IFIT2	interferon-induced protein with tetratricopeptide repeats 2	12.7	60.5
IFIT3	interferon-induced protein with tetratricopeptide repeats 3	6.0	25.7
IFIT3	interferon-induced protein with tetratricopeptide repeats 3	6.2	35.6
IFIT5	interferon-induced protein with tetratricopeptide repeats 5	-	3.6
IFIT5	interferon-induced protein with tetratricopeptide repeats 5	-	4.1
IFITM1	interferon induced transmembrane protein 1 (9-27)	3.6	8.4
IFITM1	interferon induced transmembrane protein 1 (9-27)	-	8.4
IFNB1	interferon, beta 1, fibroblast	-	104.0
INDO	indoleamine-pyrrole 2,3 dioxygenase	-	38.6
IRF1	interferon regulatory factor 1	-	8.3
IRF2	interferon regulatory factor 2	-	2.5
IRF7	interferon regulatory factor 7	-	8.2
ISG20	interferon stimulated exonuclease gene 20kDa	-	6.9
ISG20	interferon stimulated exonuclease gene 20kDa	-	13.6
ISGF3G	interferon-stimulated transcription factor 3, gamma 48kDa	3.3	4.3
LBA1	lupus brain antigen 1	-	3.2
MX1	myxovirus (influenza virus) resistance 1, interferon-inducible protein p78 (mouse)	8.3	84.9
MX2	myxovirus (influenza virus) resistance 2 (mouse)	-	28.9
NMI	N-myc (and STAT) interactor	-	2.9
NOD27	nucleotide-binding oligomerization domains 27	-	9.6
OAS1	2',5'-oligoadenylate synthetase 1, 40/46kDa	-	13.3
OAS1	2',5'-oligoadenylate synthetase 1, 40/46kDa	2.3	11.4
OAS2	2'-5'-oligoadenylate synthetase 2, 69/71kDa	7.8	22.4
OAS2	2'-5'-oligoadenylate synthetase 2, 69/71kDa	-	22.2
OAS2	2'-5'-oligoadenylate synthetase 2, 69/71kDa	8.9	49.3
OAS3	2'-5'-oligoadenylate synthetase 3, 100kDa	-	3.5
OASL	2'-5'-oligoadenylate synthetase-like	12.1	33.1
OASL	2'-5'-oligoadenylate synthetase-like	10.6	22.8

PDCD1LG1	CD274 antigen	-	32.2
PHF11	PHD finger protein 11	-	2.6
PIK3AP1	phosphoinositide-3-kinase adaptor protein 1	-	2.8
PLAUR	plasminogen activator, urokinase receptor ; plasminogen activator, urokinase receptor	-	2.1
PLSCR1	phospholipid scramblase 1	-	3.3
PLSCR1	phospholipid scramblase 1	-	3.4
PLSCR1	Phospholipid scramblase 1	-	3.3
PRKRA	Protein kinase, interferon-inducible double stranded RNA dependent activator	-	2.3
PRKRA	Protein kinase, interferon-inducible double stranded RNA dependent activator	-	2.7
PRKRA	Protein kinase, interferon-inducible double stranded RNA dependent activator	-	2.7
RSAD2	radical S-adenosyl methionine domain containing 2	6.5	147.0
SOCS1	suppressor of cytokine signaling 1	-	21.3
SOCS3	suppressor of cytokine signaling 3	-	2.5
SOCS3	suppressor of cytokine signaling 3	-	2.7
SP100	nuclear antigen Sp100	-	3.2
SP100	nuclear antigen Sp100	-	2.6
SP100	nuclear antigen Sp100	-	2.1
SP100	nuclear antigen Sp100	-	4.4
SP100	nuclear antigen Sp100	-	2.3
SP110	SP110 nuclear body protein	-	4.6
SP110	SP110 nuclear body protein	-	5.1
SP110	SP110 nuclear body protein	-	5.8
SP110	SP110 nuclear body protein	-	10.0
SP110	SP110 nuclear body protein	-	10.3
STAT1	Signal transducer and activator of transcription 1, 91kDa	-	3.3
STAT1	signal transducer and activator of transcription 1, 91kDa	-	5.5
STAT1	signal transducer and activator of transcription 1, 91kDa	-	2.3
STAT2	signal transducer and activator of transcription 2, 113kDa	-	6.8
STAT2	signal transducer and activator of transcription 2, 113kDa	-	2.2
TAP2	transporter 2, ATP-binding cassette, sub-family B (MDR/TAP)	-	2.1
TNFSF10	tumor necrosis factor (ligand) superfamily, member 10 ; tumor necrosis factor (ligand) superfamily, member 10	19.9	29.8
TNFSF10	tumor necrosis factor (ligand) superfamily, member 10 ; tumor necrosis factor (ligand) superfamily, member 10	-	26.9
TNFSF10	Tumor necrosis factor (ligand) superfamily, member 10 ; Tumor necrosis factor (ligand) superfamily, member 10	4.7	41.7
TNFSF13B	tumor necrosis factor (ligand) superfamily, member 13b	-	18.8
TNFSF13B	tumor necrosis factor (ligand) superfamily, member 13b	4.3	20.2
TRIM21	tripartite motif-containing 21	-	5.8
TRIM22	tripartite motif-containing 22	-	4.6
TSPAN12	tetraspanin 12	-	2.2
ZC3HAV1	zinc finger CCCH-type, antiviral 1	-	2.7
ZC3HAV1	zinc finger CCCH-type, antiviral 1	-	2.3
ZC3HAV1	zinc finger CCCH-type, antiviral 1	-	3.4

Cell Death

Gene Symbol	Description	H1N1	H9N2
BIRC4BP	XIAP associated factor-1	-	3.4
BIRC4BP	XIAP associated factor-1	-	27.6
BIRC4BP	XIAP associated factor-1	-	242.0
BTG1	B-cell translocation gene 1, anti-proliferative	-	2.5
CASP1	caspase 1, apoptosis-related cysteine peptidase (interleukin 1, beta, convertase)	-	2.6
CASP1	caspase 1, apoptosis-related cysteine peptidase (interleukin 1, beta, convertase)	-	3.5
CASP1	caspase 1, apoptosis-related cysteine peptidase (interleukin 1, beta, convertase)	-	5.7
CASP1	caspase 1, apoptosis-related cysteine peptidase (interleukin 1, beta, convertase)	-	7.5
CASP1 ; COP1	caspase 1, apoptosis-related cysteine peptidase (interleukin 1, beta, convertase) ; caspase-1 dominant-negative inhibitor pseudo-ICE	-	7.2
CD38	CD38 antigen (p45)	-	5.8
OPTN	optineurin	-	2.1
SOCS3	suppressor of cytokine signaling 3	-	2.5
SOCS3	suppressor of cytokine signaling 3	-	2.7
THAP2	THAP domain containing, apoptosis associated protein 2	10.4	5.9
TNFAIP3	tumor necrosis factor, alpha-induced protein 3	-	2.6
TNFAIP6	tumor necrosis factor, alpha-induced protein 6	-	2.7
TNFAIP6	tumor necrosis factor, alpha-induced protein 6	-	2.8
TNFSF10	tumor necrosis factor (ligand) superfamily, member 10 ; tumor necrosis factor (ligand) superfamily, member 10	19.9	29.8
TNFSF10	tumor necrosis factor (ligand) superfamily, member 10 ; tumor necrosis factor (ligand) superfamily, member 10	-	26.9
TNFSF10	Tumor necrosis factor (ligand) superfamily, member 10 ; Tumor necrosis factor (ligand) superfamily, member 10	4.7	41.7
TNFSF13B	tumor necrosis factor (ligand) superfamily, member 13b	4.3	20.2
TNFSF13B	tumor necrosis factor (ligand) superfamily, member 13b	-	18.8

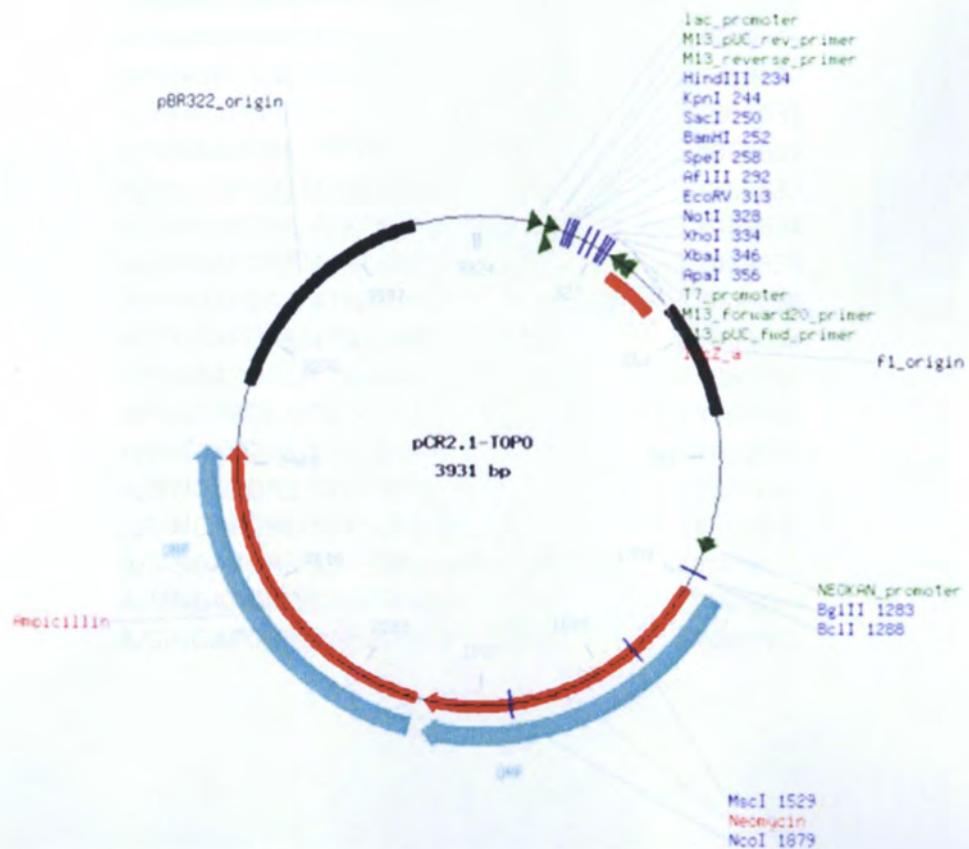
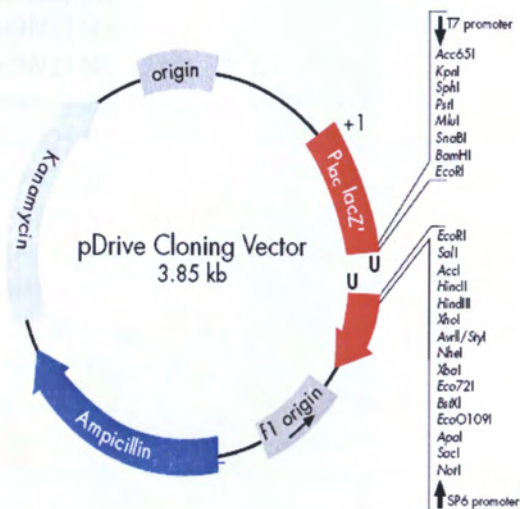
6. Cloning Vector for H9N2 gene for sequencing

pDrive Cloning Vector

Positions of various elements

Vector size (bp)	3851
Multiple cloning site	266-393
lacZ α -peptide	216-593
T7 RNA polymerase promoter	239-258
T7 transcription start	256
SP6 RNA polymerase promoter	398-417
SP6 transcription start	400
Ampicillin resistance gene	1175-2032
Kanamycin resistance gene	2181-2993
pUC origin	3668
Phage f1 origin	588-1043
Primer binding sites:*	
M13 forward (-20)	431-447
M13 forward (-40)	451-467
M13 reverse	209-224
T7 promoter primer	239-258
SP6 promoter primer	400-418

* Primer sequences are provided below



7. Accession Number List of Influenza Virus Sequence Used in This Experiment

Sequence	Accession
A/DUCK/MALAYSIA/01 (H9N2) PB2	CY073797
A/DUCK/MALAYSIA/01 (H9N2) PB1	CY073798
A/DUCK/MALAYSIA/01 (H9N2) PA	CY073799
A/DUCK/MALAYSIA/01 (H9N2) HA	CY073800
A/DUCK/MALAYSIA/01 (H9N2) NP	CY073801
A/DUCK/MALAYSIA/01 (H9N2) NA	CY073802
A/DUCK/MALAYSIA/01 (H9N2) M	CY073803
A/DUCK/MALAYSIA/01 (H9N2) NS	CY073804
A/SINGAPORE/276/2009 (H1N1) PA	CY069618
A/SINGAPORE/276/2009 (H1N1) HA	CY069619
A/SINGAPORE/276/2009 (H1N1) NP	CY069620
A/SINGAPORE/276/2009 (H1N1) NA	CY069621
A/SINGAPORE/276/2009 (H1N1) M	CY069622
A/SINGAPORE/276/2009 (H1N1) NS	CY069623
A/SINGAPORE/471/2009 (H1N1) PB1	CY069624
A/SINGAPORE/471/2009 (H1N1) PA	CY069625
A/SINGAPORE/471/2009 (H1N1) HA	CY069626
A/SINGAPORE/471/2009 (H1N1) NP	CY069627
A/SINGAPORE/471/2009 (H1N1) NA	CY069628
A/SINGAPORE/471/2009 (H1N1) M	CY069629
A/SINGAPORE/471/2009 (H1N1) NS	CY069630
A/SINGAPORE/478/2009 (H1N1) PB2	CY069631
A/SINGAPORE/478/2009 (H1N1) PB1	CY069632
A/SINGAPORE/478/2009 (H1N1) PA	CY069633
A/SINGAPORE/478/2009 (H1N1) HA	CY069634
A/SINGAPORE/478/2009 (H1N1) NP	CY069635
A/SINGAPORE/478/2009 (H1N1) NA	CY069636
A/SINGAPORE/478/2009 (H1N1) M	CY069637
A/SINGAPORE/478/2009 (H1N1) NS	CY069638
A/SINGAPORE/527/2009 (H1N1) PB1	CY069639
A/SINGAPORE/527/2009 (H1N1) PA	CY069640
A/SINGAPORE/527/2009 (H1N1) HA	CY069641
A/SINGAPORE/527/2009 (H1N1) NP	CY069642
A/SINGAPORE/527/2009 (H1N1) NA	CY069643
A/SINGAPORE/527/2009 (H1N1) M	CY069644
A/SINGAPORE/527/2009 (H1N1) NS	CY069645